



**AFEAS**

**Alternative Fluorocarbons Environmental Acceptability Study**

*JKETON 02*

*86940000-222*  
*119*

The West Tower, Suite 400 1333 H Street N.W. Washington, D.C. 20005  
• Tel: 202-898-0906 Fax: 202-789-1206 •

24 March 1994

Document Processing Center (TS-790)  
Office of Pesticides and Toxic Substances  
U.S. Environmental Protection Agency  
401 M Street SW  
Washington, DC 20460

**Contains No CBI**

RECEIVED  
OFFICE OF PESTICIDES  
& TOXIC SUBSTANCES  
MARCH 29 PM 2:51

Re: 8(d) Health and Safety Reporting Rule (Notification/Reporting), OPTS-84024A;  
FRL-3528-4; Significant New Use Rule and Addition to Health and Safety Data Reporting  
Rule, OPTS-50574B; FRL-3743-6

COMPOUND	TSCA CHEMICAL SUBSTANCE INVENTORY NAME	CAS NUMBER
----------	---	------------

*86940000213*  
*TO*  
*86940000222*

HCFC-21	Methane, dichloro-fluoro-	75-43-4
HCFC-22	Methane, chloro-difluoro-	75-45-6
HCFC-147b	Ethane, 1-chloro-1,1-difluoro-	75-68-3
HFC-152a	Ethane, 1,1-difluoro-	75-37-6
HCFC-133a	Ethane, 2-chloro-1,1,1-trifluoro-	75-88-7
HCFC-123	Ethane, 2,2-dichloro-1,1,1-trifluoro-	306-83-2
HFC-125	Ethane, pentafluoro-	354-33-6
HFC-134a	Ethane, 1,1,1,2-tetrafluoro-	811-97-2
HCFC-132b	Ethane, 1,2-dichloro-1,1-difluoro	1649-08-7
HCFC-141b	Ethane, 1,1-dichloro-1-fluoro-	1717-00-6
HCFC-124	Ethane, 2-chloro-1,1,1,2-tetrafluoro	2873-89-0

Dear Coordinator:

As required under the subject TSCA 8(d) rule published at 54FR8484, the Alternative Fluorocarbons Environmental Acceptability Study (AFEAS) submits on behalf and at the request of its sponsors the following information on studies to investigate the potential atmospheric environmental effects of the subject 8(d) chemicals. AFEAS is a consortium of 12 fluorocarbon manufacturers organized to fund environmental studies on HCFCs and HFCs. The AFEAS companies are:

**AFEAS Member Companies:** Akzo Chemicals International BV (Neth.), Allied-Signal Inc. (USA), Asahi Glass Co., Ltd. (Japan), Ausimont S.p.A. (Italy), Daikin Industries, Ltd. (Japan), E.I. du Pont de Nemours & Co., Inc. (USA), Elf Atochem S.A. (France), Hoechst AG (Germany), ICI Chemicals & Polymers, Ltd. (UK), LaRoche Chemicals Inc. (USA), Rhône-Poulenc Chemicals Ltd. (UK), and Solvay S.A. (Belgium).

0003

Akzo Chemicals BV  
AlliedSignal Inc.  
Asahi Glass Co., Ltd.  
Ausimont S.p.A.  
Daikin Industries, Ltd.  
E.I. du Pont de Nemours & Co., Inc.  
Elf Atochem S.A. / Elf Atochem North America  
Hoechst AG  
ICI Chemicals & Polymers, Ltd.  
LaRoche Chemicals Inc.  
Rhône-Poulenc Chemicals, Ltd.  
Solvay S.A.

AFEAS has recently approved for funding the following reportable projects:

- Principal Investigator: T.L. Bott  
Stroud Water Research Center, 512 Spencer Road, Avondale, Pennsylvania 19311  
Title: Incorporation into Biomass AFEAS Ref. #SP91-18.13/BP93-21
- Principal Investigator: R. Kannuck, P. Rardon, and W. Kenyon  
DuPont Haskell Laboratory, P.O. Box 50 Elkton Road, Newark, Delaware 19714-0050  
Title: Trifluoroacetic Acid: Terrestrial Plant Toxicity AFEAS Ref. #SP91-18.14/BP93-14
- Principal Investigator: T.L. Bott  
Stroud Water Research Center, 512 Spencer Road, Avondale, Pennsylvania 19311  
Title: Effects on Normal Acetate Metabolism AFEAS Ref. #SP91-18.15/BP93-20
- Principal Investigator: S.E. Schwarzbach, J.P. Skorupa, and J. Sefchick  
U.S. Fish and Wildlife Service, Sacramento Field Office, 3310 El Camino Avenue - Suite 130, Sacramento, California 95825  
Title: Review of Evaporative Concentration Potential of Conservative Soluble Tracers in Selected Wetland Systems AFEAS Ref. #SP91-18.16/BP93-22
- Principal Investigator: P. Newman, M.R. Schoeberl, and R.B. Rood  
NASA Goddard Space Flight Center, Greenbelt, Maryland  
Title: Field Support for the Airborne Southern Hemisphere Ozone Measurement and the Measurements for Assessing the Effects of Stratospheric Aircraft Mission (ASHOE/MAESA) AFEAS Ref. #P93-41b.c

The following AFEAS-sponsored projects have been completed; the final reports are provided for:

- Principal Investigator: O. Rattigan and R.A. Cox 86940000213  
University of Cambridge, Lensfield Road, Cambridge CB2 1EW, UK  
Title: Spectra and Photochemistry of Degradation Products of HCFCs and HFCs  
AFEAS Ref. #P90-007



**AFEAS**  
**Alternative Fluorocarbons Environmental Acceptability Study**

0 0 0 4

- Principal Investigator: R. Zellner, A. Hoffmann, V. Mörs, and W. Malm  
Universität Göttingen, 37077 Göttingen, Germany  
Title: Time Resolved Studies of Intermediate Products in the Oxidation of HCFCs and HFCs  
86940000214 AFEAS Ref. #P91-065
- Principal Investigator: J.M. Lobert, T.J. Baring - University of Colorado, Boulder, Colorado; J.H. Butler, S.A. Montzka, R.C. Myers, and J.E. Elkins - NOAA/CMDL, Boulder, Colorado  
86940000215 AFEAS Ref. #P91-068
- Principal Investigator: E.C. Tuazon and R. Atkinson, Statewide Air Pollution Research Center, University of California, Riverside, California 92521  
Title: Experimental Investigation of the Products Formed from the Tropospheric Reactions of Alternative Fluorocarbons  
86940000216 AFEAS Ref. #P91-082
- Principal Investigator: C. George, J.Y. Saison, J.L. Ponche, P. Mirabel  
Université Louis Pasteur, Strasbourg, France  
Title: Kinetics of Mass Transfer of COF<sub>2</sub>, CF<sub>3</sub>COF, and CF<sub>3</sub>COCl at the Air/Water Interface  
86940000217 AFEAS Ref. #P92-089
- Principal Investigator: K.-D. Asmus  
Hahn-Meitner-Institut Berlin, Glienicke Strasse 100, D-14109 Berlin, Germany  
Title: Exploratory Study on the Possible Degradation of Trifluoroacetic Acid by Semi-conducting Material  
86940000218 AFEAS Ref. #P93-110
- Principal Investigator: H. Sidebottom  
University College Dublin, Department of Chemistry, Dublin, Ireland  
Title: STEP-Halocside/AFEAS Workshop on Kinetics and Mechanisms for the Reactions of Halogenated Organic Compounds in the Troposphere  
86940000219 AFEAS Ref. #SP91-15
- Principal Investigator: R. Thompson  
Brixham Environmental Laboratory, Zeneca Ltd., Brixham, Devon UK  
86940000220 1. Title: Sodium Trifluoroacetate: Determination of its Effect in Soil on Seed Germination and Early Plant Growth of Wheat AFEAS Ref. #SP91-18.6  
86940000221 2. Title: Sodium Trifluoroacetate: Determination of its Effect in Soil on Seed Germination and Early Plant Growth of Sunflower and Mung Bean AFEAS Ref. #SP91-18.6  
86940000222 3. Title: Sodium Trifluoroacetate: Toxicity to Duckweed AFEAS Ref. #SP91-18.7

You may contact me at (202) 898-0906 if you have any questions regarding this submission.

Sincerely,

*Katie D. Smythe*  
Katie D. Smythe  
AFEAS Program Administrator



**AFEAS**  
Alternative Fluorocarbons Environmental Acceptability Study

0005

86940000219



COMMISSION OF THE  
EUROPEAN COMMUNITIES



**AFEAS**  
Alternative  
Fluorocarbons  
Environmental  
Acceptability  
Study

219

**Kinetics and Mechanisms for the Reactions of  
Halogenated Organic Compounds in the Troposphere.**

**STEP - HALOCSIDE/AFEAS WORKSHOP**

**DUBLIN 23 - 25 March 1993**



**University College Dublin**

0 0 0 6



86948000219

**Kinetics and Mechanisms for the Reactions of  
Halogenated Organic Compounds in the Troposphere.**

**STEP - HALOCSIDE/AFEAS WORKSHOP**

**DUBLIN 23 - 25 March 1993**

**LEGAL NOTICE**

Neither the Commission of the European Communities nor AFEAS is responsible for the use which might be made of the following information.

Printed by Campus Printing Unit,  
Chemistry Department,  
University College Dublin,  
Ireland.

0 0 0 8

## CONTENTS

### Summary:

	page
Rate constants for the reactions of OH with HFC-134a(CF <sub>3</sub> CH <sub>2</sub> F) and HFC-134(CHF <sub>2</sub> CHF <sub>2</sub> ). W.B. DeMore.	1
Atmospheric removal processes and lifetimes of CH <sub>3</sub> F, CH <sub>2</sub> F <sub>2</sub> , CHF <sub>3</sub> , C <sub>2</sub> H <sub>5</sub> F, C <sub>4</sub> H <sub>2</sub> F <sub>8</sub> and C <sub>5</sub> H <sub>2</sub> F <sub>10</sub> . A.M. Schmoltner, R.K. Talukdar, R.F. Warren, A. Mellouki, L. Goldfarb, T. Gierczak, S.A. McKeen and A.R. Ravishankara.	7
Laboratory studies of some halogenated hydrocarbons :measurements of rates of reaction with OH and comments on interferences in OH kinetics. C.E. Canosa-Mas, R.K. Connell, D.J. Kinnison, C.J. Percival and R.P. Wayne.	12
Gas phase reaction rate studies and gas and liquid phase absorption cross-section measurements for CFC alternatives. M.J. Kurylo, R.E. Huie, Z. Zhang, R.D. Saini, S. Padmaja, R. Liu, A. Fahr, W. Braun and E.P. Hunter.	19
A kinetic study of the OH + CCl <sub>3</sub> CHO reaction and a theoretical interpretation of the reactivity of OH with haloacetaldehydes. M.T. Rayez, S. Teton, A. Chichinin, G. Poulet, G. LeBras, D. Scollard, J. Treacy and H. Sidebottom.	26
Rate constants of reactions of fluoro(chloro) ethyl peroxy radicals with NO. V. Pultau and J. Peeters.	34

	page
Pulse radiolysis and FTIR studies of the atmospheric chemistry of halogenated alkyl peroxy radicals. O.J. Nielsen, J. Sehested, T. Ellerman and T.J. Wallington.	41
Formation and thermal decomposition of $\text{CCl}_3\text{C}(\text{O})\text{O}_2\text{NO}_2$ and $\text{CF}_3\text{C}(\text{O})\text{O}_2\text{NO}_2$ . I. Barnes, K.H. Becker, F. Kirchner, F. Zabel, H. Richer and J. Sodeau.	52
Rate constants for reactions of perhaloalkyl peroxy radicals with alkenes. R.E. Huie, Z.B. Alfassi and P. Neta.	59
The kinetics and mechanisms of processes involved in the atmospheric degradation of hydrochlorofluoro carbons and hydrofluorocarbons. G.D. Hayman.	65
Tropospheric transformation products of a series of hydrofluorocarbons and hydrochlorofluorocarbons. E.C. Tuazon and R. Atkinson.	75
Time resolved studies of intermediate products in the oxidation of HCFCs and HFCs. R. Zellner, A. Hoffman, V. Mors and W. Malms.	80
Photochemical studies of 1,1,1,2-tetrafluoroethane (HFC-134a). O.V. Rattigan, D.M. Rowley, O. Wild, R.L. Jones and R.A. Cox.	88
Predicted lifetimes of hydrofluorocarbons(HFCs) and hydrofluoroethers(HFEs) from simple correlations. D.L. Cooper, T.P. Cunningham, N.L. Allan and A. McCulloch.	98

	page
Two-dimensional assessment of the degradation of HFC-134a: tropospheric accumulations and deposition of trifluoroacetic acid. J.M. Rodriguez, M.K.W. Ko, N.D. Sze and C.W. Heisey.	104
A global three-dimensional study of the degradation of HCFCs and HFC-134a in the troposphere. M. Kanakidou, F.J. Dentener and P.J. Crutzen.	113
Absorption cross-sections and photolysis studies of halogenated carbonyl compounds. Photo-oxidation studies on CF <sub>3</sub> -containing CFC-substitutes. R. Meller, D. Boglu and G.K. Moortgat.	130
Rate constants for the reaction of CF <sub>3</sub> O radicals with hydrocarbons at 298 K. C. Kelly, J. Treacy, H.W. Sidebottom and O.J. Nielsen.	139
Long-path FTIR spectroscopic study of the reactions of CF <sub>3</sub> OO and CF <sub>3</sub> O radicals with NO <sub>2</sub> . J. Chen, V. Young, T. Zhu and H. Niki.	150
Studies of the atmospheric oxidation mechanisms of some CFC replacement compounds. T.J. Bevilacqua, D.R. Hanson, N.R. Jensen and C.J. Howard.	163
Atmospheric chemistry of CF <sub>3</sub> O radicals: reaction with H <sub>2</sub> O. T.J. Wallington, M.D. Hurley, W.F. Schneider, J. Sehested and O.J. Nielsen.	170
The possible atmospheric importance of the reaction of CF <sub>3</sub> O radicals with ozone. P. Biggs, C.E. Canosa-Mas, D.E. Shallcross, R.P. Wayne, C. Kelly and H.W. Sidebottom.	177
The photolysis and chlorine-atom initiated photo-oxidation of trifluoroacetaldehyde. H.R. Richer, J.R. Sodeau and I. Barnes.	182

	page
Thermodynamic properties for atmospheric degradation of HFC-134a and HFC-23. D.A. Dixon and R. Fernandez.	189
Experimental determination of uptake coefficients for acid halides. Ch. George, J.L. Ponche and Ph. Mirabel.	196
An aerosol chamber technique for the determination of the uptake of carbonyl halides by submicron aqueous solution droplets: phosgene. W. Behnke, M. Elend, H.U. Kruger and C. Zetzsch.	203
Formation of $\text{OClO}$ and $\text{Cl}_2\text{O}_3$ on ice in the $\text{Cl}/\text{O}_3$ system at temperatures below $-60^\circ\text{C}$ and some results for the $\text{Br}/\text{O}_3$ system. U. Kirchner, M. Liesner, Th. Benter and R.N. Schindler.	210

0 0 1 2

Summary:

Research carried out over the two years since the previous STEP-HALOCSIDE/AFEAS Workshop (May 1991) has provided detailed kinetic and mechanistic data for the atmospheric breakdown of hydrofluorocarbons (HFCs) and hydrochlorofluorocarbons (HCFCs), proposed as alternatives for chlorofluorocarbons (CFCs). Laboratory studies on these compounds have now reached a stage where their environmental acceptability can be judged on the basis of firm scientific evidence. Although a few areas still exist where further research is required, it now seems timely to review the progress made since the publication of the WMO Scientific Assessment of Ozone Depletion (1991).

The dominant loss process for HFCs and HCFCs in the atmosphere is through reaction with the OH radical, with minor contributions from reactions with O(<sup>1</sup>D) and Cl atoms in the stratosphere. Photolysis of HCFCs is also important in the stratosphere and leads directly to the formation of Cl atoms. Rate constant data for the OH radical reactions have been determined in various laboratories, employing different experimental techniques, and have been critically evaluated. The uncertainty in the values is of the order of ±20%. In order to calculate the tropospheric lifetimes of these compounds an estimate of the hydroxyl concentration field is required. The average lifetimes of the HCFCs and HFCs are generally calculated by scaling to the average tropospheric lifetime of methyl chloroform, for which an independent estimate has been obtained from analysis of the measured concentrations of this compound and of its estimated emissions. Errors in the tropospheric lifetime of methyl chloroform are likely to be in excess of 10% and hence the overall error in the absolute atmospheric lifetimes of HFCs and HCFCs are probably in the region of ±40%. Relative to one another, their lifetimes are much less uncertain. Absorption cross-sections for HFCs and HCFCs are now reasonably well known and provide photolytic loss rates for HCFCs in the stratosphere. Photolysis of HFCs is of no atmospheric significance.

Reaction of OH radicals with HCFCs and HFCs leads to formation of haloalkyl radicals, which under atmospheric conditions form the corresponding peroxy radicals. A generalized scheme for the subsequent reactions of these radicals is shown in Figure 1. The peroxy radicals may react with NO, NO<sub>2</sub> and HO<sub>2</sub> radicals under tropospheric conditions. The available evidence suggests that the major loss process, for conditions typical of the troposphere, is

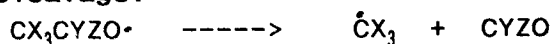
by reaction with NO to give the alkoxy radical. The hydroperoxides, pernitrites and nitrates have been shown to have limited stability and transport to the stratosphere will be negligible. Thermal decomposition or photolysis of these species either leads to regeneration of  $CX_3CYZO\cdot$  or formation of  $CX_3CYO\cdot$ .

There are a number of possible reaction pathways for the degradation of haloalkoxy radicals:

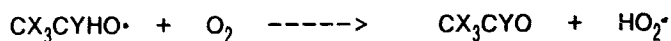
C-Cl bond cleavage:



C-C bond cleavage:



hydrogen abstraction:



Experimental data concerning the reactions of haloalkoxy radicals has come mainly from chlorine atom initiated oxidation of halogenated alkanes and alkenes, although oxidation has also been initiated via OH radical reactions and photolysis. A number of general conclusions concerning the relative importance of the various reaction channels may be drawn from the results of the experimental data:

- (1)  $CX_2ClO$  radicals (X=H, Cl or F) eliminate a Cl atom except for  $CH_2ClO\cdot$  where reaction with  $O_2$  is the dominant reaction.
- (2)  $CH_2FO$  and  $CHF_2O$  radicals react with  $O_2$  to give the corresponding carbonyl fluorides and  $HO_2$  radicals. Fluorine atom loss or reaction with  $O_2$  are unimportant for  $CF_3O$  radicals. The chemistry of these species is discussed in detail below.
- (3)  $CX_3CH_2O$  radicals (X=H, Cl or F) react predominantly with  $O_2$  to form the aldehyde and  $HO_2$  radicals.
- (4)  $CX_3CCl_2O$  and  $CX_3CFCIO$  radicals decompose by Cl atom elimination rather than C-C bond fission.
- (5)  $CX_3CF_2O$  radicals undergo C-C bond breaking.

0 0 1 4

- (6)  $CX_3CHYO$  radicals ( $Y=Cl$  or  $F$ ) have two important reaction channels. The relative importance of the C-C bond breaking process and reaction with  $O_2$  is a function of temperature,  $O_2$  pressure and the total pressure and hence varies considerably with altitude. Recent laboratory results for the  $CF_3CHFO$  radical, when used in tropospheric model calculations, indicate that 35 to 40% of HFC-134a released into the atmosphere will be converted to  $CF_3CFO$ .

Halogenated aldehydes,  $CX_3CHO$ , are formed as primary products in the OH initiated oxidation of HFCs and HCFCs of structure  $CX_3CH_3$ . These species may further degrade by photolysis or by reaction with OH radicals, with typical lifetimes of the order of several days. The reported experimental data show that photolysis, to form  $CX_3$  radicals, is the dominant removal process for  $CX_3CHO$ . However, the minor channel involving reaction with OH radicals can lead to formation of acyl peroxy nitrates, which appear to be thermally stable under conditions typical of the upper troposphere. It is therefore expected that their lifetimes will be controlled by photolysis and can be approximated to that of  $CH_3C(O)O_2NO_2$ . The yields of the acyl peroxy nitrates will be largely dependent on the stabilities of the precursor radicals,  $CX_3\dot{C}O$ . Kinetic studies show that whereas  $CF_3\dot{C}O$  is relatively stable and leads to formation of  $CF_3C(O)O_2$ ,  $CCl_3\dot{C}O$  rapidly decomposes. It is hence possible that  $CF_2Cl\dot{C}O$  and  $CFCl_2\dot{C}O$  radicals are sufficiently stable that small amounts of  $CF_2ClC(O)O_2NO_2$  and  $CFCl_2C(O)O_2NO_2$  may result from the oxidation of  $CF_2ClCH_3$  and  $CFCl_2CH_3$  and might give rise to a minor flux of chlorine into the stratosphere.

Reactions of OH radicals with the fully halogenated carbonyl compounds  $CCl_2O$ ,  $CClFO$ ,  $CF_2O$ ,  $CX_3CFO$  and  $CX_3CClO$  have been shown to be unimportant and absorption cross section measurements indicate that only for  $CCl_2O$  and  $CX_3CClO$  is photolysis important in the troposphere. Photolysis and reaction with OH radicals may be important for  $CHClO$  in the troposphere whereas both these sinks are negligible for  $CHFO$ . In the troposphere, the carbonyl halides and acid halides are likely to be removed by heterogeneous processes. All of these compounds are soluble in water, where they react further forming halogenated acids or hydrogen halides and carbon dioxide. The rate of these processes depends on both the Henry's constant and the hydrolysis rate constant. These data have now been determined for most of the compounds and the lifetimes estimated suggest that the major sink is by uptake in atmospheric and ocean

0 0 1 5

waters with a geographical distribution depending on the local rate at which the parent HFC or HCFC decomposes. This, in turn, will depend on the local OH concentration. Trifluoroacetic acid is the hydrolysis product of both  $\text{CF}_3\text{CFO}$  and  $\text{CF}_3\text{CClO}$  and at the present time its environmental fate is uncertain. It appears to be resistant to abiotic decomposition although recent results seem to indicate that surface photolysis of this compound may have some importance.

Trifluoromethyl radicals are produced as reaction intermediates in the atmospheric degradation of HFCs and HCFCs which contain the  $\text{CF}_3$  group. Further reaction of  $\dot{\text{C}}\text{F}_3$  with  $\text{O}_2$  and  $\text{NO}$  leads to the formation of  $\text{CF}_3\text{O}$  radicals. The possible reactions of  $\text{CF}_3\text{O}$  in the troposphere and the stratosphere are given in Figure 2. The available kinetic and mechanistic evidence indicates that the loss of  $\text{CF}_3\text{O}$  radicals in the troposphere is largely dominated by hydrogen abstraction from  $\text{CH}_4$  and possibly  $\text{H}_2\text{O}$  to form  $\text{CF}_3\text{OH}$ , and by reaction with  $\text{NO}$  to form  $\text{CF}_2\text{O}$ . Although  $\text{CF}_3\text{OH}$  is relatively unstable under laboratory conditions, this is probably due to heterogeneous processes. It seems likely, therefore, that  $\text{CF}_3\text{OH}$  loss in the troposphere will largely take place at aerosol surfaces or by hydrolysis in cloud water. Reaction with  $\text{CH}_4$  and  $\text{NO}$  will also be major sinks for  $\text{CF}_3\text{O}$  in the stratosphere.  $\text{CF}_3\text{OH}$  is expected to be photochemically stable in this region and by analogy with structurally similar compounds, reaction with  $\dot{\text{O}}\text{H}$  will be very slow. Circulation back to the troposphere and loss by hydrolysis is likely to be the sink for this species. The lifetime of  $\text{CF}_2\text{O}$ , formed by the reaction of  $\text{CF}_3\text{O}$  with  $\text{NO}$ , is sufficiently long that diffusion into the troposphere followed by hydrolysis is the major fate of this compound. Recently it has been proposed that the reaction of  $\text{CF}_3\text{O}$  with  $\text{O}_3$  may be important in the stratosphere leading to the catalytic loss of  $\text{O}_3$ . The importance of this chain process depends critically on a number of factors: the rate constants for the reactions of  $\text{CF}_3\text{O}$  with  $\text{O}_3$  and for the sink reactions with  $\text{CH}_4$ ,  $\text{NO}$  and possibly  $\text{NO}_2$ , the relative concentrations of these species and the levels of  $\text{CF}_3$  radicals generated from HCFCs and HFCs in the stratosphere. The limited experimental data seem to suggest that  $\text{O}_3$  loss due to reaction with  $\text{CF}_3\text{O}$  radicals will be minor.

The major conclusions that can be drawn from recent laboratory-based studies are:

- Calculated atmospheric lifetimes for HFCs and HCFCs may have substantial uncertainties arising, mainly, from uncertainties in the OH radical rate constant data and tropospheric OH field strengths. The absolute fluxes of unchanged HFCs and HCFCs into the stratosphere will be subject to the same uncertainties but relative to each other the fluxes are much more certain.

- Irrespective of the flux of unchanged HFCs and HCFCs to the stratosphere, the amounts of degradation products diffusing into the stratosphere are expected to be minimal. Thus, chlorine-containing products from the degradation of HCFCs in the troposphere will not contribute significantly to chlorine loading in the stratosphere.

- Tentative evidence for the involvement of the  $CF_3O$  radical in catalytic cycles leading to loss of  $O_3$  in the stratosphere has been reported. The available data indicate that  $O_3$  loss through this cycle will be small, if not negligible.

Archie McCulloch,  
ICI Chemicals and  
Polymers Limited,  
Runcorn, U.K.

Howard Sidebottom,  
University College Dublin,  
Ireland.

Figure 1: Atmospheric Degradation Scheme for HFC/HCFC.

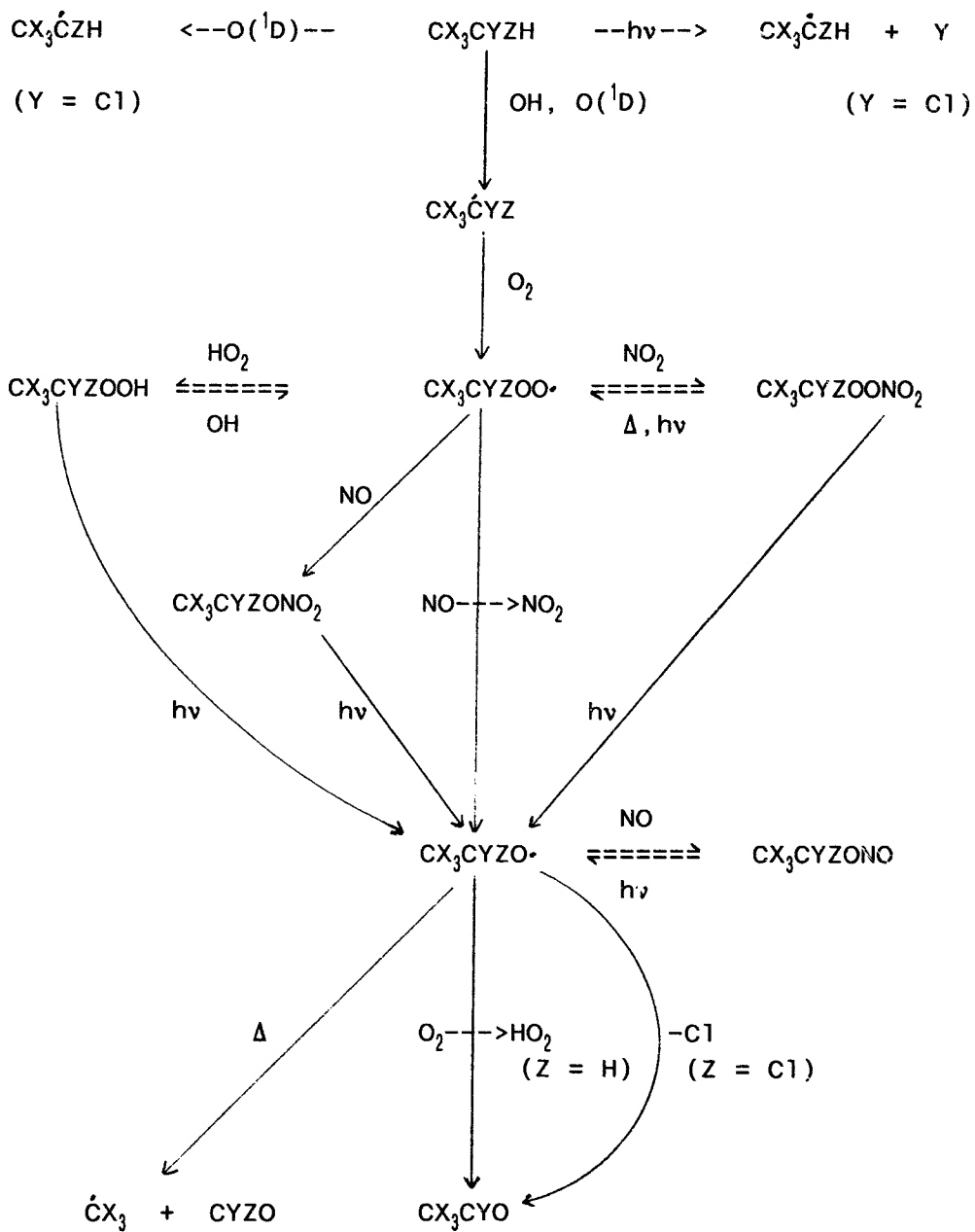
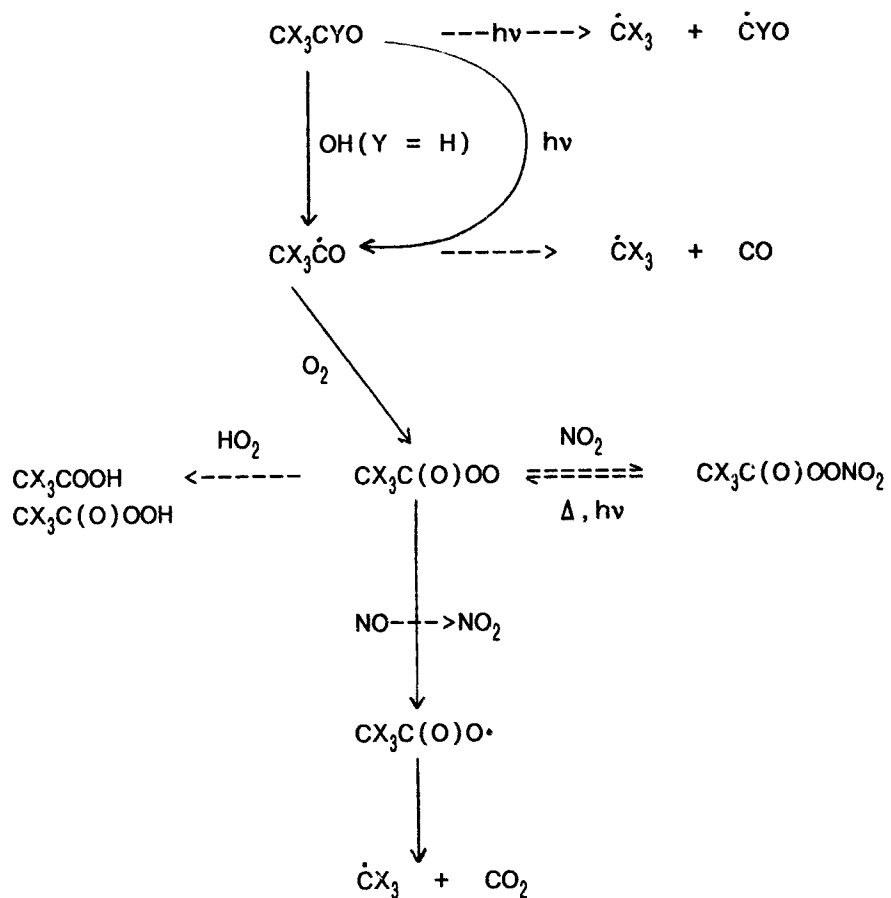
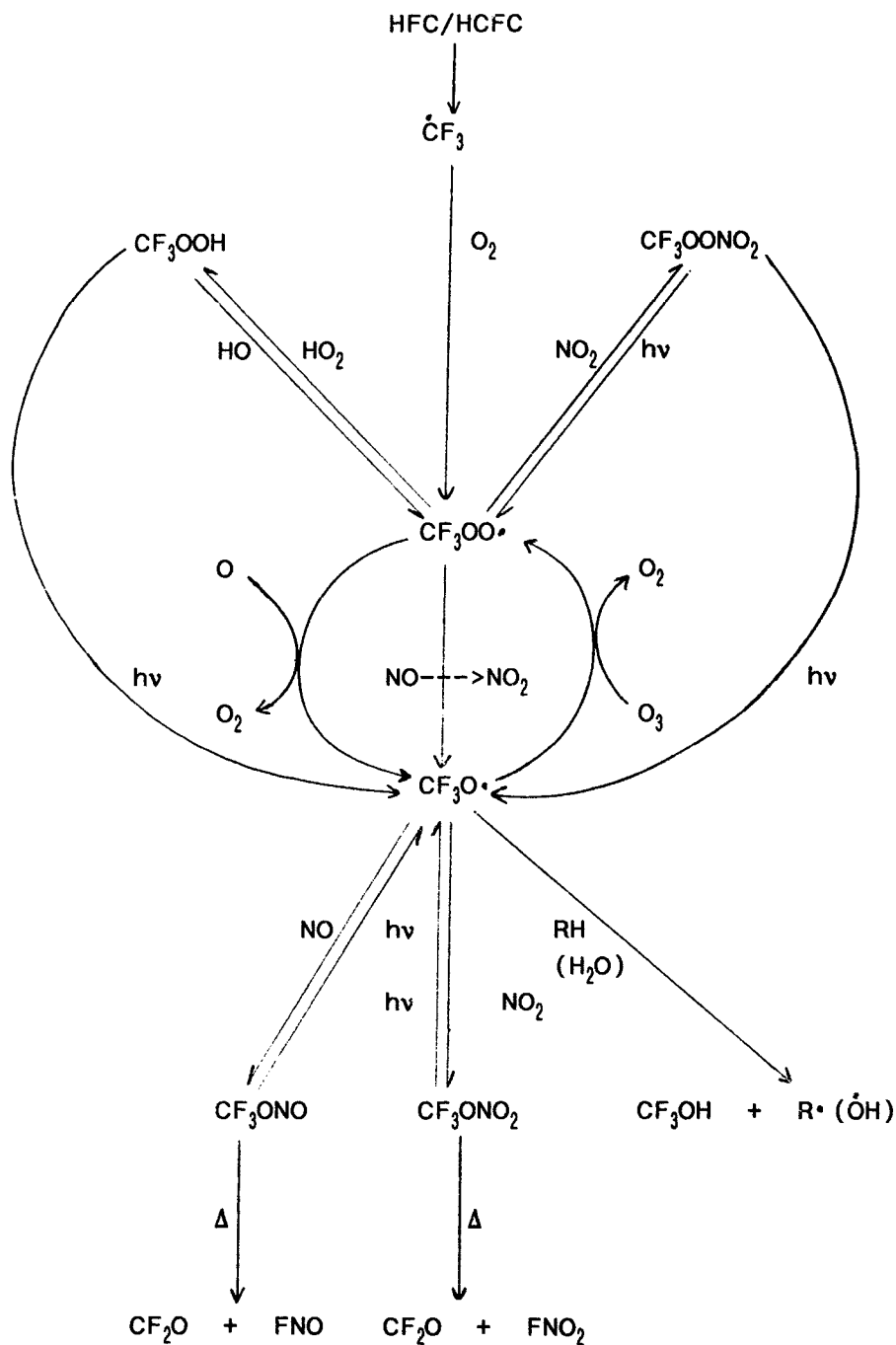


**Figure 1: Continued**



0019

**Figure 2: Atmospheric Reactions of the CF<sub>3</sub> Radical.**



## Rate Constants for the Reactions of OH With HFC-134a (CF<sub>3</sub>CH<sub>2</sub>F) and HFC-134 (CHF<sub>2</sub>CHF<sub>2</sub>)

W. B. DeMore

Jet Propulsion Laboratory, California Institute of Technology  
Pasadena, California, U. S. A.

Recent results from this laboratory[1] have indicated that the currently accepted rate constant for HFC-134a may be too high. Also, the data base for HFC-134 is limited to the early study of Clyne and Holt [2]. In the present work relative rate measurements have been made to better establish the rate constants for these two HFCs. The results provide information on the internal consistency of the recommended rate constants for the reference reactants CH<sub>4</sub>, CH<sub>3</sub>CCl<sub>3</sub>, and HFC-125.

The experimental method was similar to that previously used to measure relative rate constants for OH reactions with CH<sub>4</sub> and CH<sub>3</sub>CCl<sub>3</sub> [3]. The OH radicals were produced by UV photolysis of O<sub>3</sub> in the presence of water vapor in a slow-flow, temperature-controlled photochemical reactor. All experiments were at atmospheric pressure. Each reactant is depleted by the OH reaction in a manner similar to that of the atmosphere. The rate constant ratio is obtained from the relation:

$$\frac{k_{\text{reactant}}}{k_{\text{reference}}} = \frac{\ln(DF)_{\text{reactant}}}{\ln(DF)_{\text{reference}}} \quad (\text{I})$$

The quantity DF (depletion factor) is given by:

$$DF = \frac{(\text{Initial Conc.})}{(\text{Final Conc.})} \quad (\text{II})$$

Initial reactant concentrations were in the range 10<sup>14</sup> to 10<sup>15</sup> cm<sup>-3</sup>, and depletion factors were normally about 1.1 to 1.5. Concentrations were monitored with a Nicolet 20SX FTIR operated at 0.5 cm<sup>-1</sup> resolution in the absorbance mode using a White cell with a three-meter path length. Infrared spectra of HFC-134a and HFC-134 are shown in Figures 1 and 2. The photolysis cell was quartz with a water jacket for temperature control. The light source was a low pressure Hg lamp.

Figure 3 shows 298 K data plotted according to Equation I for HFC-134a and HFC-134, both with reference to CH<sub>3</sub>CCl<sub>3</sub>. The ratio of slopes is 1.5, which indicates that the reaction of HFC-134 with OH is 1.5 times faster than that of HFC-134a at 298 K.

Six rate constant ratios and their temperature dependences were measured: k(CH<sub>3</sub>CCl<sub>3</sub>)/k(134a), k(CH<sub>4</sub>)/k(134a), k(125)/k(134a), k(CH<sub>3</sub>CCl<sub>3</sub>)/k(134), k(134)/k(134a), and k(134)/k(125). The results for all ratios measured are shown in Arrhenius form in Figure 4(a-f).

Table 1 summarizes all the ratios measured, in Arrhenius form, as derived from linear least squares fits of the data shown in Figure 2. Table 2 lists the calculated rate constants for HFC-134a, based on the three reference compounds used. Table 3 shows the resulting rate constants for HFC-134.

Table 1. Ratios Measured and Their Temperature Dependence

Ratio	Arrhenius Expression <sup>a</sup>	Ratio at 298 K
k(CH <sub>3</sub> CCl <sub>3</sub> ) / k(134a)	(1.22 ± 0.17) exp ((219 ± 44)/T)	2.54
k(CH <sub>4</sub> ) / k(134a)	(2.24 ± 0.78) exp((-82 ± 115)/T)	1.70
k(125) / k(134a)	(0.48 ± 0.12) exp ((12 ± 79)/T)	0.50
k(CH <sub>3</sub> CCl <sub>3</sub> ) / k(134)	(0.84 ± 0.10) exp ((212 ± 37)/T)	1.71
k(134a) / k(134)	(0.85 ± 0.07) exp ((-80 ± 25)/T)	0.65
k(125) / k(134)	(0.48 ± 0.11) exp ((-109 ± 77)/T)	0.33

(a) Errors shown are standard deviations. Actual uncertainties are approximately a factor of 1.3 in the A-factor ratios and 75-125 K in the ΔE/R values.

Table 2. Derived Rate Constants for HFC-134a and Comparison with Previous Recommendations.

k (134a)	k(298 K)	Reference Compound	Reference Rate Constant	Source
<u>This work</u>				
$1.5 \times 10^{-12} \exp(-1769/T)$	$3.9 \times 10^{-15}$	CH <sub>3</sub> CCl <sub>3</sub>	$1.8 \times 10^{-12} \exp(-1550/T)$	JPL 92-20
$1.3 \times 10^{-12} \exp(-1738/T)$	$3.8 \times 10^{-15}$	CH <sub>4</sub>	$2.9 \times 10^{-12} \exp(-1820/T)$	JPL 92-20
$1.2 \times 10^{-12} \exp(-1712/T)$	$3.8 \times 10^{-15}$	CF <sub>3</sub> CF <sub>2</sub> H	$5.6 \times 10^{-13} \exp(-1700/T)$	JPL 92-20
<u>JPL 92-20</u>				
$1.7 \times 10^{-12} \exp(-1750/T)$	$4.8 \times 10^{-15}$			
<u>IUPAC</u>				
$8.4 \times 10^{-13} \exp(-1535/T)$	$4.9 \times 10^{-15}$			

Units are cm<sup>3</sup>/molecule-s.

Table 3. Derived Rate Constants for HFC-134 and Comparison with Previous Recommendations.

k (134)	k(298 K)	Reference Compound	Reference Rate Constant	Source
<u>This work</u>				
$2.1 \times 10^{-12} \exp(-1762/T)$	$5.7 \times 10^{-15}$	CH <sub>3</sub> CCl <sub>3</sub>	$1.8 \times 10^{-12} \exp(-1550/T)$	JPL 92-20
$1.5 \times 10^{-12} \exp(-1660/T)$	$5.7 \times 10^{-15}$	CF <sub>3</sub> CFH <sub>2</sub>	$1.3 \times 10^{-12} \exp(-1740/T)$	This work <sup>a</sup>
$1.2 \times 10^{-12} \exp(-1591/T)$	$5.8 \times 10^{-15}$	CF <sub>3</sub> CF <sub>2</sub> H	$5.6 \times 10^{-13} \exp(-1700/T)$	JPL 92-20
<u>JPL 92-20</u>				
$8.7 \times 10^{-12} \exp(-1500/T)$	$5.7 \times 10^{-15}$			
<u>IUPAC</u>				
-----	$5.7 \times 10^{-15}$			

Units are cm<sup>3</sup>/molecule-s.

(a.) See Discussion Section.

Some consistency checks may be noted in Table 1. The ratio  $k(134a)/k(134a)$ , when calculated from the ratios of each HFC versus CH<sub>3</sub>CCl<sub>3</sub>, is 0.68 at 298 K, compared to the directly measured value 0.65. Similarly, the same ratio obtained from the HFC-125 ratios is 0.66. The temperature dependences and A-factor ratios are slightly different, although within experimental error, and all indicate a higher E/R for HFC-134a compared to HFC-134.

The previously measured ratio  $k(\text{CH}_3\text{CCl}_3)/k(\text{CH}_4)$  [3] can also be compared with the value calculated from the data of Table 1, using the ratios for CH<sub>3</sub>CCl<sub>3</sub> and CH<sub>4</sub> versus HFC-134a. The result is  $0.54 \exp(301/T)$ , compared to the directly measured value of  $0.62 \exp(291/T)$ .

#### Discussion

The derived rate constants for both HFC-134a and HFC-134 (Tables 2 and 3) from the different reference compounds are in remarkably good agreement. This implies that the rate constant data used for the reference compounds are self-consistent. It seems clear, however, that the presently recommended rate constant for HFC-134a in JPL 92-20[4] and IUPAC[5] is high by about 25%, from the standpoint of consistency with the reference compounds. Both the JPL 92-20 and the IUPAC recommendations for HFC-134a are based on recent and extensive absolute measurements of the rate constant for this reaction. All studies report higher rate constants for HFC-134a

than would be consistent with the present work, although the actual data points of Gierczak et al., [6] near 298 K are only about 12% higher than those of the present work. The reason for higher results in other studies is not known, although absolute rate measurements for OH reactions sometimes give high values as a result of impurity effects, secondary reactions, or wall losses. [7,8].

The present results for HFC-134a imply that the atmospheric lifetime is 25% longer than would be calculated from presently recommended rate constants [JPL 92-20, 1992; IUPAC, 1992] Based on the ratio  $k(\text{CH}_3\text{CCl}_3)/k(134a)$  from the present work (Table 1), the lifetime of HFC-134a with respect to OH loss is 2.7 times longer than that of  $\text{CH}_3\text{CCl}_3$  at an average atmospheric temperature of 277 K.

The previous database for HFC-134 is limited to the work of Clyne and Holt [1979], who obtained the rate constant expression  $k = 2.8 \times 10^{-12} \exp(-1800/T)$  for the temperature range 294-434 K. This corresponds to a  $k(298 \text{ K})$  value which is about 17% higher than that of the present work. The JPL 92-20 recommendation,  $8.7 \times 10^{-13} \exp(-1500/T)$  is based only on the Clyne and Holt data at 294 K ( $k = 5.3 \times 10^{-15} \text{ cm}^3/\text{molec}\cdot\text{s}$ ), with the temperature dependence being an estimate. From this expression,  $k(298 \text{ K}) = 5.7 \times 10^{-15}$ . Thus the JPL 92-20 recommendation agrees with the present work at 298 K.

Based on the three rate constants obtained in the present work for both HFC-134a and HFC-134 (Tables 2 and 3), the following expressions are recommended:

$$\begin{aligned}k(134a) &= 1.3 \times 10^{-12} \exp(-1740/T) \\k(298 \text{ K}) &= 3.8 \times 10^{-15} \text{ cm}^3/\text{molec}\cdot\text{s}\end{aligned}$$

$$\begin{aligned}k(134) &= 1.6 \times 10^{-12} \exp(-1680/T) \\k(298 \text{ K}) &= 5.7 \times 10^{-15} \text{ cm}^3/\text{molec}\cdot\text{s}\end{aligned}$$

These were obtained by averaging the Arrhenius parameters in Tables 2 and 3, respectively. They are consistent with the directly measured ratio  $k(134)/k(134a)$  (Table 1). The absolute uncertainty for both rate constants at 298 K is probably 10% or less, considering the excellent agreement from different reference compounds. The uncertainties in the E/R values are about  $\pm 150 \text{ K}$ .

This work was carried out by the Jet Propulsion Laboratory, California Institute of Technology, under contract with the National Aeronautics and Space Administration.

#### References

1. DeMore, W. B., Rates of Hydroxyl Reactions with some HFCs, Optical Methods in Atmospheric Chemistry, 1715, 72-76, 1992a.
2. Clyne, M. A. A., P. M. Holt, Reaction Kinetics Involving Ground and Excited Hydroxyl Radicals, Part 2. Rate Constants for Reactions of OH with Halogenomethanes and Halogenoethanes, J. Chem. Soc. Faraday Trans. 2, 75, 582, 1979.
3. DeMore, W. B., Relative Rate Constants for the Reactions of OH with Methane and Methyl Chloroform, Geophys. Res. Lett., 19, 1367-1370, 1992b.
4. JPL 92-20, Chemical Kinetics and Photochemical Data for Use in Stratospheric Modeling, Publication 92-20, Jet Propulsion Laboratory, California Institute of Technology, 1992.
5. IUPAC Subcommittee on Gas Kinetic Data Evaluation for Atmospheric Chemistry, Evaluated Kinetic and Photochemical Data for Atmospheric Chemistry Supp. IV, J. Phys. Chem. Ref. Data, 21, No. 6, 1125-1568, 1992.
6. Gierczak, T., R. Talukdar, G. L. Vaghjiani, E. R. Lovejoy, and A. R. Ravishankara, Atmospheric Fate of Hydrofluoroethanes and Hydrofluorochloroethanes: 1. Rate Coefficients for Reactions with OH, J. Geophys. Res. 96, 5001, 1991.
7. Jolly, G. S., G. Paraskevopolous, and D. L. Singleton, Rates of OH Radical Reactions. XII, Int. J. Chem. Kinet., 17, 1-10, 1985.
8. Wayne, R. P., C. E. Canosa-Mas, A. C. Heard, and A. D. Parr, On Discrepancies Between Different Laboratory Measurements of Kinetic Parameters for the Reaction of Hydroxyl Radical with Halocarbons, Atmospheric Environment, 26A, 2371-2379, 1992.

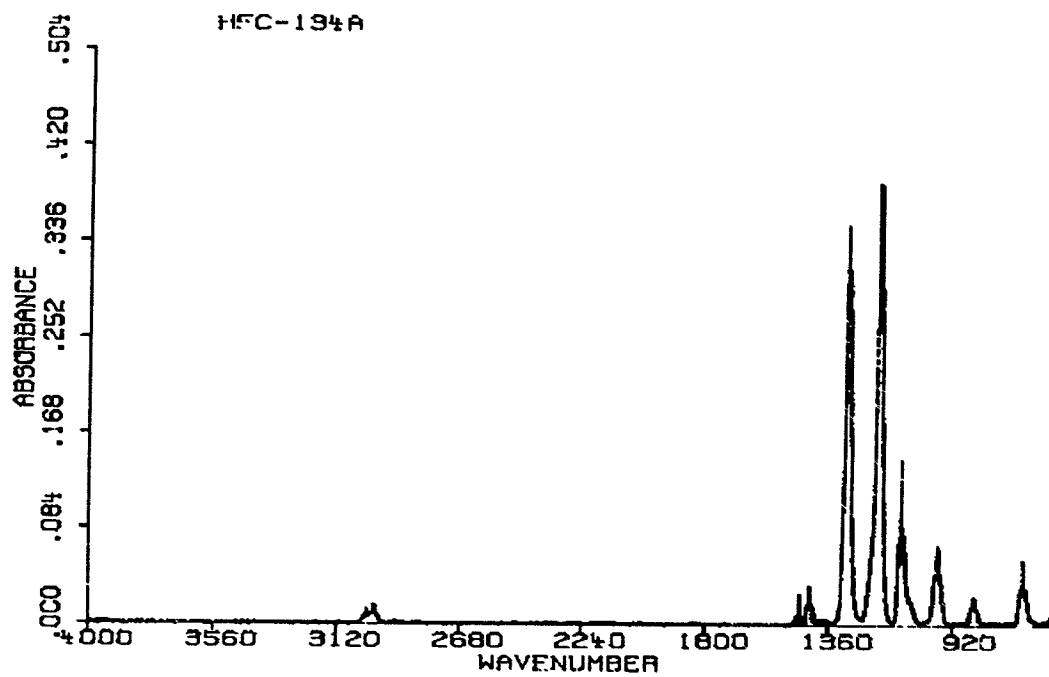


Figure 1. Infrared spectrum of HFC-134a in the absorbance mode.

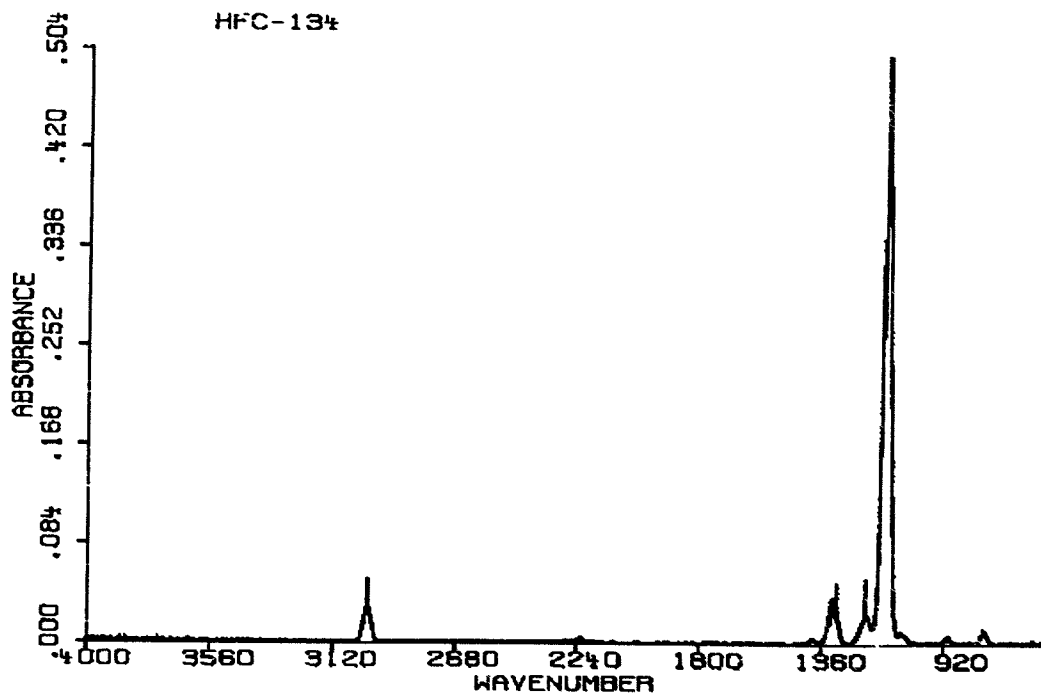


Figure 2. Infrared spectrum of HFC-134 in the absorbance mode.

0 0 - 2 4

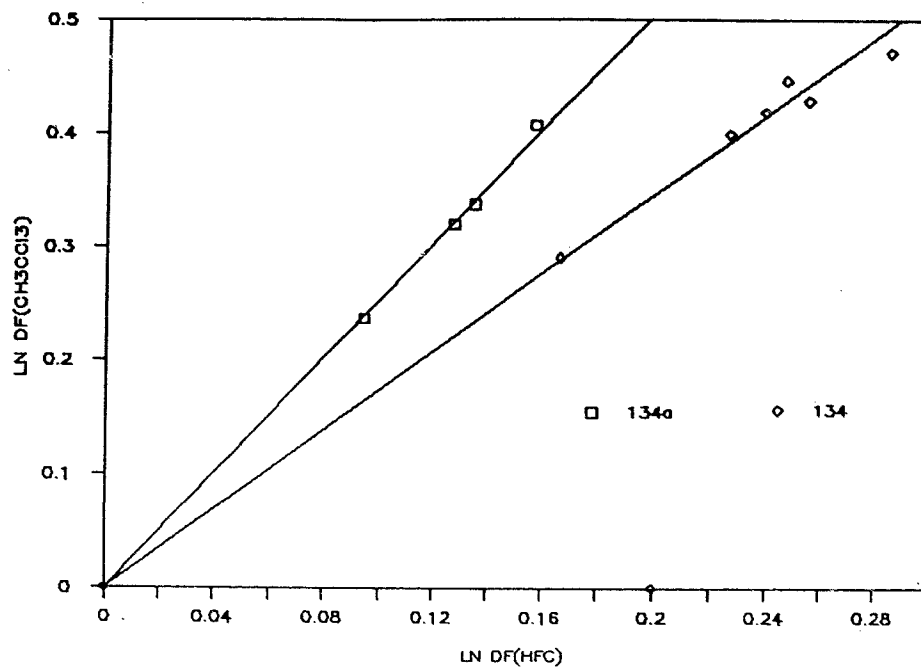


Figure 3. Relative depletions factors at 298 K for HFC-134a and HFC-134 versus  $\text{CH}_3\text{COCl}_3$ , plotted according to Equation I.

0025

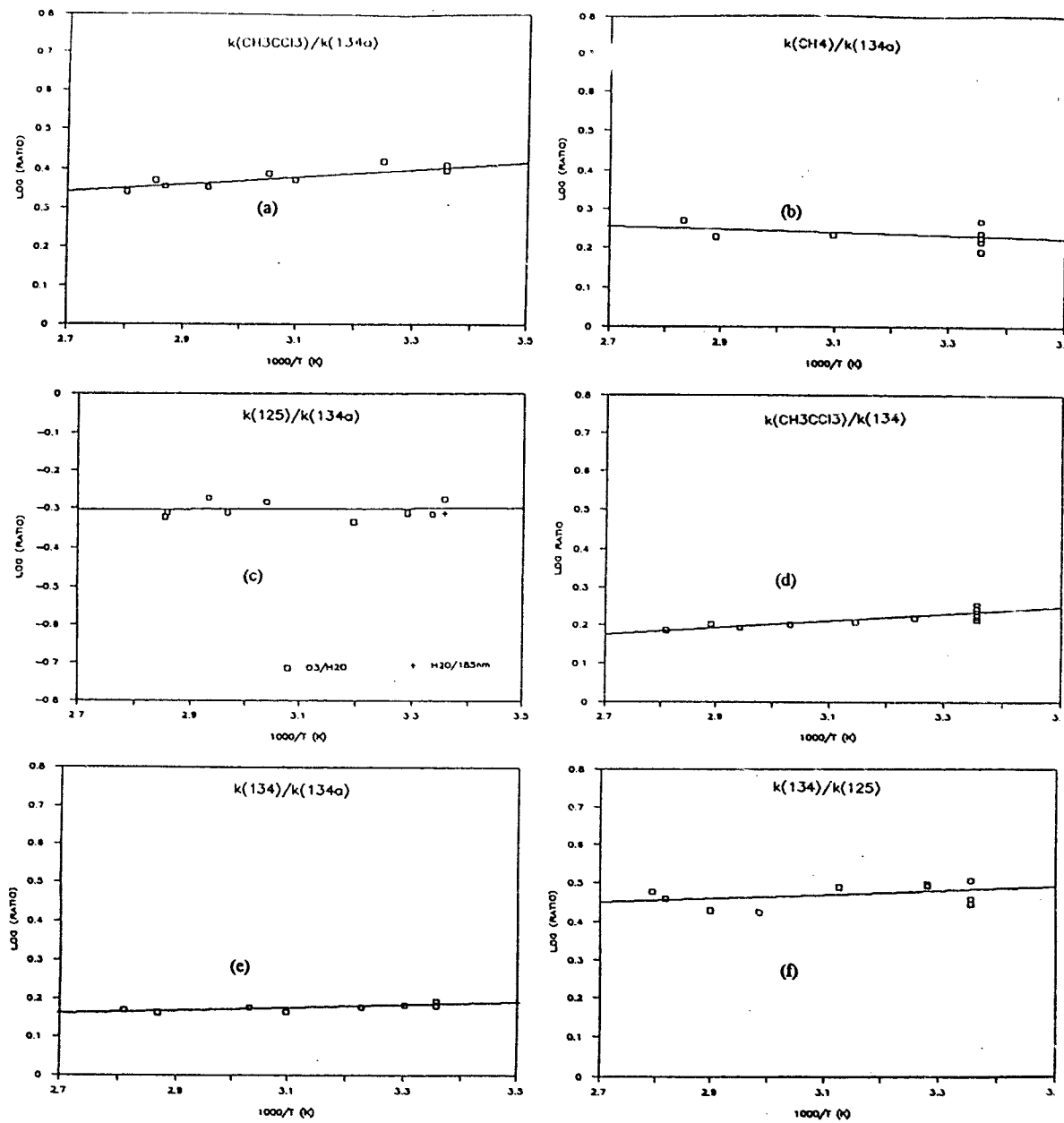


Figure 4. Arrhenius plots of the six rate constant ratios measured. The 125/134a graph, (c), includes the result from reference 1, showing good agreement with the present work.

0026

## Atmospheric Removal Processes and Lifetimes of CH<sub>3</sub>F, CH<sub>2</sub>F<sub>2</sub>, CHF<sub>3</sub>, C<sub>2</sub>H<sub>5</sub>F, C<sub>4</sub>H<sub>2</sub>F<sub>8</sub> and C<sub>5</sub>H<sub>2</sub>F<sub>10</sub>

A. M. Schmoltner<sup>a</sup>, R. K. Talukdar<sup>a</sup>, R. F. Warren<sup>a,b</sup>, A. Mellouki<sup>a,c</sup>, L. Goldfarb<sup>d</sup>, T. Gierczak<sup>e</sup>, S. A. McKeen<sup>a</sup>, and A. R. Ravishankara<sup>d</sup>

National Oceanic and Atmospheric Administration, Aeronomy Laboratory, Boulder, CO 80303, USA

<sup>a</sup> Also affiliated with the Cooperative Institute for Research in Environmental Sciences, University of Colorado, Boulder, Colorado, USA.

<sup>b</sup> Current address: Centre for Environmental Technology, Imperial College of Science, Technology, and Medicine, 48 Prince's Gardens, London SW7 2PE, UK.

<sup>c</sup> Current address: C.N.R.S., L.C.S.R., 1C, Avenue de la Recherche Scientifique, 45071 Orléans, Cédex 2, France.

<sup>d</sup> Also affiliated with the Department of Chemistry and Biochemistry, University of Colorado, Boulder, Colorado, USA.

<sup>e</sup> Current address: Department of Chemistry, Warsaw University, ul. Zwirki y Wigury 101, 02-089, Warszawa, Poland.

### Introduction

Hydrofluorocarbons (HFCs) are important substitutes for chlorofluorocarbons (CFCs). Since they do not contain chlorine, they are not expected to harm the ozone layer. However, they strongly absorb IR radiation in wavelength regions where CO<sub>2</sub> and H<sub>2</sub>O do not absorb, and are therefore greenhouse gases. In order to calculate their global warming potentials, their atmospheric lifetimes are needed.

The dominant loss process for HFCs in the atmosphere is their reaction with OH, with minor contributions from reactions with O(<sup>1</sup>D) and Cl in the stratosphere. UV photolysis does not contribute to tropospheric or stratospheric removal of HFCs since they do not absorb at wavelengths greater than about 145 nm [1]. We report here measurements of the reaction rate coefficients of OH and O(<sup>1</sup>D) with CH<sub>3</sub>F, CH<sub>2</sub>F<sub>2</sub>, CHF<sub>3</sub>, C<sub>2</sub>H<sub>5</sub>F, C<sub>4</sub>H<sub>2</sub>F<sub>8</sub> and C<sub>5</sub>H<sub>2</sub>F<sub>10</sub>, as

0 0 2 7

well as calculated values of their atmospheric lifetimes. A detailed report will be published elsewhere[2].

### Experiments and Results

The extensively purified HFC samples used in this study were carefully analyzed for impurities. In none of the reactions the impurities can contribute more than about 2% to the measured rate coefficients.

The techniques employed in this study have been described in detail elsewhere [3]. Briefly, the OH reaction rate coefficients were measured using the pulsed-photolysis / pulsed laser-induced fluorescence technique. A gas mixture containing the HFC, He buffer gas, and the OH precursor was flowed through a thermostatted reaction cell. Photolysis and probe lasers intersected in the cell at 90°. OH was produced from the photolysis of HONO (at 355 nm), H<sub>2</sub>O<sub>2</sub> or HNO<sub>3</sub> (at 266 nm), or H<sub>2</sub>O dissociated by a flash lamp (165-185 nm). OH was probed by exciting it at 281.9 nm from a pulsed tunable dye laser and collecting the resultant fluorescence with a photomultiplier mounted orthogonally to both laser beams. The delay between the two lasers was varied and thus temporal profiles of OH were obtained. The measurements were carried out under pseudo-first order conditions in OH, i.e. [HFC] >> [OH], at various concentrations of the HFCs, to obtain the second order rate coefficients. Experimental conditions, such as [OH]<sub>0</sub>, total pressure, laser fluence or lamp power, OH source, and linear gas flow rate were varied to check for possible errors. Rate coefficients were measured over a range of temperatures, typically from 243 to 373 K, and fit to Arrhenius expressions. The results obtained are summarized in Table 1. The errors listed are at the 95% confidence limit and include an estimated 5% systematic error in the determination of the HFC concentrations.

The rate coefficients for reaction of O(<sup>1</sup>D) with the HFCs were determined using the laser-photolysis / resonance fluorescence technique, described in detail in Ref. 4. Briefly, mixtures of HFC, He and ozone were flowed through a reaction cell. 248 nm laser pulses from a KrF excimer laser dissociated the ozone to give 90% O(<sup>1</sup>D) and 10% O(<sup>3</sup>P). A CW microwave-

0 0 2 8

**Table 1: Summary of rate coefficient parameters for the OH + HFC reactions determined in the present work.**

compound	A, cm <sup>3</sup> molecule <sup>-1</sup> s <sup>-1</sup>	E/R, K	ΔE/R,K	k(298), cm <sup>3</sup> molecule <sup>-1</sup> s <sup>-1</sup>	f(298)
CH <sub>3</sub> F	1.75x10 <sup>-12</sup>	1300	100	2.23x10 <sup>-14</sup>	1.17
CHF <sub>3</sub>	6.93x10 <sup>-13</sup>	2300	100	3.08x10 <sup>-16</sup>	1.09
C <sub>2</sub> H <sub>5</sub> F	2.69x10 <sup>-12</sup>	750	100	2.17x10 <sup>-13</sup>	1.13
C <sub>4</sub> H <sub>2</sub> F <sub>8</sub>	7.71x10 <sup>-13</sup>	1550	60	4.25x10 <sup>-15</sup>	1.20
C <sub>5</sub> H <sub>2</sub> F <sub>10</sub>	6.46x10 <sup>-13</sup>	1600	50	3.01x10 <sup>-15</sup>	1.12

f(298) is at the 95% confidence level.

$$f(T) = f(298) \cdot \exp[\Delta E/R \cdot (1/T - 1/298)]$$

powered resonance lamp was used to excite the O(<sup>3</sup>P) at about 130 nm, and the fluorescence was collected with a photomultiplier at right angles to both the laser and the lamp. O(<sup>3</sup>P) was formed primarily from reaction of O(<sup>1</sup>D) with ozone and quenching of O(<sup>1</sup>D) by the HFC. Analysis of the measured O(<sup>3</sup>P) profiles yielded information on the processes of interest, namely the overall rate coefficients for the loss of O(<sup>1</sup>D) due to reaction with the HFCs, and the fractions of these rate coefficients attributed to quenching of O(<sup>1</sup>D) to O(<sup>3</sup>P). From this information the rate coefficients for loss of HFC in the reaction with O(<sup>1</sup>D) (responsible for atmospheric removal of HFC) were calculated and are summarized in Table 2.

#### Atmospheric Lifetimes of the HFCs

The rate coefficients for reaction of the HFCs with OH (this work and Ref. 5), O(<sup>1</sup>D) (this work), and Cl (Ref. 6; only measured for CH<sub>3</sub>F, CH<sub>2</sub>F<sub>2</sub>, and CHF<sub>3</sub>) were incorporated into a one-dimensional photochemical model described in detail previously [7]. The model calculated the annual cycle of temperature and the O<sub>x</sub>-HO<sub>x</sub>-NO<sub>x</sub>-ClO<sub>x</sub> species concentrations from 0 to 80 km at 30° north latitude, with photolysis and reaction rate coefficients updated to Ref. 8. The OH field was normalized to obtain a 6.1-year photochemical lifetime for CH<sub>3</sub>CCl<sub>3</sub>. (Prinn [9])

0 0 2 9

**Table 2: Summary of rate coefficient parameters for the O(<sup>1</sup>D) + HFC reactions determined in the present work.**

compound	Total rate coefficient for removal of O( <sup>1</sup> D), cm <sup>3</sup> molecule <sup>-1</sup> s <sup>-1</sup>	Branching ratio for quenching	Rate coefficient for removal of HFC, cm <sup>3</sup> molecule <sup>-1</sup> s <sup>-1</sup>
CH <sub>3</sub> F	(1.65±0.15)×10 <sup>-10</sup>	0.11±0.05	(1.47±0.16)×10 <sup>-10</sup>
CH <sub>2</sub> F <sub>2</sub>	(5.13±0.33)×10 <sup>-11</sup>	0.70±0.11	(1.54±0.57)×10 <sup>-11</sup>
CHF <sub>3</sub>	(9.76±0.60)×10 <sup>-12</sup>	1.02±0.03	≤1×10 <sup>-13</sup>
C <sub>2</sub> H <sub>5</sub> F	(2.61±0.40)×10 <sup>-10</sup>	0.18±0.05	(2.14±0.35)×10 <sup>-10</sup>
C <sub>4</sub> H <sub>2</sub> F <sub>8</sub>	(1.76±0.25)×10 <sup>-11</sup>	0.97±0.09	≤2.5×10 <sup>-12</sup>
C <sub>5</sub> H <sub>2</sub> F <sub>10</sub>	(2.06±0.06)×10 <sup>-10</sup>	0.91±0.04	≤3×10 <sup>-11</sup>

deduced a total atmospheric lifetime of 5.7 years, which includes a contribution due to ocean hydrolysis corresponding to a lifetime of 85 years). The calculated lifetimes are summarized in Table 3.

The assumptions upon which the model is based are valid only for compounds with atmospheric lifetimes between 2 years (the time scale for interhemispheric mixing) and a few hundred years. Also, molecules like C<sub>2</sub>H<sub>5</sub>F will not attain a uniform spatial distribution in the troposphere, and hence our calculated lifetime is only approximate.

The results of the calculations indicate that by far the dominant removal process (≥98% of the total loss) is reaction with OH in the troposphere. Even in the stratosphere, reactions with O(<sup>1</sup>D) and Cl typically play only minor roles.

**Table 3: Atmospheric lifetimes and annually averaged fractional losses in the atmosphere due to OH, O(<sup>1</sup>D), and Cl calculated using the 1-dimensional model.**

compound	atmospheric lifetime	loss due to OH	loss due to O( <sup>1</sup> D)	loss due to Cl
CH <sub>3</sub> F	3 years	0.99	3.0×10 <sup>-3</sup>	7.8×10 <sup>-3</sup>
CH <sub>2</sub> F <sub>2</sub>	6 years	1.00	1.4×10 <sup>-3</sup>	2.0×10 <sup>-3</sup>
CHF <sub>3</sub>	270 years	1.00	7.3×10 <sup>-4</sup>	4.1×10 <sup>-4</sup>
C <sub>2</sub> H <sub>5</sub> F	90 days	1.00	5.1×10 <sup>-5</sup>	-
C <sub>4</sub> H <sub>2</sub> F <sub>8</sub>	16 years	1.00	9.0×10 <sup>-4</sup>	-
C <sub>5</sub> H <sub>2</sub> F <sub>10</sub>	23 years	0.98	1.5×10 <sup>-2</sup>	-

## References

- [1] Sandorfy, C. *Atmos. Env.* **1976**, *10*, 343, and Refs. therein.
- [2] Schmoltner, A. M.; Talukdar, R. K.; Warren, R. F.; Mellouki, W.; Goldfarb, L.; Gierczak, T.; McKeen, S. A.; Ravishankara, A. R. *J. Phys. Chem.*, submitted, 1993
- [3] Vaghjiani, G. L.; Ravishankara, A. R. *J. Phys. Chem.* **1989**, *93*, 1948.
- [4] Warren, R.; Gierczak, T.; Ravishankara, A. R. *Chem. Phys. Lett.* **1991**, *183*, 403.
- [5] Talukdar, R.; Mellouki, A.; Gierczak, T.; Burkholder, J. B.; McKeen, S. A.; Ravishankara, A. R. *J. Phys. Chem.* **1991**, *95*, 5815.
- [6] Thompson, J. E. Master's thesis, University of Colorado, Boulder, 1993.
- [7] Orlando, J. J.; Burkholder, J. B.; McKeen, S. A.; Ravishankara, A. R. *J. Geophys. Res.* **1991**, *96*, 5013.
- [8] DeMore, W. B.; Sander, S. P.; Golden, D. M.; Hampson, R. F.; Kurylo, M. J.; Howard, C. J.; Ravishankara, A. R.; Kolb, C. E.; Molina, M. J. *Chemical Kinetics and Photochemical Data for Use in Stratospheric Modeling*, Evaluation No. 10, JPL Publication 92-20, 1992.
- [9] Prinn, R.; Cunnold, D.; Simmonds, P.; Alyea, F.; Boldi, R.; Crawford, A.; Fraser, P.; Gutzler, D.; Hartley, D.; Rosen, R.; Rasmussen, R. *J. Geophys. Res.* **1992**, *97*, 2445.

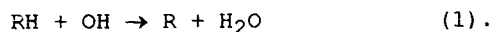
**Laboratory studies of some halogenated hydrocarbons:  
measurements of rates of reaction with OH and comments on  
interferences in OH kinetics.**

C.E.Canosa-Mas, R.K.Connell, D.J.Kinnison,  
C.J.Percival, and R.P.Wayne.

Physical Chemistry Laboratory, South Parks Road,  
Oxford, England, OX1 3QZ.

**1. Introduction.**

The hydroxyl radical, OH, is the primary initiator of hydrocarbon oxidation in the troposphere. Compounds containing hydrogen are likely to be attacked by OH



Knowledge of the rate coefficient for the reaction of OH with hydrocarbons, hydrofluorochlorocarbons (HCFCs), and hydrofluorocarbons (HFCs) is important. The results determined from kinetic measurements are used in evaluating the lifetimes of the HCFCs and HFCs in the atmosphere and in atmospheric models as well. Discrepancies in rate constant determinations are a cause for concern. Whilst a rogue value can be eliminated by an evaluation panel, the origin of the discrepancies is one of our goals.

We have determined rate constants for the reaction of OH with several HCFCs/HFCs in a newly constructed discharge-flow resonance fluorescence system. Wayne *et al.* [1] have considered three possible sources of interferences in the determination of OH rate constants: i) impurities; ii) secondary reactions involving OH; and iii) heterogeneous (surface) reactions.

Previous measurements made in our laboratory [2] on a different system for reactions of OH with HCFCs and HFCs agree with other research groups for some compounds and disagree for other compounds.

Wayne et al.[1] have shown that impurities and secondary reactions are unlikely to be the source of the interferences in the reaction of OH with  $\text{CH}_3\text{CFCl}_2$  (HCFC-141b) in their system. We have found that the impurity levels for unsaturated species in HCFC/HFC samples barely exceed 100 ppm. Zhang et al.[3] have redetermined the rate constant for the reaction of OH with HCFC-141b and their study shows that impurities do not contribute to the rate constant in their system either. Our attention has been focused on the nature of the surface of the flow tube. Surface effects have been reported by various research groups, for example in the reaction of OH with dimethylsulphide[4-6], the reaction of OH with ketene[7], and in general by Wayne et al.[1] and Howard[8].

## 2. Experimental

A discharge-flow resonance fluorescence system was used to make the kinetic measurements. The flow tube (100 cm in length and 3.4 cm i.d.) was fabricated from stainless steel and was internally lined with PTFE. Seven injectors were equally spaced 10 cm apart starting from the centre of the detection cell. The OH radical was generated by passing  $\text{H}_2$  diluted in helium through a microwave discharge upstream and mixing it with  $\text{NO}_2$  diluted in helium. Hydroxyl radical concentrations were measured by irradiating with light from an OH discharge lamp and detecting the resonance fluorescence orthogonally by an EMI 9597 QA photomultiplier with an interference filter (308 nm) and honeycomb fitted before the front window of the PMT. The signal from the PMT was processed by an EMI amplifier/discriminator and was passed into a rate meter and then to a chart recorder.

An Edwards E1M80 backing pump connected to a Roots blower provided the necessary pumping for the flow tube. A calibrated flow meter (Jencons RS3) was used in all experiments for the main helium flow (BOC commercial grade), and calibrated mass flow controllers (Tylan FC-260) were used for all other flows.

Linear flow velocities ranged from 5 to 15  $\text{ms}^{-1}$  and the flow tube pressure, typically 2-5 torr, was measured by a capacitance manometer (MKS Baratron).

The concentration of OH used in experiments was  $(5-10) \times 10^{10}$  molecule  $\text{cm}^{-3}$  and the concentration of the co-reactant used in experiments was roughly  $(1-20) \times 10^{14}$  molecule  $\text{cm}^{-3}$ , giving  $[\text{co-reactant}]/[\text{OH}] = 1000-20,000$  and hence allowing the use of pseudo-first order conditions. Experiments at elevated temperatures were performed by heating the flow tube with a Hotfoil G4 heating tape controlled by a Cal 9900 temperature controller. Experiments at sub-ambient temperatures were carried out by encasing the flow tube in a cold box in which solid carbon dioxide was placed. The temperature was monitored by six evenly spaced thermocouples along the flow tube and kept constant by gently heating the tube to the required temperature. Sub-ambient temperatures were maintained for up to two hours.

### 3. Results and discussion

The kinetics were performed in our system by normalizing the OH concentration,  $[\text{OH}]_t$ , to fluorescence signals,  $[\text{OH}]_0$  when no co-reactant was present. It was assumed that the OH concentrations were proportional to the fluorescence intensities. We extracted the pseudo first order rate constant,  $k'$ , from  $\ln[\text{OH}]_0/\ln[\text{OH}]_t = k't$ , where  $k' = k[\text{co-reactant}]$  and  $k$  is the second-order rate constant for the reaction. A summary of rate constants measured at room temperature is shown in table 1. A typical second-order plot is shown in figure 1, for the reaction of OH with  $\text{CH}_3\text{CHF}_2$  (HFC-152a). A straight line is obtained which passes through the origin. A similar case is shown in figure 2 but with the experimental point at the origin omitted to demonstrate that the line in fact passes through the origin without that point being included in the linear regression analysis. However, good behaviour of this kind is not always observed, as shown in figure 3 for the reaction of OH with  $\text{CH}_3\text{CFCl}_2$  (HCFC-141b); a positive intercept is clearly apparent. The intercept lies outside the 95% confidence error limits. Forcing the gradient through the origin yields a rate coefficient a factor of two larger than the recommended value.

The assumption that the rate constant for wall loss of OH,  $k_w$ , is constant throughout the experiment, as the co-reactant concentration is

changed, may not be valid. We have observed an interesting phenomenon with our co-workers in Germany. Figure 4 shows a second-order plot for the reaction of OH with methylvinylloxirane using a discharge-flow-mass-spectrometer system described previously[9]. The important difference compared with the apparatus used in Oxford is that the OH radical was injected through a moveable inlet and the flow tube was coated with halocarbon wax. The observed loss of OH, and hence  $k'$ , is much greater than expected at low concentrations of co-reactant and  $k'$  does not increase linearly with [co-reactant]; at higher concentrations, the plot becomes linear. The intercepts are very high for reactions of OH with epoxides, of the order  $300 \text{ s}^{-1}$  to  $600 \text{ s}^{-1}$ . In systems where OH is injected through a moveable inlet, it is often assumed that the intercept in the second-order plot is the rate constant for the wall loss. However, this assumption can only be valid if  $k_w$  is not a function of the co-reactant concentration. Measurements of the OH as a function of distance along the flow tube in the absence of co-reactant show that  $k_w$  is less than  $30 \text{ s}^{-1}$  for halocarbon wax, Teflon(PTFE), phosphoric acid, and boric acid surfaces used in discharge-flow OH kinetics. The abnormally high intercept of the linear portion of the second-order plot thus suggests that the surface activity is modified by the presence of the co-reactant. One simple approach to this problem is to postulate the existence of just two types of wall site, one appropriate to the "clean" surface when no reactant is present, and the other occupied by the reactant. If the fraction of covered sites is  $\theta$ , the expression for  $k'$  now becomes

$$k' = k[\text{co-reactant}] + \{\theta k_w^\infty + (1-\theta)k_w^0\}$$

$k_w^\infty$  is the rate constant for wall loss of OH when the surface is completely covered by the co-reactant and  $k_w^0$  is the rate constant for wall loss of OH in the absence of co-reactant (i.e. ca.  $30 \text{ s}^{-1}$ ). If we assume that the adsorption of the co-reactant on the flow tube wall can be described by Langmuir's isotherm[10], then it follows that  $\theta = K[\text{RH}] / (1 + K[\text{RH}])$  where  $K$  is the Langmuir constant and  $[\text{RH}]$  is the co-reactant concentration.

$$k' = k[\text{RH}] + \{(k_w^\infty - k_w^0)K[\text{RH}] / (1 + K[\text{RH}])\} + k_w^0$$

At high concentrations of co-reactant,  $k'$  therefore reduces to  $k[\text{RH}] + k_w^\infty$ ; when no co-reactant is added,  $k' = k_w^0$ .

It must be stressed that the quantity  $k'$  defined here is measured only in experiments such as those in which the OH is admitted into the flow tube through a sliding injector. In collaboration with our co-workers in Germany, data for the reaction of OH with methylvinylloxirane have been fitted to a function based on the form just derived. The rate constant for the reaction of OH with methylvinylloxirane is three orders of magnitude larger than the rate constant for the reaction of OH + HCFC-141b. The adsorption of HCFC-141b seems less severe than that of methylvinylloxirane, and the technique used in Oxford would not reveal an adsorption of HCFC-141b so obviously as in the methylvinylloxirane case. We believe that some adsorption of HCFC-141b may still occur in our system with the Teflon lined tube, but the effect on the kinetics appears much less pronounced. The adsorption of material on the flow tube wall is dependent on the nature of the surface (i.e. the coating).

Our results shown in table 1 are in good agreement with the values recommended by NASA[11] and IUPAC[12] evaluation panels. Experiments will be conducted employing a selection surfaces to elucidate further the rôle played by adsorption in interfering with kinetic measurements in systems containing the hydroxyl radical.

#### **Acknowledgements.**

DJK kindly thanks Dr R.N.Schindler and Mr T.Jungkamp for the use of their data and the Department of the Environment for the supply of compounds and for the support of a CASE studentship awarded by SERC.

#### **4. References.**

1. Wayne R.P, Canosa-Mas C.E, Heard A.C, and Parr A.D. Atmos. Environ. 26A, 13, (1992) 2371-2379.
2. Brown A.C, Canosa-Mas C.E, Parr A.D, and Wayne R.P Atmos.Envir. Vol 24A, 9, (1990) 2499
3. Zhang Z, Huie R.E, and Kurylo M.J. J.Phys Chem. 96, (1992)1533-1535

4. Abbat J.P.D, Fenter F.F, and Anderson J.G.  
J.Phys.Chem. 96, 4, (1992) 1780
5. MacLeod H, LeBras G, and Poulet G.  
J.Chim. Phys. 80, (1983) 287
6. Hsu Y.C, Chen D.S, and Lee Y.P.  
Int.J.Chem.Kinet. 19, (1987) 1073.
7. Oehlers C, Temps F, Wagner H.Gg, and Wolf M.  
Ber. Bunsenges. Phys. Chem.96, 2 (1992) 171.
- 8.Howard C.J. J.Phys Chem 83,1 (1979) 3
9. Schonle G, Rahman M.M, and Schindler R.N.  
Ber. Bunseges.Phys Chem. 91, (1987) 66-75.
10. Atkins P.W. Physical chemistry 3ed.(1986) 777.
11. NASA Panel for data evaluation. Chemical kinetics and photochemical data for use in stratospheric modelling. JPL 92-1 (1992) Evaluation no.10.
12. Atkinson R, Baulch D.L, Cox R.A, Hampson R.F, Kerr J.A, and Troe J.  
IUPAC subcommittee on gas kinetic data evaluation for atmospheric chemistry. Atmos. Environ 26A, 7, (1992) 1187-1230.

Table 1. A summary of the rate constants determined in our system for the reaction of HCFC/HFC with OH at room temperature.

Compound	HCFC/HFC identification	k cm <sup>3</sup> molecule <sup>-1</sup> s <sup>-1</sup>
CH <sub>3</sub> CFCl <sub>2</sub>	HCFC-141b	(5.4±1.6)×10 <sup>-15</sup>
CH <sub>3</sub> CF <sub>2</sub> Cl	HCFC-142b	(2.2±0.3)×10 <sup>-15</sup>
CH <sub>3</sub> CHF <sub>2</sub>	HCFC-152a	(3.3±0.2)×10 <sup>-14</sup>
CHCl <sub>2</sub> CF <sub>3</sub>	HCFC-123	(3.1±0.2)×10 <sup>-14</sup>
CH <sub>3</sub> CCl <sub>3</sub>	HCFC-140	(1.0±0.2)×10 <sup>-14</sup>
CCl <sub>3</sub> CHO	CHLORAL	(1.3±0.2)×10 <sup>-12</sup>
CH <sub>3</sub> CFCl <sub>2</sub>	HCFC-141b	A = 4.8×10 <sup>-13</sup> E <sub>a</sub> /R =1327±220 K <sup>-1</sup>

0 0 3 3

Figure 1. A second-order plot for the reaction of OH with  $\text{CHCl}_2\text{CF}_3$  (HCFC-123).

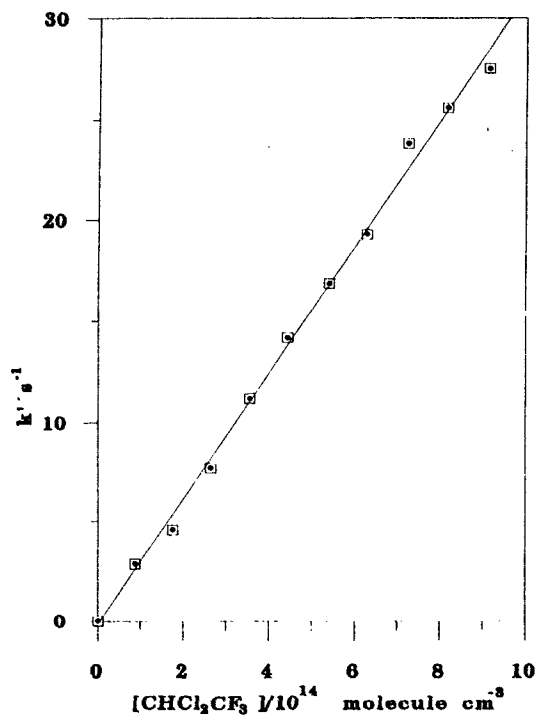


Figure 2. A second-order plot for the reaction of OH with  $\text{CH}_3\text{CHF}_2$  (HCFC-152a).

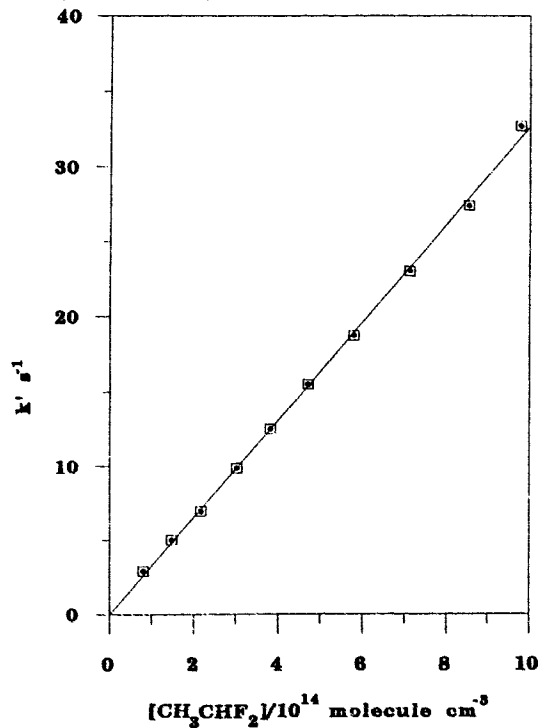


Figure 3. A comparison of data of Brown et al to this work for the reaction of OH with HCFC-141b at room temperature.

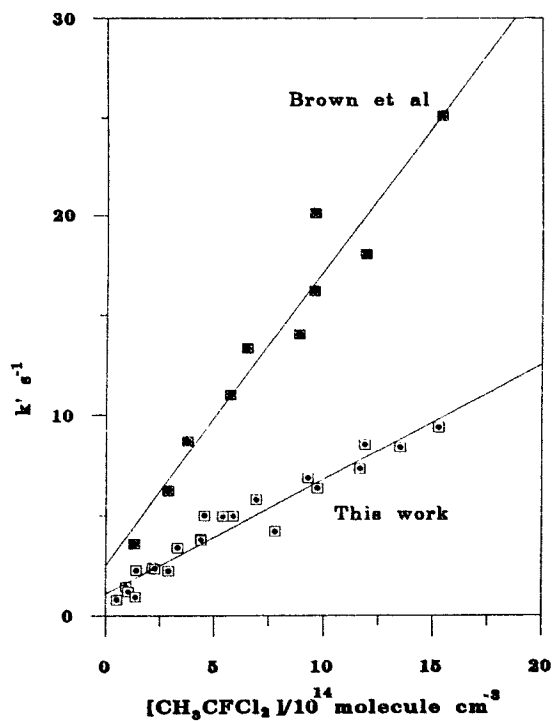
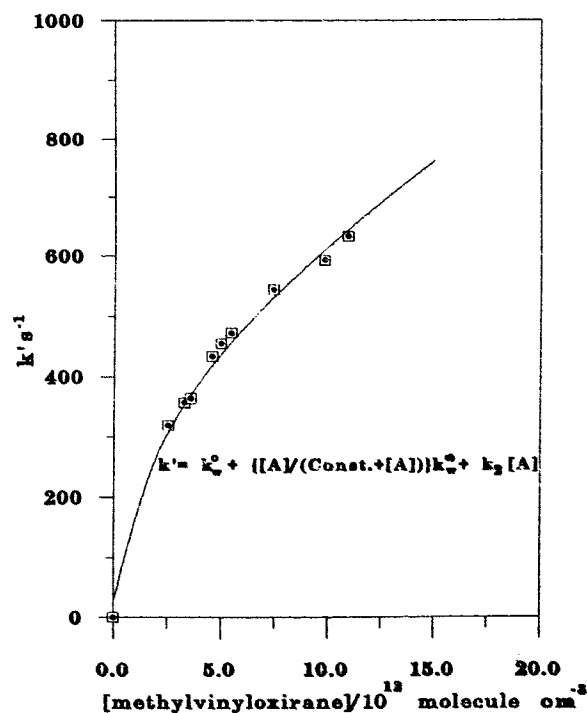


Figure 4. A second-order plot for the reaction of OH with methylvinylloxirane showing the curved character of the plot.



0038

Gas Phase Reaction Rate Studies and  
Gas and Liquid Phase Absorption Cross-Section Measurements  
for CFC Alternatives

M. J. Kurylo, R. E. Huie, Z. Zhang, R. D. Saini,  
S. Padmaja, R. Liu, A. Fahr, W. Braun, and E. P. Hunter

Chemical Kinetics and Thermodynamics Division  
National Institute of Standards and Technology  
Gaithersburg, MD 20899 USA

### Introduction

Because of scientific evidence that has identified atmospheric chlorine and bromine (and their associated oxides, ClO and BrO) as the principal catalytic agents for the destruction of stratospheric ozone in the polar regions and as strong contributors to ozone loss at mid-latitudes [1], international environmental legislation has established phaseout deadlines for chlorofluorocarbons (CFCs) as well as other halogenated compounds. Thus, the environmental and technological acceptability of suitable industrial alternatives to the banned chemicals have become the subjects of considerable research activity.

Critical to an assessment of the environmental acceptability of CFC alternatives is a detailed understanding of the atmospheric degradation of such compounds. Our research focuses on two areas of investigation (chemical reactivity and photolysis) that, to a large extent, control atmospheric degradation mechanisms. In the troposphere, the atmospheric lifetimes of most chemicals are governed primarily by their rates of reaction with OH radicals and, to a lesser degree, by solar photolysis. However, in the stratosphere, ultraviolet photolysis can play a very important role in defining a chemical's atmospheric lifetime and also specifies the amount and altitude of release of chlorine (important in quantifying ozone depletion potentials).

Over the past several years, researchers in our laboratories have been conducting a comprehensive program of investigation on the reactivities of a large number of atmospheric trace gases and proposed CFC alternatives with respect to the OH radical. The relatively low reactivity of some of these chemicals (having OH rate constants in the  $10^{-15}$  cm<sup>3</sup> molecule<sup>-1</sup> s<sup>-1</sup> range) coupled with the need for very precise and accurate rate constant determinations has required increased sample purification and measurement sensitivity. More recently, we have begun to focus on the determination of UV absorption cross-sections for CFC alternates using both gas phase and liquid phase measurements. These new studies have quantitatively characterized the roles of sample/window absorption and scattered light in our experiments and permit extension of the measurements to longer wavelengths where the absorption cross-sections are quite small and are often are subject to large uncertainties as evidenced by differences in values reported in the literature. This paper summarizes our completed and ongoing OH reaction studies with CFC alternatives and a few other related atmospheric trace gases using an improved version of the flash photolysis resonance fluorescence technique that was developed in our laboratories nearly 25 years ago. These studies have sought to minimize the unwanted effects due to reactive impurities as well as secondary reactions associated with primary reaction and/or photolysis products. Similarly, an update on recent UV absorption cross-section measurements is presented, highlighting our recently developed methodology of using liquid phase results to extend the gas phase measurements to regions of extremely low absorptivity.

## Experimental

**Rate Constant Measurements:** The flash photolysis resonance fluorescence technique was employed for all OH reaction rate studies as described in earlier publications from our laboratory.[2,3] A double-walled, thermally controlled Pyrex reaction cell (100 cm<sup>3</sup> volume) reaction cell was used in a "slow flow" mode. Reaction mixtures were generated and used in two different manners. First, they could be prepared manometrically in glass storage bulbs and slowly flowed through the cell at total pressures between 5 and 200 Torr (1 Torr  $\approx$  0.133 kPa) at a typical flow rate of 0.36 cm<sup>3</sup> s<sup>-1</sup>. Alternatively, they could be prepared just upstream from the cell by the confluence of separate flows of organic reactant, OH photolytic precursor, and inert diluent gas. OH radicals were typically produced by the flash photolysis ( $\lambda \geq 165$  nm) of 0.1-0.2 Torr of H<sub>2</sub>O and monitored over several reaction e-folding times following the flash by their resonance fluorescence at 308 nm ( $A^2\Sigma^+ \rightarrow X^2\Pi$ , 0-0 band). The latter was excited by a microwave-powered cw OH resonance lamp ( $\sim$ 1 Torr of He saturated with water vapor) and monitored at right angles to both the flash and resonance lamps through an interference filter. Both specially fabricated N<sub>2</sub> or commercially available Xe flash lamps were employed for the OH production, the latter type providing a faster repetition rate and better flux reproducibility. The fluorescence decay (directly proportional to the OH concentration at the low concentrations generated) was recorded on a microcomputer based multi-channel scaler as a summation of multiple flash photolysis experiments. These OH decay curves were then analyzed using a weighted linear least squares routine ( $\ln(\text{fluorescence signal})$  vs. time) to derive the first order decay rates. Several such determinations were made for each set of experimental conditions. In all cases, the hydrocarbon reactant was in great excess over the OH concentration ( $10^{10}$  -  $10^{11}$  molecules cm<sup>-3</sup>) so that first order kinetic behavior applied to the OH radical disappearance and the decays were extremely well represented by an exponential fit. Thus, first order decay rates were determined over a range of reactant concentration (at each temperature in temperature dependent studies) and the second order rate constants were derived from weighted linear least squares plots of the decay rate vs. concentration data. The reactant cell temperature was controlled by the passage of appropriate heating or cooling fluids between the walls of the vessel.

**UV Cross-Section Measurements:** The spectrometer system used for the gas phase measurements has been described previously.[4,5] It consists of a 1 m normal incidence vacuum monochromator employing a 600 lines/mm grating blazed at 150 nm and provided with a 20 cm cell. Interchangeable vacuum UV and UV photomultipliers, analog to digital circuitry, computer-controlled wavelength stepping motor drive, and computerized data acquisition complete the experimental arrangement. Data for diffuse absorbers such as those discussed here only required measurements every 0.2 nm and a precision (as determined from measurement repeatability) was approximately 2%. For the liquid phase measurements, a dual-beam Cary 219 spectrophotometer was employed along with three pairs of precision cells (0.01, 1.0, and 5.0 cm in length). Wavelength accuracy was verified using the 279.3 nm and 287.6 nm lines of a holmium oxide glass filter and the precision of the liquid phase measurements was determined from a comparison of absorption cross-sections obtained at a given wavelength using the various cells.

In most cases, hydrocarbon samples were obtained as special preparations from industrial or other research labs. The purity of such samples were verified using gas chromatography and gas chromatography / mass spectrometry. When necessary, repurification was performed by vacuum distillation techniques. Ultra high purity inert diluent gases were used from commercial suppliers.

## Results and Discussion

**OH Rate Constants:** The results of our past few years of research on the chemical reactivity of atmospheric trace gases and CFC alternatives towards OH are presented in Tables I and II. In cases where there are other recent studies that have taken care to exclude kinetic effects due to reactive impurities and secondary reactions, agreement with the present results are quite good. This level of agreement among the published data and recommended kinetic parameters for atmospheric modeling are detailed in the latest publication by the NASA Panel for Data Evaluation.[6] For the more recent, yet unpublished, work from our laboratory (HFC-227ea, HFC-245ca, and methane) we have only published data from other laboratories for methane with which to compare our results. Our methane rate constants compare quite favorably with those from the very recent study by Vaghjiani and Ravishankara[7], which indicate a significantly slower rate of reaction between methane and OH in the atmosphere and are the basis for the latest modeling recommendations[6]. The level of agreement between the present results and those of reference [7] can be seen from Figure 1 where, despite differences in the Arrhenius parameters derived from the individual data sets, agreement between the measured values is better than 10% over the entire temperature range of measurement below 300K.

The primary utility of the kinetic data present herein is in the calculation of atmospheric lifetimes. While exact lifetime calculations are best performed using a full atmospheric photochemical model and must take into account loss mechanisms other than gas phase reaction or photolysis, an estimate of the tropospheric lifetime can be obtained by a comparison with that for methyl chloroform ( $\text{CH}_3\text{CCl}_3$ ). [8] Such a calculation assumes that the reaction with OH is the dominant tropospheric loss mechanism for both  $\text{CH}_3\text{CCl}_3$  and the compound of interest and, hence is useful only in a semi-quantitative manner to compare the relative lifetimes of species whose atmospheric photochemistries are similar. The overall atmospheric lifetime is then calculated from the sum of the reciprocals of the tropospheric lifetime and the stratospheric lifetime (estimated from modeling calculations). [1] Considering only tropospheric loss due to reaction with OH, the tropospheric lifetime for any compound can be approximated by the tropospheric lifetime of  $\text{CH}_3\text{CCl}_3$  multiplied by the ratio of rate constants (at 277K) for the reaction of OH with  $\text{CH}_3\text{CCl}_3$  and the compound of interest. A tropospheric lifetime for  $\text{CH}_3\text{CCl}_3$  of approximately 7.0 years with respect to reaction with OH can be calculated by adjusting the total lifetime of 5.7 years[9] for the estimated 85 year lifetime due to ocean loss and the 47 year lifetime calculated for stratospheric loss. [1] Thus, using a value for the rate constant for  $\text{OH} + \text{CH}_3\text{CCl}_3$  of  $6.7 \times 10^{-15}$  from reference [6] the tropospheric lifetimes of the compounds listed in Table I can be calculated.

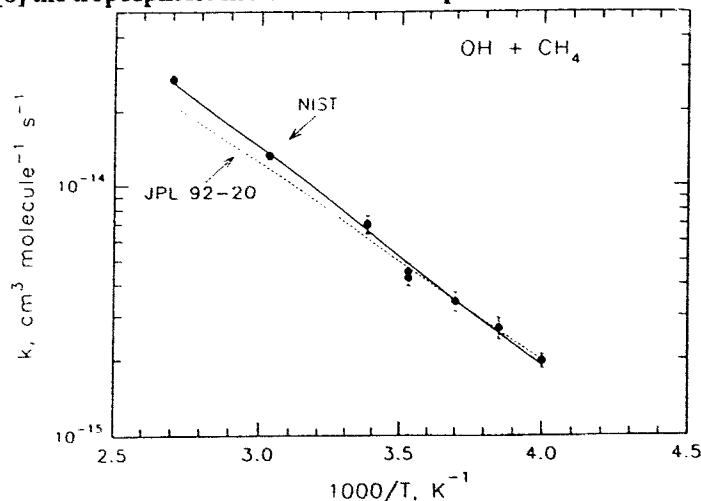


Figure 1: Arrhenius plot of our recent data for the reaction  $\text{OH} + \text{CH}_4$ . The Arrhenius fit to our data is given by the solid line. The dashed line is calculated from the Arrhenius parameters recommended in reference [6] as derived from the data of reference [7].

Table I: Rate constant summary for the reactions of OH with various atmospheric trace gases and possible CFC alternatives as a function of temperature.

Compound	A-Factor <sup>a</sup>	E/R±(ΔE/R)	k(298K) <sup>b</sup>	k(277K) <sup>b</sup>	ΔT (K)	Ref.
CH <sub>2</sub> FCF <sub>3</sub> (HFC-134a)	3.7	1990±280	0.46	0.28	270-400	[10,11]
CH <sub>3</sub> CHF <sub>2</sub> (HFC-152a)	0.96	940±130	4.1	3.2	270-400	[10]
CF <sub>3</sub> CHF <sub>2</sub> CF <sub>3</sub> (HFC-227ea)	0.37	1620±100	0.16	0.11	270-365	[12]
CHF <sub>2</sub> CF <sub>2</sub> CH <sub>2</sub> F (HFC-245ca)	2.9	1660±170	1.1	0.73	260-365	[12]
CHF <sub>2</sub> CF <sub>2</sub> CF <sub>2</sub> CHF <sub>2</sub> (HFC-338pcc)	0.78	1510±260	0.49	0.33	245-419	[13]
CF <sub>3</sub> CHFCHFCF <sub>2</sub> CF <sub>3</sub> (HFC-43-10-mee)	0.42	1400±180	0.38	0.27	250-400	[13]
CHCl <sub>2</sub> CF <sub>3</sub> (HCFC-123)	1.1	1040±140	3.4	2.6	270-400	[10]
CH <sub>3</sub> CFCl <sub>2</sub> (HCFC-141b)	1.42	1620±290	0.62	0.41	250-400	[10,11]
CH <sub>3</sub> CF <sub>2</sub> Cl (HCFC-142b)	0.98	1660±200	0.37	0.24	270-400	[10,11]
CF <sub>3</sub> CF <sub>2</sub> CHCl <sub>2</sub> (HCFC-225ca)	1.92	1290±90	2.5	1.8	270-400	[14]
CF <sub>2</sub> ClCF <sub>2</sub> CHFCI (HCFC-225cb)	0.68	1300±180	0.87	0.62	289-400	[14]
CH <sub>4</sub> (Methane)	6.3	2030±100	0.69	0.41	260-330	[12]
CH <sub>3</sub> Br (Methyl Bromide)	5.79	1560±150	3.1	2.1	250-400	[15]
CCl <sub>2</sub> CH <sub>2</sub> (1,1-Dichloroethene)	2.30	-472±105	1120	1260	240-400	[16]
cis-CHClCHCl (cis-1,2-Dichloroethene)	2.21	-65±89	275	279	240-400	[16]
trans-CHClCHCl (trans-1,2-Dichloroethene)	0.937	-283±85	242	260	240-400	[16]

a in units of 10<sup>-12</sup> cm<sup>3</sup> molecule<sup>-1</sup> s<sup>-1</sup>  
b in units of 10<sup>-14</sup> cm<sup>3</sup> molecule<sup>-1</sup> s<sup>-1</sup>

0042

Table II: Rate constant summary for the room temperature reactions of OH with various fluorinated ethers.

Compound	k(298K) <sup>a</sup>	Ref.
CF <sub>3</sub> OCH <sub>3</sub> (Trifluoromethyl Methyl Ether)	2.14	[17]
CF <sub>3</sub> OCHF <sub>2</sub> (Trifluoromethyl Difluoromethyl Ether)	0.35	[17]
CHF <sub>2</sub> OCHF <sub>2</sub> (Bis-Difluoromethyl Ether)	2.47	[17]
CF <sub>3</sub> CH <sub>2</sub> OCH <sub>3</sub> (1,1,1-Trifluoroethyl Methyl Ether)	62.4	[17]
CF <sub>3</sub> CH <sub>2</sub> OCHF <sub>2</sub> (1,1,1-Trifluoroethyl Difluoromethyl Ether)	1.23	[17]
cyclo-CF <sub>2</sub> CHF <sub>2</sub> O (1,1,2,3,3-Pentafluorooxetane)	0.25	[17]
cyclo-(CF <sub>2</sub> ) <sub>3</sub> O (Perfluorooxetane)	<0.02	[17]

<sup>a</sup> in units of 10<sup>-14</sup> cm<sup>3</sup> molecule<sup>-1</sup> s<sup>-1</sup>

**UV Absorption Cross-Sections:** Despite the significant attention that has recently been given to the determination of the cross-sections for the solar photolysis of many atmospherically important compounds, significant differences still occasionally exist between results reported in the literature, particular in regions of low absorptivity. Possible sources of measurement errors in such regions include adsorption of the compound on the optical windows, scattered light contributions, fluctuations and drift in the monitoring light intensity, and sample impurities. We have conducted systematic studies of such contributing factors in our gas phase studies. In addition, we have also adopted an alternative approach to the measurement of small cross-sections, namely the determination of the absorption cross-sections in the liquid phase and the translation of the liquid phase results into gas phase cross-sections. As described in our first publication utilizing this technique[4], the conversion can be accomplished by using a small, empirically determined wavelength shift. Using this methodology, the composite gas phase and adjusted liquid phase data for CF<sub>3</sub>CF<sub>2</sub>CHCl<sub>2</sub> (HCFC-225ca) from 170-270 nm and CF<sub>2</sub>ClCF<sub>2</sub>CHFCl (HCFC-225cb) from 170-250 nm can be represented by the equations

$$\log_{10}(\sigma_{225ca}) = -17.966 + (4.542 \times 10^{-2}X) - (2.306 \times 10^{-3}X^2) + (1.042 \times 10^{-5}X^3)$$

and

$$\log_{10}(\sigma_{225cb}) = -17.714 - (2.175 \times 10^{-2}X) - (1.484 \times 10^{-3}X^2) + (1.147 \times 10^{-5}X^3)$$

where  $\sigma$  is in units of cm<sup>2</sup> and  $X = (\lambda - 160 \text{ nm})$ .

A similar study has been conducted for HCFC-141b (CH<sub>3</sub>CFCl<sub>2</sub>) and a manuscript is in press.[18] A plot of both the gas phase and unshifted liquid phase data is shown in Figure 2. Using the overlap region between 230-240 nm to determine a wavelength shift of 3.5 nm, the gas phase data from 190-240 nm can be combined with the shifted liquid phase data from 230-260 nm to give an absorption spectrum where the cross-sections (in units of cm<sup>2</sup>) are given by

$$\log_{10}(\sigma_{141b}) = -971.66885 + 17.6328 \lambda - (12.1201 \times 10^{-2}\lambda^2) + (3.68081 \times 10^{-4}\lambda^3) - (4.18928 \times 10^{-7}\lambda^4)$$

This procedure permits a determination of small gas phase cross-sections (from the liquid phase data) in a measurement region where (as shown in the figure) the gas phase data themselves exhibit significant flare-off due to scattered light effects

Experiments have now also been performed for  $\text{CH}_3\text{CCl}_3$  (methyl chloroform) and  $\text{CF}_3\text{CHCl}_2$  (HCFC-123) and are underway for  $\text{CF}_3\text{CHFCl}$  (HCFC-124) and  $\text{CH}_3\text{CF}_2\text{Cl}$  (HCFC-142b). A temperature controlled assembly that permits the near simultaneous acquisition of both gas phase and liquid phase data has been fabricated and should permit extension of these measurements to a wide variety of compounds as a function of temperature in the near future.

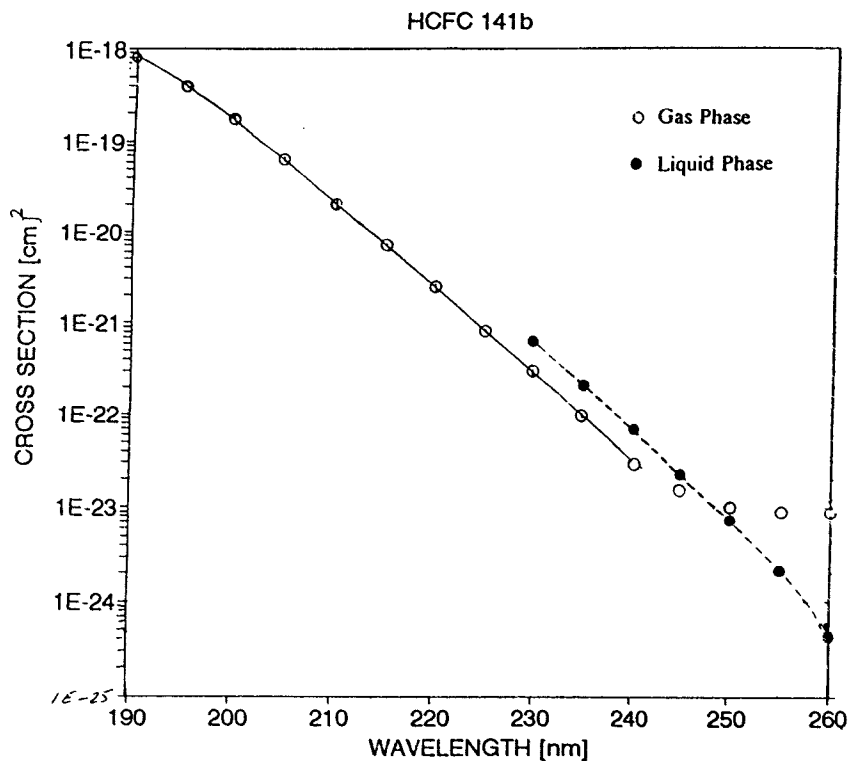


Figure 2: Gas and liquid phase absorption cross-section data for HCFC-141b ( $\text{CH}_3\text{CFCl}_2$ ). The lines drawn through the data indicate the wavelength regions over which the two data sets were used to derive the composite fit as described in the text.

#### Acknowledgment

Both the kinetics and absorption cross-section measurements were performed at the National Institute of Standards and Technology laboratories with the partial support of NASA's Upper Atmosphere Research Program.

0 0 4 4

## References

- [1] World Meteorological Organization Global Ozone Research and Monitoring Project - Report No. 25; "Scientific Assessment of Ozone Depletion: 1991".
- [2] Wallington, T. J., Neuman, D. M., and Kurylo, M. J., *Int. J. Chem. Kinetics*, **19**, (1987) 725.
- [3] Kurylo, M. J., Cornett, K. D., and Murphy, J. L., *J. Geophys. Res.*, **87** (1982) 3081.
- [4] Braun, W., Fahr, A., Klein, R., Kurylo, M. J., and Huie, R. E., *J. Geophys. Res.*, **96** (1991) 13009.
- [5] Klein, R., Braun, W., Fahr, A., Mele, A., and Okabe, H., *J. Res. Natl. Inst. Std. and Tech.*, **95** (1009) 337.
- [6] DeMore, W. B., Sander, S. P., Golden, D. M., Hampson, R. F., Kurylo, M. J., Howard, C. J., Ravishankara, A. R., Kolb, C. E., and Molina, M. J., "Chemical Kinetics and Photochemical Data for Use in Stratospheric Modeling", JPL Publication 92-20 (August 15, 1992).
- [7] Vaghjiani, G. L. and Ravishankara, A. R., *Nature*, **350** (1991) 406.
- [8] Prather, M. and Spivakovsky, C. M., *J. Geophys. Res.*, **95** (1990) 18723.
- [9] Prinn, R., Cunnold, D., Simmonds, P., Alyea, F., Boldi, R., Crawford, A., Fraser, P., Gutzler, D., Hartley, D., Rosen, R., and Rasmussen, R., *J. Geophys. Res.*, **97** (1992) 2445.
- [10] Liu, R., Huie, R. E., and Kurylo, M. J., *J. Phys. Chem.*, **94** (1990) 3247.
- [11] Zhang, Z., Huie, R. E., and Kurylo, M. J., *J. Phys. Chem.*, **96** (1992) 1533.
- [12] Unpublished results; manuscript in preparation.
- [13] Zhang, Z., Saini, R. D., Kurylo, M. J., and Huie, R. E., *Chem. Phys. Lett.*, **200** (1992) 230.
- [14] Zhang, Z., Liu, R., Huie, R. E., and Kurylo, M. J., *Geophys. Res. Lett.*, **18** (1991) 5.
- [15] Zhang, Z., Saini, R. D., Kurylo, M. J., and Huie, R. E., *Geophys. Res. Lett.*, **19** (1992) 2413.
- [16] Zhang, Z., Liu, R., Huie, R. E., and Kurylo, M. J., *J. Phys. Chem.*, **95** (1991) 194.
- [17] Zhang, Z., Saini, R. D., Kurylo, M. J., and Huie, R. E., *J. Phys. Chem.*, **23** (1992) 9301.
- [18] Fahr, A., Braun, W., and Kurylo, M. J., *J. Geophys. Res.*, in press (1993).

**A kinetic study of the OH + CCl<sub>3</sub>CHO reaction and a theoretical interpretation of the reactivity of OH with haloacetaldehydes.**

M.T. Rayez<sup>x</sup>, S. Téton<sup>+</sup>, A. Chichinin<sup>+</sup>, G. Poulet<sup>+</sup>,  
G. Le Bras<sup>+</sup>, D. Scollard<sup>\*</sup>, J. Treacy<sup>\*</sup> and H. Sidebottom<sup>\*</sup>

<sup>x</sup> Laboratoire de Physico-Chimie Théorique, URA503 - CNRS  
Université de Bordeaux I - 33405 Talence-Cedex (France).

<sup>+</sup> Laboratoire de Combustion et Systèmes Réactifs,  
CNRS - 45071 - Orléans - Cedex 2 (France).

<sup>\*</sup> Department of Chemistry,  
University College Dublin - Belfield, Dublin4 (Ireland).

**1 - Introduction :**

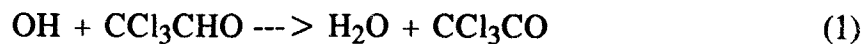
The haloacetaldehydes, CX<sub>3</sub>CHO (X = H, F and/or Cl) are intermediates in the atmospheric degradation of haloethanes CX<sub>3</sub>CH<sub>3</sub>. The CX<sub>3</sub>CHO species further degrade through photolysis or OH reaction. A knowledge of the kinetics and mechanism of these removal steps is required to estimate the atmospheric lifetimes of CX<sub>3</sub>CHO and the relative yields of the halogenated species produced. The OH + CX<sub>3</sub>CHO reaction may be particularly important since it can lead to the production of PAN-type compounds which might be sufficiently long-lived to transport chlorine into the stratosphere.

The rate constants for the reaction of OH with several chloro-fluoro acetaldehydes have been recently measured using complementary techniques (the literature results are summarized in reference 1). Agreement between the data sets is satisfactory except for the reaction OH + CCl<sub>3</sub>CHO for which a discrepancy of a factor 2 exists between the different determinations. The substantial data base now available for k (OH + CX<sub>3</sub>CHO) can be used to interpret the reactivity of OH with haloacetaldehydes using both empirical and semi-empirical methods.

The present paper reports a new determination for the rate constant of the reaction OH + CCl<sub>3</sub>CHO and also on empirical and semi-empirical calculations concerning the reactivity of OH with CX<sub>3</sub>CHO.

## 2. Kinetic study of the reaction $\text{OH} + \text{CCl}_3\text{CHO}$

The reaction of OH with  $\text{CCl}_3\text{CHO}$  :



has been studied in Orléans using the discharge flow-EPR method. The pseudo-first order kinetics of OH were monitored by gas phase EPR, in the presence of excess of  $\text{CCl}_3\text{CHO}$ . Initial concentrations of the reactants were :  $[\text{OH}]_0 = (0.4 - 2.8) \times 10^{12} \text{ cm}^{-3}$  and  $[\text{CCl}_3\text{CHO}]_0 = (0.03 - 1.79) \times 10^{14} \text{ cm}^{-3}$ . The internal wall of the flow tube was coated with halocarbon wax in order to minimize wall reactions. The pseudo-first order plot,  $-\ln[\text{OH}]/\text{dt} = k_1 [\text{CCl}_3\text{CHO}]$ , is represented in Figure 1.

The rate constant derived at 298 K is :

$$k_1 = (0.89 \pm 0.15) \times 10^{-12} \text{ cm}^3 \text{ molecule}^{-1} \text{ s}^{-1}$$

The error is two standard deviations.

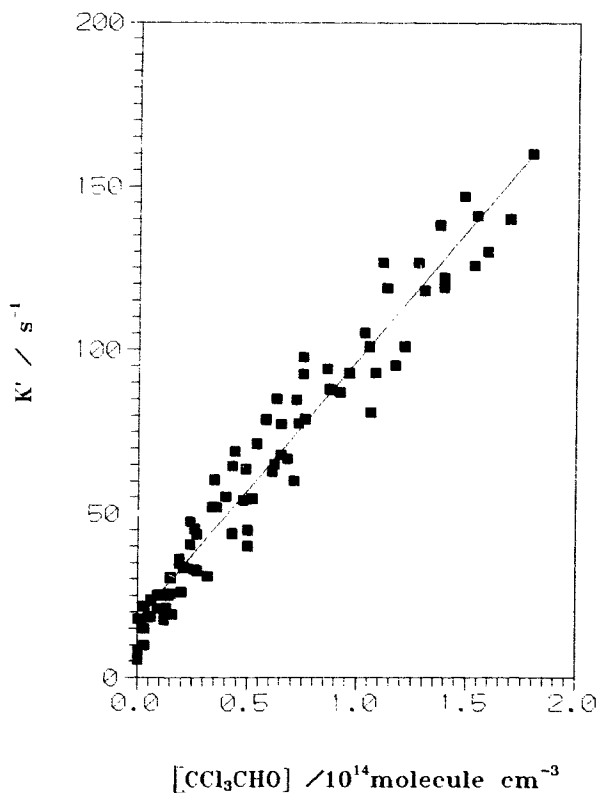


Figure 1 : Reaction  $\text{OH} + \text{CCl}_3\text{CHO}$  : pseudo-first order plot.

This value can be compared with the literature values (reported in reference 1) and the two recent determinations obtained using pulse radiolysis - UV absorption [2] and discharge flow-UV absorption techniques [3]. The values given in Table I range from  $0.86 \times 10^{-12}$  to  $2.0 \times 10^{-12} \text{ cm}^3 \text{ molecule}^{-1} \text{ s}^{-1}$ .

k ( $10^{-12} \text{ cm}^3 \text{ molecule}^{-1} \text{ s}^{-1}$ )	Technique	Reference
$1.6 \pm 0.3$	DF-RF	Dobé et al, (1989)
$\geq 1.2$	RR	Starcke et al, (1990)
$1.8 \pm 0.3$	RR	Nelson et al, (1990)
$2.0 \pm 0.2$	RR	Zabel et Becker, (1991)
$1.6 \pm 0.2$	RR	Scollard et al, (1991)
$0.86 \pm 0.09$	LP-RF	Balestra et al (1992)
$1.37 \pm 0.14$	LP-RF	Scollard et Téton, (1992)
$1.28 \pm 0.25$	DF-RF	Canosa-Mas et al, (1992)
$1.68 \pm 0.27$	PR-UV	Nielsen (1992)
$0.89 \pm 0.15$	DF-EPR	This work (1993)

Table I : Rate constant of the reaction  $\text{OH} + \text{CCl}_3\text{CHO}$  at 298 K.  
 DF-RF : discharge flow-resonance fluorescence, RR : relative rate, LP-RF : laser photolysis - resonance fluorescence, PR-UV : pulse radiolysis - UV absorption, DF-EPR : discharge flow-electron paramagnetic resonance.

The discrepancy of a factor of 2 between the rate constants is outside the reported experimental errors of the measurements. There is no evident explanation for such large variations in the data.

0 0 4 A

### 3. Theoretical interpretation of the reactivity of OH with haloacetaldehydes

The data base available for theoretical interpretation includes the rate constant values for the reactions of OH with  $\text{CH}_3\text{CHO}$ ,  $\text{CH}_2\text{ClCHO}$ ,  $\text{CHCl}_2\text{CHO}$ ,  $\text{CCl}_3\text{CHO}$ ,  $\text{CHClFCHO}$ ,  $\text{CCl}_2\text{FCHO}$ ,  $\text{CHF}_2\text{CHO}$  and  $\text{CF}_3\text{CHO}$ .

On an empirical basis, a linear relationship was found [4] between  $\ln k_{298\text{K}}$  and the electronegativity of the  $\text{CX}_3$  group in  $\text{CX}_3\text{CHO}$  (Figure 2). The electronegativity scale used was that of Huheey [5] which takes into account the bonding of  $\text{CX}_3$  to  $\text{CHO}$ .

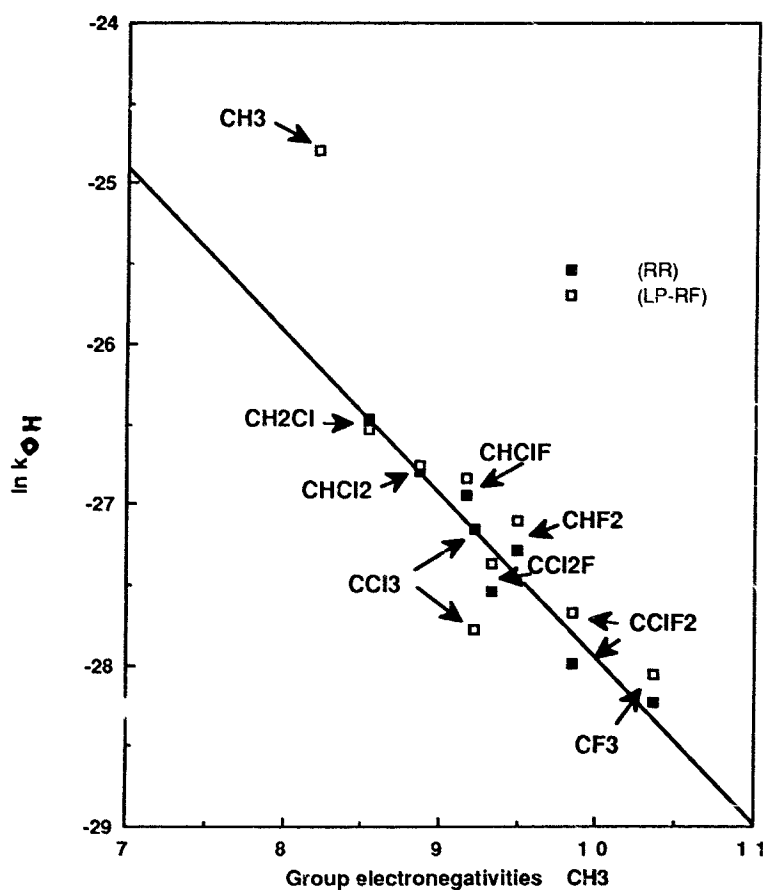


Figure 2 : Plot of  $\ln k_{\text{OH}}$  against the group electronegativities of  $\text{CX}_3$  in  $\text{CX}_3\text{CHO}$ .  $k_{\text{OH}}$  are from reference 1.

The linearity of the plot suggests that the group electronegativities represent a measure of the inductive effect of  $\text{CX}_3$  in the transition state of the

reaction. The free energy of activation for  $\text{OH} + \text{CX}_3\text{CHO}$  would therefore seem to be a strong function of the electron withdrawing effect of the substituents.

In order to further investigate the electron withdrawing effect suggested by the empirical method described above, the MNDO-PM3 [6] semi-empirical molecular orbital method has been employed to calculate the energies, geometries and net electronic charge distributions for reactants and transition states [7, 8]. Calculation of the electron densities on the aldehydic hydrogen atom shows that the net positive charge increases with the degree of halogenation of the methyl group. As expected for reaction with the electrophilic OH radical, there is a good correlation between the rate constants and the net charge on the abstracted hydrogen atom, (Figure 3).

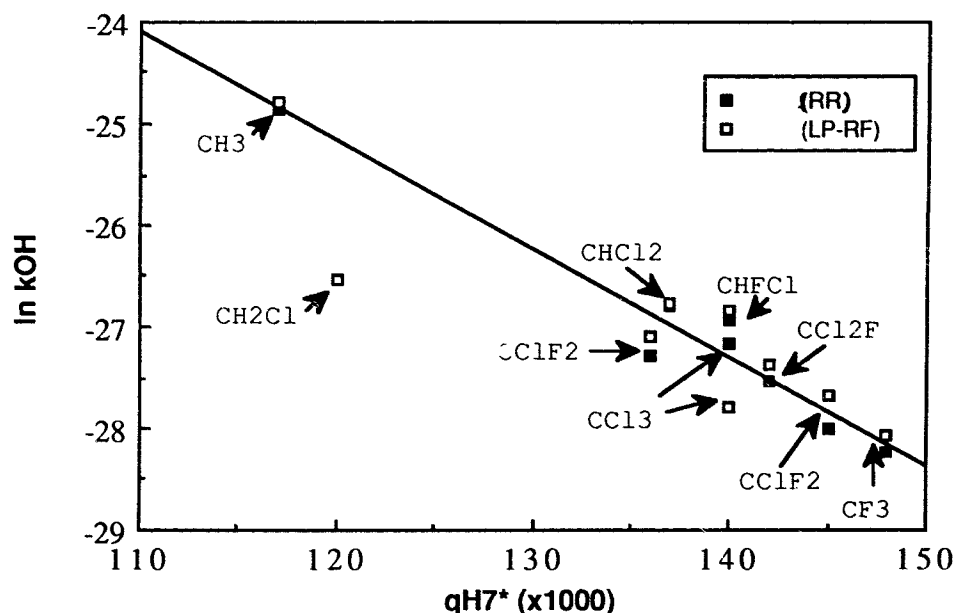


Figure 3 : Plot of  $\ln k_{\text{OH}}$  for  $\text{OH} + \text{CX}_3\text{CHO}$  reactions as a function of the net electronic charge of the H atom of the carbonyl group in the transition state.

The reaction of the OH radicals with the aldehydes are all highly exothermic and hence the transition states are expected to be reactant-like throughout the series. Our calculations confirm this suggestion since the results show that in the transition states, the aldehydic C-H bond increases by only

0 0 5 0

about 0.15 Å, whereas the incipient H-O bond of the product H<sub>2</sub>O molecule is lengthened by at least 0.4 Å relative to the equilibrium bond distance in H<sub>2</sub>O.

Calculation of the charge distributions within the transition states shows how the approach of the OH radical creates a charge displacement in both the reactant species. For the transition state, the net charges on the CX<sub>3</sub> and CO groups and on the aldehydic hydrogen atom become more positive, whereas the negative charge on the oxygen atom of the OH radical increases when compared to the reactant compounds. These changes in the electron densities decrease as the electronegativity of the CX<sub>3</sub> group increases. The polarity of the incipient bond between the aldehydic hydrogen and the oxygen atom of the OH group is hence greatest for reaction with CH<sub>3</sub>CHO and is reduced on halogenation, for example :

### CH<sub>3</sub>CHO

reactants :	10 <sup>3</sup> q :	-5	-36	40	-176	176
		CH <sub>3</sub> CO	-----	H	+	O ----- H

transition state :	10 <sup>3</sup> q :	55	-6	117	-341	176
		CH <sub>3</sub> CO	.....	H	.....	O ----- H

	10 <sup>3</sup> q	60	30	77	-165	0
--	-------------------	----	----	----	------	---

$$10^3(q_H - q_O) = 458$$

### CCl<sub>3</sub>CHO

reactants :	10 <sup>3</sup> q :	-92	12	80	-176	176
		CCl <sub>3</sub> CO	-----	H	+	O ----- H

transition state :	10 <sup>3</sup> q :	-35	22	140	-305	179
		CCl <sub>3</sub> CO	.....	H	.....	O ----- H

	10 <sup>3</sup> q	57	10	60	-129	3
--	-------------------	----	----	----	------	---

$$10^3(q_H - q_O) = 445$$

Thus the smaller the electron withdrawing effect of the  $CX_3$  group in the reactant aldehyde, the greater is the potential for charge separation between the H and O atoms of the forming H-O bond in the transition state, thereby increasing the stability of the transition state with respect to the reactants. The linearity of the free energy plot of the experimental rate constant data against the polarity of the incipient H-O bond,  $q_H - q_O$ , given in Figure 4, provides support for this conclusion.

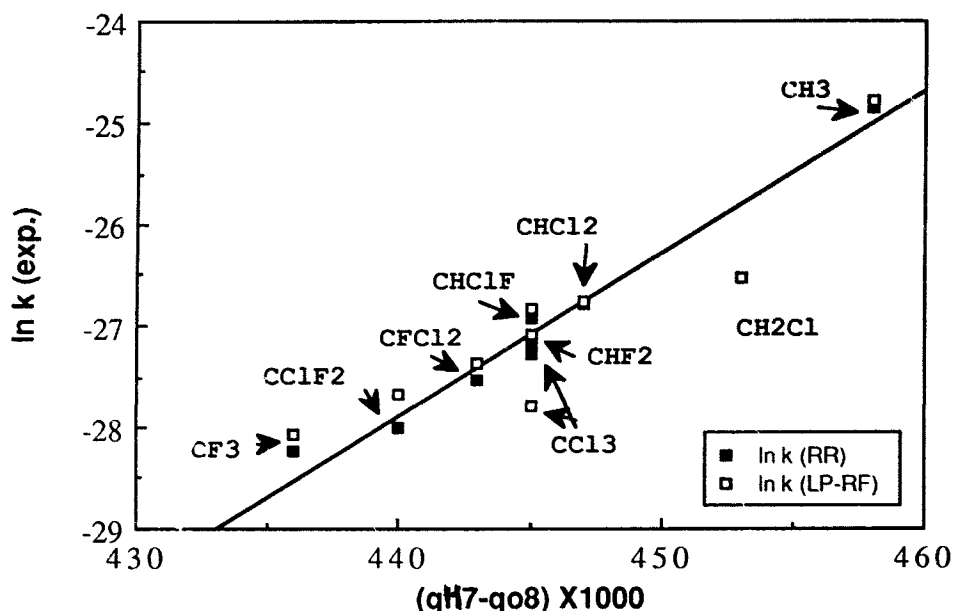


Figure 4 : Plot of  $\ln k_{OH}$  against the polarity of the incipient H-O bond.

#### Conclusions :

For the  $OH + CCl_3CHO$  reaction an uncertainty of a factor 2 still remains on the experimental determinations of the rate constant at 298 K. For the  $OH + CX_3CHO$  reactions, both empirical and quantum mechanical calculations indicate that the changes in reactivity are mainly due to inductive effects in the transition states. The experimental determinations of  $k$  ( $OH + CX_3CHO$ ) indicate that the  $OH$  reaction could compete with photolysis to remove  $CX_3CHO$  in the atmosphere. For  $CCl_3CHO$ , the lifetime towards  $OH$  reaction is of the order of the week, and the photolysis lifetime of 7 hours, assuming a photodissociation quantum yield of unity [9]. This photolysis lifetime however represents a lower limit since the quantum yield would be expected to be lower than unity. If the  $OH$  reaction significantly competes with photolysis, this can be a source of the PAN type compound,  $CCl_3C(O)O_2NO_2$ , which can be long-lived enough to transport chlorine to the stratosphere.

References :

- 1 Scollard, D.J., Treacy, J.J., Sidebottom, H.W., Balestra-Garcia, C., Laverdet, G., Le Bras, G., Mac Leod, H., and Téton, S., *J. Phys. Chem.* 97 (1993) 4683.
- 2 Nielsen, O.J., private communication.
- 3 Canosa-Mas, C.E., Kinnison, D.J., and Wayne, R.P., private communication.
- 4 Scollard, D.J., PhD thesis, Dublin 1992.
- 5 Huheey, J.E., *J. Phys. Chem.* 67 (1963) 1501.
- 6 Stewart, J.J.P., *J. Comp. Chemistry* 10, (1989) 209  
Stewart, J.J.P., *J. Comp. Chemistry* 10, (1989) 221.
- 7 Rayez, M.T., Rayez, J.C., Berces, T., and Lendvay, G., *J. Phys. Chem.* 97 (1993) 5570.
- 8 Rayez, M.T., Scollard, D.J., Treacy, J.J., Sidebottom, H.W., Balestra-Garcia, C., Téton, S., and Le Bras, G. submitted for publication.
- 9 Pirre, M., private communication.

# Rate constants for reactions of fluoro(chloro)ethylperoxy radicals with NO

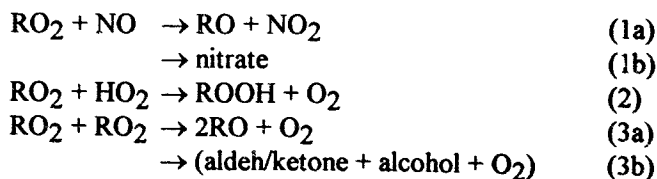
V. Pultau and J. Peeters  
K.U. Leuven, Depart. of Chemistry  
Celestijnenlaan 200F  
3001 Leuven (Heverlee)  
Belgium

## 1. Introduction

In this research concerning the alternative hydrofluoro(chloro)carbons, rate constants were measured for reactions of nitric oxide with fluoro(chloro)ethylperoxy radicals (briefly RO<sub>2</sub>) resulting from the tropospheric degradation of H(C)FC's.

In the atmosphere, the H(C)FC's will react with OH-radicals to produce an haloalkylradical which will result in a peroxyradical through subsequent reaction with O<sub>2</sub>.

Three major reaction routes are open to the peroxyradical:



In order to predict the fate of the RO<sub>2</sub>-radicals in the troposphere, the rate constants of the competing reactions above must be known.

In this work, a direct measurement was made of the rate coefficient  $k_1$ , at 290K, for RO<sub>2</sub> from HFC 134a, HFC 143a and HCFC 142b. The  $k_1$  are derived from the shape of NO<sub>2</sub>-growth profiles upon reacting the peroxyradical with an excess NO, at various NO-concentrations.

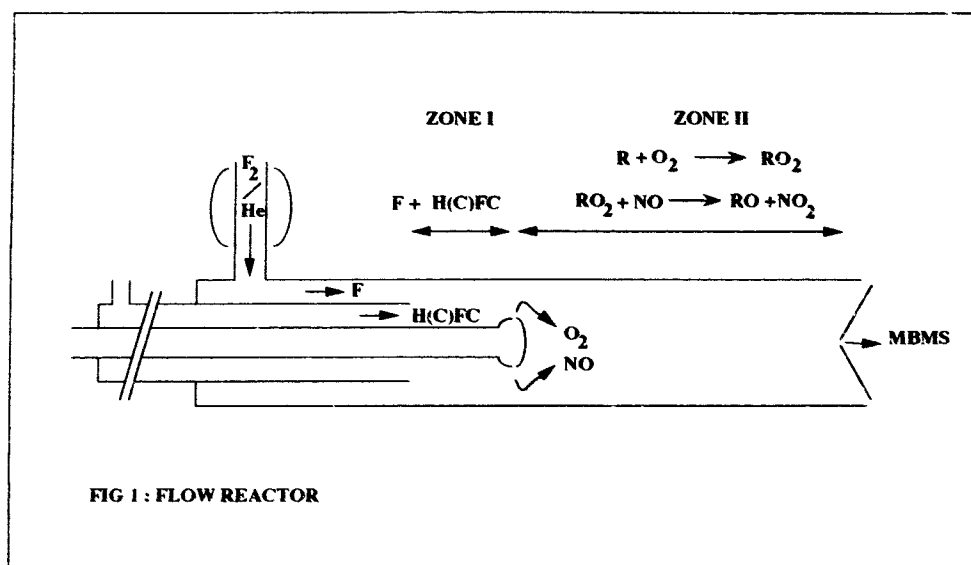
To this end, the Discharge-Flow-technique in combination with Molecular Beam Sampling Mass Spectrometry (EI) was applied.

The method was validated earlier on the basis of the known  $k(\text{CF}_3\text{O}_2 + \text{NO})$  rate constant. [1]

## 2. Experimental

The apparatus comprises a conventional fast-flow reactor and a three-stage differentially-pumped molecular beam sampling system with an Extranuclear Quadrupole Mass spectrometer housed in the last stage. The flow reactor consists of a 2,8 cm inner diameter quartz tube, with a side arm equipped with a microwave cavity, and a set of two coaxial, movable injector tubes (see fig. 1). In zone I, F-atoms, created upstream from F<sub>2</sub> in a microwave discharge (F<sub>2</sub> dissociation yield ≈98%) are converted into haloalkyl radicals through reaction with a large excess of the appropriate H(C)FC. In zone II, where a very high amount of O<sub>2</sub> and a smaller amount of NO is added, the haloalkylradicals rapidly lead to RO<sub>2</sub> which subsequently reacts with NO, yielding NO<sub>2</sub> and haloalkylnitrate. The  $i(\text{NO}_2^+)$ -versus-time profiles are

monitored by moving the two coaxial injectors together towards the sampling point, i.e. by changing the length of zone II (from 0 to 24 cm) at constant length of zone I (4cm). The rate constants of the  $RO_2 + NO$ -reactions were derived from the *shape* of the  $i(NO_2^+)(t)$  profiles at various NO-concentrations. The  $NO_2^+$ -signals are recorded at an electron energy of 40 eV or 14 eV; the lower value was chosen for the cases where H(C)FC can give rise to an  $m/e=46$  fragmentation.

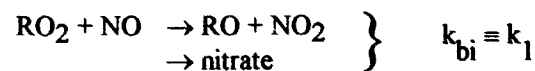


The experiments were performed at a total pressure of 2 torr (He = bath gas) at 290 K. The average flow velocity was about 1800 cm/s.

The  $RO_2$  radicals were created by reacting F-atoms ( $[F]_0 \approx 5 \cdot 10^{12}$  molec  $cm^{-3}$ ) with a large excess of H(C)FC ( $[H(C)FC] \approx 5 \cdot 10^{14}$ ), resulting in  $RO_2$  through subsequent reaction of the so formed R-radical with a large excess of  $O_2$  ( $[O_2] \approx 5 \cdot 10^{13}$ ). The concentration of NO ranges from  $10^{13}$  to  $5 \cdot 10^{13}$  molec  $cm^{-3}$ .

### 3. Data analysis

The data analysis consists of two steps. The first is an analytical approach based on a simple model, containing only:



At constant [NO], the  $NO_2$ -growth is then given by:

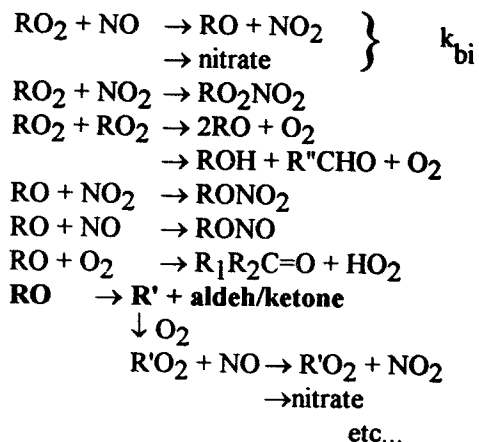
$$[NO_2] = cst(1 - e^{-kt})$$

$$k = k_{bi}[NO]$$

0 0 5 5

This simple approach gives us a first approximation of  $k$  (and  $k_1$ ) and allows one to establish the time-scale zero and to make the appropriate corrections for diffusional transport.

Secondly, in a kinetic modelling approach, the  $k_1$ -value is improved by including all side-effects that influence the  $\text{NO}_2^+$  profile shape. The extended reaction mechanism adopted thereto comprises all reactions of probable importance, i.a. secondary  $\text{NO}_2$ -formation and  $\text{NO}_2$ -removal as well as mutual reaction of  $\text{RO}_2$ ; this second step also takes into account the decrease of the  $\text{NO}$ -concentration and contribution to the  $\text{NO}_2^+$ -signal from fragment ions of nitrates and pernitrates:



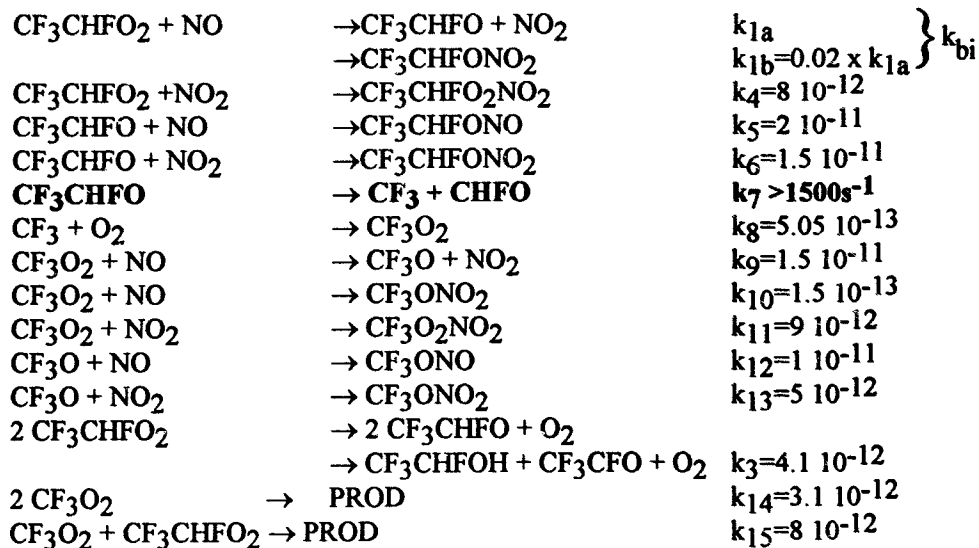
In our conditions, the reaction of  $\text{RO} + \text{O}_2$  will be slow because of the low  $\text{O}_2$  concentration. Thus the most important reaction pathways of  $\text{RO}$  will be the  $\text{RO} + \text{NO}$ -reaction or, in some cases, the thermal decomposition of  $\text{RO}$ . When  $\text{RO}$  decomposes it leads through subsequent reactions to a delayed formation of a second  $\text{NO}_2$ .

It must be emphasized that only a few of the above reactions are of importance; sensitivity analysis reveals that for each of the cases considered here the  $\text{NO}_2^+$  profile shape is determined predominantly by the rate constant  $k_1$  of the  $\text{RO}_2 + \text{NO}$  reaction. Numerical integration of the full set of kinetic equations for different "trial" values of  $k_1$ , and comparison of the generated  $\text{NO}_2^+$ -profiles with the experimental  $i(\text{NO}_2^+)$ -shape provides the best  $k_1$ -value. The computed  $\text{NO}_2^+$  signal is taken as the weighted sum of  $[\text{NO}_2]$ , [nitrates] and [pernitrates], with sensitivity ratios 1 : 3 : 1.1 at 40 eV [1]; at 14 eV, the relative sensitivities of nitrates and pernitrates w.r.t.  $\text{NO}_2$  are approximately 3 times lower. Thus, at each  $[\text{NO}]$ , a first-order  $k = k_{bi}[\text{NO}]$  is "reconstituted". The slope of the resulting  $k$  vs.  $[\text{NO}]$  plot gives  $k_{bi}$  together with its 95% confidence interval.

#### 4. Results

##### 1. $\text{CF}_3\text{CHFO}_2 + \text{NO}$ ( $\text{RO}_2$ arising from HFC 134a)

The extended model is given below; the adopted rate constants, known or estimated, are for our experimental conditions.



In this case, the main fate of the alkoxyradical,  $\text{CF}_3\text{CHFO}$  is fast decomposition to  $\text{CF}_3$  and  $\text{CHFO}$ . The evidence is three-fold: i) fairly large  $\text{CHFO}$ -signals were observed; ii) there was no significant reduction of the  $\text{CHFO}$ -signal upon increasing  $[\text{NO}]$ , which means that the  $\text{CF}_3\text{CHFO} + \text{NO}$ -reaction can only barely compete with the decomposition, iii) the final  $\text{NO}_2$ -signals at large  $[\text{NO}]$  were markedly higher than obtained for  $\text{RO}_2 = \text{CF}_3\text{O}_2$  in identical conditions. The delayed secondary  $\text{NO}_2$  formation here causes an underestimation of  $k_1$  by  $\sim 50\%$  in the simplified single-step approach. The final  $k_1 (= k_{1a} + k_{1b})$  value deduced from the full model for the  $\text{CF}_3\text{CHFO}_2 + \text{NO}$ -reaction is  $(1.56 \pm 0.45) \cdot 10^{-11} \text{ cm}^3 \text{ molec}^{-1} \text{ s}^{-1}$ ; the error indicated is  $2\sigma$ , including an estimated systematic error of 30%.

Our present result is 20% higher than the values reported by Wallington and Nielsen [7] and by Howard et al. [6].

Figure 2 shows the plot of the pseudo first order rate constant versus the  $\text{NO}$ -concentration based on the extended model.

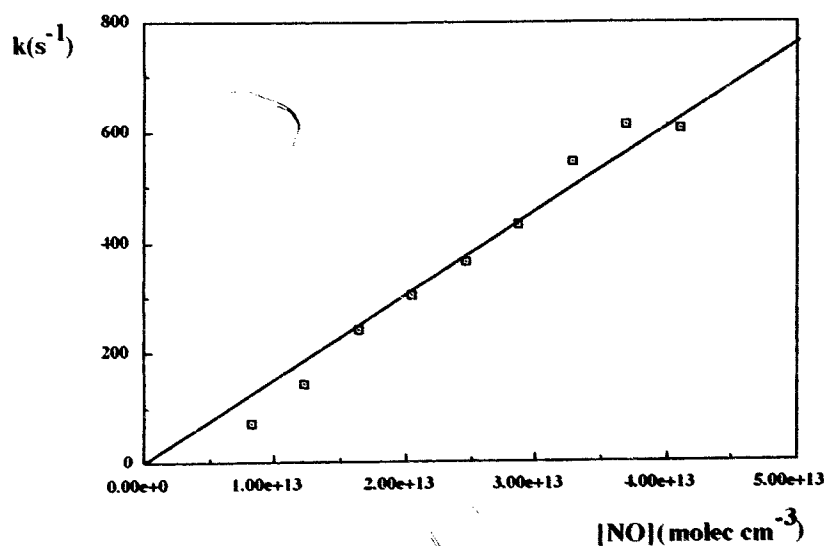


figure 2:  $k$  vs.  $[\text{NO}]$

0 0 5 7

## 2. $\text{CF}_3\text{CH}_2\text{O}_2 + \text{NO}$ ( $\text{RO}_2$ arising from HFC 143a)

In this case the extended mechanism only includes 12 reactions, because in contrast with the  $\text{CF}_3\text{CHFO}_2$  reaction, the  $\text{CF}_3\text{CH}_2\text{O}$  alkoxyradical does not decompose. Indeed, concurring with Howard et al. [6], we did not find any evidence for decomposition products and the magnitude of the measured  $\text{NO}_2$ -signals gives no indication for secondary  $\text{NO}_2$ -formation. Our findings are in keeping with the unfavourable energetics for the decomposition of  $\text{CF}_3\text{CH}_2\text{O}$  to  $\text{CF}_3$  and  $\text{CH}_2\text{O}$ . The main fate of the alkoxyradical in our case is reaction with  $\text{NO}$  to form a nitrite.

The extended modelling procedure results in a bimolecular rate constant for the  $\text{CF}_3\text{CH}_2\text{O}_2 + \text{NO}$ -reaction of  $(1.15 \pm 0.30) 10^{-11} \text{ cm}^3 \text{ molec}^{-1} \text{ s}^{-1}$ , this result is here only 30% above that of the simple, single-step model.

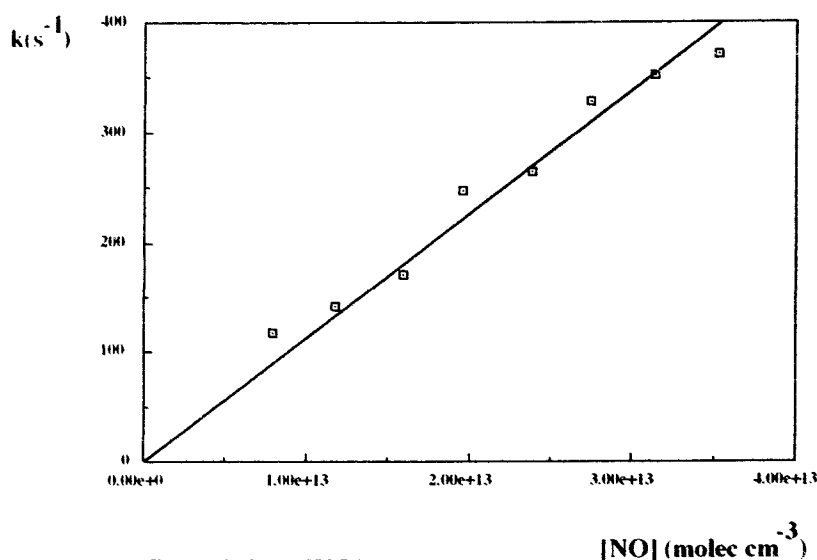


figure 3: k vs. [NO]

## 3. $\text{CF}_2\text{ClCH}_2\text{O}_2 + \text{NO}$ ( $\text{RO}_2$ arising from HCFC 142b)

Also in this case no decomposition of the alkoxyradical occurs, and the kinetics are uncomplicated, with the  $\text{NO}_2^+$ -shape determined almost uniquely by  $k_1$ . Only the mutual  $\text{RO}_2$  reaction appears to have a slight effect.

We did not complete the full analysis yet, but as usual we expect an increase in  $k$ -value of ~ 30%, which would result in a bimolecular rate constant for the  $\text{CF}_2\text{ClCH}_2\text{O}_2 + \text{NO}$ -reaction of  $\sim 1.3 10^{-11} \text{ cm}^3 \text{ molec}^{-1} \text{ s}^{-1}$

Figure 3 shows the plot of  $k$  versus the  $\text{NO}$ -concentration, for the simple model.

0 0 5 8

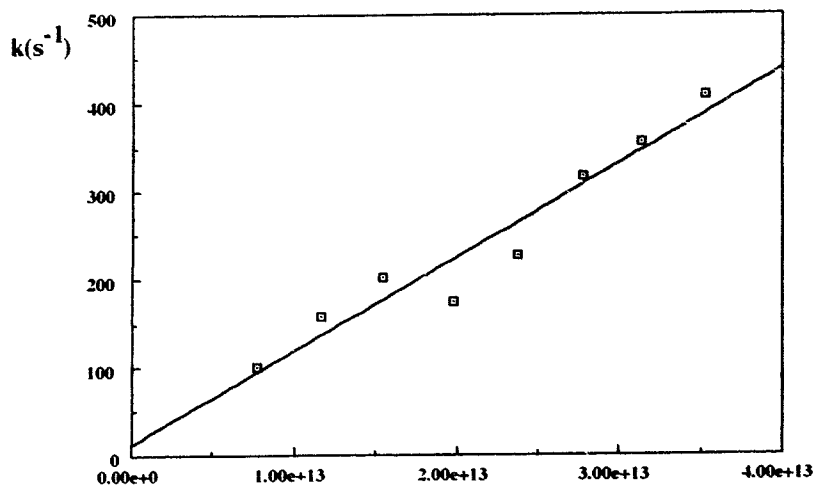


figure 4:  $k$  vs.  $[\text{NO}]$  (simple model)  $[\text{NO}]$ (molec  $\text{cm}^{-3}$ )

## 5. Conclusions

Table 1: Rate constants of  $\text{RO}_2 + \text{NO}$  reactions at 290K.

$\text{RO}_2$	rate coefficient *	reference
$\text{CF}_3\text{O}_2$	1.53	[1]
	1.78	[2]
	1.45	[3]
$\text{CCl}_3\text{O}_2$	1.86	[4]
	1.7	[3]
$\text{CFCl}_2\text{O}_2$	1.45	[3]
	1.60	[5]
$\text{CF}_2\text{ClO}_2$	1.6	[3]
$\text{CF}_3\text{CHFO}_2$	1.56	this work
$\text{CF}_3\text{CH}_2\text{O}_2$	1.3	[6]
	1.28	[7]
	1.3	[6]
$\text{CF}_3\text{CCl}_2\text{O}_2$	1.15	this work
	1.5-2.0	[8]
$\text{CF}_3\text{CF}_2\text{O}_2$	1.4	[6]
$\text{CF}_2\text{ClCH}_2\text{O}_2$		this work

\* in units of  $10^{-11} \text{ cm}^3 \text{ molec}^{-1} \text{ s}^{-1}$

The present results are listed in table 1, together with  $k(\text{RO}_2 + \text{NO})$  data for other haloalkylperoxyradicals. All data are in fairly narrow range, from 1.15 to  $2.10 \cdot 10^{-11}$

$\text{cm}^3\text{molec}^{-1}\text{s}^{-1}$ , i.e. appreciably higher than the rate constants for  $\text{CH}_3\text{O}_2 + \text{NO}$  and  $\text{C}_2\text{H}_5\text{O}_2 + \text{NO}$  (both near  $7.5 \cdot 10^{-12}$ ). A closer inspection of the results for the halogenated radicals reveals a slight trend: the reactivity towards NO increases with the number of electronegative substituents (F, Cl,  $\text{CF}_3$ ,  $\text{CF}_2\text{Cl}$ ) on the  $\alpha$ -carbon. This observation confirms earlier conclusions [1].

As regards the fate of the H(C)FC degradation products, our results strongly support earlier findings that  $\text{CF}_3\text{CHFO}$  decomposition in  $\text{CF}_3$  plus CHFO is a fast process [9,10]. On the other hand,  $\text{CF}_3\text{CH}_2\text{O}$  and  $\text{CF}_2\text{ClCH}_2\text{O}$  decompose only slowly and their major tropospheric reaction route is expected to be H-abstraction by  $\text{O}_2$ .

## 6. References

- [1] Peeters J., Vertommen J. and Langhans I.  
Ber. Bunsenges. Phys. Chem. **96**, 431, 1992
- [2] J.C. Plumb and K.R. Ryan  
Chem. Phys. Lett. **92**, 236, 1982
- [3] A.M. Dognon, F. Caralp and R. Lesclaux  
J. Chim. Phys-Chim. Biol. **82**, 349, 1985
- [4] K.R. Ryan and I.C. Plumb  
Int. J. Chem. Kin. **16**, 591, 1984
- [5] R. Lesclaux and F. Caralp  
Int. J. Chim. Kin. **16**, 1117, 1984
- [6] C.J. Howard, T.J. Bevilacqua, D.R. Hanson and N.R. Jensen  
results presented at the AFEAS-Workshop, March 1993, Dublin
- [7] T.J. Wallington and O.J. Nielsen  
Chem. Phys. Lett. **187**, 33, 1991
- [8] G.D. Hayman, M.E. Jenkin, T.P. Murrels and S.J. Shalliker  
Step-Halocside/AFEAS Workshop, Dublin 1991, p 79
- [9] R. Zellner, A. Hoffmann, D. Bingemann, V. Mors and J.P. Kohlmann  
Step-Halocside/AFEAS Workshop, Dublin 1991, p 94
- [10] M.M. Maricq and J.J. Szenté  
J. Phys. Chem. **96**, 10862, 1992

# Pulse radiolysis and FTIR studies of the atmospheric chemistry of halogenated alkyl peroxy radicals.

Ole John Nielsen, Jens Sehested, Thomas Ellerman and Timothy J. Wallington\*

Chemical Reactivity Section  
ES&T Department  
Risø National Laboratory  
DK-4000 Roskilde, Denmark

## 1. Introduction

By international agreement, industrial production of CFCs will be phased out. Hydrofluorocarbons (HFCs) are one class of potential CFC substitutes. Prior to large scale industrial use, it is important to establish the environmental impact of the release of HFCs into the atmosphere. Following release, HFCs will react with OH radicals in the lower atmosphere to produce fluorinated alkyl radicals which will, in turn, react with O<sub>2</sub> to give peroxy radicals. There is relatively little information available concerning the atmospheric fate of the fluorinated alkyl peroxy radicals.

As part of a collaborative study between Risø and Ford on the atmospheric fate of HFCs, we have conducted experimental studies of a series of HFCs: CH<sub>3</sub>F, CH<sub>2</sub>F<sub>2</sub>, CHF<sub>3</sub>, CF<sub>3</sub>CFH<sub>2</sub>, CF<sub>2</sub>HCF<sub>2</sub>H, and CF<sub>3</sub>CF<sub>2</sub>H. A pulse radiolysis technique was used to measure the UV absorption spectrum, self reaction kinetics, and the rate of reaction with NO of the peroxy radicals. The products following the self reaction of the peroxy radicals were determined using a FTIR spectrometer coupled to an atmospheric reactor. Selected results from both experimental systems will be reported.

## 2. Experimental

Two different experimental systems were used as part of the present work. A pulse radiolysis transient UV kinetic spectrometer was used to study the UV absorption spectrum and self reaction kinetics of RO<sub>2</sub> radicals, while a Fourier

---

\* permanent address: SRL-E3083, Ford Motor Company, P.O. Box 2053, Dearborn, Michigan 48121-2053, USA

transform infrared (FTIR) spectrometer was used to investigate the products following the self reaction of  $\text{RO}_2$  radicals. The experimental systems have been described in detail in previous publications [1,2] and will only be discussed briefly here.

Peroxy radicals were generated by the radiolysis of  $\text{SF}_6/\text{O}_2/\text{HFC}$  gas mixtures in a one liter stainless steel reactor with a 30 ns pulse of 2 MeV electrons from a Febetron 705B field emission accelerator.  $\text{SF}_6$  was always in great excess and was used to generate fluorine atoms:



Two sets of experiments were performed using the pulse radiolysis system. First, the ultraviolet absorption spectrum of  $\text{RO}_2$  radicals was measured by observing the maximum in the transient UV absorption at short times (10-40  $\mu\text{sec}$ ). Second, using a longer time scale (0.5-2 msec), the subsequent decay of the absorption was monitored to determine the kinetics of reaction (4):



To monitor the transient UV absorption, the output of a pulsed 150 Watt xenon arc lamp was multi-passed through the reaction cell using internal White cell optics (40 cm path-length). Reagent concentrations used were;  $\text{SF}_6$ , 948 mbar;  $\text{O}_2$ , 2 mbar; and HFC 50 mbar. All experiments were performed at  $298 \pm 2\text{K}$ . Ultra high purity  $\text{O}_2$  was supplied by L'Air Liquide,  $\text{SF}_6$  (99.9%) was supplied by Gerling and Holz and HFCs (>99%) was obtained from Fluorochem. All reagents were used as received.

The FTIR system was interfaced to a 140 liter pyrex reactor. Radicals were generated by the UV irradiation of mixtures of HFC and  $\text{Cl}_2$  in air at 700 torr total pressure at 298K using 22 blacklamps (GE-BLB-40). The loss of reactants and the formation of products were monitored by FTIR spectroscopy, using an analyzing path-length of 28 meters and a resolution of  $0.25\text{cm}^{-1}$ . Infrared spectra were derived from 128 co-added spectra. Reference spectra were acquired by expanding known volumes of a reference material into the reactor. Ultra pure synthetic air was supplied by Matheson Gas Products, and HFCs were obtained from PCR, Inc. at a stated purity of >99%.

### 3. Results

The UV spectra of  $\text{CH}_2\text{FO}_2$ ,  $\text{CHF}_2\text{O}_2$ ,  $\text{CF}_3\text{O}_2$ ,  $\text{CF}_3\text{CF}_2\text{O}_2$ ,  $\text{CF}_2\text{HCF}_2\text{O}_2$ , and  $\text{CF}_3\text{CFHO}_2$  radicals were measured using the pulse radiolysis technique. After the pulse radiolysis of HFC/ $\text{O}_2$ / $\text{SF}_6$  mixtures a rapid increase in absorption in the ultraviolet was observed, followed by a slower decay. No absorption was observed in the absence of  $\text{SF}_6$ . We ascribe the UV absorption following radiolysis of HFC/ $\text{O}_2$ / $\text{SF}_6$  mixtures to the formation of fluorinated peroxy radicals and their subsequent loss by self reaction.

To illustrate some typical data we present here detailed results for  $\text{CH}_2\text{FO}_2$  [3]. Results for  $\text{CHF}_2\text{O}_2$  [4],  $\text{CF}_3\text{O}_2$  [5],  $\text{CF}_3\text{CF}_2\text{O}_2$  [6],  $\text{CF}_2\text{HCF}_2\text{O}_2$  [7], and  $\text{CF}_3\text{CFHO}_2$  [8] radicals are available elsewhere.

Measurement of absolute absorption spectra requires calibration of the initial F atom concentration. Additionally, experimental conditions have to be chosen such that there is stoichiometric conversion of F atoms to the appropriate radical. The yield of F atoms was established by two techniques. First, by monitoring the transient absorption at 216.4 nm due to methyl radicals produced by radiolysis of  $\text{SF}_6/\text{CH}_4$  mixtures and using a value of  $4.12 \times 10^{-17} \text{ cm}^2 \text{ molecule}^{-1}$  for  $\sigma(\text{CH}_3)$  at 216.4 nm [9]. Second, by monitoring the transient absorption at 250 nm due to  $\text{CH}_3\text{O}_2$  radicals following radiolysis of  $\text{SF}_6/\text{CH}_4/\text{O}_2$  mixtures and using  $\sigma(\text{CH}_3\text{O}_2) = 3.92 \times 10^{-18} \text{ cm}^2 \text{ molecule}^{-1}$  at 250 nm [10]. Values of  $[\text{F}]_0$  derived from both methods differed by less than 10%.

To work under conditions where the F atoms are converted stoichiometrically into  $\text{CH}_2\text{FO}_2$  radicals, it is necessary to consider potential interfering secondary chemistry. Potential complications include: (ii) competition for the available F atoms by reaction with molecular oxygen;



(ii) reaction of  $\text{CH}_2\text{F}$  radicals with  $\text{CH}_2\text{FO}_2$  radicals:



and (iii) reaction of F atoms with  $\text{CH}_2\text{F}$  and/or  $\text{CH}_2\text{FO}_2$  radicals:



0 0 6 3

The rate constant for reaction (5) has been measured previously in our laboratory [11],  $k_5 = 1.4$  and  $2.0 \times 10^{-13} \text{ cm}^3 \text{ molecule}^{-1} \text{ sec}^{-1}$  at 600 and 1000 mbar of  $\text{SF}_6$  diluent, respectively. There are no literature data concerning the kinetics of reactions (6-8). Hence, we cannot calculate their importance. Instead, to check for the presence of complications in our experiments caused by unwanted radical-radical reactions, two series of experiments were performed. First, the transient absorption at 240 nm was observed in experiments using  $[\text{CH}_3\text{F}] = 10$  mbar,  $[\text{O}_2] = 40$  mbar, and  $[\text{SF}_6] = 550$  mbar with the radiolysis dose varied by over an order of magnitude. Figure 1 shows the observed maximum of the transient absorption of  $\text{CH}_2\text{FO}_2$  at 240 nm as a function of the dose. Second, the maximum in the transient absorption was measured in experiments using full dose,  $[\text{CH}_3\text{F}] = 10$  mbar,  $[\text{O}_2] = 40$  mbar with the  $\text{SF}_6$  concentration varied between 50 and 950 mbar. Figure 2 shows the maximum absorption at 240 nm plotted as a function of  $\text{SF}_6$  concentration. From Figure 1 and 2 it can be seen that, with the exception of the data obtained using full dose and  $\text{SF}_6$  concentrations greater than 600 mbar, the initial absorption was linear with both the radiolysis dose and the  $\text{SF}_6$  concentration. Under our experimental conditions, the formation of  $\text{CH}_2\text{FO}_2$  increased linearly with the initial yield of F atoms and hence reactions (6-8) are of negligible importance. For experiments employing the full radiolysis dose and  $\text{SF}_6$  concentrations greater than 600 mbar initial absorptions were 10-20% lower than expected based upon extrapolation of the data obtained at lower  $\text{SF}_6$  concentrations. This behaviour is ascribed to secondary chemistry at high F atom concentrations resulting in incomplete conversion of F into  $\text{CH}_2\text{FO}_2$ . Consequentially, the majority of our experiments were performed using  $[\text{SF}_6] < 600$  mbar.

To test for complications caused by reaction (5), experiments were performed with the  $\text{CH}_3\text{F}$  concentration varied over the range 0.8-20 mbar with all other parameters fixed (full dose,  $[\text{SF}_6] = 550$  mbar,  $[\text{O}_2] = 40$  mbar). Within our experimental reproducibility ( $\pm 5\%$ ) no effect on the maximum transient absorption at 220 nm was discernable indicating that the formation of  $\text{FO}_2$  radicals is not significant under our experimental conditions. Using a value for  $\sigma(\text{FO}_2)$  at 220 nm of  $1.34 \times 10^{-17} \text{ cm}^2 \text{ molecule}^{-1}$  [12], we calculate that less than 2% of the fluorine atoms react to form  $\text{FO}_2$  under experimental conditions of  $[\text{CH}_3\text{F}] = 10$  mbar and  $[\text{O}_2] = 40$  mbar. This observation, combined with a previous measurement of  $k_5 = 1.4 \times 10^{-13} \text{ cm}^3 \text{ molecule}^{-1} \text{ sec}^{-1}$  at 600 mbar of  $\text{SF}_6$  diluent [18], leads to a lower limit for the rate constant of the reaction of F with  $\text{CH}_3\text{F}$  of  $k(\text{F} + \text{CH}_3\text{F}) \geq 3 \times 10^{-11} \text{ cm}^3 \text{ molecule}^{-1} \text{ sec}^{-1}$ .

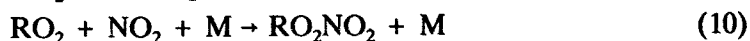
The solid lines in Figures 1 and 2 are linear least squares fits to the data obtained using  $\text{SF}_6$  concentrations less than 600 mbar and have slopes of  $0.324 \pm 0.012$  and  $(5.67 \pm 0.26) \times 10^{-4}$  respectively (errors represent  $2\sigma$ ). From these slopes absorbances

( $\log_{10}$ ) of 0.324 and 0.567 are calculated for experiments using full radiolysis dose and either 550 or 1000 mbar of  $\text{SF}_6$  respectively. Combining these initial absorbances with the calibrated yield of F atoms of  $2.7 \times 10^{15} \text{ cm}^{-3}$  at 1000 mbar of  $\text{SF}_6$  at full irradiation dose gives  $\sigma_{\text{CH}_2\text{FO}_2}(240 \text{ nm}) = (4.19 \pm 0.16)$  and  $(4.03 \pm 0.18) \times 10^{-18} \text{ cm}^2$  molecule $^{-1}$ , respectively. Within the quoted errors these determinations are in agreement. We choose to quote the average of these values with error limits which encompass the uncertainties associated with each determination, hence  $\sigma_{\text{CH}_2\text{FO}_2}(240 \text{ nm}) = (4.11 \pm 0.26) \times 10^{-18} \text{ cm}^2$  molecule $^{-1}$ . Errors quoted thus far represent the statistical uncertainty associated with our measurements, we estimate that, in addition, there is 10% uncertainty in the absolute calibration of the F atom yield. Combining the statistical and possible systematic errors, we arrive at  $\sigma_{\text{CH}_2\text{FO}_2}(240) = (4.11 \pm 0.67) \times 10^{-18} \text{ cm}^2$  molecule $^{-1}$ .

To map out the absorption spectrum of  $\text{CH}_2\text{FO}_2$  radicals, experiments were performed to measure the initial absorption between 220 and 300 nm following the pulsed irradiation of  $\text{SF}_6/\text{CH}_3\text{F}/\text{O}_2$  mixtures with  $\text{SF}_6 = 550$  mbar. Initial absorptions were then scaled to that at 240 nm and converted into absolute absorption cross sections. Results are shown in Figure 3.

The pulse radiolysis technique was also used to measure the UV spectra of  $\text{CHF}_2\text{O}_2$ ,  $\text{CF}_3\text{O}_2$ ,  $\text{CF}_3\text{CF}_2\text{O}_2$ ,  $\text{CF}_2\text{HCF}_2\text{O}_2$ , and  $\text{CF}_3\text{CFHO}_2$  radicals. In general, there is reasonable agreement between the various studies. For  $\text{CF}_3\text{CFHO}_2$  the spectra of Wallington and Nielsen [8] and Maricq and Szenté [13] are in agreement. However, the data from Jemi-Alade et al. [14] is approximately 40% lower. Wallington and Nielsen [8] and Maricq and Szenté [13] both used the reaction of F atoms with HFC-134a as a source of  $\text{CF}_3\text{CFHO}_2$  radicals. Jemi-Alade et al. [14] employed the reaction of Cl atoms with HFC-134a. Chlorine atoms react slowly with HFC-134a, and fluorine atom attack is three orders of magnitude more rapid. A possible explanation for the anomalously low absorption cross sections reported by Jemi-Alade et al. is the loss of Cl atoms with a reactive impurity in their work.

The fate of  $\text{RO}_2$  radicals in the atmosphere is determined by reaction with  $\text{NO}$ ,  $\text{NO}_2$ ,  $\text{HO}_2$ , or other  $\text{RO}_2$  radicals:

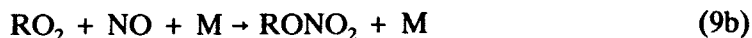


The relative importance of reactions 9-12 depends on  $\text{NO}$ ,  $\text{NO}_2$ ,  $\text{HO}_2$  and  $\text{RO}_2$  concentrations as well as the values of the respective rate constants  $k_9$ - $k_{12}$ . In remote

0 0 6 5

areas  $\text{NO}_x$  concentrations as low as 1 ppt have been measured [15], decreasing the importance of reactions 9 and 10. However, in urban areas with higher  $\text{NO}_x$  concentration reaction 9 and 10 will be the major sink for  $\text{RO}_2$  radicals.

The reaction of  $\text{RO}_2$  radicals with  $\text{NO}$  can proceed through two channels:



In this work we have used the pulse radiolysis technique to investigate reaction 2 for a number of alkyl and halogenated alkyl peroxy radicals:  $\text{CH}_3\text{O}_2$ ,  $\text{C}_2\text{H}_5\text{O}_2$ ,  $(\text{CH}_3)_3\text{CCH}_2\text{O}_2$ ,  $(\text{CH}_3)_3\text{CC}(\text{CH}_3)_2\text{CH}_2\text{O}_2$ ,  $\text{CH}_2\text{FO}_2$ ,  $\text{CH}_2\text{ClO}_2$ ,  $\text{CH}_2\text{BrO}_2$ ,  $\text{CHF}_2\text{O}_2$ ,  $\text{CF}_2\text{ClO}_2$ ,  $\text{CHF}_2\text{CF}_2\text{O}_2$ ,  $\text{CF}_3\text{CF}_2\text{O}_2$ ,  $\text{CFCl}_2\text{CH}_2\text{O}_2$ , and  $\text{CF}_2\text{ClCH}_2\text{O}_2$ .

The formation of  $\text{NO}_2$  from reaction (9a) was followed by monitoring the absorption of  $\text{NO}_2$  at both 400 and 450 nm in order to assure that there was no interference from other transient species in the system. The observed formation of  $\text{NO}_2$  was always first order. No significant difference between experiments done at 400 and 450 nm was detected. Detailed information on these experiments and results are given by Sehested et al. [16]. In Table 1 our results have been compared with results from previous investigations published in the literature. In Figure 4 the rate constant has been plotted to indicate structure reactivity relationships.

## Acknowledgements

The authors wish to acknowledge the financial support of the Commission of the European Communities.

## REFERENCES

1. O.J. Nielsen, Risø-R-480 (1984).
2. T.J. Wallington and S.M. Japar, *J. Atmos. Chem.*, **9** (1989) 399.
3. T.J. Wallington, J.C. Ball, O.J. Nielsen, and E. Bartkiewicz, *J. Phys. Chem.*, **96** (1992) 1241.
4. O.J. Nielsen, T. Ellermann, E. Bartkiewicz, T.J. Wallington, and M.D. Hurley, *J. Phys. Chem.*, **96** (1992) 82.
5. O.J. Nielsen, T. Ellermann, J. Sehested, E. Bartkiewicz, T.J. Wallington, and M.D. Hurley, *J. Phys. Chem.*, **96** (1992) 1009.
6. J. Sehested, T. Ellermann, O.J. Nielsen, T.J. Wallington, and M.D. Hurley, accepted for publication in *Int. J. Chem. Kinet.* (1993).
7. O.J. Nielsen, T. Ellermann, J. Sehested, and T.J. Wallington, *J. Phys. Chem.*, **96** (1992) 10875.
8. T.J. Wallington and O.J. Nielsen, *Chem. Phys. Lett.*, **187** (1991) 33.
9. T. MacPherson, M.J. Pilling, and M.J.C. Smith, *J. Phys. Chem.*, **89** (1985) 2268.
10. T.J. Wallington, P. Dagaut, and M.J. Kurylo, *Chem. Rev.*, **92** (1992) 667.
11. T. Ellermann, J. Sehested, O.J. Nielsen, P. Pagsberg, and T.J. Wallington, *Chem. Phys. Lett.*, submitted (1993).
12. P. Pagsberg, E. Ratajczak, and A. Sillesen, *Chem. Phys. Lett.*, **141** (1987) 88.
13. M.M. Maricq and J.J. Szente, *J. Phys. Chem.*, **96** (1992) 10862.
14. A.A. Jemi-Alade, P.D. Lightfoot, and R. Lesclaux, *Chem. Phys. Lett.*, **179** (1991) 119.
15. B.A. Ridley, M.A. Carroll, and G.L. Gregory, *J. Geophys. Res.* **92** (1987) 2025.
16. J. Sehested, O.J. Nielsen, and T.J. Wallington, *Chem. Phys. Lett.*, submitted (1993).
17. H. Adachi and N. Basco, *Chem. Phys. Lett.*, **63**, (1979) 490.

18. R.A. Cox and G.S. Tyndall, *J. Chem. Soc. Faraday Trans. 2* 76, (1980) 153.
19. S.P. Sander and R.T. Watson, *J. Phys. Chem.* 85, (1980) 2960.
20. R. Simonaitis and J. Heicklen, *J. Phys. Chem.* 95, (1981) 2946.
21. I.C. Plumb, K.R. Ryan, J.R. Steven, and M.F.R. Mulcahy, *J. Phys. Chem.* 85, (1981) 3136.
22. A.R. Ravishankara, F.L. Eisele, N.M. Kreutter and P.H. Wine, *J. Chem. Phys.* 74 (1981) 2267.
23. R. Zellner, B. Fritz, and K. Lorentz, *J. Atm. Chem.* 4, (1986) 241.
24. H. Adachi and N. Basco, *Chem. Phys. Lett.* 67 (1979) 324.
25. I.C. Plumb, K.R. Ryan, J.R. Steven, and M.F.R. Mulcahy, *Int. J. Chem. Kinet.* 14 (1982) 183.
26. H. Adachi and N. Basco, *Int. J. Chem. Kinet.* 14, (1982) 1243.
27. J. Peeters, J. Vertommen, and I. Langhans, *Ber. Bunsenges. Phys. Chem.* (1992) in press.
28. I.C. Ryan and K.R. Ryan, *Chem. Phys. Lett.* 92 (1982) 236.
29. A.M. Dognon, F. Caralp, and R. Lesclaux, *J. Chim. Phys.* 82 (1985) 349.
30. J. Sehested and O.J. Nielsen, submitted for publication in *Chem. Phys. Lett.* (1993).
31. P. Lesclaux and F. Caralp, *Int. J. Chem. Kinet.* 16 (1984) 1117.
32. K.R. Ryan and I.C. Plumb, *Int. J. Chem. Kinet.* 16 (1984) 591.
33. T.J. Wallington and O.J. Nielsen, *Chem. Phys. Lett.* 187, (1991) 33.

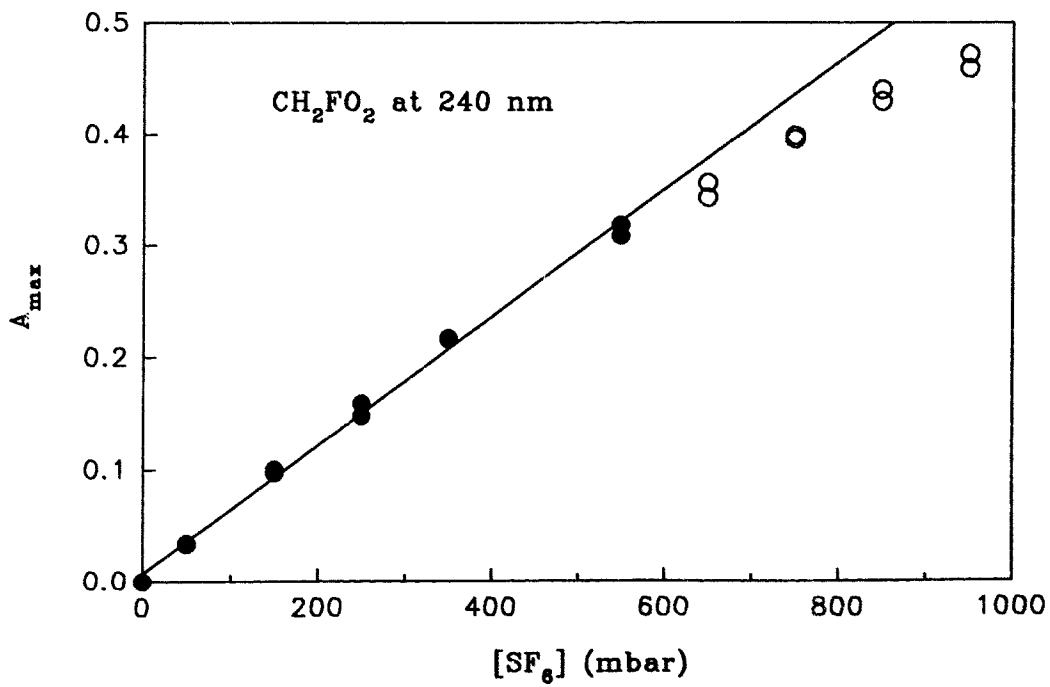
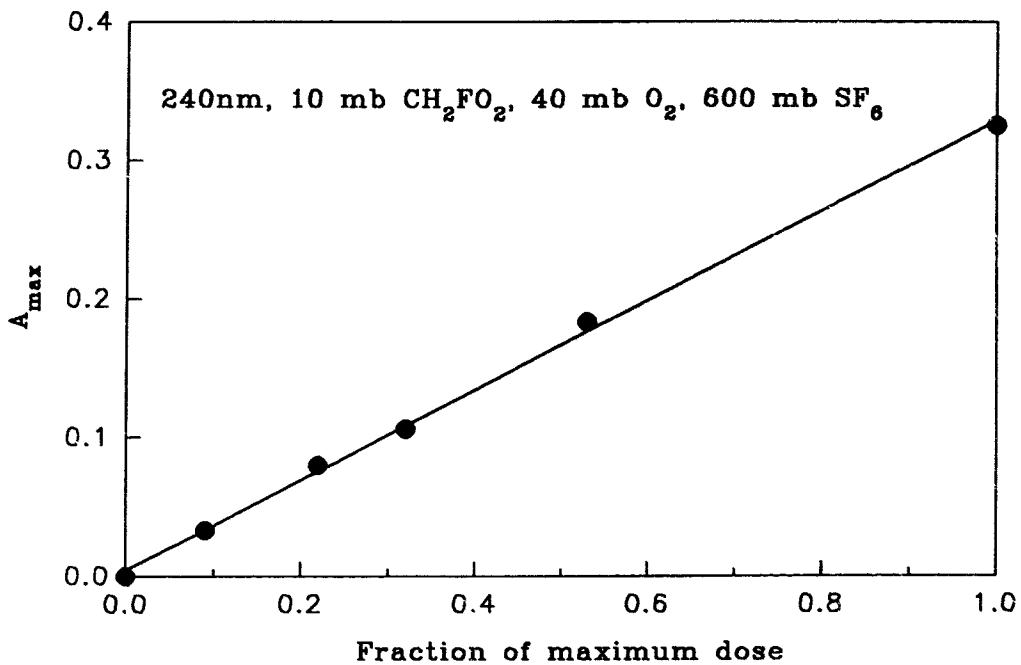


Table 1. Summary of rate constants for RO<sub>2</sub>+NO → products reactions

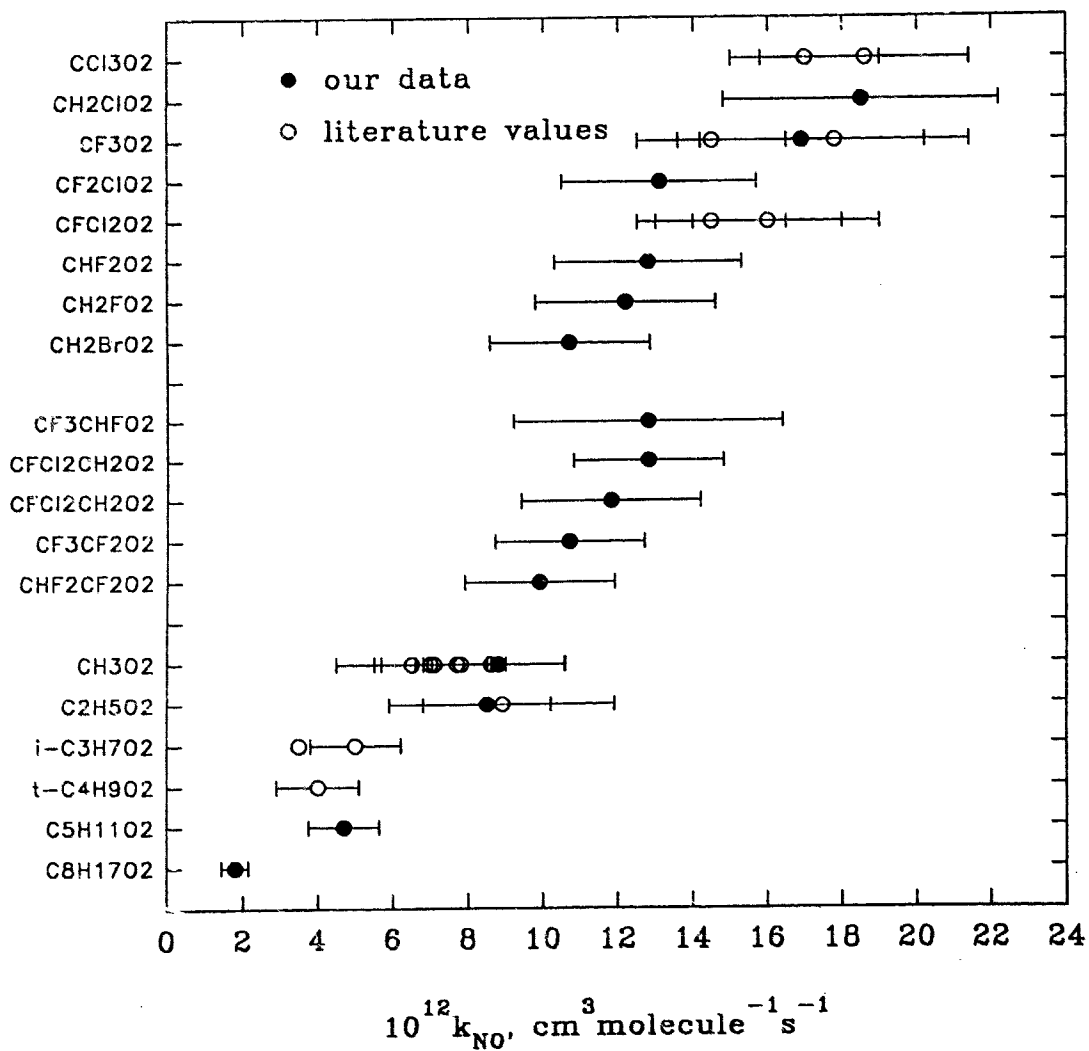
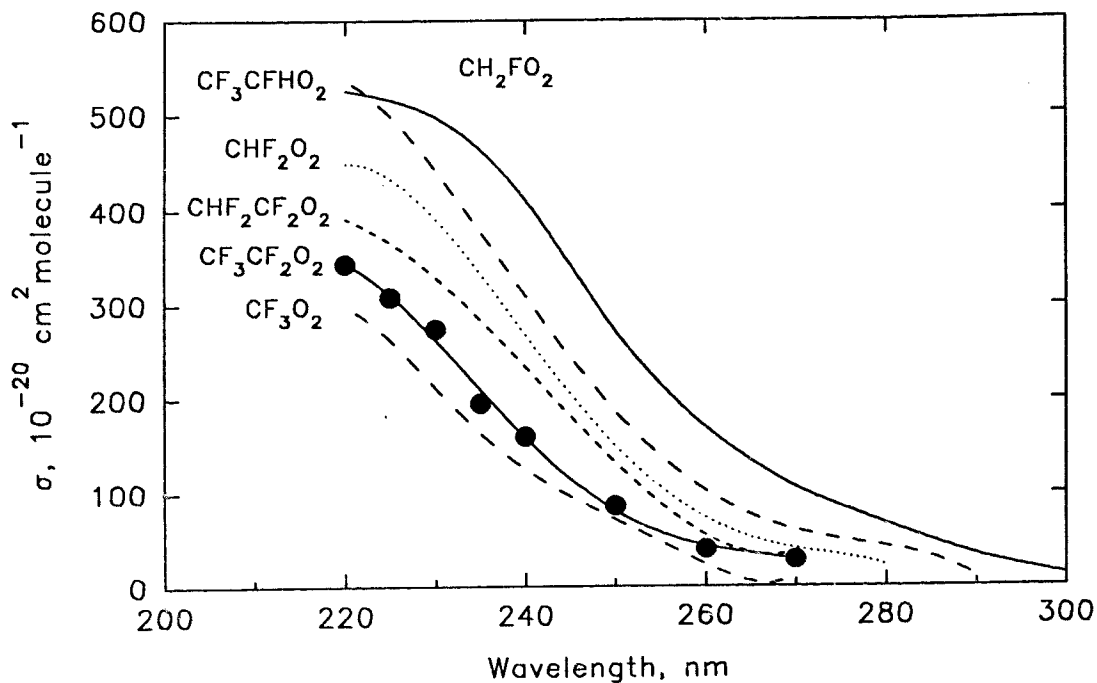
Species	Technique <sup>a)</sup>	10 <sup>12</sup> k <sub>2</sub> <sup>b)</sup>	Reference
CH <sub>3</sub> O <sub>2</sub>	FP-UV	3.0±0.2	[17]
	DF-MS	6.5±2.0	[18]
	FP-UV	7.1±1.4	[19]
	FP-UV	7.7±0.9	[20]
	DF-MS	8.6±2.0	[21]
	LP-LIF	7.8±1.2	[22]
	LP-LA	7.0±1.5	[23]
	PR-UV	8.8±1.4	This work
C <sub>2</sub> H <sub>5</sub> O <sub>2</sub>	FP-UV	2.7±0.2	[24]
	DF-MS	8.9±3.0	[25]
	PR-UV	8.5±1.2	This work
<i>i</i> -C <sub>3</sub> H <sub>7</sub> O <sub>2</sub>	FP-UV	3.5±0.2	[26]
	DF-MS	5.0±1.2	[27]
<i>t</i> -C <sub>4</sub> H <sub>9</sub> O <sub>2</sub>	DF-MS	4.0±1.1	[17]
(CH <sub>3</sub> ) <sub>3</sub> CCH <sub>2</sub> O <sub>2</sub>	PR-UV	4.7±0.4	This work
(CH <sub>3</sub> ) <sub>3</sub> C(CH <sub>3</sub> ) <sub>2</sub> CH <sub>2</sub> O <sub>2</sub>	PR-UV	1.8±0.2	This work
CH <sub>2</sub> FO <sub>2</sub>	PR-UV	12.5±1.3	This work
CH <sub>2</sub> ClO <sub>2</sub>	PR-UV	18.7±2.0	This work
CH <sub>2</sub> BrO <sub>2</sub>	PR-UV	10.7±1.1	This work
CHF <sub>2</sub> O <sub>2</sub>	PR-UV	12.6±1.6	This work
CF <sub>3</sub> O <sub>2</sub>	DF-MS	17.8±3.6	[28]
	LP-MS	14.5±2.0	[29]
	PR-UV	16.9±2.6	[30]
CF <sub>2</sub> ClO <sub>2</sub>	LP-MS	16.0±3	[19]
	PR-UV	13.1±1.2	This work
CFCl <sub>2</sub> O <sub>2</sub>	LP-MS	16.0±2.0	[31]
	LP-MS	14.5±2.0	[19]
CCl <sub>3</sub> O <sub>2</sub>	DF-MS	18.6±2.8	[32]
	LP-MS	17.0±2.0	[19]
CF <sub>3</sub> CHFO <sub>2</sub>	PR-UV	12.8±3.6	[33]
CHF <sub>2</sub> CF <sub>2</sub> O <sub>2</sub>	PR-UV	>9.7±1.3	This work
CF <sub>3</sub> CF <sub>2</sub> O <sub>2</sub>	PR-UV	>10.7±1.5	This work
CFCl <sub>2</sub> CH <sub>2</sub> O <sub>2</sub>	PR-UV	12.8±1.1	This work
CF <sub>2</sub> ClCH <sub>2</sub> O <sub>2</sub>	PR-UV	11.8±1.0	This work

<sup>a)</sup> FP-UV, Flash Photolysis - UV Absorption; DF-MS, Discharge Flow - Mass Spectrometry; LP-LIF, Laser Photolysis - Laser Induced Fluorescence; LP-LA, Laser Photolysis - Laser Absorption; PR-UV, Pulse Radiolysis - UV Absorption; LP-MS, Laser Photolysis - Mass Spectrometry

<sup>b)</sup> in units of cm<sup>3</sup>molecule<sup>-1</sup>s<sup>-1</sup>



0 0 7 8



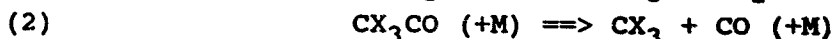
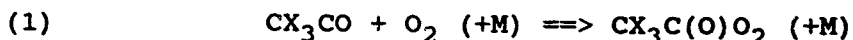
Formation and thermal decomposition of  $\text{CCl}_3\text{C}(\text{O})\text{O}_2\text{NO}_2$  and  
 $\text{CF}_3\text{C}(\text{O})\text{O}_2\text{NO}_2$

I. Barnes, K. H. Becker, F. Kirchner, and F. Zabel  
University of Wuppertal, Physikalische Chemie / FB 9,  
Gaußstr. 20, 5600 Wuppertal 1, Germany

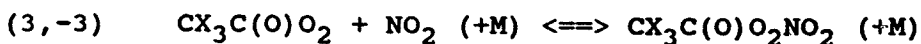
and

H. Richer and J. Sodeau  
School of Chemical Sciences, University of East Anglia,  
Norwich, Norfolk, NR4 7TJ, U.K.

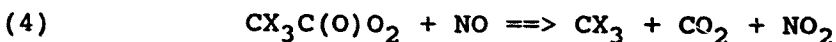
Degradation of 1,1,1-trihaloethanes in the atmosphere proceeds via trihaloacetaldehydes (see e. g. [1] for  $\text{CH}_3\text{CCl}_3$ ). Two competing pathways exist for the halogenated acetyl radicals which are formed from these aldehydes through H atom abstraction by OH:



The  $\text{CX}_3\text{C}(\text{O})\text{O}_2$  radicals formed in reaction (1) may add  $\text{NO}_2$  to give thermally unstable peroxy nitrates:



The impact of these species as temporary reservoirs of X depends on their thermal lifetimes. Ultimately, reaction of  $\text{CX}_3\text{C}(\text{O})\text{O}_2$  with NO will also lead to  $\text{CX}_3$  radicals:



The relative importance of reactions (1) and (2) is uncertain mainly due to unknown C-C bond strengths in the acetyl radicals.

In the present study, the relative rates of reactions (1) and (2) were determined for  $\text{X} = \text{Cl}$  and  $\text{X} = \text{F}$  by measuring the yields of CO and  $\text{CX}_3\text{C}(\text{O})\text{O}_2\text{NO}_2$ , the latter of which is rapidly formed from  $\text{CX}_3\text{C}(\text{O})\text{O}_2$  in the presence of  $\text{NO}_2$ . These results allow an estimation of the fate of  $\text{CCl}_3\text{CO}$  and  $\text{CF}_3\text{CO}$  in the troposphere. In addition, the unimolecular decomposition rate constants  $k_{-3}$  of  $\text{CCl}_3\text{C}(\text{O})\text{O}_2\text{NO}_2$  and  $\text{CF}_3\text{C}(\text{O})\text{O}_2\text{NO}_2$  have been measured as a function of temperature and pressure, thus complementing earlier studies from the Wuppertal laboratory on the thermal decomposition of  $\text{CF}_2\text{ClC}(\text{O})\text{O}_2\text{NO}_2$  and  $\text{CFCl}_2\text{C}(\text{O})\text{O}_2\text{NO}_2$  [2].

## Experimental

Experiments were performed in a 420 l temperature regulated DURAN glass chamber. The reactor is surrounded by 20 photolysis lamps for the generation of radicals and equipped with a White mirror system for in situ long-path (50.4 m) IR absorption measurements using an FTIR spectrometer.  $CX_3CO$  radicals were generated by continuous photolysis of  $CX_3CHO/Cl_2/O_2/NO_2/N_2$  mixtures. The yields of CO and  $CX_3C(O)O_2NO_2$  were measured as a function of time. The partial pressure of oxygen was varied between 200 and 975 mbar for  $CCl_3CHO$  and between 5 and 19 mbar for  $CF_3CHO$ . The total pressure was kept constant by addition of nitrogen to 975 mbar. The following relationship applies for the reaction conditions of this work:

$$(I) \quad k_2/k_1 = \frac{\Delta [CO][O_2]}{\Delta [CX_3C(O)O_2NO_2]}$$

Thus by measuring  $\Delta [CO]$  and  $\Delta [CX_3C(O)O_2NO_2]$  as a function of temperature, the temperature dependence of  $k_2/k_1$  and thereby the difference of the activation energies of reactions (1) and (2) can be determined.

In the second part of this work, the temperature and pressure dependence of  $k_{-3}$  was measured. Both peroxy nitrates, in particular  $CCl_3C(O)O_2NO_2$ , were prepared in the presence of high  $O_2$  partial pressures in order to suppress reaction (2), and then diluted with  $N_2$ . Thermal decomposition of  $CX_3C(O)O_2NO_2$  was initiated by addition of - 0.3 mbar NO. The following relationship holds for the first order disappearance rate constant of  $CX_3C(O)O_2NO_2$ ,  $k_{-3,eff}$ :

$$(II) \quad (k_{-3,eff})^{-1} = (k_{-3})^{-1} \times \left\{ 1 + \frac{k_3[NO_2]}{k_4[NO]} \right\}$$

At low  $[NO_2]/[NO]$  ratios,  $k_{-3,eff}$  approaches  $k_{-3}$ .

## Results

In figures 1 and 2, the logarithm of the measured ratios  $\Delta [CO][O_2]/\Delta [CX_3C(O)O_2NO_2]$  is plotted as a function of  $T^{-1}$ . Arbitrary units are used because the IR absorption coefficients of  $CX_3C(O)O_2NO_2$  are not accurately known.

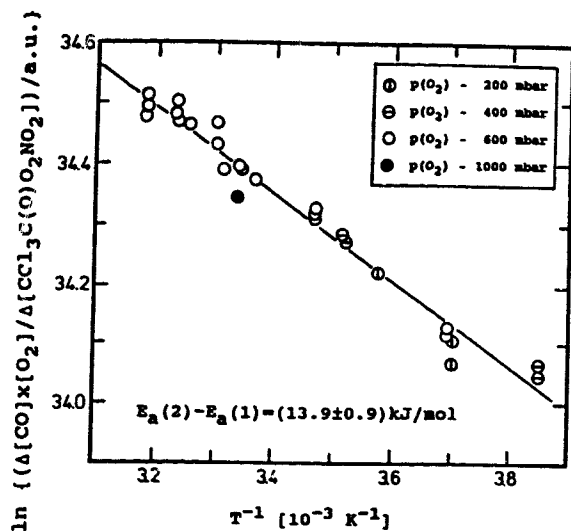


Fig. 1: Temperature dependence of  $k_2/k_1$  for  $\text{CCl}_3\text{CO}$

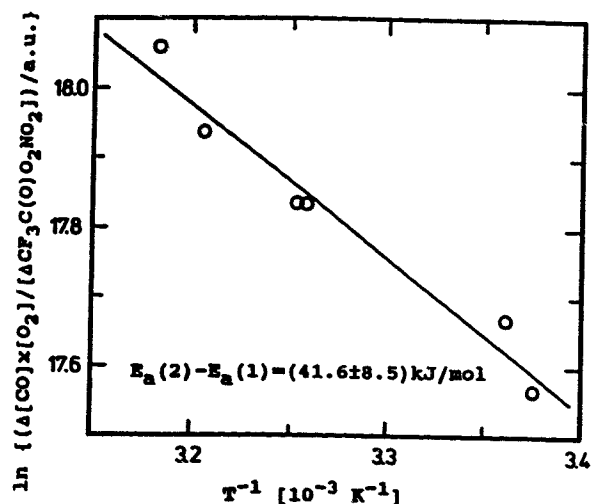
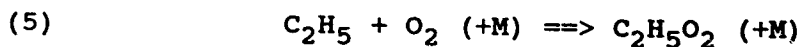


Fig. 2: Temperature dependence of  $k_2/k_1$  for  $\text{CF}_3\text{CO}$

It was verified that  $\Delta[\text{CO}][\text{O}_2]/\Delta[\text{CX}_3\text{C}(\text{O})\text{O}_2\text{NO}_2]$  is independent of the partial pressure of  $\text{O}_2$ . The slopes of the Arrhenius type plots of figs. 1 and 2 are equal to the difference of activation energies of reactions (2) and (1). Using the activation energy of the similar reaction



(- 0.8 kJ/mol [4]) as an approximation for the temperature dependence of  $k_1$ , the values  $(13.1 \pm 0.9)$  and  $(40.8 \pm 8.5)$  kJ/mol (2 $\sigma$ ) were derived for the activation energies of the thermal decomposition of  $\text{CCl}_3\text{CO}$  and  $\text{CF}_3\text{CO}$  radicals, respectively, at 1000 mbar.

Thermal decomposition of  $\text{CX}_3\text{C}(\text{O})\text{O}_2\text{NO}_2$  was measured in the temperature range 305 - 325 K and the pressure range 8 - 1000 mbar. First order wall loss of  $\text{CX}_3\text{C}(\text{O})\text{O}_2\text{NO}_2$  occurred and was taken into account. Due to the relatively high partial pressures of  $\text{O}_2$ , considerable transformation of  $\text{NO}$  to  $\text{NO}_2$  by the reaction  $2 \text{NO} + \text{O}_2 \Rightarrow 2 \text{NO}_2$  occurred, and the  $[\text{NO}]/[\text{NO}_2]$  ratio slowly changed with time. Therefore,  $k_{-3,\text{eff}}$  had to be corrected for the non-negligible  $[\text{NO}_2]/[\text{NO}]$  ratio according to eq. (II). As  $k_3$  and  $k_4$  are not known for  $\text{CX}_3\text{C}(\text{O})\text{O}_2$  radicals, the value  $k_3/k_4 = 0.5$  was used which is close to the experimental values of  $k_3/k_4$  for  $\text{CH}_3\text{C}(\text{O})\text{O}_2$  and  $\text{C}_6\text{H}_5\text{C}(\text{O})\text{O}_2$  [3]. The difference between  $k_{-3,\text{eff}}$  and  $k_{-3}$  amounted to 10 - 30 %. Arrhenius plots for the thermal decomposition rate

constants of  $\text{CCl}_3\text{C}(\text{O})\text{O}_2\text{NO}_2$  and  $\text{CF}_3\text{C}(\text{O})\text{O}_2\text{NO}_2$  thus obtained are shown in figs. 3 and 4 for different total pressures.

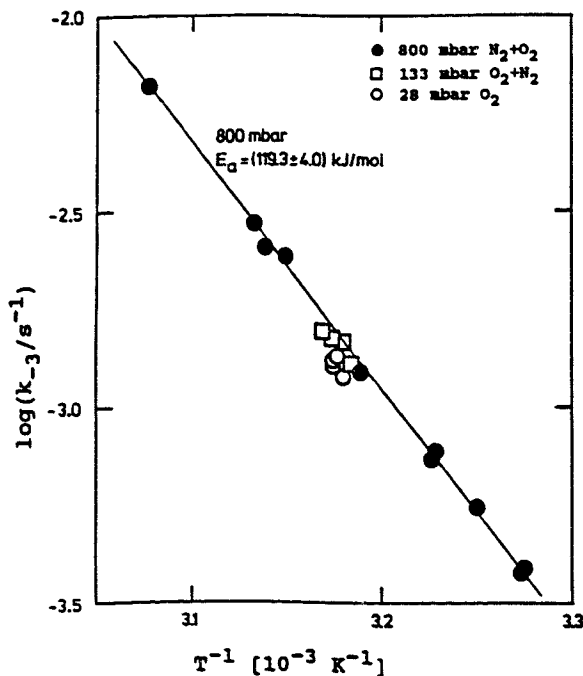


Fig.3: Arrhenius plot for thermal decomposition of  $\text{CCl}_3\text{C}(\text{O})\text{O}_2\text{NO}_2$

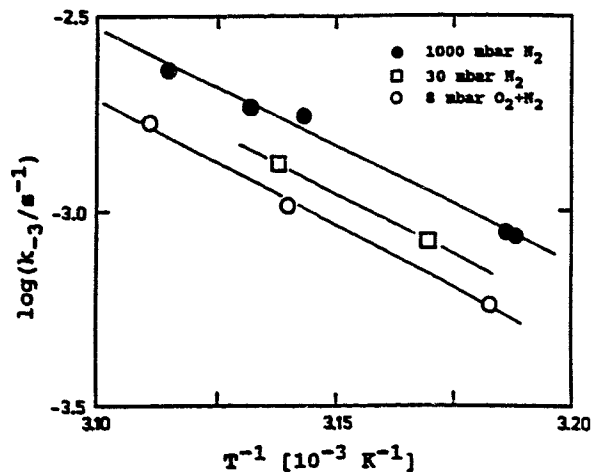


Fig.3: Arrhenius plot for thermal decomposition of  $\text{CF}_3\text{C}(\text{O})\text{O}_2\text{NO}_2$

### Discussion

It has been assumed that the Arrhenius pre-exponential factor for reaction (2) is low, corresponding to a tight transition state. This being true, the reaction should be close to the high pressure limit at a total pressure of 1 atm. In table 1, the activation energy of  $k_2$  for  $\text{CF}_3\text{CO}$  at 1 atm from this work is compared with previous determinations [5,6] and a theoretical estimate for the high pressure value by Francisco [7]. Furthermore, the experimental activation energies of  $k_2$  are compared with calculated heats of reaction based on  $\Delta H_{\text{R},298}^{\circ}(\text{CH}_3\text{CO})$  [8],  $\Delta H_{\text{R},298}^{\circ}(\text{CH}_3\text{OO})$  [3] and thermochemical additivity rules [9]. Both data show good agreement (see table 1) suggesting that there is only a small (if any) barrier for the recombination of  $\text{CX}_3$  and  $\text{CO}$ . This is in contrast to the theoretical work of Francisco suggesting a barrier of 20.9 kJ/mol for the recombination of  $\text{CF}_3$  and  $\text{CO}$  [7].

Table 1.

Activation energies and heats of reaction of reaction (2)

	CCl <sub>3</sub> CO	Ref.	CF <sub>3</sub> CO	Ref.
E <sub>a∞</sub> (3) [kJ/mol]	13.1±5.1	this work	≥41.8	5
			83.1	6
			47.7	7
			40.8±9.9	this work
E <sub>a∞</sub> (-3) [kJ/mol]			20.9	7
ΔH <sub>R,298</sub> <sup>o</sup> (3) [kJ/mol]	14.5±8.8	a	29.3	7
			52.1±17.2	a

Note: <sup>a</sup> based on ΔH<sub>R,298</sub><sup>o</sup>(CH<sub>3</sub>CO) [8], ΔH<sub>R,298</sub><sup>o</sup>(CH<sub>3</sub>OO) [3] and thermochemical additivity rules [9]

The measured ratios  $k_2/k_1$  can directly be applied to estimate the relative importance of reactions (1) and (2) under tropospheric conditions. When equal Arrhenius pre-exponential factors of  $k_2$  are assumed for CCl<sub>3</sub>CO and CF<sub>3</sub>CO, it is suggested from the above data that CCl<sub>3</sub>CO radicals predominantly decompose under all tropospheric conditions whereas the major fraction of the CF<sub>3</sub>CO radicals add O<sub>2</sub> and are able to form a stable PAN-type peroxyxynitrate (table 2).

Table 2.

Atmospheric Fate of CX<sub>3</sub>CO Radicals

	CCl <sub>3</sub> CO	CF <sub>3</sub> CO
Fraction of CX <sub>3</sub> CO loss by thermal decomposition in the lower troposphere (298 K, 1000 mbar)	92 %	1.3 %
Fraction of CX <sub>3</sub> CO loss by thermal decomposition in the upper troposphere (220 K, 100 mbar)	89 %	0.02 %

$\text{CCl}_3\text{C}(\text{O})\text{O}_2\text{NO}_2$  and  $\text{CF}_3\text{C}(\text{O})\text{O}_2\text{NO}_2$  are stable peroxy nitrates like PAN. The values for  $k_{-3}$  from this work fit well into a series of decomposition rate constants of other (substituted) acetyl peroxy nitrates. It can be seen from table 3 that within this group of peroxy nitrates substitution on the methyl group by electron drawing atoms or groups results in additional thermal stabilisation of the peroxy nitrate.

Table 3.

Kinetic parameters of thermal decomposition of  $\text{RO}_2\text{NO}_2$  in nitrogen

R	T [K]	$P_{\text{tot}}$ [mbar]	$k_{-3}(298\text{K})^{\text{a}}$ [ $\text{s}^{-1}$ ]	$E_{\text{a}}$ [kJ/mol]	A [ $10^{16}\text{s}^{-1}$ ]	Ref.
$\text{CH}_3\text{OCO}$	301-320	1000	0.00084	107.0±2.2	0.48	[10]
$\text{CH}_3\text{CO}^{\text{b}}$	297-326	1000	0.00040	112.9±1.9	2.5	[11]
$\text{C}_6\text{H}_5\text{CO}$	301-321	1000	0.00031	116.4±3.8	7.9	[12]
$\text{ClCO}$	300-324	800	0.00017	115.1±3.2	2.6	[10]
$\text{CCl}_3\text{CO}$	305-325	800	0.00012 <sup>b</sup>	119.3±4.0 <sup>b</sup>	9.6 <sup>b</sup>	this work
$\text{CFCl}_2\text{CO}$	311-323	1000	0.00011	(118.2) <sup>c</sup>	(6) <sup>d</sup>	[2]
$\text{CF}_2\text{ClCO}$	313-322	1000	0.00009	(118.9) <sup>c</sup>	(6) <sup>d</sup>	[2]
$\text{CF}_3\text{CO}$	314-321	1000	0.00008	(119.2) <sup>c</sup>	(6) <sup>d</sup>	this work

Notes: <sup>a</sup> calculated from the two subsequent columns; <sup>b</sup> in 800 mbar  $\text{N}_2+\text{O}_2$ ; <sup>c</sup> from measured rate constants and estimated pre-exponential factor; <sup>d</sup> estimated

From the data of the present work it may be concluded that  $\text{CCl}_3\text{C}(\text{O})\text{O}_2\text{NO}_2$  cannot act as a reservoir of chlorine in the atmosphere as the precursor radical  $\text{CCl}_3\text{CO}$  will predominantly thermally decompose.  $\text{CF}_3\text{C}(\text{O})\text{O}_2\text{NO}_2$  may act as a temporary reservoir of fluorine but its ozone depletion potential is zero because it contains neither chlorine nor bromine. However, the equally stable peroxy nitrates  $\text{CFCl}_2\text{C}(\text{O})\text{O}_2\text{NO}_2$  and  $\text{CF}_2\text{ClC}(\text{O})\text{O}_2\text{NO}_2$  might carry small amounts of chlorine into the stratosphere.

## References

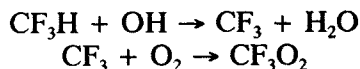
- [1] L. Nelson, I. Shanahan, H. W. Sidebottom, J. Treacy, and O. J. Nielsen, *Int. J. Chem. Kinet.* 22(1990)577
- [2] K. H. Becker and F. Zabel, AFEAS-Project No. CTR90-5/P90-020 "Thermal Decomposition of  $\text{CClF}_2\text{CH}_2\text{O}_2\text{NO}_2$ ,  $\text{CCl}_2\text{FCH}_2\text{O}_2\text{NO}_2$ ,  $\text{CClF}_2\text{C}(\text{O})\text{O}_2\text{NO}_2$  und  $\text{CCl}_2\text{FC}(\text{O})\text{O}_2\text{NO}_2$ ", Final Report, 1991
- [3] P. D. Lightfoot, R. A. Cox, J. N. Crowley, M. Destriau, G. D. Hayman, M. E. Jenkin, G. K. Moortgat and F. Zabel, *Atmos. Environ.* 26A(1992)1805
- [4] R. Atkinson, D. L. Baulch, R. A. Cox, R. F. Hampson Jr., J. A. Kerr and J. Troe, *J. Phys. Chem. Ref. Data* 21(1992)1125
- [5] J. C. Amphlett and E. Whittle, *Trans. Faraday Soc.* 63(1967)80
- [6] J. A. Kerr and J. P. Wright, *J. Chem. Soc. Faraday Trans I* 81(1985)1471
- [7] J. S. Francisco, *Chem. Phys. Lett.* 191(1992)7
- [8] J. T. Niiranen, D. Gutman,, and L. N. Krasnoperov, *J. Phys. Chem.* 96(1992)5881
- [9] S. W. Benson, "Thermochemical Kinetics", 2nd ed., Wiley, New York, 1976
- [10] F. Kirchner, G. Libuda and F. Zabel, XXIth Int. Symp. Gas Kinetics, Assisi (Italy), 2 - 7 Sept. 1990, Book of Abstracts
- [11] I. Bridier, F. Caralp, H. Loirat, R. Lesclaux, B. Veyret, K. H. Becker, A. Reimer, and F. Zabel, *J. Phys. Chem.* 95(1991)3594
- [12] F. Kirchner, F. Zabel and K. H. Becker, *Chem. Phys. Lett* 191(1992)169

## Rate Constants for Reactions of Perhaloalkylperoxyl Radicals with Alkenes

R. E. Huie, Z. B. Alfassi, and P. Neta

Chemical Kinetics and Thermodynamics Division  
National Institute of Standards and Technology  
Gaithersburg, Maryland 20899 USA

**Introduction.** The reactions of hydroxyl radicals with hydrofluorocarbons and hydrochlorofluorocarbons in the atmosphere result in the formation of halogenated peroxyl radicals, for example



These radicals are expected generally to react with NO, NO<sub>2</sub>, or with other peroxyl radicals, including HO<sub>2</sub>. Other reactions of peroxyl radicals, for example with alkenes, are considered to be too slow to be of any importance in the atmosphere. Whereas this is clearly true for the non-halogenated alkyl peroxyl radicals, halogenation may increase the reactivity of these radicals sufficiently that other reaction pathways become important, particularly with alkenes. Over the past several years, we have been engaged in the study of the liquid-phase reactivity of halogenated peroxyl radicals, primarily their electron-transfer reactions [1-8]. We have now extended these studies to several reactions of halogenated peroxyl radicals with alkenes in a number of solvents, in order to determine if these reactions might be rapid enough to be of importance in the atmosphere.

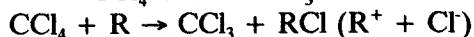
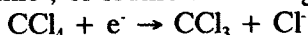
**Experimental Methods.** The rate constants for reactions of perhaloalkylperoxyl radical with the various alkenes were determined by pulse radiolysis. The irradiation of a solvent by ionizing radiation results in the formation of a solvated electron and a radical cation



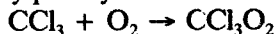
The radical cation can deprotonate,



often yielding an additional reducing radical. Halogenated alkyl radicals are produced by the reduction of chlorine-, bromine-, or iodine-containing halocarbons, for example

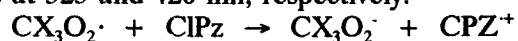


In the presence of oxygen, haloalkylperoxyl radicals are formed



Direct kinetic-spectrophotometric measurements of the decay of the peroxyl radical or the buildup of the substrate radical are not possible with alkanes and alkenes because these radicals absorb only in the UV where measurements are hampered by the absorption of some of the radical precursors, reactants, or solvents. Therefore, we have determined the rate constants by competition kinetics using chlorpromazine (CIPz) as a reference. In triethylamine, where CIPz is insoluble, we used trolox. The rate of oxidation of CIPz and trolox has been determined directly by following the formation of

their radicals at 525 and 420 nm, respectively.



The addition of alkenes to solutions of CIPz or trolox leads to competition which will result in enhanced rate constant of formation ( $k_{\text{obs}}$ ) and decreased yield of CIPz or trolox radicals. The rate constant for the competing reaction was derived from the effect of substrate concentration on the kinetics and on the yield.

**Results.** We have measured rate constants in methanol for the reactions of  $\text{CCl}_3\text{O}_2\cdot$ ,  $\text{CBr}_3\text{O}_2\cdot$ , and  $\text{CF}_3\text{CCl}_2\text{O}_2\cdot$  with a number of alkenes (Table I).

**Table I.** Rate Constants for Reactions of  $\text{CF}_3\text{CCl}_2\text{O}_2\cdot$ ,  $\text{CCl}_3\text{O}_2\cdot$ , and  $\text{CBr}_3\text{O}_2\cdot$  Radicals with Alkenes in Methanolic Solutions

Substrate	k, L mol <sup>-1</sup> s <sup>-1</sup>			
	$\text{CF}_3\text{CCl}_2\text{O}_2$	$\text{CCl}_3\text{O}_2$	$\text{CBr}_3\text{O}_2$	$\sigma^*$
2-buten-1-ol	4.9x10 <sup>4</sup>	2.6x10 <sup>4</sup>	2.3x10 <sup>4</sup>	1.54
3-methyl-3-buten-1-ol	9.3x10 <sup>4</sup>	5.0x10 <sup>4</sup>	5.0x10 <sup>4</sup>	1.16
3-methyl-2-buten-1-ol	3.3x10 <sup>5</sup>	1.6x10 <sup>5</sup>	1.2x10 <sup>5</sup>	1.05
cyclohexene	2.1x10 <sup>5</sup>	9.5x10 <sup>4</sup>	9.1x10 <sup>4</sup>	0.74
2-methyl-3-ethyl-2-pentene	9.7x10 <sup>6</sup>	3.2x10 <sup>6</sup>	2.5x10 <sup>6</sup>	-0.20
2,3-dimethyl-2-butene	3.1x10 <sup>7</sup>	1.4x10 <sup>7</sup>	1.0x10 <sup>7</sup>	0.00
1,2-dimethylcyclohexene	8.0x10 <sup>6</sup>	3.4x10 <sup>6</sup>	3.3x10 <sup>6</sup>	-0.24
styrene	5.7x10 <sup>5</sup>	3.2x10 <sup>5</sup>	2.1x10 <sup>5</sup>	2.07

With the exception of styrene, the rate constants for the alkenes correlate with Taft's  $\sigma^*$  substituent constant [9]. The rate constants for the reactions of  $\text{CCl}_3\text{O}_2\cdot$  and  $\text{CBr}_3\text{O}_2\cdot$  are similar and about a factor of two to three less than the rate constants for  $\text{CF}_3\text{CCl}_2\text{O}_2\cdot$ . Although these rate constants are much faster than for non-halogenated alkyl peroxy radicals [10], they are somewhat slower than the values for  $\text{C}_4\text{F}_9\text{O}_2\cdot$ , which reach  $6 \times 10^8 \text{ L mol}^{-1}\text{s}^{-1}$  [7].

We have investigated the effect of solvent on the rate constants of the reactions of  $\text{CCl}_3\text{O}_2\cdot$  with 2,3-dimethyl-2-butene and cyclohexene (Table II).

**Table II.** Solvent Effects on Rate Constants for Reactions of  $\text{CCl}_3\text{O}_2$  Radicals with 2,3-Dimethyl-2-butene (DMB) and Cyclohexene (CH)

Solvent	k, L mol <sup>-1</sup> s <sup>-1</sup>	
	DMB	CH
$\text{CH}_3\text{CN}$	$2.3 \times 10^7$	$8.5 \times 10^4$
MeOH	$1.4 \times 10^7$	$9.5 \times 10^4$
acetone	$1.3 \times 10^7$	$4.9 \times 10^4$
DMF	$1.2 \times 10^7$	$8.0 \times 10^4$
$\text{HCONHCH}_3$	$\sim 1.2 \times 10^7$	$6.6 \times 10^4$
t-BuOH	$7.7 \times 10^6$	$7.6 \times 10^4$
dioxane	$6.9 \times 10^6$	$9.7 \times 10^4$
$\text{CCl}_4$ :dioxane	$4.3 \times 10^6$	
2-PrOH	$4.1 \times 10^6$	$7.9 \times 10^4$
DMSO	$3.3 \times 10^6$	$1.3 \times 10^5$
$(\text{CH}_2\text{OH})_2$	$\leq 1 \times 10^5$	
triethylamine	$\leq 3 \times 10^{4c}$	$\leq 3 \times 10^{4c}$

We have also measured rate constants for the reactions of  $\text{CCl}_3\text{O}_2$  with three unsaturated alcohols in both methanol and water (Table III).

**Table III.** Rate Constants for Reaction of  $\text{CCl}_3\text{O}_2$  with Unsaturated Alcohols

Substrate	k, L mol <sup>-1</sup> s <sup>-1</sup>	
	$\text{H}_2\text{O}$ :2-PrOH: $\text{CCl}_4$ (90:10:0.1)	Methanol: $\text{CCl}_4$ (9:1)
2-buten-1-ol	$9.0 \times 10^4$	$2.6 \times 10^4$
3-methyl-3-buten-1-ol	$3.8 \times 10^5$	$5.0 \times 10^4$
3-methyl-2-buten-1-ol	$6.8 \times 10^5$	$1.6 \times 10^5$

**Discussion.** The rate constant for the addition of  $(\text{CH}_3)_3\text{CO}_2$  to 2,3-dimethyl-2-butene in benzyl chloride is  $22 \text{ L mol}^{-1}\text{s}^{-1}$  [11]. Substitution of halogens for  $\text{CH}_3$ - groups clearly results in a tremendous activation of the peroxy radical toward addition. We found no particular correlation of the reactivity with any of the usual solvent parameters. The very low results for the reactions in ethylene glycol and triethylamine are surprising. We note that the former solvent is highly viscous and the latter is a very strong base. From these results, however, we do not yet know the reactivity of halogenated peroxy radicals towards alkenes in the *gas phase*. There are a few reactions of alkenes which have been investigated in both the gas and liquid phases. In Tables IV and V, we compare reported results for the reactions of  $\text{O}_3$  in  $\text{CCl}_4$  and  $\text{NO}_3$  in  $\text{CH}_3\text{CN}$  with the gas-phase results.

**Table IV.** Rate constants for reactions of  $\text{O}_3$  with alkanes in  $\text{CCl}_4$  and in the gas-phase

Substrate	$k \times 10^3 \text{ (L mol}^{-1} \text{ s}^{-1}\text{)}$	
	$\text{CCl}_4$ [12]	gas phase [13]
Ethene	25	1.0
Propene	80	6.4
1-Butene	79 <sup>a</sup>	6.2
2-Methylpropene	97	7.0
<i>cis</i> -2-Butene	163	76
<i>trans</i> -2-Butene		106
2-Methyl-2-butene	167	239
2,3-Dimethyl-2-butene	200	634

a. for 1-pentene and 1-hexene

**Table V** Rate constants for reactions of  $\text{NO}_3\cdot$  radicals with alkanes, alkenes, and arenes in acetonitrile and in the gas-phase

Substrate	k ( $\text{L mol}^{-1} \text{s}^{-1}$ )	
	$\text{CH}_3\text{CN}$ [14]	gas phase [15]
n-hexane	$5.9 \times 10^5$	$6.3 \times 10^4$
cyclohexane	$1.0 \times 10^6$	$8.1 \times 10^4$
methylcyclohexane	$1.6 \times 10^6$	
2-chloropropane	$2.7 \times 10^4$	
1-hexene	$2.7 \times 10^8$	
<i>trans</i> -2-hexene	$1.5 \times 10^9$	
2-butene		$2.3 \times 10^8$
2,3-dimethyl-2-butene	$3.5 \times 10^9$	$2.8 \times 10^{10}$
cyclopentene	$2.9 \times 10^9$	$2.7 \times 10^8$
cyclohexene	$3.1 \times 10^9$	$3.2 \times 10^8$
cycloheptene	$4.8 \times 10^9$	$2.9 \times 10^8$
<i>trans</i> -1,2-dichloroethylene	$1.7 \times 10^7$	$6.7 \times 10^4$
trichloroethylene	$2.0 \times 10^7$	$1.8 \times 10^5$
tetrachloroethylene	$9.9 \times 10^6$	$< 3 \times 10^4$
toluene	$8.8 \times 10^7$	$4.7 \times 10^4$
ethylbenzene	$1.2 \times 10^8$	$\leq 4 \times 10^5$
isopropylbenzene	$2.3 \times 10^7$	

For the reactions of  $\text{O}_3$  with alkenes, the rate constants are initially lower in the gas phase than in the liquid phase; as the reactivity of the alkene increases, however, the rate constant becomes greater in the gas phase than in the liquid phase. For the  $\text{NO}_3$  reactions, the rate constants are less in the gas phase, up to the reaction of  $\text{NO}_3$

with 2,3-dimethyl-2-butene. As the reactivity increases, the ratio of the rate constants ( $k_{ACN}/k_{gas}$ ) decreases. These results suggest that the gas phase rate constants for the reactions of the halogenated peroxy radicals with the more reactive alkenes will be near, or even greater than, the liquid phase values.

#### References

1. Huie, R. E. and Neta, P. *Int. J. Chem. Kinet.*, **18**, 1185 (1986).
2. Brault, D., Neta, P., and Patterson, L. K. *Chem. -Biol. Interact.*, **54**, 289 (1985).
3. Mosseri, S., Alfassi, Z. B., and Neta, P. *Int. J. Chem. Kinet.*, **19**, 309 (1987).
4. Alfassi, Z. B., Mosseri, S., and Neta, P. *J. Phys. Chem.*, **91**, 3383 (1987).
5. Neta, P., Huie, R. E., Mosseri, S., Shastri, L. T. V., Mittal, J. P., Maruthamuthu, P. and Steenken, S. *J. Phys. Chem.*, **93**, 4099 (1989).
6. Neta, P., Huie, R. E., Maruthamuthu, P., and Steenken, S. *J. Phys. Chem.*, **93**, 7654 (1989).
7. Nahor, G and Neta, P. *Int. J. Chem. Kinet.*, **23**, 941 (1991).
8. Alfassi, Z. B., Huie, R. E., Kumar, M., and Neta, P. *J. Phys. Chem.*, **96**, 767 (1992).
9. Taft, R. W., Jr. in Steric Effects in Organic Chemistry, M. S. Newman, ed., Wiley, New York, 1956, p. 619.
10. Howard, J. A.; Scaiano, J. C. in Landolt-Börnstein Numerical Data and Functional Relationships in Science and Technology. New Series, Group II: Atomic and Molecular Physics, Hellwege, K.-H.; Madelung, O., eds., Springer-Verlag, Berlin, 1984, Vol. 13, Fischer, H., ed., Part D.
11. Koelewijn, P. *Rec. Trav. Chim. Pays-Bas*, **91**, 1275 (1972).
12. Williamson, D. G. and Cvetanović, R. J. *J. Am. Chem. Soc.*, **90**, 3668 (1969).
13. Huie, R. E. and Herron, J. T. *Int. J. Chem. Kinet., Symp.* **1**, 165 (1975).
14. Alfassi, Z. B., Padmaja, S., Neta, P., and Huie, R. E., *J. Phys. Chem.*, in press.
15. Wayne, R.P.; Barnes, I.; Biggs, P.; Burrows, J. P.; Canosa-Mas, C. E.; Hjorth, J.; LeBras, G.; Moortgaat, G. K.; Perner, D.; Poulet, G.; Restelli, G.; Sidebottom, H. *The Nitrate Radical, Physics, Chemistry and the Atmosphere*, Air Pollution Research Report 31, Commission of the European Community, 1990 (also published as *Atmos. Environ.* **1991**, *25A*, 1).

*The Kinetics and Mechanisms of Processes Involved in the Atmospheric Degradation of Hydrochlorofluorocarbons and Hydrofluorocarbons*

G D HAYMAN

Chemical Kinetics Section  
AEA Consultancy Services  
Building 551  
Harwell Laboratory  
Didcot, Oxon, OX11 0RA  
United Kingdom

**Introduction**

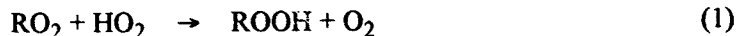
Under the terms of the Copenhagen amendment to the Montreal Protocol, the production of fully-halogenated chlorofluorocarbons (CFCs) will cease from the beginning of 1995. The chemical industry has identified a number of substitute compounds with similar physico-chemical properties to the CFCs being phased-out. The replacement compounds - the hydrochlorofluorocarbons (HCFCs) and hydrofluorocarbons (HFCs) - have been assessed [1,2] and are predicted to cause significantly less (HCFCs) or no stratospheric ozone depletion (HFCs) compared to the CFCs, as well as being less active as Greenhouse gases, both these features a result of the shorter residence times of the substitute compounds in the atmosphere.

The shorter lifetime results from the presence of hydrogen in the molecule which makes them susceptible to attack by OH radicals in the troposphere, a fate not open to the CFCs. As the oxidation of the HCFCs and HFCs occurs primarily in the troposphere, it is important to define the subsequent reaction pathways occurring following attack by OH radicals and to identify and quantify the yields of products formed in the degradation of the HCFC or HFC. These data will be used to address issues such as

- (1) the identity of the products deposited to ground, and,
- (2) whether chlorine present in the degradation products formed from the HCFCs in the troposphere could be transported to the stratosphere,

so that a full assessment of the potential environmental effects of using HCFCs and HFCs can be made.

In this paper, experimental studies on the kinetics and mechanisms of processes occurring in the atmospheric degradation of HFC-134a ( $\text{CF}_3\text{CH}_2\text{F}$ ) and HCFC-142b ( $\text{CF}_2\text{ClCH}_3$ ) are reported. The laser flash photolysis technique has been used to determine room-temperature rate coefficients for the reactions of the atmospheric radical,  $\text{HO}_2$  with the peroxy radicals derived from HCFC-142b ( $\text{CF}_2\text{ClCH}_2\text{O}_2$ ) and HFC-134a, ( $\text{CF}_3\text{CHFO}_2$ ).



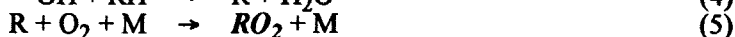
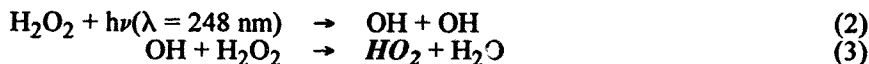
where  $\text{R} = \text{CF}_2\text{ClCH}_2$  (from HCFC-142b) and  $\text{CF}_3\text{CHF}$  (from HFC-134a).

In a separate set of experiments, the mechanism of the degradation of HCFC-142b has been investigated using long pathlength FT-IR spectroscopy.

**Experimental**

**(a) The Laser Flash Photolysis Apparatus**

The laser flash photolysis technique with UV absorption detection has been described in a number of recent papers [3,4]. The present experiments utilised the 248 nm laser photolysis of mixtures containing  $\text{H}_2\text{O}_2$ , HCFC-142b or HFC-134a,  $\text{O}_2$  and  $\text{N}_2$ . The peroxy radicals of interest were generated in the following reaction sequence.



Transient absorption traces were recorded following the laser flash using a storage oscilloscope and transferred to a microcomputer. The individual absorption traces were co-added to improve the signal-to-noise ratio before subsequent storage and analysis on the microcomputer.

As the absorption cross-sections of both HCFC-142b and HFC-134a are small in the wavelength region from 220 to 250 nm [1], the concentrations of HFC-134a and HCFC-142b in the reaction mixture were calculated by noting the reduction in the  $\text{H}_2\text{O}_2$  absorption at 220 or 230 nm as the reaction mixture was diluted on addition of the freon. The concentration of the freon could also be determined from the volumetric flows of the reagents used but this was less reliable. The two methods gave concentrations which agreed within 15%.

The experiments undertaken with the HFC-134a reaction system used concentrations of HFC-134a in the range from 0.5 to  $10.0 \times 10^{18}$  molecule  $\text{cm}^{-3}$ , concentrations of  $\text{O}_2$  between  $0.1$  and  $2.4 \times 10^{19}$  molecule  $\text{cm}^{-3}$  with  $\text{N}_2$  added as necessary to ensure the total pressure in the cell was atmospheric pressure. There was less freedom to vary the  $\text{H}_2\text{O}_2$  concentrations and experiments were conducted with  $\text{H}_2\text{O}_2$  concentrations between  $2.0$  to  $3.5 \times 10^{16}$  molecule  $\text{cm}^{-3}$ . In the HCFC-142b experiments, the concentrations of HCFC-142b used were between  $3.0$  to  $5.5 \times 10^{18}$  molecule  $\text{cm}^{-3}$ , the  $\text{O}_2$  concentration was altered between  $0.7$  and  $2.5 \times 10^{18}$  molecule  $\text{cm}^{-3}$  with  $\text{N}_2$  again added as the diluent.

In both reaction systems, the relative concentrations of  $\text{H}_2\text{O}_2$  and the freon (HFC-134a or HCFC-142b) used, together with the reactivity of these compounds towards OH radicals indicated that  $\text{HO}_2$  would be produced in larger concentrations than those of the  $\text{RO}_2$  radical. This ensures that the major loss process for the  $\text{RO}_2$  radicals is reaction with  $\text{HO}_2$  (1) and the self-reactions of the  $\text{RO}_2$  radicals (6) are reduced in importance.



#### (b) *The Long Pathlength FT-IR Spectrometer*

The experiments undertaken to investigate the degradation mechanism of HCFC-142b used long pathlength infrared absorption spectroscopy. Mixtures containing  $\text{Cl}_2/\text{HCFC-142b}/\text{O}_2/\text{N}_2$  were added from a gas manifold to a reaction vessel, 15 cm in diameter and 100 cm in length. Infrared transmission spectra of the gases present in the reaction vessel were recorded using a FT-IR spectrometer (Mattson Galaxy 4020,  $1 \text{ cm}^{-1}$  resolution). The strength of the absorption bands due to the parent HCFC meant that the shortest pathlength possible was used (4 passes, pathlength = 320 cm).

Initially, mixtures containing no HCFC-142b were admitted into the reaction vessel and a transmission spectrum recorded. This was used as the reference spectrum for the particular experimental run. HCFC-142b was then added to the reaction mixtures and after allowing the system to stabilise, the cell was isolated and a second transmission spectrum was recorded. The two spectra were ratioed to give an absorption spectrum corresponding to that of HCFC-142b.

The mixture in the reaction vessel was irradiated for set periods of time at 350 nm using up to 6 blacklight fluorescent tubes. After each exposure period, the blacklights were switched off and a new transmission spectrum recorded. The transmission spectra were ratioed to that recorded with no HCFC-142b present to give the corresponding composite absorption spectra.

A number of experiments were conducted using different initial concentrations of the reagents.

$$\begin{aligned} [\text{HCFC-142b}] &= (0.1-27.0) \times 10^{17} \text{ molecule cm}^{-3} \\ [\text{Cl}_2] &= (2.0-4.5) \times 10^{16} \text{ molecule cm}^{-3} \\ [\text{O}_2] &= (0.9-24.0) \times 10^{18} \text{ molecule cm}^{-3} \\ [\text{N}_2] &= (0.4-24.0) \times 10^{18} \text{ molecule cm}^{-3} \end{aligned}$$

Most of the experiments used concentrations of HCFC-142b which were 100 times greater than those of Cl<sub>2</sub> so that the initial stages of the degradation could be investigated. However, a number of experiments were undertaken in which the initial concentration of Cl<sub>2</sub> was greater than that of HCFC-142b so that significant oxidation of HCFC-142b to final products resulted.

### Samples

The sample of HFC-134a was supplied by ICI plc at a stated purity of 99.6%. An analysis was provided with the sample which indicated that the major impurity was HFC-134. The HCFC-142b sample was supplied by Solvay at a stated purity of >99.99% with the major impurity being CClF=CH<sub>2</sub> (7 ppmv).

### Results

#### (a) The Laser Flash Photolysis Experiments - The Kinetics of the Reaction, RO<sub>2</sub> + HO<sub>2</sub>

Transient absorption profiles were recorded at 220, 230 and 240 nm following the 248 nm laser flash photolysis of H<sub>2</sub>O<sub>2</sub>/HCFC-142b or HFC-134a/O<sub>2</sub>/N<sub>2</sub> mixtures. The wavelengths used correspond to wavelengths where the various peroxy radicals, HO<sub>2</sub> [5] and CF<sub>3</sub>CHFO<sub>2</sub> [5-8] or CF<sub>2</sub>ClCH<sub>2</sub>O<sub>2</sub> [5,6,9] are known to absorb. Figure 1 shows the composite absorption profiles recorded using the HFC-134a reaction system.

Table 1 - Reaction Mechanism Used to Derive the Kinetic Data for the Reaction CF<sub>3</sub>CHFO<sub>2</sub> + HO<sub>2</sub>

Reaction	Rate Expression	Ref.
H <sub>2</sub> O <sub>2</sub> + hv (λ = 248 nm) → OH + OH	instantaneous	
OH + H <sub>2</sub> O <sub>2</sub> → HO <sub>2</sub> + H <sub>2</sub> O	1.7x10 <sup>-12</sup>	[10]
OH + RH (R=CF <sub>3</sub> CHF) → RO <sub>2</sub> + H <sub>2</sub> O	4.8x10 <sup>-15</sup>	[10]
RO <sub>2</sub> + RO <sub>2</sub> → RO + RO + O <sub>2</sub>	6.0x10 <sup>-12</sup>	[8]
RO <sub>2</sub> + RO <sub>2</sub> → CF <sub>3</sub> COF + CF <sub>3</sub> CHFOH + O <sub>2</sub>	1.0x10 <sup>-12</sup>	[8]
RO + O <sub>2</sub> → CF <sub>3</sub> COF + HO <sub>2</sub>	9.0x10 <sup>-16</sup>	[8,11]
RO (+O <sub>2</sub> ) → CF <sub>3</sub> O <sub>2</sub> + HO <sub>2</sub>	2.1x10 <sup>4</sup>	[8]
CF <sub>3</sub> O <sub>2</sub> + CF <sub>3</sub> O <sub>2</sub> → CF <sub>3</sub> O + CF <sub>3</sub> O + O <sub>2</sub>	3.1x10 <sup>-12</sup>	[8]
CF <sub>3</sub> O <sub>2</sub> + CF <sub>3</sub> CHFO <sub>2</sub> → CF <sub>3</sub> O + CF <sub>3</sub> C'FO + O <sub>2</sub>	8.0x10 <sup>-12</sup>	[8]
CF <sub>3</sub> O + RH → RO <sub>2</sub> + CF <sub>3</sub> OH	1.1x10 <sup>-15</sup>	[12]
CF <sub>3</sub> O + H <sub>2</sub> O <sub>2</sub> → HO <sub>2</sub> + CF <sub>3</sub> OH	set to k[OH+H <sub>2</sub> O <sub>2</sub> ]	[10]
HO <sub>2</sub> + HO <sub>2</sub> → H <sub>2</sub> O <sub>2</sub> + O <sub>2</sub>	3.5x10 <sup>-12</sup> to allow for the high [HFC] used	[13]
RO <sub>2</sub> + HO <sub>2</sub> → products	optimised	
CF <sub>3</sub> O <sub>2</sub> + HO <sub>2</sub> → CF <sub>3</sub> OOH + O <sub>2</sub>	2.0x10 <sup>-12</sup> , from present analysis	

The analysis of these datasets was undertaken using numerical integration of an assumed reaction mechanism (see table 1 above for the mechanism used for HFC-134a). The sources of the kinetic and mechanistic parameters are given in the table. There is some disagreement in the literature concerning the UV absorption cross-sections of CF<sub>3</sub>CHFO<sub>2</sub> [5-8] and CF<sub>2</sub>ClCH<sub>2</sub>O<sub>2</sub> [5,6,9]. In this study, the cross-sections determined at Risø are used for the two radicals [7,9]. In the case of HFC-134a, there is supporting evidence from the Ford group [8] that the higher values should be preferred.

Table 2 summarises the kinetic results obtained for reaction (7) following the analysis of the experimental datasets recorded using the numerical integration program, *FACSIMILE* [14].



Table 2 - Kinetic Data Obtained for  $\text{CF}_3\text{CHFO}_2 + \text{HO}_2$  at  $(296 \pm 2)\text{K}$

	$10^{-18}$ [HFC-134a] /molecule $\text{cm}^{-3}$	$10^{12}$ Rate Coefficient / $\text{cm}^3$ molecule $^{-1}$ $\text{s}^{-1}$
Sample 1 (500g, 99.6%)	2.0 ( $\text{N}_2$ carrier)	$4.5 \pm 1.6$
	0.4 ( $\text{N}_2$ )	$11.8 \pm 8.0^*$
	0.5 ( $\text{N}_2$ )	$3.3 \pm 2.2$
Sample 2 (9.5kg, 99.6%)	1.7 ( $\text{N}_2$ )	$2.7 \pm 0.7$
	3.1 ( $\text{N}_2$ )	$2.7 \pm 0.7$
	4.7 ( $\text{N}_2$ )	$4.4 \pm 2.4$
Sample 3 (9.5kg, 99.6%)	2.7 ( $\text{N}_2$ )	$6.8 \pm 1.8$
	4.0 ( $\text{N}_2$ )	$4.4 \pm 0.6$
	4.2 ( $\text{O}_2$ )	$4.4 \pm 0.8$
	10.7 ( $\text{O}_2$ )	$2.3 \pm 1.0$
	7.3 ( $\text{O}_2$ )	$3.2 \pm 0.9$
Weighted mean ( $\pm 1\sigma$ , excluding high value *)		$4.1 \pm 1.1$

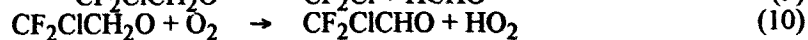
A weighted mean of the individual results (excluding the high value) gives the following room-temperature rate coefficients where the errors represent two standard deviations and include the uncertainties in the reported cross-sections.

$$k_7 = (4.1 \pm 2.2) \times 10^{-12} \text{ cm}^3 \text{ molecule}^{-1} \text{ s}^{-1}$$

The analysis indicated that the rate coefficient for the reaction between  $\text{CF}_3\text{O}_2$  and  $\text{HO}_2$  (8) was slower than that derived for the reaction between  $\text{CF}_3\text{CHFO}_2$  and  $\text{HO}_2$ . An upper limit of  $2 \times 10^{-12} \text{ cm}^3 \text{ molecule}^{-1} \text{ s}^{-1}$  was determined for  $k_8$ .



Only a limited set of experiments were conducted on the HCFC-142b reaction system. An assumed reaction mechanism (not given) was used to analyse the experimental data. It was assumed in the analysis that the oxy radical,  $\text{CF}_2\text{ClCH}_2\text{O}$ , did not undergo thermal decomposition (9) but reacted with  $\text{O}_2$  to give  $\text{HO}_2$  (10) as suggested by presentations made at this workshop [15,16].



The results of the numerical modelling analysis gave a rate coefficient for reaction (11)



of  $k_{11} = (6.9 \pm 2.6) \times 10^{-12} \text{ cm}^3 \text{ molecule}^{-1} \text{ s}^{-1}$ .

(b) *The FT-IR Experiments - The Degradation Mechanism of HCFC-142b*

Absorption spectra were recorded at specific times during the 350 nm photolysis of  $\text{Cl}_2/\text{HCFC-142b}/\text{O}_2/\text{N}_2$  mixtures. The spectra were dominated by the absorption bands due to HCFC-142b and a significant part of the absorption spectrum was obscured. However, it was apparent that, although the intensity of the HCFC-142b did not change during the course of the photolysis experiments, new absorption bands were being formed. Figures 2a and 2b show the composite absorption spectra recorded after 4500 s for experiments conducted at low and high  $\text{O}_2$  concentrations. Table 3 lists the new absorption features seen with assignments (bands due to HCFC-142b are not included).

Table 3 - *Absorption Features Observed during the 350 nm Photolysis of  $\text{Cl}_2/\text{HCFC-142b}/\text{O}_2/\text{N}_2$  Mixtures (excluding HCFC-142b bands)*

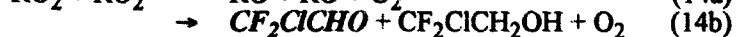
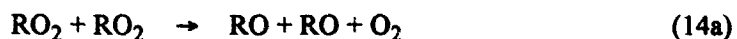
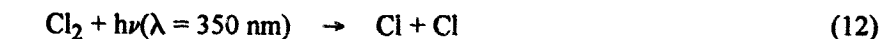
(a) Experiments Undertaken at low  $[\text{O}_2]$  ( $1.0 \times 10^{18}$  molecule  $\text{cm}^{-3}$ )

Wavenumber of band ( $\text{cm}^{-1}$ )	Assignment	Ref.
774 and 1942	$\text{COF}_2$	[17]
1818 and 3580	$\text{CF}_2\text{ClCOOH}$	[18]
2143	$\text{CO}$	[17]
2349	$\text{CO}_2$	[17]
2885	$\text{HCl}$	[17]

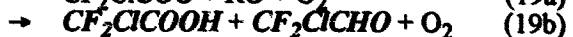
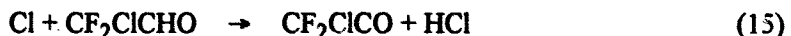
(b) Experiments Undertaken at high  $[\text{O}_2]$  ( $2.4 \times 10^{19}$  molecule  $\text{cm}^{-3}$ )

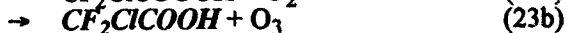
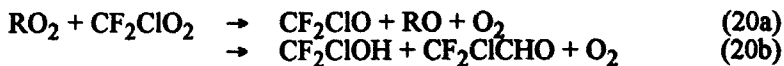
Wavenumber of band ( $\text{cm}^{-1}$ )	Assignment	Ref.
774 and 1942	$\text{COF}_2$	[17]
1778	$\text{CF}_2\text{ClCHO}$	[19]
1818 and 3580	$\text{CF}_2\text{ClCOOH}$	[18]
2143	$\text{CO}$	[17]
2349, 3609 and 3716	$\text{CO}_2$	[17]
2885	$\text{HCl}$	[17]

The origin of the product absorption bands observed can be rationalised as follows. The Cl-initiated oxidation of HCFC-142b, by analogy with the reactions of simple hydrocarbons, leads to the formation of the peroxy radical,  $\text{CF}_2\text{ClCH}_2\text{O}_2$ , (reactions 12, 13, 5) and the first stable product,  $\text{CF}_2\text{ClCHO}$ , by the reaction sequence (14a, b), (10).



As the reaction of Cl atoms with HCFC-142b (13) is relatively slow [9], significant oxidation of  $\text{CF}_2\text{ClCHO}$  occurs [reactions (15) to (23)] leading to the end oxidation product,  $\text{COF}_2$ .





CO was observed in the composite absorption spectrum which could provide evidence for the thermal decomposition of the oxy radical,  $\text{CF}_2\text{ClCH}_2\text{O}$ , reaction (9). If this were the case, CO would be formed from the oxidation of HCHO [reactions (24) and (25)].



There was no evidence for the formation of HCHO. This might arise because its concentration was suppressed by its rapid oxidation by Cl atoms. However, papers presented at this workshop [15,16] have indicated that the oxy radical,  $\text{CF}_2\text{ClCH}_2\text{O}$ , does not decompose significantly at low pressures (*i.e.* reaction (9) does not seem to occur) and CO could be formed from the thermal decomposition of the radical,  $\text{CF}_2\text{ClCO}$ , reaction (26) [20]. Decomposition of  $\text{CF}_2\text{ClCO}$  would be in competition with its reaction with  $\text{O}_2$  (reaction 16).



Reactions (16) and (26) are consistent with the observed decrease in yield of CO as the  $\text{O}_2$  concentration was increased. In addition, the yield of  $\text{CF}_2\text{ClCOOH}$  was found to increase if higher  $[\text{O}_2]$  concentration were used which suggested that more  $\text{CF}_2\text{ClCOO}_2$  radicals were present under these conditions. At this stage, a qualitative interpretation of the spectral data is not able to distinguish between one or the other of the reaction pathways (or indeed both) giving rise to the CO observed.

### Discussion and Atmospheric Implications

#### (a) Kinetics Study of the Reaction, $\text{RO}_2 + \text{HO}_2$

These measurements represent the first determination of the kinetics of the reactions between  $\text{HO}_2$  and  $\text{RO}_2$  radicals derived from HFC-134a and HCFC-142b. The rate coefficients have similar magnitudes to the corresponding rate coefficients for the reactions between  $\text{CH}_3\text{O}_2$  and  $\text{HO}_2$  [5] or  $\text{C}_2\text{H}_5\text{O}_2 + \text{HO}_2$  [5]. The importance of these reactions with  $\text{HO}_2$  in the troposphere depends on the magnitude of the rate coefficients for reaction of the peroxy radicals with NO and  $\text{HO}_2$  and the ambient concentrations of NO and  $\text{HO}_2$ . The tropospheric abundances of  $\text{HO}_2$  and NO are very similar. As the rate coefficient for reaction of  $\text{RO}_2$  with NO for these radicals is about three times greater at room temperature [18,21,22] than that determined in this work for the rate coefficient for reaction with  $\text{HO}_2$ , the dominant loss reaction for  $\text{RO}_2$  radicals is *via* reaction with NO.

The temperature dependencies of the reactions of  $\text{RO}_2$  with both  $\text{HO}_2$  and NO are not known. If the temperature-dependent parameters given for the reactions of  $\text{CH}_3\text{O}_2$  with  $\text{HO}_2$  and NO are considered [5], the reaction of  $\text{RO}_2$  with  $\text{HO}_2$  would become progressively more important as the temperature is lowered.

The products of the reaction of  $\text{RO}_2$  radicals with  $\text{HO}_2$  are expected to be hydroperoxides, ROOH, which are photo-oxidants. The fate of the hydroperoxide is reaction with OH, photolysis or physical deposition to the ground. The relative efficiency of these three processes determines the atmospheric effect of the  $\text{RO}_2 + \text{HO}_2$  reaction. Deposition of the

hydroperoxide to the ground or reaction of the hydroperoxide with OH radicals leads to net loss of HO<sub>x</sub> from the atmosphere. Photolysis leads to the same reaction product as if the peroxy radical had reacted with NO and converts the HO<sub>2</sub> radical into OH.

If a molecular channel exists for the reaction of CF<sub>3</sub>CHFO<sub>2</sub> with HO<sub>2</sub>, then this could be a source of CF<sub>3</sub>COF - a precursor to trifluoroacetic acid - in low-NO<sub>x</sub> environments. Further studies are needed to determine the products of this reaction.



#### (b) *Degradation Mechanism of HCFC-142b*

Previous studies by Edney and Driscoll [23] and Tuazon and Atkinson [24] used low concentrations of HCFC-142b which resulted in the quantitative conversion of HCFC-142b into COF<sub>2</sub>. No definitive information could be derived on the exact mechanism leading to the formation of COF<sub>2</sub>. The thrust of the present study was to determine the extent to which the oxy radical, CF<sub>2</sub>ClCH<sub>2</sub>O, thermally decomposed (9) or reacted with O<sub>2</sub> (10) so as to deduce the partitioning between C<sub>1</sub>- and C<sub>2</sub>-containing products. This would allow the route(s) leading to COF<sub>2</sub> to be determined. It was unfortunately apparent, even in these experiments, that the limited range of concentrations of HCFC-142b which could be used together with the low reactivity of HCFC-142b towards Cl-atoms has meant that significant oxidation of the intermediate products has occurred.

It is clear that a quantitative analysis of the spectral data is required to define the reaction mechanism more precisely and so identify the route leading to the formation of COF<sub>2</sub>. The exact route is important because the more COF<sub>2</sub> formed following the thermal decomposition of the oxy radical, CF<sub>2</sub>ClCH<sub>2</sub>O, reaction (9), the smaller will be the yield of C<sub>2</sub>-containing products such as CF<sub>2</sub>ClCHO. The yield of CF<sub>2</sub>ClCHO and its oxidation determine the abundance of the PAN-type species, CF<sub>2</sub>ClCOO<sub>2</sub>NO<sub>2</sub>, which, when formed in the upper troposphere, is sufficiently long lived for it to be transported into the stratosphere. Once in the stratosphere, these PAN species can release their chlorine and so cause ozone loss.

Many of the reaction products predicted by the above mechanism were not observed due to the greater reactivity of these compounds to Cl atoms compared to the parent HCFC. However, the production of CF<sub>2</sub>ClCOOH *via* a homogeneous gas-phase mechanism is of interest as it potentially represents a source of halogenated acetic acids in the atmosphere in addition to those formed by hydrolysis of halogenated acetyl halides such as CF<sub>3</sub>COCl and CF<sub>3</sub>COF. Quantitative analysis of the IR data is required so that the source of CF<sub>2</sub>ClCOOH can be identified and the significance of these laboratory observations for the atmosphere can be assessed.

#### *Acknowledgements*

The author gratefully acknowledges the support for this work provided by the following organisations: the *Alternative Fluorocarbons Environmental Acceptability Study* (CTR92-35/P91-086), the Commission of the European Communities (EV5V-CT91-0024) and the UK Department of the Environment (PECD 7/12/81).

I am grateful to Archie McCulloch (ICI plc) for the provision of the sample of HFC-134a and to Dr James Franklin for the sample of HCFC-142b used in this work.

#### *References*

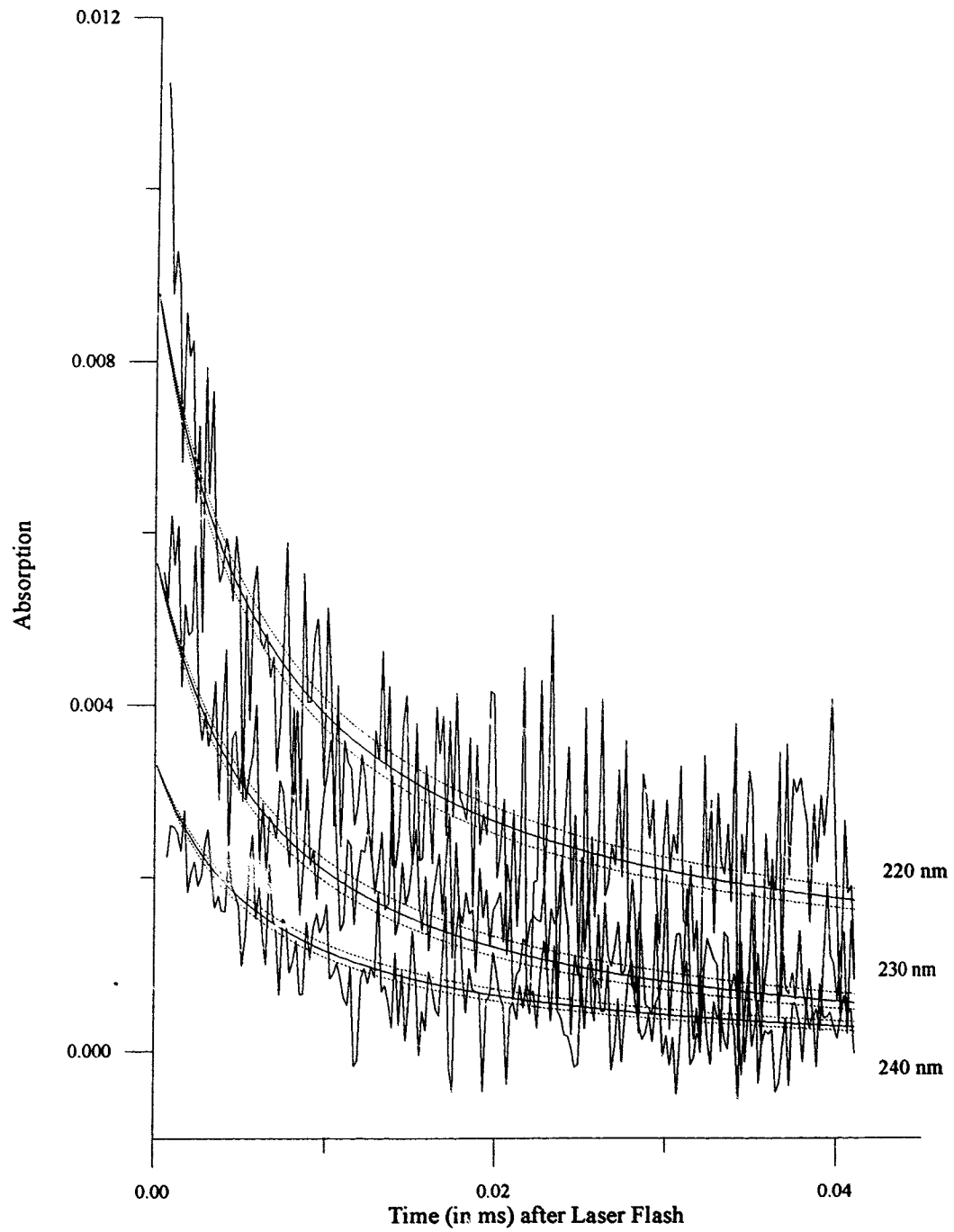
- [1] *Scientific Assessment of Stratospheric Ozone : 1989 (1990)* World Meteorological Organisation Report Number 20, Volume II - AFEAS Report, World Meteorological Organisation, Geneva, Switzerland.
- [2] *Scientific Assessment of Ozone Depletion: 1991 (1992)* World Meteorological Organisation Report Number 25, World Meteorological Organisation, Geneva, Switzerland.

- [3] Murrells, T P, Jenkin, M E, Shalliker, S J and Hayman, G D, *Laser Flash Photolysis Study of the UV Spectrum and Kinetics of Reactions of HOCH<sub>2</sub>CH<sub>2</sub>O<sub>2</sub> Radicals*, Journal of the Chemical Society, Faraday Transactions 87 (1991) 2351-2360.
- [4] Jenkin, M E, Murrells, T P, Shalliker, S J and Hayman, G D, *Kinetics and Product Study of the Self-Reactions of Allyl and Allylperoxy Radicals at 296 K*, Journal of the Chemical Society, Faraday Transactions 89 (1993) 433-446.
- [5] Lightfoot, P D, Cox, R A, Crowley, J N, Destriau, M, Hayman, G D, Jenkin, M E, Moortgat, G K, and Zabel, F, *Atmospheric Environment* 26A (1992) 1805-1961.
- [6] Jemi-Alade, A A, Lightfoot, P D, and Lesclaux, R, *Chemical Physics Letters* 179, (1991) 119-124.
- [7] Wallington, T J, and Nielsen, O J, *Chemical Physics Letters* 187 (1991) 33-39.
- [8] Maricq, M M, and Sente, J J, *Journal of Physical Chemistry* (1992) submitted for publication.
- [9] Wallington, T J, and Nielsen, O J, *International Journal of Chemical Kinetics* 23 (1991) 785-798.
- [10] DeMore, W B, Molina, M J, Sander, S P, Golden, D M, Hampson, R F, Kurylo, M J, Howard, C J, and Ravishankara, A R, *JPL Publication 92-20* (1992) Jet Propulsion Laboratory, Pasadena, California, USA.
- [11] Wallington, T J, Hurley, M D, Ball, J C, and Kaiser, E W, *Environmental Science and Technology* 26 (1992) 1318-1324.
- [12] Sehested, J, and Wallington, T J, *Journal of Physical Chemistry* (1992) submitted for publication.
- [13] Atkinson, R, Baulch, D L, Cox, R A, Hampson, R F, Kerr, J A, and Troe, J, *Atmospheric Environment* 26A (1992) 1187-1230.
- [14] Curtis, A R, and Sweetenham, W P, *FACSIMILE/CHEKMAT Users Manual*. (1988) AERE-R12805, Harwell Laboratory, Oxfordshire, UK.
- [15] Pultau, V, and Peeters, J, Paper presented at this workshop.
- [16] Zellner, R, Hoffman, A, Mors, V, and Malms, W, Paper presented at this workshop.
- [17] Herzberg, G, *Infrared and Raman Spectroscopy of Polyatomic Molecules*, (1945) Van Nostrand Reinhold, New York.
- [18] The bands occur in a similar position to those of CF<sub>3</sub>COOH as given in the gas-phase EPA FT-IR library.
- [19] Rattigan, O, *private communication*.
- [20] Barnes, I, Becker, K H, Kirchner, F, Zabel, F, Richter, Sodeau, J R, Paper presented at this workshop.
- [21] Nielsen, O J, Sehested, J, Ellerman, T, and Wallington, T J, Paper presented at this workshop.
- [22] Bevilacqua, T J, Hanson, D R, Jensen, N R, and Howard, C J, Paper presented at this workshop.
- [23] Edney, E O, and Driscoll, D J, *International Journal of Chemical Kinetics* 24 (1992) 1067-1081.
- [24] Tuazon, E, and Atkinson, R, Pages 88-93 of the Proceedings of the CEC/AFEAS workshop held in Dublin, May 1991.

### Figure Captions

- Figure 1 Transient absorption profiles recorded at 220, 230 and 240 nm following the 248 nm excimer laser photolysis of H<sub>2</sub>O<sub>2</sub>/HFC-134a/O<sub>2</sub>/N<sub>2</sub> mixtures. The full line is a simulation using the optimised rate coefficient and the dotted lines correspond to a change in the rate coefficient by  $\pm 2.0 \times 10^{-12}$  cm<sup>3</sup> molecule<sup>-1</sup> s<sup>-1</sup>.
- Figure 2 The FT-IR absorption spectrum recorded prior to (figure 2a) and after 4500s (figure 2b) of photolysis at 350 nm of Cl<sub>2</sub>/HCFC-142b/O<sub>2</sub>/N<sub>2</sub> mixtures. The experiment used the following initial concentrations (in molecule cm<sup>-3</sup>): [HCFC-142b] =  $2.7 \times 10^{18}$ ; [Cl<sub>2</sub>] =  $2.4 \times 10^{16}$ ; [O<sub>2</sub>] =  $2.1 \times 10^{19}$  and [N<sub>2</sub>] =  $4.6 \times 10^{17}$ . Note the appearance of the band at 1778 cm<sup>-1</sup> due to CF<sub>2</sub>ClCHO and the absorptions due to CF<sub>2</sub>ClCOOH which were more pronounced in this experiment using a high [O<sub>2</sub>].

Figure 1



0 0 9 3

Figure 2a

Pre-photolysis Infrared Absorption Spectrum of HCFC-142b

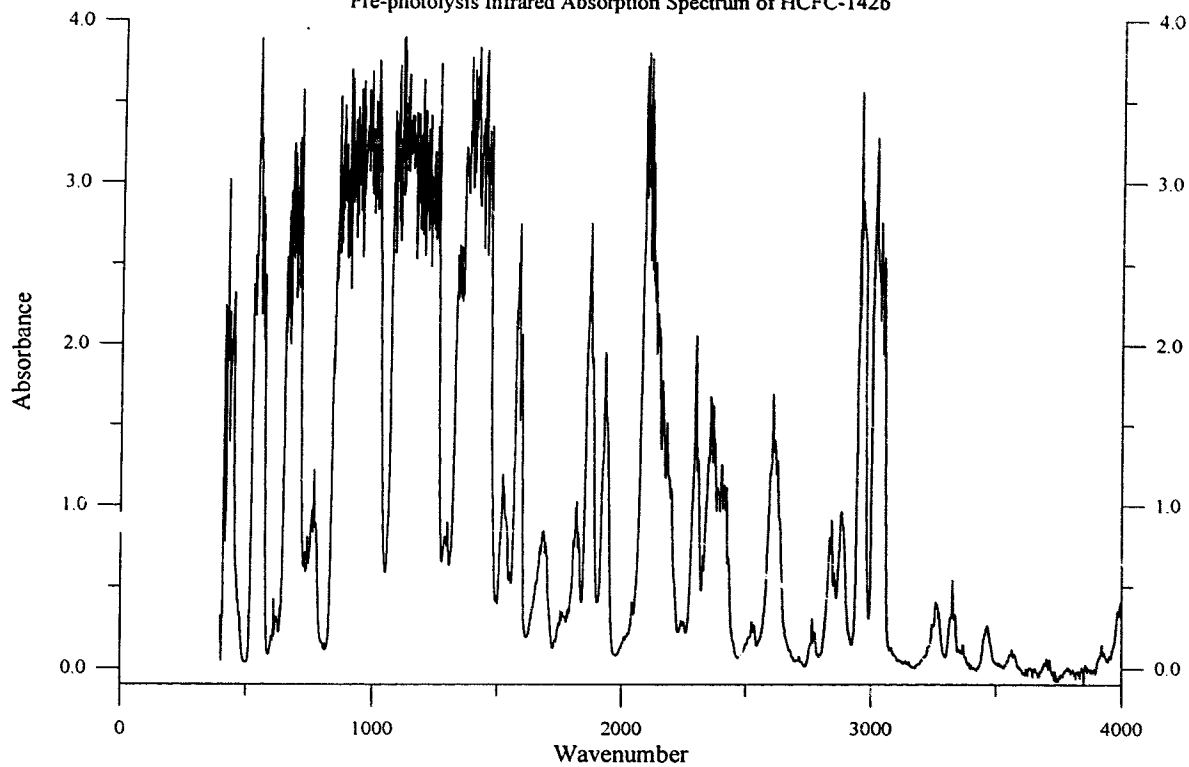
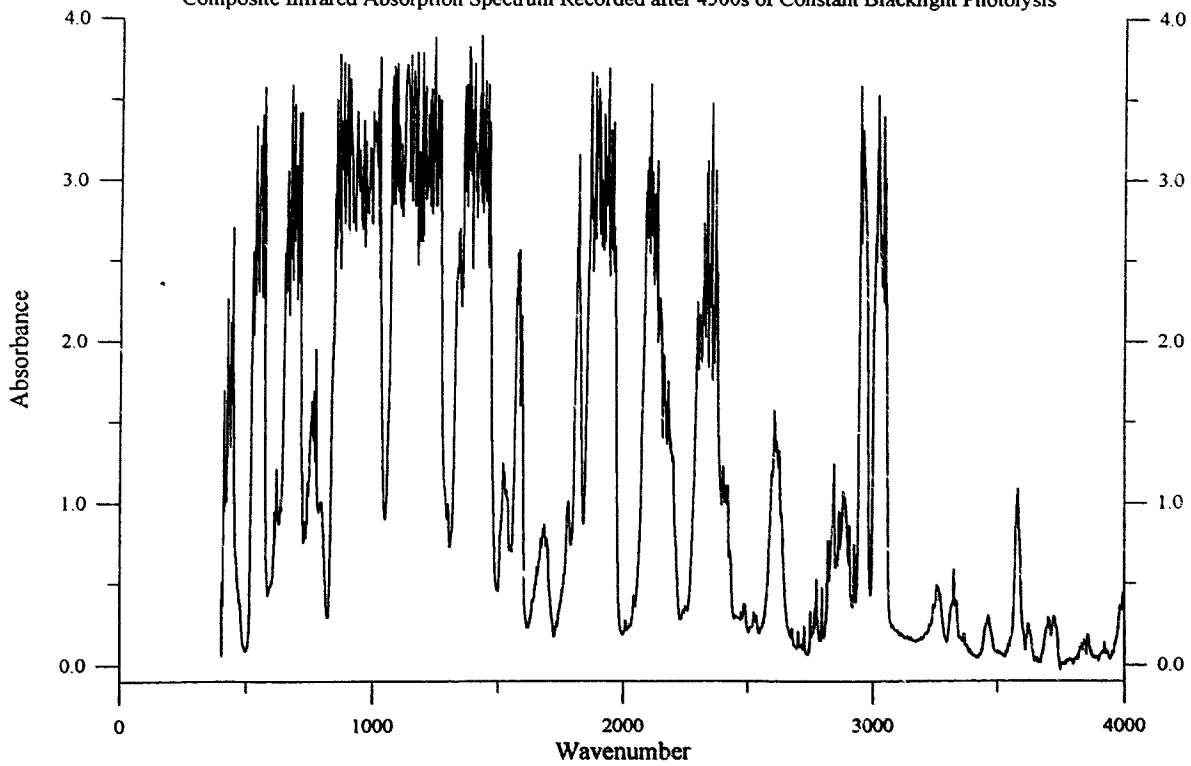


Figure 2b

Composite Infrared Absorption Spectrum Recorded after 4500s of Constant Blacklight Photolysis



0094

## Tropospheric Transformation Products of a Series of Hydrofluorocarbons and Hydrochlorofluorocarbons

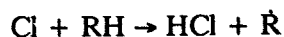
Ernesto C. Tuazon and Roger Atkinson  
Statewide Air Pollution Research Center  
University of California  
Riverside, California 92521, U.S.A.

### Introduction

A series of hydrofluorocarbons (HFCs) and hydrochlorofluorocarbons (HCFCs) are being considered as replacements for the chlorofluorocarbons (CFCs) currently in use. The presence of a hydrogen atom in the HFCs and HCFCs allows reaction with the OH radical to occur, via H-atom abstraction, and this H-atom abstraction process is sufficiently fast (the room temperature rate constants for the OH radical reactions with the HFCs and HCFCs are  $\sim 10^{(14 \pm 1)} \text{ cm}^3 \text{ molecule}^{-1} \text{ s}^{-1}$ ) that a major fraction of the emitted HFCs and/or HCFCs will react in the troposphere and hence not be transported into the stratosphere. In order to assess the environmental impacts of releasing these HFCs and/or HCFCs into the atmosphere, the tropospheric loss processes of the HFCs and HCFCs, the spectrum of products formed from their tropospheric degradation reactions, and the effects of these chemicals and their further transformation products on the ecosystem need to be understood. In this experimental program, we are investigating the products formed from the chlorine atom-initiated reactions of the HFCs and HCFCs shown in Table 1.

### Experimental

Experiments were carried out in a 5800 liter evacuable, Teflon-coated chamber equipped with an in situ multiple reflection optical system interfaced to a Nicolet 7199 Fourier transform infrared (FT-IR) absorption spectrometer. Irradiation was provided by a 24 kiloWatt xenon arc. Since the OH radical reaction rate constants for the HFCs and HCFCs are too low to allow a significant fraction of the HCFC or HFC to react under our experimental conditions, the haloalkyl radicals were generated by use of the analogous Cl atom reactions:



Chlorine atoms were produced by the photolysis of  $\text{Cl}_2$ . For the experiments conducted to date, the initial reactant concentrations (in molecule  $\text{cm}^{-3}$  units) were: HCFC or HFC,  $(1.2-2.5) \times 10^{14}$ ;  $\text{Cl}_2$ ,  $(1.2-16) \times 10^{14}$ . For the majority of the experiments conducted, the diluent gas was  $\text{O}_2 + \text{N}_2$  (with typically 150 Torr of  $\text{O}_2$ ) at a total pressure of 740 Torr, and the temperature was maintained at  $298 \pm 2$  K. For HFC-134a, experiments were carried out as a function of temperature (273-320 K),  $\text{O}_2$  partial pressure (1-600 Torr), and total pressure (150-740 Torr).

Table 1. HFCs and HCFCs being investigated

HFC or HCFC	
CHFCl <sub>2</sub>	HCFC-21
CHF <sub>2</sub> Cl	HCFC-22
CH <sub>2</sub> FCl	HCFC-31
CF <sub>3</sub> CHCl <sub>2</sub>	HCFC-123
CF <sub>3</sub> CHFCl	HCFC-124
CFCl <sub>2</sub> CH <sub>3</sub>	HCFC-141b
CF <sub>2</sub> ClCH <sub>3</sub>	HCFC-142b
CF <sub>3</sub> CF <sub>2</sub> CHCl <sub>2</sub>	HCFC-225ca
CF <sub>2</sub> ClCF <sub>2</sub> CHFCl	HCFC-225cb
CH <sub>3</sub> F	HFC-41
CF <sub>3</sub> CHF <sub>2</sub>	HFC-125
CF <sub>3</sub> CH <sub>2</sub> F	HFC-134a
CHF <sub>2</sub> CH <sub>3</sub>	HFC-152a

The concentrations of the reactants and products were monitored by FT-IR absorption spectroscopy. Authentic samples of the HFCs and HCFCs and of several product species were used to determine the absorption spectra and cross-sections. For C(O)FCl and HC(O)F, the absorption spectra and cross-sections were obtained from the irradiation of Cl<sub>2</sub>-CHFCl<sub>2</sub>-air (C(O)FCl) and Cl<sub>2</sub>-CH<sub>2</sub>FCl-air and Cl<sub>2</sub>-CH<sub>3</sub>F-air (HC(O)F) mixtures, assuming that the COFCl and HC(O)F yields were unity (no other products were observed).

### Results and Discussion

The HFCs and HCFCs studied, the products observed, and the measured product yields at 298 ± 2 K and in the presence of 740 Torr total pressure of synthetic air are given in Table 2. Our results for HFC-134a are discussed in more detail below.

HCFC-21, HCFC-22, HCFC-31, HFC-41, HCFC-123, HCFC-124, HFC-125 and HFC-152a. Our product data [1] show that under atmospheric conditions the intermediate alkoxy radicals react by the routes:

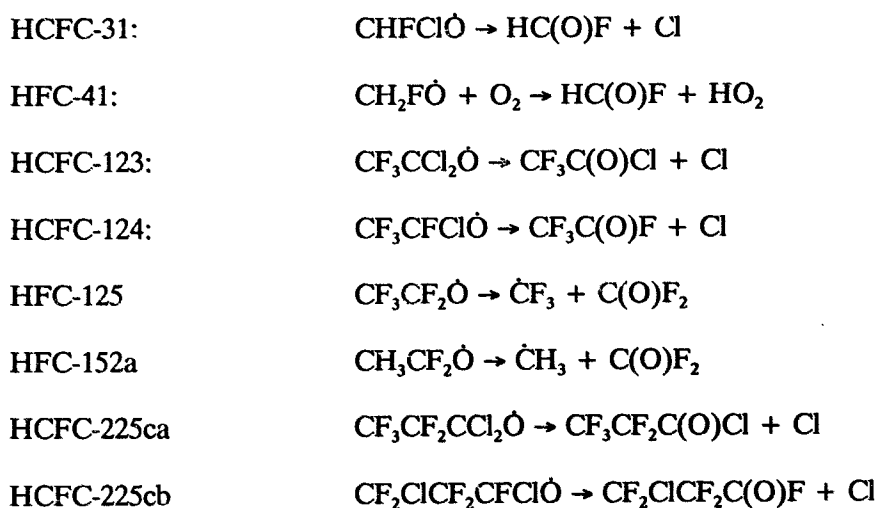


0 0 9 6

Table 2. Products and product yields for the Cl atom-initiated reactions of HFCs and HCFCs at  $298 \pm 2$  K and 740 Torr of air

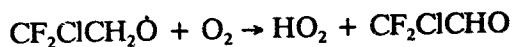
HFC or HCFC	Products	Yield (%)
$\text{CHFCl}_2$ (HCFC-21)	$\text{C(O)FCl}$	100 (assumed)
$\text{CHF}_2\text{Cl}$ (HCFC-22)	$\text{C(O)F}_2$	100
$\text{CH}_2\text{FCl}$ (HCFC-31)	$\text{HC(O)F}$	100 (assumed)
$\text{CH}_3\text{F}$ (HFC-41)	$\text{HC(O)F}$	100 (assumed)
$\text{CF}_3\text{CHCl}_2$ (HCFC-123)	$\text{CF}_3\text{C(O)Cl}$	$98.0 \pm 0.5$
$\text{CF}_3\text{CHFCl}$ (HCFC-124)	$\text{CF}_3\text{C(O)F}$	$101 \pm 1$
$\text{CFCl}_2\text{CH}_3$ (HCFC-141b)	$\text{C(O)FCl}$	$99.5 \pm 0.8$
$\text{CF}_2\text{ClCH}_3$ (HCFC-142b)	$\text{C(O)F}_2$	$100 \pm 1$
$\text{CF}_3\text{CF}_2\text{CHCl}_2$ (HCFC-225ca)	$\text{CF}_3\text{CF}_2\text{C(O)Cl}$	100
$\text{CF}_2\text{ClCF}_2\text{CHFCl}$ (HCFC-225cb)	$\text{CF}_2\text{ClCF}_2\text{C(O)F}$	100
$\text{CHF}_2\text{CF}_3$ (HFC-125)	$\text{C(O)F}_2$ $\text{CF}_3\text{OOOCF}_3$	$\sim 100^a$
$\text{CH}_3\text{CHF}_2$ (HFC-152a)	$\text{C(O)F}_2$	$92.2 \pm 1.2$

<sup>a</sup>Initial yield.



with the  $\dot{\text{C}}\text{F}_3$  radical from HFC-125 leading to further production of  $\text{C}(\text{O})\text{F}_2$  as the reaction proceeds. For HFC-152a, 99% of the Cl atom-initiated reaction is expected to proceed via formation of the  $\text{CH}_3\text{CF}_2\dot{\text{O}}$  radical [1]; the 92% yield of  $\text{C}(\text{O})\text{F}_2$  indicates that other products are formed, and indeed unidentified weak residual IR absorption bands were observed [1].

HFC-141b and -142b. Irradiations of  $\text{Cl}_2\text{-CF}_2\text{ClCH}_3\text{-air}$  and  $\text{Cl}_2\text{-CFCl}_2\text{CH}_3\text{-air}$  mixtures led to the formation of  $\text{C}(\text{O})\text{F}_2$  and  $\text{C}(\text{O})\text{FCl}$ , respectively, in 100% yields. These data do not allow us to discriminate between the two possible alkoxy radical reaction channels (taking the  $\text{CF}_2\text{ClCH}_2\dot{\text{O}}$  radical as an example) [1]:

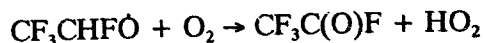
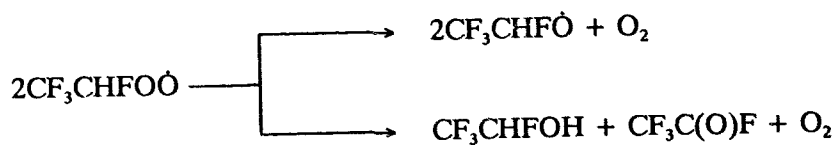


or



since the aldehydes ( $\text{CF}_2\text{ClCHO}$ ,  $\text{CFCl}_2\text{CHO}$  and  $\text{HCHO}$ ) are either known, or are expected, to react with Cl atoms with rate constants which are orders of magnitude higher than those for the parent HCFCs.

HFC-134a.  $\text{CF}_3\text{C}(\text{O})\text{F}$ ,  $\text{HC}(\text{O})\text{F}$ ,  $\text{C}(\text{O})\text{F}_2$ ,  $\text{CF}_3\text{OOOCF}_3$  and  $\text{CF}_3\text{OOC}(\text{O})\text{F}$  were observed as products [2]. The  $\text{CF}_3\text{C}(\text{O})\text{F}$  yield increased with the  $\text{O}_2$  concentration, and with decrease in temperature and total pressure (showing that the decomposition pathway is in the fall-off region below one atmosphere total pressure). Our data are consistent with the reaction sequence [2]





products

Assuming that under tropospheric conditions the  $\text{CF}_3\text{CHFOO}$  radical produces only the  $\text{CF}_3\text{CHFO}$  radical, then our data give the following  $\text{CF}_3\text{C(O)F}$  yields [2].

$\text{CF}_3\text{C(O)F}$  yield<sup>a</sup>

Altitude (km)	T (K)	P (Torr)	Yield (%)
	298	760	18
0	288	760	25
5	259	407	44
10	230	202	71
15	213	92	80

#### Acknowledgment

This research was supported by SPA-AFEAS Contracts No. CTR90-3/P90-001 and CTR91-28/P91-082.

#### References

1. Tuazon, E. C. and Atkinson, R. *J. Atmos. Chem.* (1993), in press.
2. Tuazon, E. C. and Atkinson, R. *J. Atmos. Chem.* (1993), in press.

Time Resolved Studies of Intermediate Products in the  
Oxidation of HCFC's and HFC's

R. Zellner, A. Hoffmann, V. Mörs, W. Malm

Institut für Physikalische und Theoretische Chemie  
Universität Essen, 4300 Essen, FRG

**Introduction**

HCFC's and HFC's are being considered as potential substitutes of CFC's in a large number of applications. With full substitution it may be anticipated that the global consumption of HCFC's and HFC's will at least equal the present day consumption of CFC's. Hence an assessment of the environmental acceptability of these compounds is of vital importance prior to the implementation of larger industrial production. The environmental assessment of alternative CFC's has to follow various routes which are well defined in the AFEAS initiative [1]. One of these is the determination of the tropospheric degradation products.

Product studies of photooxidation products have hitherto been successfully performed using FTIR-analysis of stable end products [2-5]. In the present paper we present the application of a technique in which the photooxidation is pulse-initiated and products resulting from characteristic reactions of intermediates are followed in a time-resolved mode. The advantage of this technique is that it provides a sensitive indication of the branching reactions arising from oxy reactions, independent of the nature of the individual oxy radical. Results from an application of this technique to oxidation studies of HCFC 123 ( $\text{CF}_3\text{CCl}_2\text{H}$ ), HCFC 141b ( $\text{CFCl}_2\text{CH}_3$ ), HCFC 142b ( $\text{CF}_2\text{ClCH}_3$ ), and HFC 152a ( $\text{CF}_2\text{HCH}_3$ ) are presented.

## Methodology and experimental details

The oxidation of HCFC's and HFC's under  $\text{NO}_x$ -rich simulated tropospheric conditions has been studied using laser pulse initiation combined with cw-laser long path absorption/LIF for the detection of OH and  $\text{NO}_2$ . The absolute yield and temporal behaviour of these products have been found to be sensitive indicators for the reaction behaviour of the oxy radicals ( $\text{R-CXYO}$ ) generated along the oxidation chain as shown in Fig. 1.

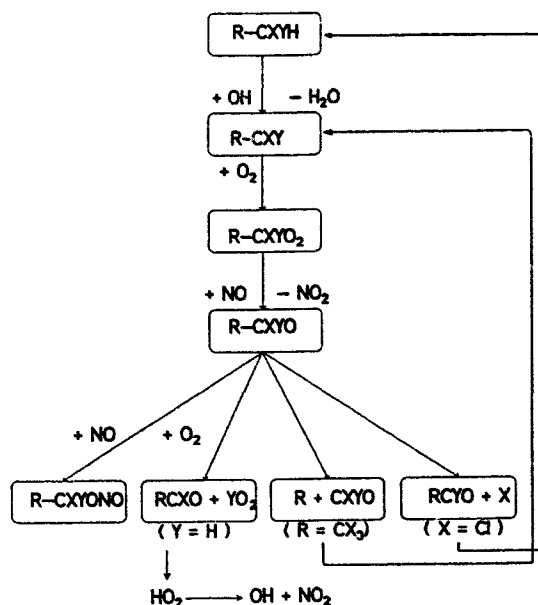


Fig.1 General oxidation scheme for halogenated alkanes. The interactions of the peroxy radicals  $\text{R-CXYO}_2$  with  $\text{NO}$ ,  $\text{NO}_2$  and  $\text{HO}_2$  are not shown.

In combination with simulation studies including detailed mechanistic schemes individual rate coefficients for the reactions of oxy radicals with  $\text{O}_2$  as well as their unimolecular fragmentations can be obtained.

The present experiments combine laser photolysis for the generation of primary oxidants such as OH and/or Cl and time resolved detection for  $\text{NO}_2$  and OH. Whereas  $\text{NO}_2$  is monitored using LIF from excitation by means of the direct output of a 9W  $\text{Ar}^+$ -laser operating at 488 nm, the detection of OH is achieved by line absorption in the center of the  $\text{Q}_{14}$  line. For this purpose an  $\text{Ar}^+$ -laser pumped narrow band ring-dye laser is internally frequency doubled. In each case (LIF and

absorption) the total path length is increased by multiply folding the laser beams via dielectrically coated mirrors in White configuration. A schematic representation of the experimental set-up is shown in Fig. 2. The detection limits in these arrangements and for total pressures of 50 mbar  $O_2$  are  $10^8 \text{ cm}^{-3}$  for the OH radicals and  $10^{11} \text{ cm}^{-3}$  for  $NO_2$  molecules. Details of the experimental arrangement have been fully described elsewhere [6]

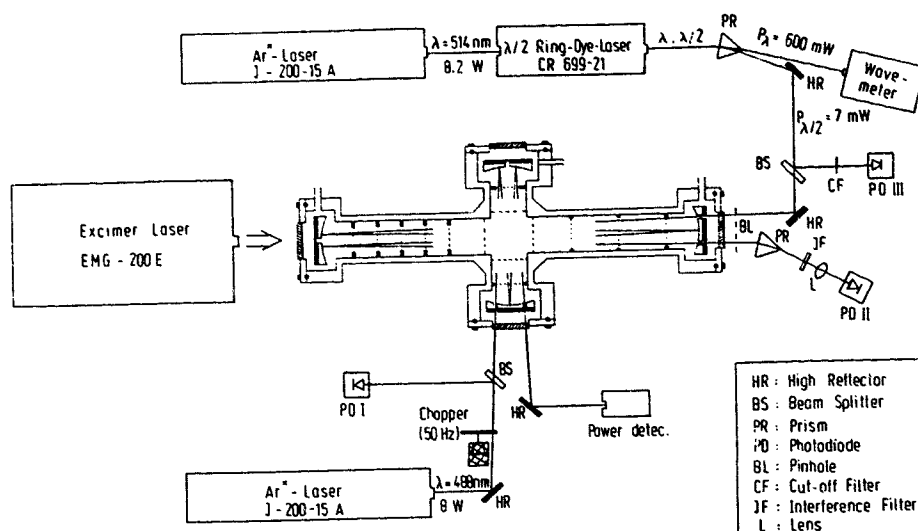


Fig. 2 Schematic representation of laser photolysis/cw-laser absorption/LIF experiment.

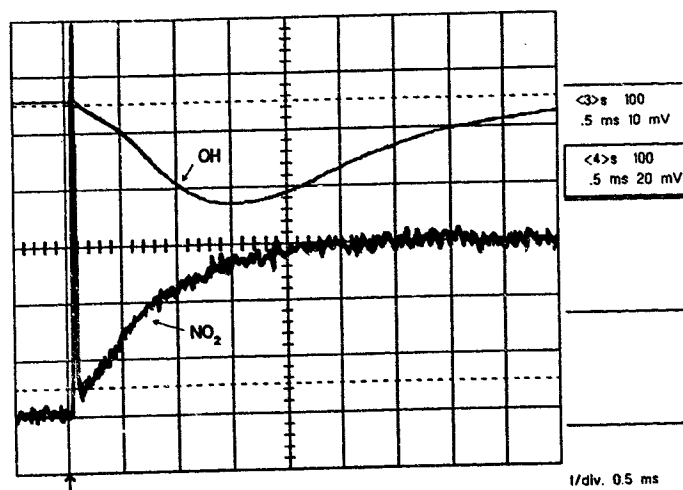


Fig. 3 Typical results obtained for the temporal behaviour of OH (from absorption measurements) and  $NO_2$  (from LIF measurements).

## Results and Discussion

### 1. HCFC 123 (CF<sub>3</sub>CCl<sub>2</sub>H)

The oxidation scheme for HCFC 123 is shown in Fig. 4

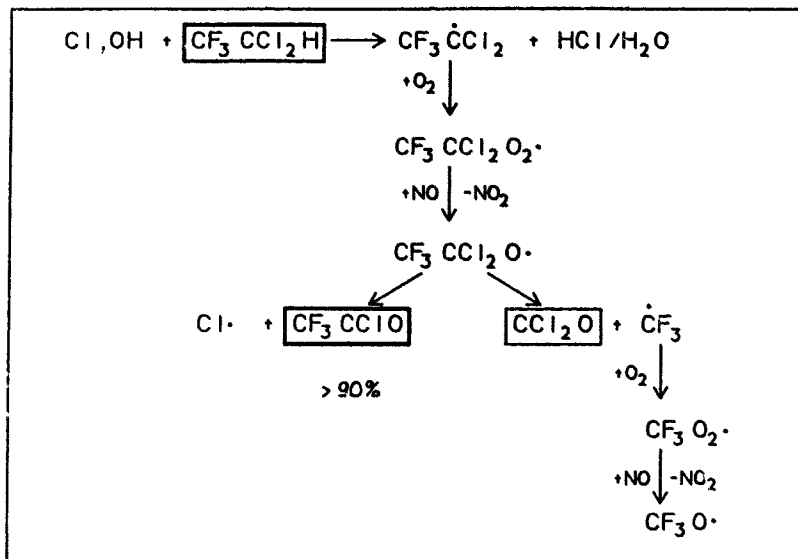


Fig. 4 Tropospheric oxidation scheme of HCFC 123

The oxy radical formed in the oxidation of this compound (CF<sub>3</sub>CCl<sub>2</sub>O) can only react by C-C bond fission or Cl-elimination. This is reflected in the amount and the temporal behaviour of NO<sub>2</sub> which is measured in our experiment. Whereas C-C bond fission generates CF<sub>3</sub> radicals which in their subsequent oxidation form CF<sub>3</sub>O, the elimination of Cl atoms is chain propagating. As a consequence this channel provides enhanced NO<sub>2</sub> formation. For the unimolecular decomposition of CF<sub>3</sub>CCl<sub>2</sub>O a rate coefficient for the thermal elimination of a Cl-atom of  $k(\text{C-Cl}) = 1.4 \times 10^4 \text{ s}^{-1}$  at 298 K has been determined. The branching ratio for C-Cl bond fission relative to C-C bond fission is found to  $(12 \pm 4)$ . As a consequence the oxidation of HCFC 123 is predicted to yield CF<sub>3</sub>CClO as the main carbonyl product.

2. HCFC 141b (CFCl<sub>2</sub>CH<sub>3</sub>)

The oxidation scheme for HCFC 141b is shown in Fig. 5

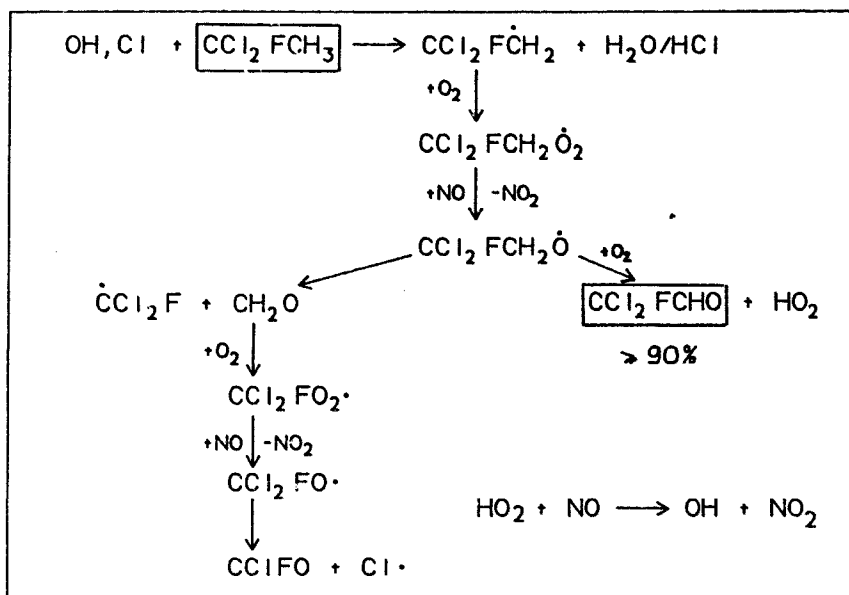


Fig.5 Tropospheric oxidation scheme of HCFC 141b

The oxy radical formed in the oxidation of this compound (CCl<sub>2</sub>FCH<sub>2</sub>O) can in principle react by C-C bond fission or by H atom abstraction by O<sub>2</sub>. Since the latter pathway forms HO<sub>2</sub> (and sequently OH), both NO<sub>2</sub> and OH are monitored in our experiments.

For the unimolecular decomposition of CFCl<sub>2</sub>CH<sub>2</sub>O by C-C bond fission a rate coefficient at 298 K of  $k(\text{C-C}) = 500 \pm 500 \text{ s}^{-1}$  has been derived. The branching ratio of C-C bond fission relative to reaction of CFCl<sub>2</sub>CH<sub>2</sub>O with O<sub>2</sub> at ambient lower tropospheric conditions is determined to be  $k(\text{C-C})/k(\text{O}_2)[\text{O}_2] = 0.05 \pm 0.05$ . As a consequence the oxidation of HCFC 141b is predicted to yield CFCl<sub>2</sub>CHO as the main ( $\geq 90\%$  yield) carbonyl product.



4. HFC 152a ( $\text{CF}_2\text{HCH}_3$ )

The oxidation scheme for HFC 152a is shown in Fig. 7

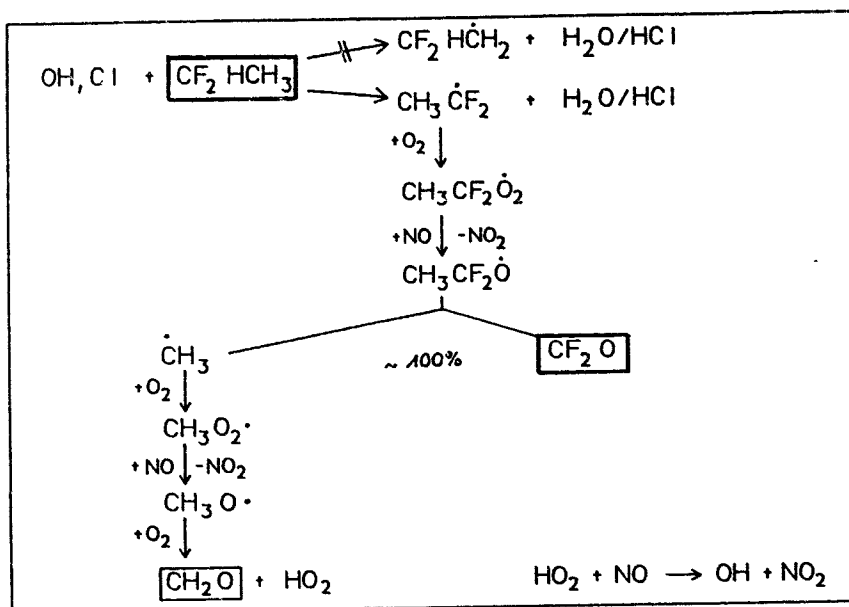


Fig. 7 Tropospheric oxidation scheme of HFC 152a

Based on former measurements [7-9] the initial oxidant attack occurs on the  $\alpha$ -carbon atom forming  $\text{CH}_3\text{CF}_2\dot{\text{O}}$  as the only oxy radical. For the unimolecular decomposition of  $\text{CH}_3\text{CF}_2\dot{\text{O}}$  by C-C bond fission a rate coefficient of  $k(\text{C-C}) \geq 1 \times 10^4 \text{ s}^{-1}$  at 298 K has been determined. Since there are no other degradation pathways of  $\text{CH}_3\text{CF}_2\dot{\text{O}}$  in the lower tropospheric and since this rate coefficient is sufficiently large we conclude that the only primary halogenated carbonyl product from the degradation of HFC 152a is  $\text{CF}_2\text{O}$ .

**Conclusions:**

By means of the observation of byproducts (such as OH and  $\text{NO}_2$ ) in the laser pulse initiated oxidation of selected HCFC's and HFC's rate constants and branching ratios for the reactions of the associated oxy radicals have been provided. In cases where Cl-elimination (HCFC 123) and/or C-C fragmentation by  $\text{CX}_2\dot{\text{O}}$  ( $\text{X}=\text{F, Cl}$ ) elimination (HCFC 123, HFC 152a) are possible, these processes occur

consequence, reactions with  $O_2$  forming  $CX_3CHO$  are the dominant reaction channels for  $CX_3CH_2O$  type oxy radicals.

### References

- [1] "Scientific Assessment of Stratospheric Ozone 1989" WMO report No. 20, Vol. II, Appendix. AFEAS report
- [2] Tuazon, E.C., and Atkinson, R., paper presented at this meeting
- [3] Meller R., Boglu, D. and Moortgart, G., paper presented at this meeting
- [4] Wallington, T.J., Hurley, U.D., Ball, J.C. and Kaiser, F.W., Environ. Sci. Techn. 26 (1992) 1318
- [5] Wallington, T.J. and Selested, J., Environ. Sci. Technol. 27 (1993) 146
- [6] Hoffmann, A., Mörs, V. and Zellner, R., Ber. Bunsenges. Phys. Chem. 96 (1992) 437
- [7] Martens, G.J., Godfroid, M., Delveaux, J. and Verbeyst, J., Int. J. Chem. Kin. 8 (1976) 153
- [8] Cadman, P. Kirk, A.W., and Trotman-Dickensen, A.F., J. Chem. Soc. Far. Trans II, 72 (1976) 1027
- [9] Tschuikow-Roux, E., Yano, T., and Niedzielsky, J., J. Chem. Phys. 82 (1985) 65

## Photochemical Studies of 1,1,1,2 Tetrafluoroethane (HFC134a)

O.V. Rattigan, D.M. Rowley, O. Wild, R.L. Jones and R.A. Cox

Centre for Atmospheric Science, Department of Chemistry, University of Cambridge,  
Lensfield Road, Cambridge CB2 1EW.

### Introduction

Hydrochlorofluorocarbons (HCFCs) and hydrofluorocarbons (HFCs) have been proposed as potential replacements for the CFCs. Their shorter atmospheric lifetimes<sup>1</sup>, coupled with reduced chlorine substitution leads to less release of chlorine in the stratosphere and hence lower ozone depletion potentials than the CFCs. In order to assess the environmental impact of HCFC and HFC release however, it is necessary to quantify the nature and yield of the products from atmospheric oxidation.

HFC-134a (CF<sub>3</sub>CH<sub>2</sub>F) is a proposed replacement for difluorodichloromethane (CFC-12) which is widely used as a refrigerant and in air conditioning systems. In the troposphere OH initiated oxidation of HFC-134a leads to the formation of the peroxy radical CF<sub>3</sub>CHFO<sub>2</sub> *via*:



The reaction of CF<sub>3</sub>CHFO<sub>2</sub> with NO (3) has been found to be rapid<sup>2,3</sup> and is expected to be the major loss reaction for the peroxy radical in the troposphere:



Subsequently, CF<sub>3</sub>CHFO radicals formed in reaction (3) may either react with O<sub>2</sub> to form trifluoroacetyl fluoride, CF<sub>3</sub>C(O)F, plus HO<sub>2</sub> or undergo unimolecular decomposition to form CF<sub>3</sub> radicals and formyl fluoride, HC(O)F:



The primary product distribution from the oxidation of HFC-134a therefore depends on the relative rates of reactions (4) and (5).

We have recently measured the UV absorption cross-sections for  $\text{CF}_3\text{C}(\text{O})\text{F}$  and  $\text{HC}(\text{O})\text{F}$ , and in the present work we have used this information to determine the yields of these products in the  $\text{Cl}_2$ -photosensitised oxidation of HFC-134a. Measurement of the yields as a function of  $[\text{O}_2]$  and temperature gave information of the reaction mechanism and allowed a determination of the rate constant ratio  $k_4/k_5$  in the temperature range 235 - 318 K.

During the course of this work a number of other studies of the photooxidation of HFC-134a have been carried out which have greatly aided in the understanding of the complex reaction mechanism and determination of the kinetic parameters.<sup>4-7</sup>

The fate of the  $\text{CF}_3$  radical produced in reaction (5) is still somewhat uncertain. It is likely to form  $\text{CF}_3\text{O}_2$  radicals by the addition of  $\text{O}_2$  and the self- and cross-reactions of this peroxy radical lead to  $\text{CF}_3\text{O}^8$ . Recent studies have shown that the reactivity of the  $\text{CF}_3\text{O}$  radical in H-atom abstraction from hydrocarbons is similar to that for the OH radical<sup>9,10</sup>. Sehested and Wallington found that  $\text{CF}_3\text{O}$  reacts with HFC 134a to form  $\text{CF}_3\text{OH}$  which decomposes to give  $\text{COF}_2$  and HF<sup>11</sup>. Therefore  $\text{CF}_3\text{OH}$  formation is the likely fate of  $\text{CF}_3\text{O}$  in the atmosphere.

In the present work the Cambridge 2-D model<sup>12</sup> has been used to calculate atmospheric distributions of HFC 134a following photochemical destruction. The relative importance of the thermal decomposition of  $\text{CF}_3\text{CHFO}$  compared to its reaction with  $\text{O}_2$  has been computed.

## Experimental

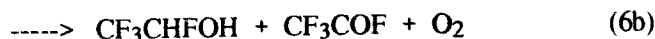
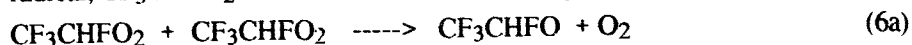
The dual beam diode array spectroscopy system used in this study has been described in detail previously.<sup>13</sup> Briefly, a 1 meter long jacketed quartz cell connected to a standard greaseless vacuum system was used as the reaction vessel. Formyl fluoride was prepared by the reaction of formic acid with benzoyl chloride using dry  $\text{KHF}_2$  at 333 K<sup>14</sup>.

## Results

Reference UV absorption spectra of pure samples of  $\text{CF}_3\text{C}(\text{O})\text{F}$  and  $\text{HC}(\text{O})\text{F}$  were recorded over a range of conditions, prior to the photooxidation study.

For the photooxidation study, mixtures of  $\text{CF}_3\text{CH}_2\text{F}$  (8 - 12 Torr),  $\text{Cl}_2$ , (1 Torr, 5% in  $\text{N}_2$ ) and  $\text{O}_2$  (20 - 730 Torr) were made up to a total pressure of 760 Torr using  $\text{N}_2$  (17 - 731 Torr) and premixed for several hours. Irradiation in the wavelength range 300 - 400 nm was

then used to drive the Cl atom initiated photooxidation of HFC 134a. The self reaction of the peroxy radical,  $\text{CF}_3\text{CHFO}_2$  was used as a route to the oxy radical  $\text{CF}_3\text{CHFO}$ :



The oxy radical then either reacts with  $\text{O}_2$ , reaction (4) or undergoes unimolecular decomposition, reaction (5). At regular intervals prior to and during this photolysis, UV spectra of the reaction mixture were recorded. Fig.1 shows three sequential spectra taken following 111, 171 and 243 seconds of irradiation. These spectra show a buildup of absorption around 230 nm, attributable to product formation and a reduction of absorption around 300 nm attributable to chlorine consumption, with increasing irradiation time.

Spectral stripping routines were applied to the sequential spectra for the identification and quantification of products formed during the photooxidation using reference spectra reported above. Chlorine cross-sections were taken from the current NASA evaluation<sup>15</sup>. Yields of the two main products were therefore expressed in terms of the molecular chlorine consumed. Errors on individual yields combined with a  $\pm 5\%$  uncertainty in cross-sections resulted in a total error on the yield of  $\pm 8\%$ . However, somewhat larger errors occurred in the  $\text{CF}_3\text{COF}$  yield due to the difficulty in subtracting the smooth  $\text{CF}_3\text{COF}$  spectrum from the composite UV spectrum of the products. Following spectral stripping of  $\text{Cl}_2$ ,  $\text{HC(O)F}$  and  $\text{CF}_3\text{C(O)F}$ , the baseline of UV absorption showed no additional significant absorbance. The combined yield  $(\text{CF}_3\text{COF} + \text{HCOF})/2$  was greater than the amount of  $\text{Cl}_2$  consumed, see Table 1. The photooxidation study was carried out at four experimental temperatures in the range 235 - 318 K, and at a range of oxygen partial pressures. IR analysis of the reaction mixture following photolysis showed in addition to the major products, absorptions attributable to  $\text{COF}_2$ , HF and  $\text{SiF}_4$ .

## Discussion

Following the self reaction of  $\text{CF}_3\text{CHFO}_2$ , either  $\text{CF}_3\text{CHFO}$  or molecular products are formed. The  $\text{CF}_3\text{CHFO}$  radicals further react and the final product distribution reflects the branching ratio between the oxy radical channels. The derived yields were analysed in two ways:

### (i) Arithmetic derivation of $k_4/k_5$

The branching ratio for the nonterminating channel of the  $\text{CF}_3\text{CHFO}_2$  radical self-reaction is defined as  $\alpha = k_{6a}/(k_{6a} + k_{6b})$ . Similarly, the branching ratio for the  $\text{CF}_3\text{CHFO}$  radical reaction with oxygen is defined as  $\beta$ .

$$\beta = k_4[\text{O}_2] / (k_4[\text{O}_2] + k_5)$$

The existence of total product yields in excess of the chlorine consumption in the present study is evidence for the further production of these products via secondary chemistry or the regeneration of  $\text{Cl}_2$ . Wallington *et al*<sup>11</sup> have shown that  $\text{CF}_3\text{O}$  radicals react with HFC-134a in this photooxidation to form  $\text{CF}_3\text{OH}$  and with excess HFC 134a (10 Torr) used in the present study this is the most probable fate of  $\text{CF}_3\text{O}$  leading to the regeneration of  $\text{CF}_3\text{CHFO}_2$  radicals. A chain reaction is therefore taking place, wherein both products  $\text{CF}_3\text{C}(\text{O})\text{F}$  and  $\text{HC}(\text{O})\text{F}$  are formed and  $\text{CF}_3\text{CHFO}_2$  is regenerated. A relationship between the yield of  $\text{HCOF}$  and  $\alpha$  and  $\beta$  was derived:

$$1/y(\text{HC}(\text{O})\text{F}) = \{(1+\alpha)/2\alpha\}[\text{O}_2] \{k_4/k_5\} + \{(1-\alpha\theta)/2\alpha\}$$

where  $\theta$  is the fractional efficiency of production of  $\text{CF}_3\text{O}$  radicals from  $\text{CF}_3$ .

A plot of  $1/y(\text{HC}(\text{O})\text{F})$  vs  $[\text{O}_2]$  at 293 K is shown in Fig 2 which shows good linearity and lends confidence to the analysis technique. Using values of  $\alpha$  from the work of Wallington *et al*<sup>4</sup>, values of  $\theta$  and  $k_4/k_5$  have been calculated.

### (ii) Kinetic Modelling

A computer simulation of the experimental system was also carried out using the FACSIMILE program. The kinetic model used was based on a reaction mechanism similar to that used by Wallington *et al*<sup>4</sup>.

The unknown rate coefficients,  $k_4$  (unimolecular decomposition of  $\text{CF}_3\text{CHFO}$ ) and  $k_1$  (the rate of  $\text{Cl}_2$  photolysis) were obtained by fitting computer-generated concentration-time data for  $\text{Cl}_2$ ,  $\text{HC}(\text{O})\text{F}$ ,  $\text{CF}_3\text{C}(\text{O})\text{F}$  and other products, to experimental data obtained in 16 experiments covering a range of temperatures and  $\text{O}_2$  partial pressures. The values of  $k_5$  obtained from the simulation are plotted in Arrhenius form in Fig 3 and are listed in table 2, together with the data from the arithmetic treatment. The agreement between the values obtained from the two methods is good.

### Conclusions

Table 2 shows the Arrhenius parameters for reaction (5) obtained from the various studies. The unimolecular decomposition  $k_5$  was calculated in each case using the expression:  $k_5 = 6.0 \times 10^{-14} \exp(-925/T) \text{ cm}^3 \text{ molecule}^{-1} \text{ s}^{-1}$  as used in this study. All values except those of Maricq and Szente<sup>7</sup> are close to the high pressure limit according to the data of Wallington *et al*<sup>4</sup>. Nevertheless the A-factors are all significantly lower than the typical value of  $10^{13} - 10^{14} \text{ s}^{-1}$ , expected for a radical decomposition at the high pressure limit<sup>16</sup>. This suggests that the reaction may not be as close to the high pressure limit as the data of Wallington *et al*<sup>4</sup>.

indicate. Further experimental investigation of the pressure dependence is clearly needed to establish this.

The recommended expression in Table 2 is based on the mean of the experimental values at 293K and the E/R values from Wallington *et al.*<sup>4</sup>, Tuazon and Atkinson<sup>5</sup> and the present work, excluding the data at 235K. The temperature dependence obtained from the present work if the 235K data are included, and from the lower pressure data of Maricq and Szente<sup>7</sup>, both lead to unrealistically low A-factors and are therefore not included in the evaluation.

### Atmospheric Modelling

The two-dimensional (latitude, height) model of Harwood and Pyle<sup>12</sup> was used to calculate the photochemical loss of HFC 134a. HFC 134a was emitted into the model between 30-50° N at ground level at a fixed rate of 10% by volume of that of CFC 11 1986 levels. Integrations up to 40 years were carried out. Fig 4 shows the HFC 134a abundances in ppt after 40 year integration with photochemical loss via the OH radical and photolysis. The even global distribution reflects the relatively long atmospheric lifetime (12-15 years) of this hydrofluorocarbon. Fig.5 shows the destruction rate in molecule cm<sup>-3</sup> s<sup>-1</sup> of HFC 134a due to loss via the OH radical. The major loss occurs in a region around the equator from 40°S to 40°N and from ground level up to 3.5 km. Fig 6 shows the fraction of CF<sub>3</sub>COF formed from the CF<sub>3</sub>CHFO radical using the recommended parameters from Table 2 and the pressure dependence of Wallington *et al.*<sup>4</sup>. As is evident approximately 25% of CF<sub>3</sub>COF is formed in the region of maximum loss of HFC 134a.

### References

1. M. Prather and C.M. Spivakovsky, *J. Geophys. Res.* **95**, (D11), 18723, (1990).
2. T.J. Wallington and O.J. Nielsen, *Chem. Phys. Lett.* **187**, 33, (1991).
3. J. Peeters and V. Pultau CF<sub>3</sub>CHFO<sub>2</sub> + NO CEC-AFEAS workshop, Leuven, September 1992.
4. T.J. Wallington, M.D. Hurley, J.C. Ball and E.W. Kaiser, *Environ. Sci. Tech.*, **26**, 1318, (1992).
5. E. Tuazon and R. Atkinson, *J. Atm. Chem.* In Press, (1992).
6. E. O. Edney and D.J. Driscoll, *Int. J. Chem. Kinet.*, **24**, 1067, (1992).
7. M.M. Maricq and J.J. Szente, *J. Phys. Chem.*, **96**, 10862, (1992).
8. M.M. Maricq and J.J. Szente, *J. Phys. Chem.*, **96**, 4925, (1992).
9. R. Zellner, *Presented at the 12<sup>th</sup> International Symposium on Gas Kinetics*, Reading, U.K. (1992)
10. H. Sidebottom, Private Communication.
11. J. Sehested and T.J. Wallington, *Environ. Sci. Tech.* Submitted (1992).

12. R.S. Harwood and J.A. Pyle, *J. Roy. Met. Soc.*, **103**, 319, (1977).
13. O. Rattigan, E. Lutman, R.L. Jones, R.A. Cox, K. Clemitshaw and J. Williams, *J. Photochem. Photobiol. A: Chem.*, **66**, 313, (1992).
14. G.A. Olah and S.J. Kuhn, *J. Am. Chem. Soc.*, **82**, 2380, (1960).
15. W.B. DeMore et al, " Chemical Kinetics and Photochemical Data for Use in Stratospheric Modeling" NASA Evaluation No. 10, Jet Propulsion Laboratory Publication 92-20, Pasadena, CA., USA (1992).
16. S.W. Benson, *Thermochemical Kinetics*, 2nd Ed. Wiley-Interscience, New York, (1976).

**Table 1: Product Yields from the photolysis of CF<sub>3</sub>CH<sub>2</sub>F/Cl<sub>2</sub>/O<sub>2</sub>/N<sub>2</sub> at 293 K**

pO <sub>2</sub> /Torr	y(CF <sub>3</sub> COF)	y(HCOF)
181.3	1.35	2.66
300.0	1.87	2.22
584.1	1.65	1.33
726.5	1.85	1.13

**Table 2: Arrhenius parameters for the reaction CF<sub>3</sub>CHFO → CF<sub>3</sub> + HC(O)F**

A / (s <sup>-1</sup> x 10 <sup>-11</sup> )	(E / R) / K	k <sub>293</sub> / (s <sup>-1</sup> x 10 <sup>-4</sup> )	Reference
45	5407	4.2	This work
16.7	5150	3.9	This work
3.6	4832	2.5	Wallington <i>et al</i> <sup>4</sup>
1.9	4760	1.7	Tuazon and Atkinson <sup>5</sup>
0.0037	2200	4.0	Maricq and Szente <sup>7</sup>
6.9	4960	3.1	RECOMMENDED

Fig. 1 Spectra showing product buildup and Cl<sub>2</sub> consumption.

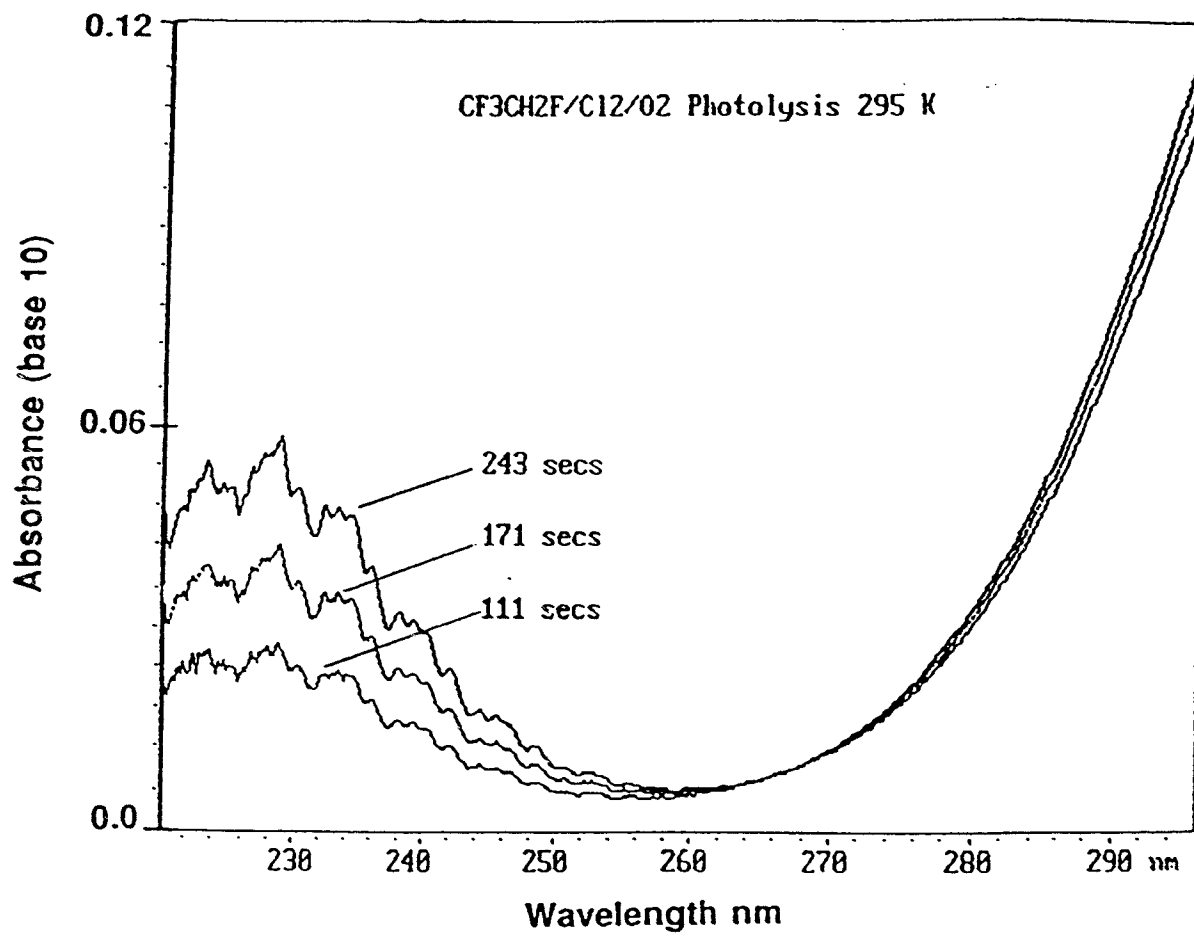
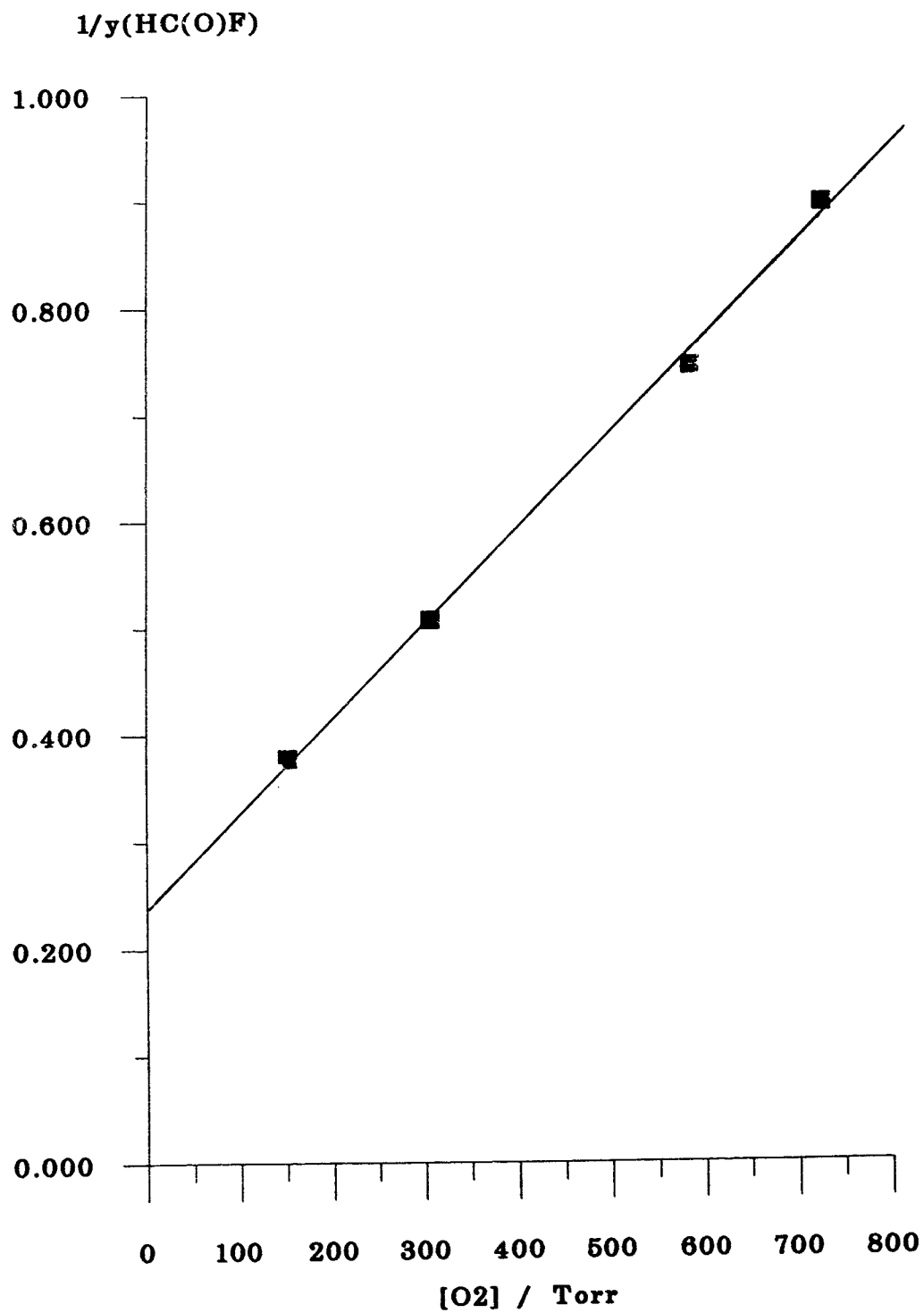


Figure 2:  $1/y(\text{HC(O)F})$  vs  $[\text{O}_2]$  at 293 K



0115

Figure 3 : k5 from 2 analyses using  
 $k_4 = (6.0 \times 10^{-14}) \exp(-925/T)$

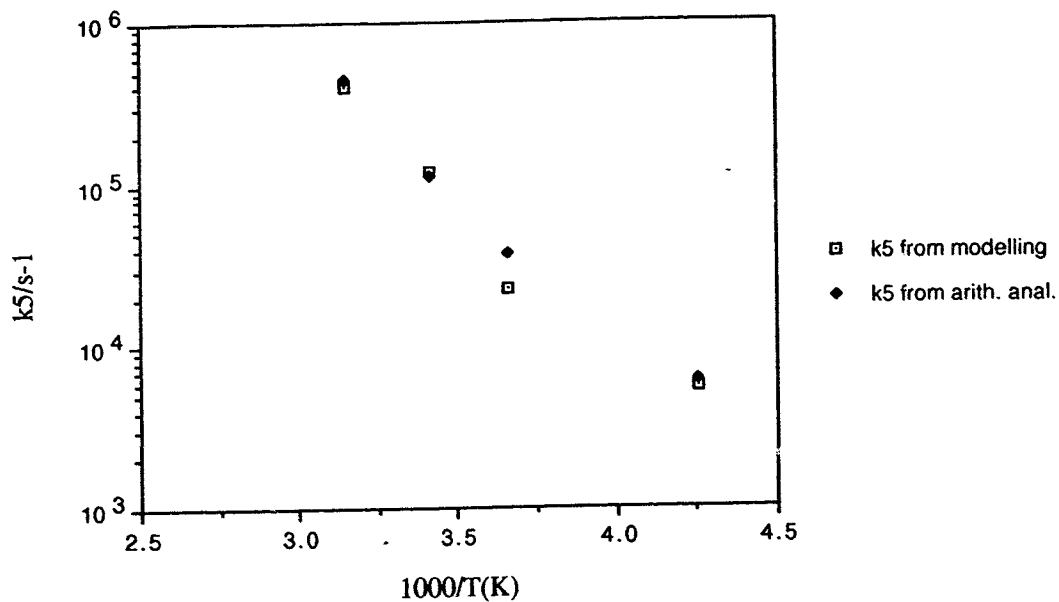


Fig. 4: Distribution of HFC 134a in ppt after 40 years integration.

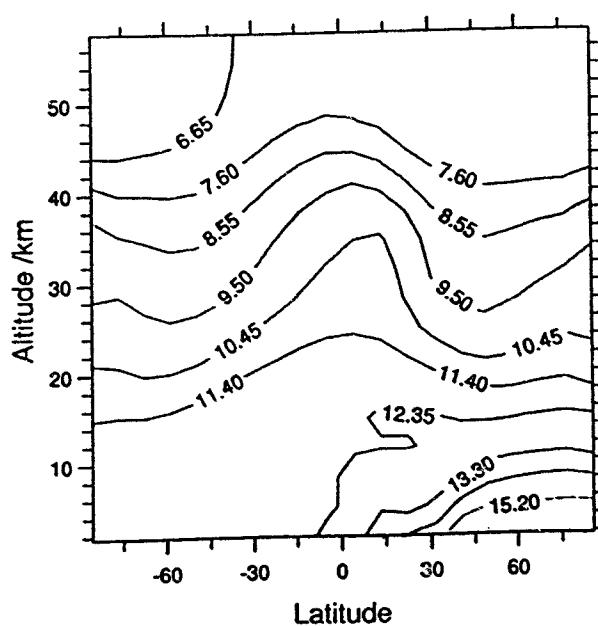


Fig. 5:  $\log_{10}$  (Annual average destruction rate of HFC 134a) molecule  $\text{cm}^{-3} \text{s}^{-1}$

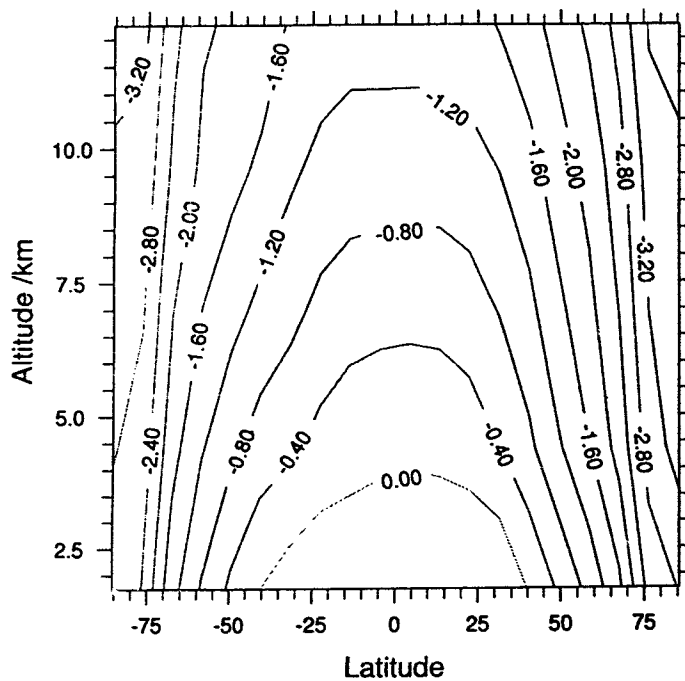
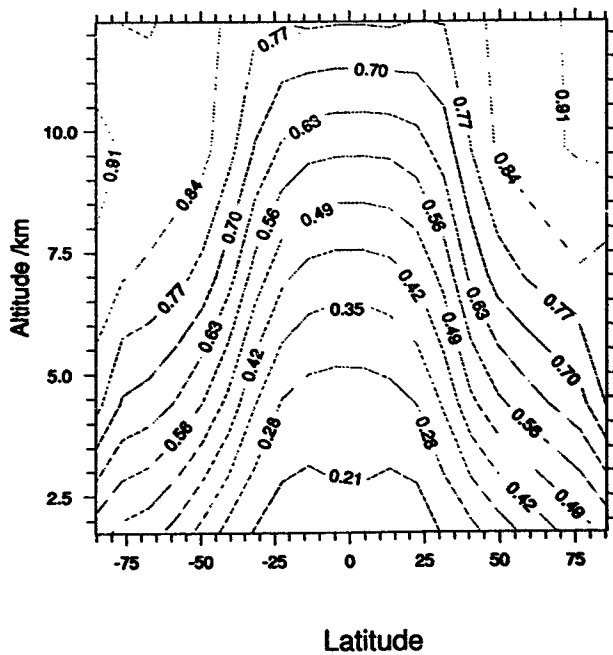


Fig. 6: Fraction of  $\text{CF}_3\text{COF}$  formed from  $\text{CF}_3\text{CHFO}$



Predicted lifetimes of hydrofluorocarbons (HFCs) and hydrofluoroethers (HFEs)  
from simple correlations

David L. Cooper<sup>1</sup>, Terry P. Cunningham<sup>1</sup>, Neil L. Allan<sup>2</sup>, and Archie McCulloch<sup>3</sup>

1 Department of Chemistry, University of Liverpool, P.O. Box 147, Liverpool L69 3BX, UK

2 School of Chemistry, University of Bristol, Cantocks Close, Bristol BS8 1TS, UK

3 Environment Department, ICI Chemicals and Polymers Ltd., P.O. Box 8, The Heath, Runcorn, Cheshire WA7 4QD, UK

In view of the role played by the reaction rates for H-atom abstraction by OH in determining the residence times of HCFCs, HFCs and HFEs, it can be useful to establish approximate correlations between kinetic data and structural information. Of particular utility would be linear relationships involving parameters readily available from relatively inexpensive self-consistent field (SCF) calculations. With this in mind, we have carried out a series of SCF geometry optimizations, using both *ab initio* and semi-empirical procedures, for fluorinated and/or chlorinated alkanes and ethers with up to four carbon atoms [1-4]. Of course, reliable predictions of the thermochemistry of such compounds require more sophisticated calculations taking appropriate account of electron correlation.

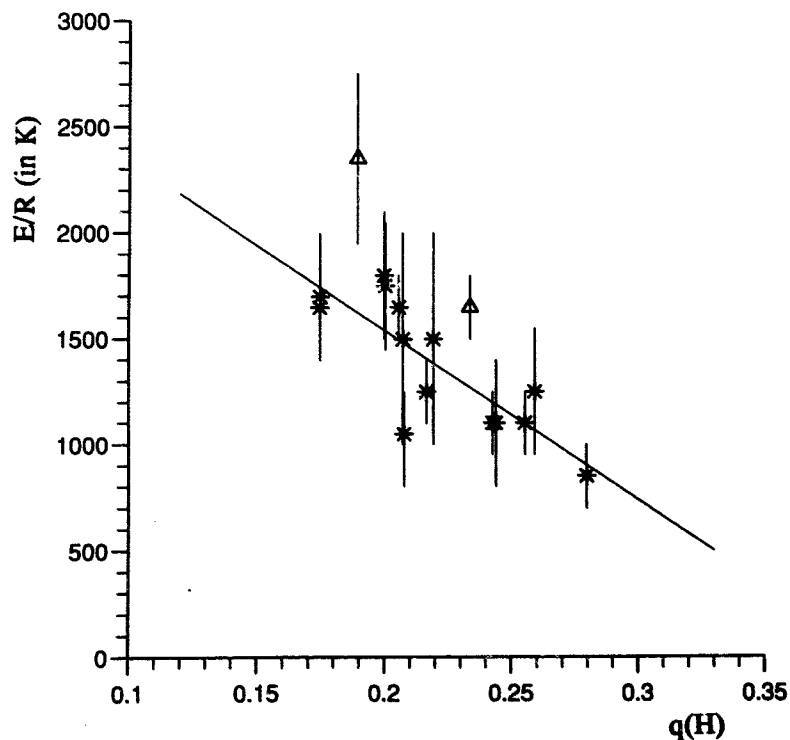
We report here two simple structure-activity relationships, one for the activation energy,  $E$ , and the other for the rate constant,  $k_{OH}$ . Activation energy data are available from a number of sources, including the useful compilation of Hampson *et al.* in the 1989 AFEAS report [5], which includes careful estimates of the likely errors. The molecules listed in Ref. 5 consist of chlorinated and/or fluorinated  $C_1$  and  $C_2$  alkanes. We have examined all these systems and, for those molecules in which there are hydrogen atoms on only one centre, we have noticed an approximate correlation between  $E$  and the calculated Mulliken charge  $q(H)$  of the abstracted H-atom [2]. The approximate linear relationship is illustrated in Figure 1 and the various data are collated in Table 1. With the exception of  $CHF_3$  and  $CHF_2Cl$ , which were excluded from the least-squares fit, the "Error", expressed as a multiple of the recommendation for the error bar on  $E/R$ , usually lies between  $\pm 1$ . This simple structure-activity relationship, which appears to hold equally well for both chlorine-bearing and chlorine-free species, could now be employed to provide useful first estimates of activation energies for larger hydrohaloalkanes and possibly hydrohaloethers.

The second type of relationship described here is based on the observation, by a number of research groups, of a statistically significant linear correlation between  $\lg(k/(cm^3s^{-1}))$  and ionization potentials for reactions with OH and  $NO_3$ . Such schemes appear to work for a wide range of organic species [6], including a few ethers and thiols. The range of  $k$ 's considered was so large that it is not clear whether the correlations would be of any practical use for a smaller range of compounds, such as HFCs, HCFCs and HFEs. Our own work for chlorine-free HFCs, using the energy of the highest occupied molecular orbital (HOMO) rather than the ionization potential, indicates that the deviations from this correlation are much smaller than we had any right to expect [3]. This is particularly true when *ab initio* wavefunctions are employed, although the scatter when using semi-empirical wavefunctions is still relatively small. Analogous studies have subsequently

**Table 1** Data for the reaction of hydroxyl with various haloalkanes. Further details are given in the text.

System	Mnemonic	E/R (in K)	q(H)	Error
CH <sub>3</sub> F	HFC-41	1700±300	0.175	-0.3
CH <sub>2</sub> F <sub>2</sub>	HFC-32	1650±200	0.175	-0.8
CH <sub>2</sub> FCI	HCFC-31	1250±200	0.217	-1.0
CH <sub>2</sub> Cl <sub>2</sub>	30	1100±250	0.243	-0.5
CHF <sub>3</sub>	HFC-23	2650±500	0.190	(+1.9)
CHF <sub>2</sub> Cl	HCFC-22	1650±150	0.234	(+2.2)
CHFCl <sub>2</sub>	HCFC-21	1100±150	0.256	-0.2
CH <sub>3</sub> CF <sub>3</sub>	HFC-143a	1750±500	0.208	+0.4
CH <sub>3</sub> CF <sub>2</sub> Cl	HCFC-142b	1650±250	0.211	+0.6
CH <sub>3</sub> CFCl <sub>2</sub>	HCFC-141b	1200±300	0.205	-1.2
CH <sub>3</sub> CCl <sub>3</sub>	140	1800±300	0.200	+0.7
CF <sub>3</sub> CH <sub>2</sub> F	HFC-134a	1750±300	0.201	+0.5
CF <sub>3</sub> CHF <sub>2</sub>	HFC-125	1750±500	0.220	+0.6
CF <sub>3</sub> CHFCI	HCFC-124	1250±300	0.260	+0.5
CF <sub>3</sub> CHCl <sub>2</sub>	HCFC-123	850±250	0.280	-0.3
CF <sub>3</sub> CH <sub>2</sub> Cl	HCFC-133a	1100±300	0.244	-0.4

**Figure 1** Graphical representation of the E/R and q(H) data listed in Table 1. The two systems excluded from the least-squares fit are marked  $\Delta$ .



been reported for reactions of OH with halogenoethenes [7], as well as for reactions of NO<sub>3</sub> with halogenobutenes (but employing only semi-empirical calculations) [8]. There is a fairly wide variation in the character of the HOMOs in all of these various systems. Consequently, attempts to rationalize the apparent success of this type of scheme in terms of frontier orbital theory are somewhat unconvincing and the correlations are, perhaps, better viewed as linear free-energy relationships, analogous to those frequently employed in organic chemistry.

For all of the chlorine-free systems considered in Ref. 5, we have marked with crosses (×) in Figure 2 the values of  $-\lg(k_{\text{OH}}/(\text{cm}^3\text{s}^{-1}))$  and the magnitudes of the corresponding *ab initio* HOMO energy ( $|\epsilon_{\text{HOMO}}|$ ). The full line is the outcome of a least-squares fit to all of these points and can be represented

$$-\lg(k_{\text{OH}}/(\text{cm}^3\text{s}^{-1})) = 0.981 |\epsilon_{\text{HOMO}}|/\text{eV} - 0.640 \quad (1)$$

There is currently interest in higher HFCs such as CF<sub>2</sub>HCF<sub>2</sub>CH<sub>2</sub>F (HFC-245ca), which has potential applications in centrifugal chillers. Furthermore, hydrofluoroethers are being considered for some situations, such as foam blowing. Consequently, we have been tempted to use Eq. 1 to provide first estimates of  $k_{\text{OH}}$  for C<sub>2</sub> HFEs [3] and for C<sub>3</sub> HFEs and HFCs [4]. A few experimental data have subsequently become available for some of these systems. We have used the results reported at this workshop by Kurylo and co-workers to update Figure 2, using the symbol Δ for HFCs and □ for HFEs. All of the data used to generate this Figure are listed in Table 2. The broken line is the outcome of a least-squares fit which takes account of the additional points and can be represented

$$-\lg(k_{\text{OH}}/(\text{cm}^3\text{s}^{-1})) = 0.867 |\epsilon_{\text{HOMO}}|/\text{eV} + 1.105 \quad (2)$$

The recently reported data lend support to our previous conjecture that simple linear relationships of this type can indeed be used to provide realistic first estimates of  $k_{\text{OH}}$  for HFEs and HFCs.

In order to facilitate further use of the structure-activity relationship, with parameters which can be refined as more data becomes available, we collect in Table 3 suitable values of  $\epsilon_{\text{HOMO}}$  from *ab initio* SCF geometry optimizations with realistic basis sets.

**Table 2** Data used to generate Figure 2.  $k_{\text{OH}}$  is given in  $\text{cm}^3\text{s}^{-1}$  and  $\epsilon_{\text{HOMO}}$  in eV.

Molecule	$k_{\text{OH}}$	$ \epsilon_{\text{HOMO}} $	Molecule	$k_{\text{OH}}$	$ \epsilon_{\text{HOMO}} $
CH <sub>3</sub> CH <sub>2</sub> F	$2.3 \times 10^{-13}$	13.65	CH <sub>2</sub> F <sub>2</sub>	$1.0 \times 10^{-14}$	14.90
CH <sub>2</sub> FCH <sub>2</sub> F	$1.1 \times 10^{-13}$	14.09	CF <sub>3</sub> CH <sub>2</sub> F	$4.8 \times 10^{-15}$	15.50
CH <sub>3</sub> CHF <sub>2</sub>	$3.7 \times 10^{-14}$	14.28	CH <sub>3</sub> CF <sub>3</sub>	$1.7 \times 10^{-15}$	15.63
CH <sub>3</sub> F	$1.8 \times 10^{-14}$	14.52	CF <sub>3</sub> CHF <sub>2</sub>	$2.5 \times 10^{-15}$	15.73
CH <sub>2</sub> FCHF <sub>2</sub>	$1.8 \times 10^{-14}$	14.55	CHF <sub>3</sub>	$2.1 \times 10^{-16}$	16.60
CHF <sub>2</sub> CHF <sub>2</sub>	$5.7 \times 10^{-15}$	14.89			
CF <sub>2</sub> HCF <sub>2</sub> CH <sub>2</sub> F	$1.1 \times 10^{-14}$	14.64	CF <sub>3</sub> CHF <sub>2</sub> CF <sub>3</sub>	$1.7 \times 10^{-15}$	16.13
CF <sub>3</sub> CH <sub>2</sub> OCH <sub>3</sub>	$6.2 \times 10^{-13}$	12.45	CF <sub>2</sub> HOCHF <sub>2</sub> H	$2.5 \times 10^{-14}$	15.16
CF <sub>3</sub> OCH <sub>3</sub>	$2.1 \times 10^{-14}$	14.11	CF <sub>3</sub> OCF <sub>2</sub> H	$3.5 \times 10^{-15}$	16.27
CF <sub>3</sub> CH <sub>2</sub> OCF <sub>2</sub> H	$1.2 \times 10^{-14}$	14.46			

Figure 2  $-\lg(k_{OH}/(\text{cm}^3\text{s}^{-1}))$  versus  $|\epsilon_{\text{HOMO}}|$  for HFCs and HFEs. Further details are given in the text.

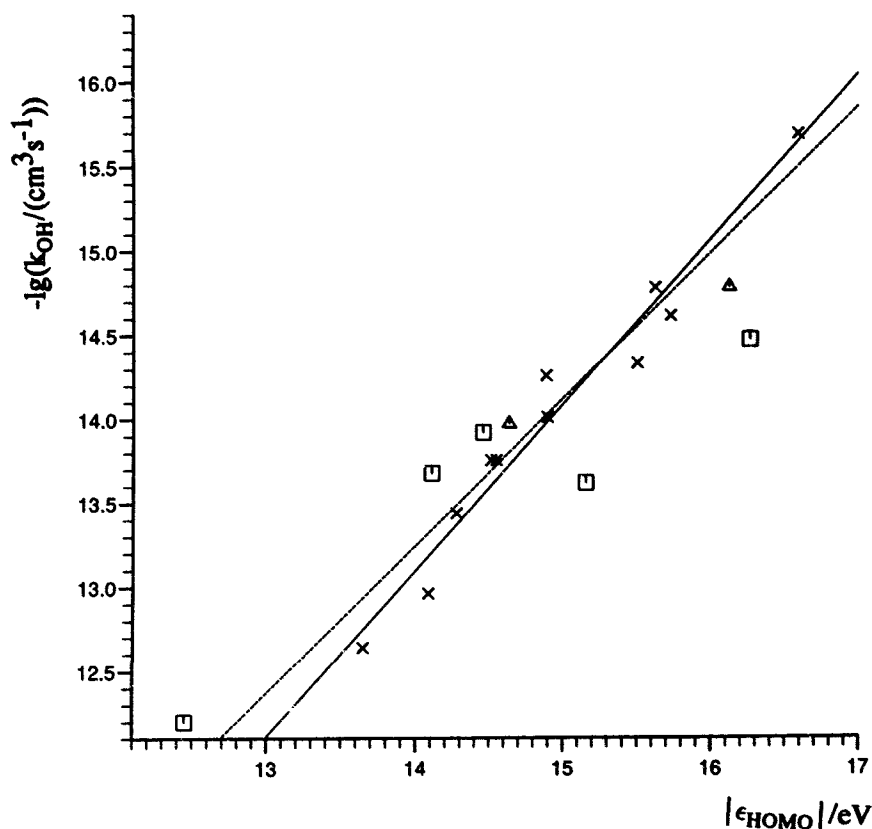
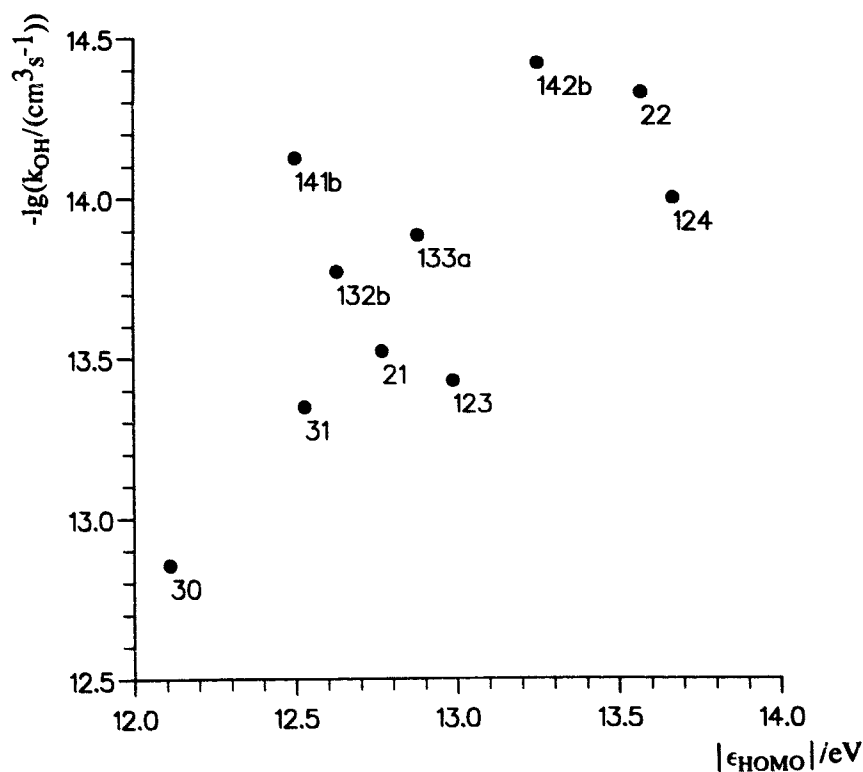


Table 3 A consistent set of *ab initio* HOMO energies ( $|\epsilon_{\text{HOMO}}|$  in eV) for various HFEs and HFCs.

CH <sub>3</sub> OCH <sub>2</sub> F	12.50	CH <sub>2</sub> FOCHF <sub>2</sub>	13.78	CHF <sub>2</sub> OCHF <sub>2</sub>	15.16
CH <sub>3</sub> OCHF <sub>2</sub>	13.43	CH <sub>3</sub> OCF <sub>3</sub>	14.11	CHF <sub>2</sub> OCF <sub>3</sub>	16.27
CH <sub>2</sub> FOCH <sub>2</sub> F	13.70	CH <sub>2</sub> FOCF <sub>3</sub>	15.09		
CHF <sub>2</sub> CF <sub>2</sub> CH <sub>3</sub>	14.39	CF <sub>3</sub> CH <sub>2</sub> CH <sub>2</sub> F	14.66	CF <sub>3</sub> CHFCHF <sub>2</sub>	15.30
CHF <sub>2</sub> CH <sub>2</sub> CHF <sub>2</sub>	14.40	CHF <sub>2</sub> CF <sub>2</sub> CHF <sub>2</sub>	15.04	CF <sub>3</sub> CH <sub>2</sub> CH <sub>2</sub> CF <sub>3</sub>	15.40
CF <sub>3</sub> CH <sub>2</sub> CH <sub>3</sub>	14.43	CF <sub>3</sub> CF <sub>2</sub> CH <sub>3</sub>	15.12	CHF <sub>2</sub> CF <sub>2</sub> CF <sub>3</sub>	15.53
CHF <sub>2</sub> CF <sub>2</sub> CH <sub>2</sub> F	14.64	CF <sub>3</sub> CH <sub>2</sub> CHF <sub>2</sub>	15.13	CF <sub>3</sub> CHFCF <sub>3</sub>	16.13
CF <sub>3</sub> CH <sub>2</sub> CF <sub>3</sub>	16.21				
CF <sub>3</sub> CH <sub>2</sub> OCH <sub>3</sub>	12.45	CH <sub>2</sub> FOCF <sub>2</sub> CHF <sub>2</sub>	14.36	CHF <sub>2</sub> OCF <sub>2</sub> CH <sub>2</sub> F	15.33
CF <sub>3</sub> CH <sub>2</sub> OCH <sub>2</sub> F	13.09	CF <sub>3</sub> CH <sub>2</sub> OCHF <sub>2</sub>	14.46	CHF <sub>2</sub> OCF <sub>2</sub> CHF <sub>2</sub>	15.45
CF <sub>3</sub> OCH <sub>2</sub> CH <sub>3</sub>	13.70	CF <sub>3</sub> OCH <sub>2</sub> CHF <sub>2</sub>	14.68	CF <sub>3</sub> OCF <sub>2</sub> CHF <sub>2</sub>	15.78
CH <sub>3</sub> OCF <sub>2</sub> CHF <sub>2</sub>	13.87	CHF <sub>2</sub> OCF <sub>2</sub> CH <sub>3</sub>	15.20	CF <sub>3</sub> OCF <sub>2</sub> CH <sub>3</sub>	15.80
CHF <sub>2</sub> OCH <sub>2</sub> CHF <sub>2</sub>	14.02	CF <sub>3</sub> OCHFCHF <sub>2</sub>	15.23	CF <sub>3</sub> CHFOCF <sub>3</sub>	15.91
CF <sub>3</sub> OCH <sub>2</sub> CH <sub>2</sub> F	14.21	CF <sub>3</sub> CHFOCHF <sub>2</sub>	15.24	CF <sub>3</sub> CF <sub>2</sub> OCHF <sub>2</sub>	16.01
CH <sub>3</sub> OCF <sub>2</sub> CF <sub>3</sub>	14.22				

The empirical correlation embodied in Eq. 1 does not hold for the HCFCs we have examined: all of the corresponding points are clumped together some distance from either of the lines shown in Figure 2. Furthermore, the range of  $k_{OH}$  values for these chlorine-bearing molecules is very small. Nonetheless, it can be seen from Figure 3 that there might still be some relationship between  $\lg(k_{OH}/(\text{cm}^3\text{s}^{-1}))$  and  $\epsilon_{HOMO}$ , but the scatter suggests that this is not worth pursuing further. In any case, it has been suggested that some HCFCs may have rather large short-term ozone-depletion potentials [9].

**Figure 3**  $-\lg(k_{OH}/(\text{cm}^3\text{s}^{-1}))$  versus  $|\epsilon_{HOMO}|$  for HCFCs. The kinetic data are taken from Ref. 5 and the orbital energies from *ab initio* calculations. The scatter is much the same when using semi-empirical techniques.



As is well known, a variety of sophisticated models are in use to predict distributions and lifetimes of halogenated systems and their various breakdown products. However, a very simple scheme, based on ratios of the reciprocal of the  $k_{OH}$  values at 277 K, using  $\text{CH}_3\text{CCl}_3$  as a reference, often produces similar results for tropospheric lifetimes. In this spirit, we have used values of  $k_{OH}$  inferred from Eq. 1 to predict approximate lifetimes for HFEs and for  $\text{C}_3$  HFCs - all of these various estimates are available from Refs. 3 and 4, and will not be repeated here. A somewhat different strategy has been adopted by Nimitz and Skaggs [10], who were able, by means of multiple regression to a wide variety of data, to estimate lifetimes of  $\text{C}_1$  and  $\text{C}_2$  HFCs and HCFCs.

It is useful to describe briefly some interesting qualitative features of our predicted lifetimes. Two-carbon HFES with at least one C atom bearing two or more hydrogens appear to have significantly shorter lifetimes than the corresponding HFCs, whereas C<sub>2</sub> HFES in which the C atoms are bonded to at most one hydrogen appear to have slightly longer lifetimes.

In general, the C<sub>3</sub> HFES appear to have shorter lifetimes than the corresponding HFCs. This is particularly true for systems which contain CH<sub>3</sub>O- or CH<sub>2</sub>FO-, although HFES which contain -CH<sub>2</sub>O- or -CHFO- also appear to have shorter lifetimes than the corresponding HFCs. Combinations of these two sets of structural units lead to particularly short lifetimes. The three-carbon HFES which do not contain such units are predicted to have *longer* lifetimes than the HFCs from which they are formally derived. It is important to note that some of the heavily-fluorinated C<sub>3</sub> HFES, which may well possess thermophysical properties suited to various applications, appear to have *shorter* lifetimes than HFC-134a. It is difficult to emphasize strongly enough the urgent need for reliable kinetic data for such systems.

#### References

- 1 Cooper, D. L., Allan, N. L. and Powell, R. L. *J. Fluoro. Chem.* **46** (1990) 317; Cooper, D. L., Wright, S. C., Allan, N. L. and Winterton, N. *J. Fluoro. Chem.* **47** (1990) 489; Cooper, D. L., Allan, N. L. and Powell, R. L. *J. Fluoro. Chem.* **49** (1990) 421.
- 2 Cooper, D. L., Allan, N. L. and McCulloch, A. *Atmos. Environ.* **24A** (1990) 2417; Cooper, D. L. and Allan, N. L. *Atmos. Environ.* **24A** (1990) 2703.
- 3 Cooper, D. L., Cunningham, T. P., Allan, N. L. and McCulloch, A. *Atmos. Environ.* **26A** (1992) 1331.
- 4 Cooper, D. L., Cunningham, T. P., Allan, N. L. and McCulloch, A. *Atmos. Environ.* **27A** (1993) 117.
- 5 Hampson R. F., Kurylo, M. J. and Sander S. P. *UNEP/WMO Scientific Assessment of Stratospheric Ozone*, Appendix, AFEAS Report, Chapter III (1989).
- 6 See, for example: Güsten H., Klasinc, L. and Marić, D. *J. Atmos. Chem.* **2** (1984) 83; Güsten, H. and Klasinc, L. *Naturwissenschaften* **73** (1986) 129; Sabljic A. and Güsten H. *Atmos. Environ.* **24A** (1990) 73.
- 7 Abbatt, J. P. D. and Anderson, J. G. *J. Phys. Chem.* **95** (1991) 2382.
- 8 Aird, R. W. S., Canosa-Mas, C. E., Cook, D. J., Marston, G., Monks, P. S., and Wayne, R. P. *J. Chem. Soc. Faraday Trans.* **88** (1992) 1093.
- 9 Solomon, S. and Albritton, D. L. *Nature* **357** (1992) 33.
- 10 Nimitz, J. S. and Skaggs, S. R. *Envir. Sci. Technol.* **26** (1992) 739.

## Two-Dimensional Assessment of the Degradation of HFC-134a: Tropospheric Accumulations and Deposition of Trifluoroacetic Acid

J. M. Rodriguez, M. K. W. Ko, N. D. Sze, and C. W. Heisey

Atmospheric and Environmental Research, Inc., 840 Memorial Dr., Cambridge, MA 02139 USA

### Introduction

Concern about potential hazards to the biosphere from degradation of substitute halocarbons has focused attention on the degradation pathways for acetyl halides of the form  $\text{CF}_3\text{C}(\text{O})\text{X}$ , (where  $\text{X}=\text{F}$  or  $\text{Cl}$ ) produced in the oxidation of HCFC-123 ( $\text{CCl}_2\text{HCF}_3$ ), HCFC-124 ( $\text{CClHFCF}_3$ ), and HFC-134a ( $\text{CF}_3\text{CFH}_2$ ). Hydrolysis of these acetyl halides in rain or cloud water results in production of trifluoroacetic acid ( $\text{CF}_3\text{C}(\text{O})\text{OH}$ ; TFA), whose subsequent removal by rainwater could lead to contamination of ground water. The work presented here concentrates on the potential production of TFA from the degradation of HFC-134a.

Figure 1 illustrates schematically the degradation of HFC-134a. Existing data (see STEP-HALOCSIDE/AFEAS Workshop, 1991) suggest that the reactions following oxidation of HFC-134a by OH occur fast enough that we can assume at each point in space

$$P(\text{CF}_3\text{CHFO}) = k_{\text{OH}}[\text{OH}][\text{HFC-134a}] \quad (1),$$

where  $k_{\text{OH}}$  is the temperature-dependent rate for reaction of HFC-134a with OH (NASA/JPL, 1992). The concentration of TFA in rainwater can be calculated based on the following information: 1) the yield of  $\text{CF}_3\text{C}(\text{O})\text{F}$  from degradation of the alkoxy radical  $\text{CF}_3\text{CHFO}$ ; 2) the portion of  $\text{CF}_3\text{C}(\text{O})\text{F}$  that hydrolyzes in clouds to form TFA; 3) the portion of TFA that is released from the cloud to the gas-phase and re-incorporated in rainwater.

Laboratory measurements during the past year (see below) have provided information on the rates of some of the above processes. This paper discusses each of these processes in light of the new data, and is thus a refinement of the calculations presented by Rodriguez et al., (1991a), and, more recently, by Rodriguez et al. (1992). In particular, new laboratory techniques (DeBruyn et al., 1992a, George et al., 1992) allow for separate determination of the Henry's Law Constant ( $H$ ,  $\text{M}/\text{atm}$ ) and hydrolysis rates ( $k_w$ ,  $\text{s}^{-1}$ ) for  $\text{CF}_3\text{C}(\text{O})\text{F}$ , thus constraining the wet removal processes for these species.

### Pertinent Processes Determining the Yield of TFA from HFC-134a

#### a. Yield of $\text{CF}_3\text{C}(\text{O})\text{F}$

Calculations presented by Rodriguez et al. (1991a) assumed that 100% of the degradation of  $\text{CF}_3\text{CHFO}$  yielded  $\text{CF}_3\text{C}(\text{O})\text{F}$ . This alkoxy radical, however, can be removed from the atmosphere through two pathways: a thermal decomposition channel, producing  $\text{HC}(\text{O})\text{F}$  and  $\text{CF}_3$ , and reaction with  $\text{O}_2$ , producing  $\text{CF}_3\text{C}(\text{O})\text{F}$ . Temperature- and pressure-dependent relative rates for these two channels have been measured by Wallington et al. (1992) and Tuazon and Atkinson (1993). Utilizing the temperature climatology in our 2-D model, we calculate yields of  $\text{CF}_3\text{C}(\text{O})\text{F}$  ranging from about 20-30% at the surface, to a maximum of about 90% in the middle/upper troposphere. Results from the two experiments are consistent with each other within the uncertainties in temperature and pressure dependence, giving an average tropospheric yield of  $\text{CF}_3\text{C}(\text{O})\text{F}$  of about 40%.

## HFC 134a Degradation

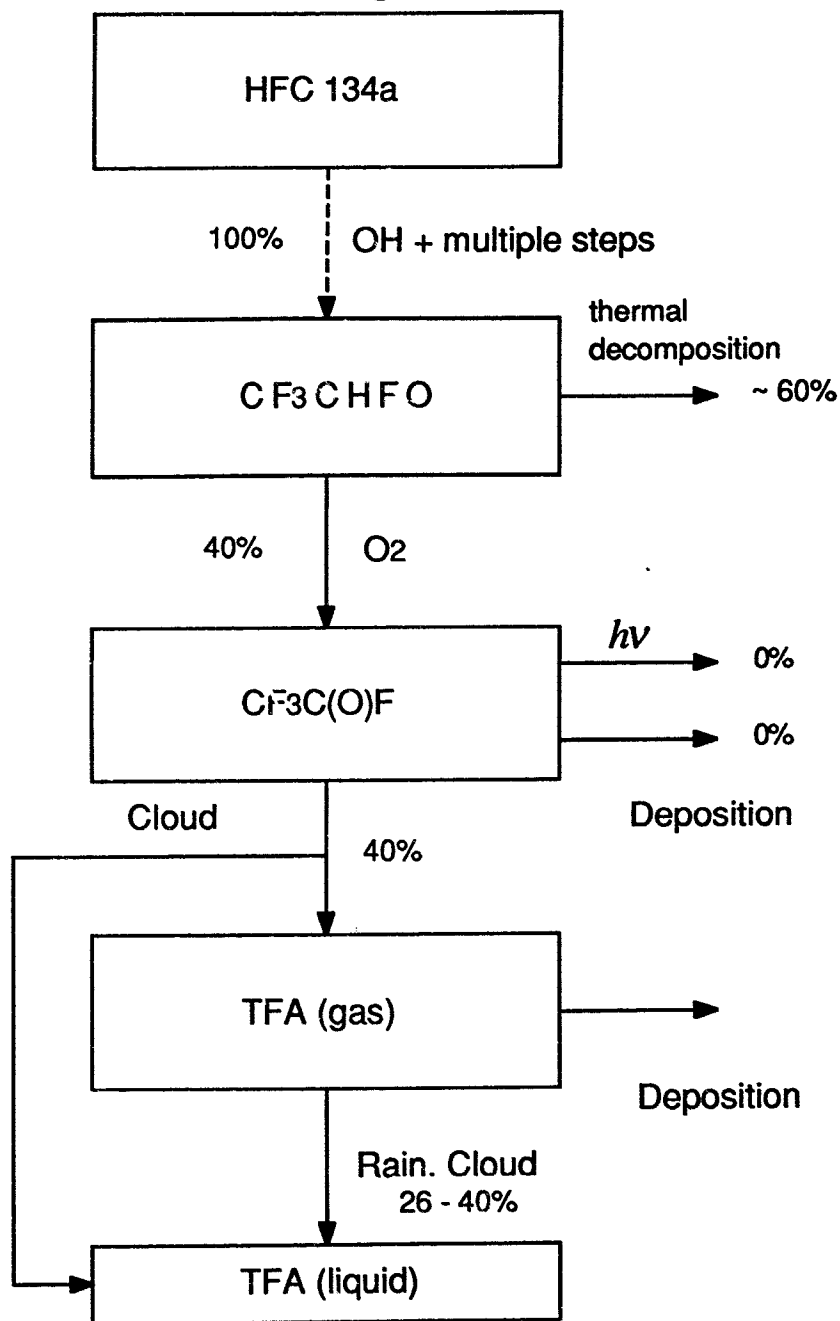


Figure 1: Schematic representation of the degradation of HFC-134a. The numbers along the different arrows denote the percent of moles of HFC-134a degraded through the corresponding pathway.

0125

b. Degradation of  $\text{CF}_3\text{C}(\text{O})\text{F}$

The acetyl halide  $\text{CF}_3\text{C}(\text{O})\text{F}$  can be transformed via three degradation processes: 1) dissolution and aqueous degradation in cloud and rainwater; 2) surface deposition on ocean and lands; 3) photolysis.

1.) Cloud and rain processes

The lifetime for chemical degradation of a trace gas in cloud water can be estimated by the expression (Wine and Chameides, 1990)

$$\tau_{\text{cloud}} (\text{days}) \approx \frac{3.9}{Hk_w} \quad (2),$$

where  $H$ , is the Henry's law constant (moles/liter/atm) and  $k_w$ , the first-order aqueous degradation rate ( $\text{s}^{-1}$ ) by hydrolysis or other processes. The above approximation is valid for  $H \leq 10^3$  moles/l/atm, and we have assumed a cloud water content of  $10^{-4} \text{ l cm}^{-2}$ . Similarly the lifetime for dissolution and removal in rainwater can be estimated by (Georgi and Chameides, 1985)

$$\tau_{\text{rain}} (\text{days}) \approx \frac{10^5}{H} \quad (3),$$

if  $H \leq 10^4$  moles/l/atm.

Wine and Chameides (1990) estimated that values of  $H$  for  $\text{CF}_3\text{C}(\text{O})\text{F}$  would be less than about 50 moles/liter/atm. Similarly, these authors indicated that aqueous degradation is expected to be dominated by hydrolysis, with  $k_w$  estimated to lie in the range  $0.001$  to  $100 \text{ s}^{-1}$ . For all reasonable estimates of  $H$  and  $k_w$ ,  $\tau_{\text{rain}} \gg \tau_{\text{cloud}}$ , and we can thus ignore the rainout process (3) for  $\text{CF}_3\text{C}(\text{O})\text{F}$ .

Hydrolysis of  $\text{CF}_3\text{C}(\text{O})\text{F}$  most probably produces TFA, which, in aqueous solutions, is almost completely dissociated into the trifluoroacetate ion ( $\text{CF}_3\text{COO}^-$ ) and  $\text{H}^+$ . We note that determination of the rate of cloud hydrolysis requires separate determination of  $H$  and  $k_w$ .

2.) Ocean/surface uptake

For a well-mixed trace species, the atmospheric lifetime for deposition on the ocean is approximately

$$\tau_{\text{dep}} (\text{days}) = \frac{9.3}{(0.7)(v_{\text{dep}})} \quad (4).$$

where  $v_{\text{dep}}$  is the deposition velocity in  $\text{cm/s}$ . Deposition to the ocean surface is parameterized following the model proposed by Liss, (1983). In this model, transfer to the ocean is envisioned in terms of an electrical circuit analogs, where different processes are represented by "resistances" (in parallel or in series). The total deposition velocity is given by:

$$\frac{1}{v_{\text{dep}}} = \frac{1}{v_{\text{air}}} + \frac{1}{v_{\text{water}}} \quad (5)$$

where  $v_{\text{air,water}}$  denote partial deposition velocities due to transfer through the atmosphere near the surface, and incorporation into the liquid surface. Equation (5) indicates that  $v_{\text{dep}}$  will be limited by the slower of the two processes.

The partial deposition velocity  $v_{\text{water}}$  can in turn be related to  $H$  and  $k_w$  (Thompson and Zafiriou, 1983). We note that

0-1-2-b

$$v_{\text{water}} \text{ (cm/s)} = 8.6 \times 10^{-2} H k_w^{1/2} \approx 6.8 \times 10^3 \gamma \quad \text{for } k_w \geq 10 \text{ s}^{-1} \quad (6a)$$

$$v_{\text{water}} \text{ (cm/s)} = 8.6 \times 10^{-2} H \quad \text{for } k_w \leq 1 \text{ s}^{-1} \quad (6b)$$

(Please note correction to equation 7 in Rodriguez et al., 1992). In equation (6a), it is assumed that the uptake coefficient  $\gamma$  is proportional to  $H k_w^{1/2}$ . For highly soluble gases,  $v_{\text{dep}}$  is determined by  $v_{\text{air}}$ . Values of  $v_{\text{air}}$  depend on meteorological conditions, surface roughness, etc (Seinfeld, 1986). We estimate  $v_{\text{air}}$  in the range of 0.3 to 1 cm/s.

Similar expressions hold for deposition over land, except that the surface terms cannot be simply related to  $H$  and  $k_w$ . Still, it is expected that highly soluble and/or reactive gases will have high surface deposition velocities, and vice-versa.

### 3.) Photolysis

Measurements of the absorption cross section of  $\text{CF}_3\text{C}(\text{O})\text{F}$  (Rattigan et al., 1992; Meller et al., 1992) indicate photolysis lifetimes of thousands of years in the troposphere. This process will thus be negligible compared to the aqueous processes and surface deposition discussed above.

### 4.) Pertinent laboratory data

Initially, experimental techniques reported only measurements for the uptake coefficient  $\gamma$  (DeBruyn et al., 1992) of  $\text{CF}_3\text{C}(\text{O})\text{F}$ . For experimental conditions where hydrolysis rates are sufficiently fast so that the equilibrium is rapidly achieved, the measured uptake coefficient is given by (DeBruyn et al., 1992b)

$$\frac{1}{\gamma} = \frac{1}{\alpha} + \frac{c}{4HRT(DK_w)^{1/2}} \quad (7)$$

where  $\alpha$  is the accommodation coefficient,  $R$  the gas constant,  $D$  the diffusion coefficient in the liquid phase,  $c$  the average thermal speed, and  $T$  the temperature. For  $\gamma \ll \alpha$ , we can disregard the first term in the right-hand side, and obtain a relation between a measured value (or upper bound)  $\gamma$  to the product  $H k_w^{1/2}$ . These measurements thus did not allow a unique determination of rates for hydrolysis, rain-out, and ocean uptake (reactions 2, 3, and 6), thus necessitating sensitivity studies for a whole range of parameters (Rodriguez et al., 1992).

Recent techniques have allowed separate determination of  $H$  and  $k_w$  by measuring time-dependent uptake coefficients before saturation is achieved (DeBruyn et al., 1992a). In this case, the uptake coefficient is given by

$$\frac{1}{\gamma(t)} \approx \frac{1}{\alpha} + \frac{c}{4HRTD^{1/2}} (1/t^{1/2} + k_w^{1/2})^{-1} \quad (8)$$

and values of  $H$  and  $k_w$  are obtained by fitting the data to the above equation.

Using the above technique for  $\text{CF}_3\text{C}(\text{O})\text{F}$ , Worsnop et al. (private communication) have obtained values of about 1 M/atm and  $10 \text{ s}^{-1}$  for  $H$  and  $k_w$ , respectively. The product of  $H k_w$  obtained from the above fits exhibits uncertainties of about factors of 3. Therefore, the hydrolysis lifetimes of order a few hours to 1 day are calculated for  $\text{CF}_3\text{C}(\text{O})\text{F}$  from equation (2). Ocean uptake velocities of about  $0.3 \text{ cm s}^{-1}$  are calculated from equations (5) and (6), corresponding to an ocean uptake lifetime of about 44 days (equation 4). We thus see that the kinetic data of Worsnop et al. indicates that removal of  $\text{CF}_3\text{C}(\text{O})\text{F}$  will be controlled primarily by cloud hydrolysis.

The hydrolysis rates values  $k_w$  of  $\text{CF}_3\text{C}(\text{O})\text{F}$  measured by Worsnop et al. are in agreement with those derived by Exner et al. (1992) from conductivity measurements in aprotic solvents and  $\text{H}_2\text{O}$ . Hydrolysis rates for  $\text{CF}_3\text{C}(\text{O})\text{Cl}$  measured by Worsnop, however, are about one order of magnitude smaller than those reported by George et al. (1992) using a similar method. Although this second group has not reported measurements for  $\text{CF}_3\text{C}(\text{O})\text{F}$ , the discrepancy in the  $\text{CF}_3\text{C}(\text{O})\text{Cl}$  values raises the question as to whether a similar discrepancy would hold for  $\text{CF}_3\text{C}(\text{O})\text{F}$ . The reason for this discrepancy has not been ascertained. A larger  $k_w$  would imply faster cloud hydrolysis. However, we note that this discrepancy introduces a negligible uncertainty in our calculations, since even for the Worsnop et al values cloud hydrolysis occurs so fast that the degradation rate of  $\text{CF}_3\text{C}(\text{O})\text{F}$  is limited by its production rates.

#### c. Degradation of TFA

We assume that, upon evaporation of cloud water, all of the acetate ions are released into the gas phase in the form of TFA. The fraction of cloud water which evaporates will depend on local conditions, but is expected to be high. It is also possible that other chemical processes in cloud water could lead to aqueous degradation of the acetate ion (Exner et al., 1992; Edney et al., 1992). Such processes could be important if their time constants were smaller than those associated with cloud evaporation and/or rainout (days to weeks). Due to the lack of quantitative information on these processes, we have not considered them in our study.

Removal of gas-phase TFA occurs through either re-incorporation in rainwater, or surface deposition. We assume that rainout removal rates for gas-phase TFA are the same as that of nitric acid, given the high solubility of TFA (Wine and Chameides, 1990). For the same reason, the surface/ocean deposition is expected to be dominated by the aerodynamic term in (5). We estimate surface deposition velocities in the range 0.3 - 1 cm/s.

#### Description of Calculations

We have carried out calculations to obtain the zonally-averaged concentration of TFA in rainwater, utilizing our 2-D model, and the latitude and seasonally dependent precipitation climatology of Jaeger (1976). We also assume that the cloud hydrolysis rate is proportional to the precipitation rate at each latitude and season. Other details of the model are given in Rodriguez et al. (1991a, b).

We adopt an upper limit of 1 day for the hydrolysis lifetime of  $\text{CF}_3\text{C}(\text{O})\text{F}$ , corresponding to a value of  $\text{H}k_w = 3.5 \text{ M/atm/s}$ . The ocean uptake is essentially controlled by the aerodynamic term, and we adopt an ocean deposition velocity of  $0.3 \text{ cm s}^{-1}$ . Further sensitivity runs (not shown) indicate that shorter hydrolysis lifetimes and faster ocean uptake yield essentially the same results, for the reasons discussed above.

Incorporation of TFA in rainwater could be reduced if gas-phase TFA is directly deposited on the surface after re-evaporation from clouds. The fraction of TFA evaporated and its deposition velocities are unknown. We thus consider cases A, B, and C, listed in Table 1. In case A, we assume that TFA formed in clouds stays in cloud water until it is rained out. For this case, surface deposition of gas-phase TFA plays no role. More realistic cases are represented by the conditions in cases B and C. In these cases, we assume that all of the TFA is re-evaporated into the gas-phase before being removed by rain or deposited on the surface. We adopt the same deposition velocity over surface and land, presumably determined by the aerodynamic resistance. Comparison of the deposition and rainout time constants suggests that surface deposition of gas-phase TFA could play a more important role in modifying the yield of TFA production.

**Table 1: Sensitivity to TFA parameters and results**

Case	Deposition Velocity for gas-phase TFA (cm/s)	Surface Uptake Lifetime for gas-phase TFA (days)	Washout Lifetime for TFA	Fraction of TFA evaporated after production	TFA conc. in rain water- Global avge. ( $\mu\text{g/l}$ ) for a 1000kT/yr source of HFC-134a
A				0%	0.94
B	0.3	31	12	100%	0.76
C	1.0	9	12	100%	0.57

### Results and Discussion

The calculated latitudinal distributions of TFA in rain are shown in Figure 2, for cases A, B, and C in Table 1. In general, higher concentrations are calculated in the tropical region due to faster degradation of HFC-134a. We note that calculated gas-phase concentrations of TFA (not shown) exhibit similar latitudinal patterns, with surface values of order 0.2-0.6 pptv.

Global average values for the three cases are listed in Table 1. If all of the HFC-134a were to be removed through the TFA channel, mass balance considerations would predict a global average rain concentration of 2.2 mg/l. Therefore, the net yield of TFA in rainwater from HFC-134a degradation ranges from 40% to 25%, depending primarily on assumptions about direct surface deposition of gas-phase TFA. The relative branching for each of the possible pathways in the HFC-134a degradation are shown in Figure 1.

We also stress that longitudinal asymmetries for the TFA concentrations could be quite large. Such asymmetries can be due to asymmetries in the precursor concentrations, OH fields, and rainfall rates, among other factors. Given that each of the above parameters can exhibit zonal asymmetries as large as factors of 3-4, we estimate that the TFA asymmetries could be of order 10-100.

Similar calculations (not shown) have been carried out for the degradation of HCFC-124 and 123, which yield  $\text{CF}_3\text{C}(\text{O})\text{F}$  and  $\text{CF}_3\text{C}(\text{O})\text{Cl}$ , respectively, with 100% efficiency (Tuazon and Atkinson, 1993). Our results indicate a 65-100% yield for HCFC-124, and about 55-75% for HCFC-123; the smaller values for HCFC-123 reflect the larger removal rate of  $\text{CF}_3\text{C}(\text{O})\text{Cl}$  by photolysis in the troposphere, compared to that of  $\text{CF}_3\text{C}(\text{O})\text{F}$  (Rattigan et al., 1992; Meller et al., 1992).

### Conclusions

We have incorporated the latest determinations of Henry's law constant and hydrolysis rate for  $\text{CF}_3\text{C}(\text{O})\text{F}$  into our 2-D model and estimated TFA concentrations in rainwater consistent with these data. As in our previous study (Rodriguez et al., 1992), we find that the TFA rainwater concentration is primarily determined by a) the yield of  $\text{CF}_3\text{C}(\text{O})\text{F}$  from degradation of the alkoxy radical  $\text{CF}_3\text{CHFO}$ , and b) the competition between removal of gas-phase TFA by rainwater and surface deposition. Our results serve to identify key processes for which laboratory/field measurements are needed. Key results of our study are as follows:

- We calculate global average concentrations of 0.6 - 0.9  $\mu\text{g/l}$  of TFA (maximum 1.2 - 1.6  $\mu\text{g/l}$  in the tropics), for a 1000 kT/year source in the Northern Hemisphere. Calculated global

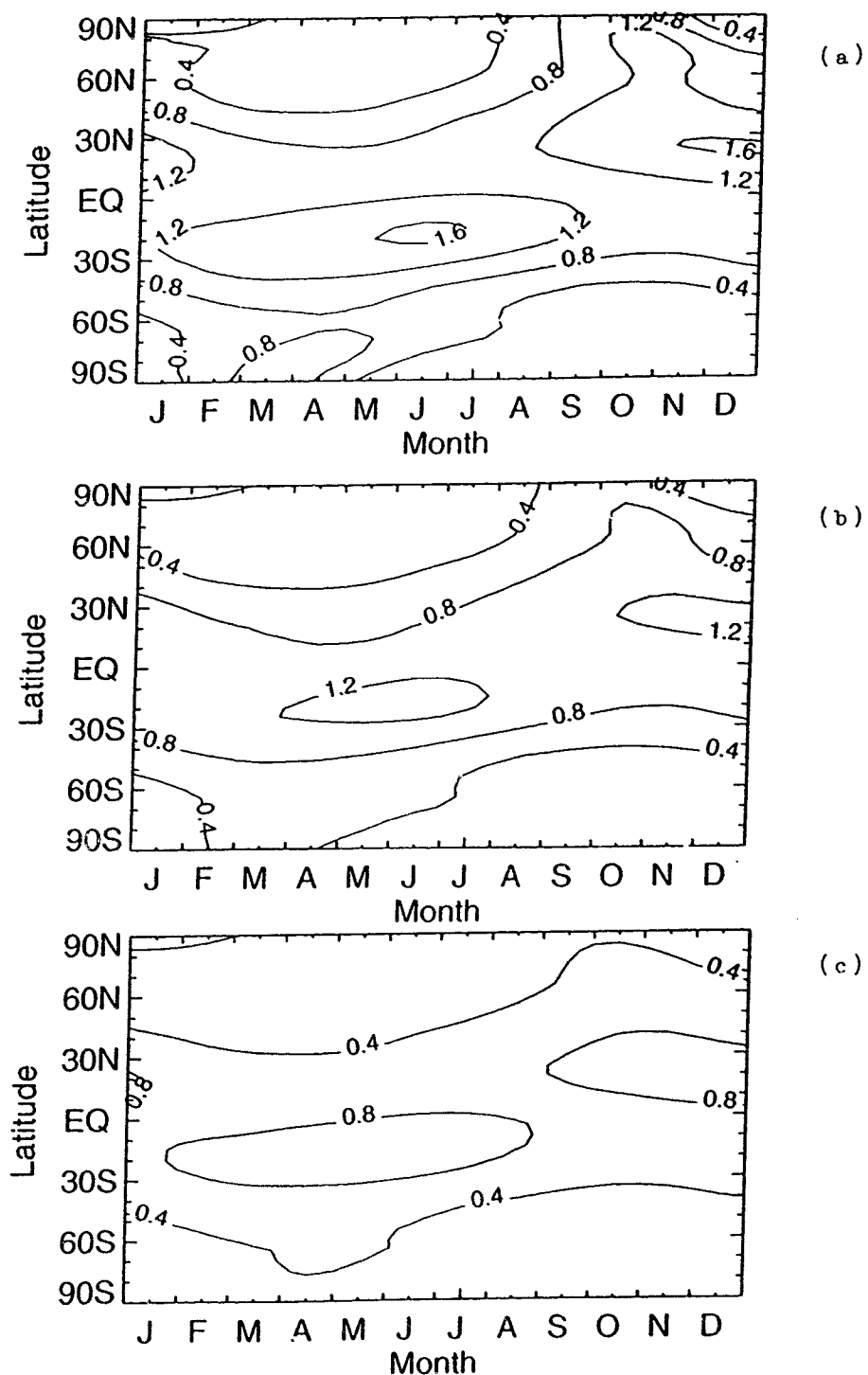


Figure 2: Calculated concentration of TFA in rainwater ( $\mu\text{g/l}$ ) as a function of latitude and season, for a 1000 kT/year source of HFC-134a in the Northern Hemisphere. Panels a, b, and c correspond to the assumptions of cases A, B, and C. See Table 1 and text for details.

average values are of order 0.6  $\mu\text{g/l}$  (maximum of 1  $\mu\text{g/l}$  in tropics) if surface deposition of gas-phase TFA is of order 1 cm/s.

- Global average concentrations of TFA in rain are primarily determined by the source strength of HFC-134a, the relative yield of  $\text{CF}_3\text{C(O)F}$  from the alkoxy radical, and the surface deposition of gas-phase TFA. These concentrations are relatively insensitive to the adopted uptake coefficient for  $\text{CF}_3\text{C(O)F}$ .
- Calculated concentrations near a local source could however be very sensitive to surface uptake and hydrolysis of  $\text{CF}_3\text{C(O)F}$ . Variations of factors of 10-100 could be expected depending on the adopted uptake coefficient.
- Our results indicate the need for the following measurements and studies:
  - a) Surface deposition velocities for TFA and  $\text{CF}_3\text{C(O)F}$ , particularly if they could be larger than 1 cm/s.
  - b) Measurement and assessment of other possible aqueous degradation mechanisms for TFA.
  - c) Regional modeling of TFA concentrations in rainwater.

#### References

- DeBruyn, W., J.A. Shorter, P. Davidovits, D.R. Worsnop, M.S. Zahniser, and C.E. Kolb (1992a) The Heterogeneous Chemistry of Carbonyl and Haloacetyl Halides. AFEAS Workshop Proceedings: *Atmospheric Wet and Dry Deposition of Carbonyl and Haloacetyl Halides*, Salway Research and Technology Center Brussels, Belgium, September 22, 1992.
- DeBruyn, W.J., S.X. Duan, X.Q. Shi and P. Davidovits, D.R. Worsnop, M.S. Zahniser, and C.E. Kolb (1992b) Tropospheric heterogeneous chemistry of haloacetyl and carbonyl halides. *Geophys. Res. Lett.*, **19**, 1939-1942.
- Edney, E.O. and D.J. Driscoll (1992) A laboratory investigation of deposition of oxidation products of HCFCs and HFCs to aqueous solutions. *Water Air, Soil Pollu.*, in press.
- Exner, M., H. Herrmann, J. Michel, and R. Zellner (1992) Hydrolysis Rate of Trifluoroacetyl Fluoride and the Decarboxylation of Trifluoroacetate Anions. AFEAS Workshop Proceedings: *Atmospheric Wet and Dry Deposition of Carbonyl and Haloacetyl Halides*, Salway Research and Technology Center Brussels, Belgium, September 22, 1992.
- George, C., J.L. Ponche, and P. Mirabel (1992) Experimental Determination of Mass Accommodation Coefficients. AFEAS Workshop Proceedings: *Atmospheric Wet and Dry Deposition of Carbonyl and Haloacetyl Halides*, Salway Research and Technology Center Brussels, Belgium, September 22, 1992.
- Giorgi, F. and W.L. Chameides (1985) The rainout parameterization in a photochemical model. *J. Geophys. Res.*, **90**, 7872-7880.
- Jaeger, L. Berichte des Deutschen Wetterdienstes Nr. 139 (18) Im Selbstverlad des Deutschen Wetterdienstes, Offenback, W. Germany, 1976.
- Liss, P.S. (1983) "Gas transfer: Experiments and geochemical implications." In *Air-Sea Exchange of Gases and Particles*, edited by P.S. Liss and W.G.N. Slinn, 241-298. D. Reidel Publishing Company.
- Meller, R. D. Boglu, G.K. Moortgat (1992) "UV Spectra of Several Halogenated Carbonyl Compounds and FTIR Studies on the Degradation of  $\text{CF}_3\text{COCl}$ , HCFC-123 and HFC-134a." In *Proceedings of Kinetics and Mechanisms for the Reactions of Halogenated Organic Compounds in Troposphere*, STEP-HALOCSIDE/AFEAS Workshop (University of Dublin), pp. 110-115.

- NASA/JPL (1992) *Chemical Kinetics and Photochemical Data for Use in Stratospheric Modeling*, Evaluation No. 10. JPL Publication 92-20, National Aeronautics and Space Administration, Jet Propulsion Laboratory, Pasadena, CA.
- Rattigan, O., R.A. Cox, and R.L. Jones (1992) "The UV Absorption Cross-Sections of  $\text{CF}_3\text{COCl}$ ,  $\text{CF}_3\text{COF}$ ,  $\text{CH}_3\text{COF}$ , and  $\text{CCl}_3\text{CHO}$ . In *Proceedings of Kinetics and Mechanisms for the Reactions of Halogenated Organic Compounds in Troposphere*, STEP-HALOCSIDE/AFEAS Workshop (University of Dublin), pp. 116-125.
- Rodriguez, J.M., M.K.W. Ko, N.D. Sze, and C.W. Heisey (1991a) "Model assessment of concentrations of trifluoroacetic acid in rainwater from degradation of HCFC/HFCs." In *Proceedings of Kinetics and Mechanisms for the Reactions of Halogenated Organic Compounds in Troposphere*, STEP-HALOCSIDE/AFEAS Workshop (University of Dublin), pp. 138-143.
- Rodriguez, J.M., M.K.W. Ko, N.D. Sze, and C.W. Heisey (1991b) "Impact of biomass burning on tropospheric CO and OH: a two-dimensional study." In *Global Biomass Burning. Atmospheric, Climatic, and Biospheric Implications*, J.S. Levene, Ed. The MIT Press, Cambridge p. 42-.
- Rodriguez, J.M., M.K.W. Ko, N.D. Sze, and C.W. Heisey (1992) Model Assessment of the Impact of Wet and Dry Deposition on the Tropospheric Abundances of Acetyl Halides and Trifluoroacetic Acid. AFEAS Workshop Proceedings: *Atmospheric Wet and Dry Deposition of Carbonyl and Haloacetyl Halides*, Salway Research and Technology Center Brussels, Belgium, September 22, 1992.
- Seinfeld, J.H. (1986) *Atmospheric Chemistry and Physics of Air Pollution*. John Wiley & Sons, New York.
- Thompson, A.M. and O.C. Zafiriou (1983) Air-Sea fluxes of transient atmospheric species. *J. Geophys. Res.*, **88**, 6696-6708.
- Tuazon, E.C., and R. Atkinson (1993) Tropospheric degradation products of  $\text{CH}_2\text{FCF}_3$  (HFC-134a). *J. Atmos. Chem.*, **16**, 301-312.
- Wallington, T.J., M.D. Hurley, J.C. Ball, and E.W. Kaiser (1992) Atmospheric chemistry of hydrofluorocarbon 134a: Fate of the Alkoxy Radical  $\text{CF}_3\text{CFHO}$ . *Environ. Sci. Technol.*, **26**, 1318-1324.
- Wine, P.H. and W.L. Chameides (1990) Scientific Assessment of Stratospheric Ozone: 1989, World Meteorological Organization, Global Ozone Research and Monitoring Project, Report No. 20, Vol. 2, 271-295.

## A global three-dimensional study of the degradation of HCFCs and HFC-134a in the troposphere.

Maria Kanakidou<sup>1</sup>, Frank J. Dentener<sup>2</sup>, Paul J. Crutzen<sup>2</sup>

<sup>1</sup> *Centre des Faibles Radioactivités, Laboratoire mixte CNRS/CEA, Domaine du CNRS F-91198 Gif-sur-Yvette Cedex, France.*

<sup>2</sup> *Max Planck Institute for Chemistry, Atmospheric Chemistry Division, P.O.Box 3060 D-6500 Mainz, Germany.*

### Introduction

The chlorofluoro- and fluoro- hydrocarbons (HCFCs and HFCs) have substantially shorter atmospheric lifetimes due to oxidation by OH radicals and they are, therefore, less aggressive towards stratospheric ozone. They thus also have significantly lower greenhouse warming potential than chlorofluorocarbons (CFCs). However, to evaluate the environmental and climatic effects of HCFC and HFC usage information on the atmospheric lifetime and the distribution of HCFCs, HFCs and their oxidation products is needed.

In the present study the 3-D global tropospheric model MOGUNTIA has been used to describe the fate of HCFC-22 (CHClF<sub>2</sub>), HCFC-123 (CF<sub>3</sub>CHCl<sub>2</sub>), HCFC-124 (CF<sub>3</sub>CHClF), HFC-134a (CF<sub>3</sub>CH<sub>2</sub>F), HCFC-141b (CH<sub>3</sub>CCl<sub>2</sub>F) and HCFC-142b (CH<sub>3</sub>CClF<sub>2</sub>), as well as their oxidation products in the troposphere.

### Model description

The model used is the climatological global 3-D model of the troposphere MOGUNTIA. It has 10° latitude x 10° longitude x 100 hPa grid boxes [1]. The model transport and stratospheric loss parameterization have been successfully tested using Kr-85 [2] and CFC-11. The model interhemispheric exchange time of 1.06 years and the loss of CFC-11 to the stratosphere (corresponding to a stratospheric lifetime of 53 years) has produced good results for CFC-11, with a maximum deviation between model results and measurements of less than 5%.

A version of the model describing O<sub>3</sub>/OH/NO<sub>x</sub>/CH<sub>4</sub>/CO/C<sub>2</sub>H<sub>6</sub>/C<sub>3</sub>H<sub>8</sub> photochemistry has previously been used to calculate the 3-D fields of monthly varying mean concentrations of OH, NO, NO<sub>2</sub> and HO<sub>2</sub> [3] and also took into account the heterogeneous chemistry of NO<sub>3</sub> and N<sub>2</sub>O<sub>5</sub> on sulfate and seasalt aerosols [4]. The OH, NO, NO<sub>2</sub> and HO<sub>2</sub> concentration fields calculated with that model have been used in this study where we consider a total of 103 gas phase reactions involved in the photochemical removal of HCFC-22, HCFC-123, HCFC-124, HFC-134a, HCFC-141b, HCFC-142b and of their oxidation products. We also consider heterogeneous removal processes (oceanic removal, washout and hydrolysis in clouds). The Henry's law coefficients, the hydrolysis rates and the literature sources used to calculate the heterogeneous loss rates are given in Table 1. To describe the influence of cloud chemistry, a three-dimensional distribution of clouds and liquid water content is derived from the NCAR statistics on different cloud types and assumptions on cloud height and liquid water content [5, 6].

**Table 1. a.** Henry's law coefficients adopted in this study.

Species	H (M.atm <sup>-1</sup> )	References
HCFC-22	exp[-8.689+205.9/(T-255.1)]#	[7]
HCFC-123	exp[-14.06+2570/T]#	[7]
HCFC-124	exp[-17.39+3229/T]#	[7]
HCFC-141b	exp[-2461+5248/T]#	[7]
HCFC-142b	exp[-15.11+2544/T]#	[7]
ROOH	300	[8]
CClF <sub>2</sub> OONO <sub>2</sub>	2.9 exp[5910*(1/T-1/298)]	taken equal to that of PAN[8]
COF <sub>2</sub>	20	[9]
COFCl	10	average of COF <sub>2</sub> and COCl <sub>2</sub>
CF <sub>3</sub> COCl	2.5	[9]
CF <sub>3</sub> COF	3	[9]
HCOF	3	based on the CF <sub>3</sub> COF
CClF <sub>2</sub> C(O)OOH	3000	assumed as suggested by [8]
CCl <sub>2</sub> FC(O)OOH	3000	"

**Table 1. b.** Hydrolysis rates adopted in this study

Species	k <sub>H</sub> (s <sup>-1</sup> )	References
HCFC-22	6. 10 <sup>-10</sup>	[8]
HCFC-123	2. 10 <sup>-9</sup>	as suggested by [8]
HCFC-124	2. 10 <sup>-9</sup>	"
HCFC-141b	2. 10 <sup>-9</sup>	"
HCFC-142b	2. 10 <sup>-9</sup>	"
ROOH	10 <sup>-4</sup>	"
CClF <sub>2</sub> OONO <sub>2</sub>	10 <sup>-4</sup>	[8]
COF <sub>2</sub>	8	[9]
COFCl	50	average of COF <sub>2</sub> and COCl <sub>2</sub>
CF <sub>3</sub> COCl	200	[9]
CF <sub>3</sub> COF	147	[9]
HCOF	0.01	see text
CClF <sub>2</sub> C(O)OOH	5.10 <sup>-4</sup>	as suggested by [8]
CCl <sub>2</sub> FC(O)OOH	5.10 <sup>-4</sup>	"

# H in mass%/kPa, T in Kelvin

The computed fields of OH concentrations reasonably reproduced the mixing ratios and the seasonal cycle of CH<sub>3</sub>CCl<sub>3</sub> measured at the ALE/GAGE network surface stations. With respect to oxidation by tropospheric OH the lifetime of CH<sub>3</sub>CCl<sub>3</sub> is calculated to be 6.5 years and the stratospheric loss alone would correspond to a lifetime of 54 years. Parameterizing the oceanic sink of CH<sub>3</sub>CCl<sub>3</sub> according to Butler et al. [10], yields a lifetime of about 63 years. The overall atmospheric lifetime of CH<sub>3</sub>CCl<sub>3</sub> is thus calculated to be 5.3 years.

The gas phase chemical reactions describing the HCFCs and HFC-134a oxidation in the troposphere and the corresponding reaction rate coefficients adopted in this study are summarized in Table 2. Simplifications are made concerning the little known chemistry of the CF<sub>3</sub>O radical. Reaction rates of the CF<sub>3</sub>O radical with NO, NO<sub>2</sub>, CO, hydrocarbons, and CH<sub>2</sub>O have been measured [11] and there is continuing research on this topic [12]. COF<sub>2</sub> has been identified as product from CF<sub>3</sub>O reaction with NO. The CF<sub>3</sub>OH formed from the reaction of CF<sub>3</sub>O with hydrocarbons is also very quickly decomposed to COF<sub>2</sub> (see detailed discussion in [11] and [12]). Thus, in order to simplify this complicated CF<sub>3</sub>O chemistry, we assume a yield of unity for COF<sub>2</sub> from the CF<sub>3</sub>O radical. Organic nitrate formation by reaction of halogenated alkylperoxy radicals with nitrogen oxide (RO<sub>2</sub> + NO → RONO<sub>2</sub>) is neglected here because the branching ratio between nitrate production and halogenated alkoxy radical formation (RO<sub>2</sub> + NO → RO + NO<sub>2</sub>) has not yet been determined. Only few of the gas phase reaction rates involved in the chemistry of HCFCs and HFC-134a have been measured at present and thus assumptions on the remainder have to be made. The results presented here strongly depend on these assumptions (Table 2) and thus the relative importance of these reactions might change when measurements become available.

**Table 2.** Gas phase reaction rates and cross-section literature sources.

Reaction	Reaction rate k	Reference
<b>HCFC-22 chemistry</b>		
CHClF <sub>2</sub> + OH → CClF <sub>2</sub> + H <sub>2</sub> O	1.2 x 10 <sup>-12</sup> exp(-1650/T)	[13]
CClF <sub>2</sub> + O <sub>2</sub> → CClF <sub>2</sub> O <sub>2</sub>	very fast	
CClF <sub>2</sub> O <sub>2</sub> + HO <sub>2</sub> → CClF <sub>2</sub> OOH + O <sub>2</sub>	6.5 x 10 <sup>-13</sup> exp(650/T)	that of C <sub>2</sub> H <sub>5</sub> O <sub>2</sub> [18]
CClF <sub>2</sub> O <sub>2</sub> + NO → CClF <sub>2</sub> O + NO <sub>2</sub>	3.1 x 10 <sup>-12</sup> exp(500/T)	[13]
CClF <sub>2</sub> O <sub>2</sub> + NO <sub>2</sub> → CClF <sub>2</sub> OONO <sub>2</sub>	k <sub>0</sub> = 4 x 10 <sup>-29</sup> (T/300) <sup>-5</sup> †	[14]
	k <sub>∞</sub> = 10 <sup>-11</sup> (T/300) <sup>-0.7</sup> , F <sub>298</sub> = 0.45	
CClF <sub>2</sub> O → COF <sub>2</sub> + Cl	very fast	
CClF <sub>2</sub> OOH + OH → CClF <sub>2</sub> O <sub>2</sub> + H <sub>2</sub> O	1.7 x 10 <sup>-12</sup> exp(220/T)	suggested for ROOH [15]
CClF <sub>2</sub> OOH $\xrightarrow{h\nu}$ CClF <sub>2</sub> O + OH	that of CH <sub>3</sub> OOH is used	[16]
CClF <sub>2</sub> OONO <sub>2</sub> $\xrightarrow{M}$ CClF <sub>2</sub> O <sub>2</sub> + NO <sub>2</sub>	k <sub>0</sub> = 5.6 x 10 <sup>-4</sup> exp(-9310/T)	[14]
	k <sub>∞</sub> = 10 <sup>16</sup> exp(-11880/T), F <sub>298</sub> = 0.4	
CClF <sub>2</sub> OONO <sub>2</sub> $\xrightarrow{h\nu}$ CClF <sub>2</sub> O <sub>2</sub> + NO <sub>2</sub>	cross-section of CCl <sub>2</sub> FOONO <sub>2</sub> * [17]	

0 1 3 5

Table 2. continued

Reaction	Reaction rate k	Reference
$\text{COF}_2 \xrightarrow{h\nu}$	extremely slow	
<b>HCFC-123 chemistry</b>		
$\text{CF}_3\text{CHCl}_2 + \text{OH} \rightarrow \text{CF}_3\text{CCl}_2 + \text{H}_2\text{O}$	$7.7 \times 10^{-13} \exp(-900/T)$	[13]
$\text{CF}_3\text{CCl}_2 + \text{O}_2 \rightarrow \text{CF}_3\text{CCl}_2\text{O}_2$	very fast	
$\text{CF}_3\text{CCl}_2\text{O}_2 + \text{NO} \rightarrow \text{CF}_3\text{CCl}_2\text{O} + \text{NO}_2$	that of $\text{CCl}_2\text{FO}_2$ is used	
$\text{CF}_3\text{CCl}_2\text{O}_2 + \text{NO}_2 \rightarrow \text{CF}_3\text{CCl}_2\text{OONO}_2$	$k_0 = 5.5 \times 10^{-29} (T/300)^{-5}$	that of $\text{CCl}_2\text{FO}_2$ [15]
	$k_\infty = 8.3 \times 10^{-12} (T/300)^{-0.7}$ , $F_c = 0.42$	
$\text{CF}_3\text{CCl}_2\text{O}_2 + \text{HO}_2 \rightarrow \text{CF}_3\text{CCl}_2\text{OOH} + \text{O}_2$	$6.5 \times 10^{-13} \exp(650/T)$	that of $\text{C}_2\text{H}_5\text{O}_2$ [18]
$\text{CF}_3\text{CCl}_2\text{OONO}_2 \xrightarrow{M} \text{CF}_3\text{CCl}_2\text{O}_2 + \text{NO}_2$	$k_0 = 3 \times 10^{-3} \exp(-10570/T)$	that of $\text{CCl}_2\text{FOONO}_2$
	$k_\infty = 2.1 \times 10^{16} \exp(-11980/T)$ , $F_c = 0.4$	[15]
$\text{CF}_3\text{CCl}_2\text{OONO}_2 \xrightarrow{h\nu} \text{CF}_3\text{CCl}_2\text{O}_2 + \text{NO}_2$	that of $\text{CCl}_2\text{FOONO}_2$	
$\text{CF}_3\text{CCl}_2\text{OOH} + \text{OH} \rightarrow \text{CF}_3\text{CCl}_2\text{O}_2 + \text{H}_2\text{O}$	$1.7 \times 10^{-12} \exp(220/T)$	70% of the total reaction [15]
$\text{CF}_3\text{CCl}_2\text{OOH} \xrightarrow{h\nu} \text{CF}_3\text{CCl}_2\text{O} + \text{OH}$	that of $\text{CH}_3\text{OOH}$	[19]
$\text{CF}_3\text{CCl}_2\text{O} \rightarrow \text{CF}_3\text{C(O)Cl} + \text{Cl}$	very fast	
$\text{CF}_3\text{C(O)Cl} \xrightarrow{h\nu, O_2} \text{CF}_3\text{O}_2 + \text{CO} + \text{Cl}$	cross sections from	[20]
<b>HCFC-124 chemistry</b>		
$\text{CF}_3\text{CHClF} + \text{OH} \rightarrow \text{CF}_3\text{CFCl} + \text{H}_2\text{O}$	$6.3 \times 10^{-13} \exp(-1250/T)$	[13]
$\text{CF}_3\text{CClF} + \text{O}_2 \rightarrow \text{CF}_3\text{CFClO}_2$	very fast	
$\text{CF}_3\text{CClFO}_2 + \text{NO} \rightarrow \text{CF}_3\text{CFClO} + \text{NO}_2$	$3.1 \times 10^{-12} \exp(500/T)$	that of $\text{CClF}_2\text{O}_2$ [13,15]
$\text{CF}_3\text{CClFO}_2 + \text{NO}_2 \rightarrow \text{CF}_3\text{CFClOONO}_2$	$k_0 = 4 \times 10^{-29} (T/300)^{-5}$	[21]
	$k_\infty = 1.1 \times 10^{-11} (T/300)^{-0.7}$ , $F_c = 0.45$	
$\text{CF}_3\text{CClFO}_2 + \text{HO}_2 \rightarrow \text{CF}_3\text{CFClOOH} + \text{O}_2$	that of $\text{C}_2\text{H}_5\text{O}_2$	[18]
$\text{CF}_3\text{CClFOONO}_2 \xrightarrow{M} \text{CF}_3\text{CFClO}_2 + \text{NO}_2$	$k_0 = 5.6 \times 10^{-14} \exp(-9310/T)$	[15]
	$k_\infty = 1.1 \times 10^{16} \exp(-11880/T)$ , $F_c = 0.4$	
$\text{CF}_3\text{CClFOONO}_2 \xrightarrow{h\nu} \text{CF}_3\text{CClFO}_2 + \text{NO}_2$	that of $\text{CCl}_2\text{FOONO}_2$	
$\text{CF}_3\text{CClFOOH} \xrightarrow{h\nu} \text{CF}_3\text{CClFO} + \text{OH}$	that of $\text{CH}_3\text{OOH}$	
$\text{CF}_3\text{CClFOOH} + \text{OH} \rightarrow \text{CF}_3\text{CClFO}_2 + \text{H}_2\text{O}$	$1.7 \times 10^{-12} \exp(220/T)$	[15]
$\text{CF}_3\text{CClFO} \rightarrow \text{CF}_3\text{COF} + \text{Cl}$	very fast	
$\text{CF}_3\text{COF} \xrightarrow{h\nu, O_2} \text{CF}_3\text{O}_2 + \text{CO} + \text{F}$	cross sections from	[20]
<b>HCFC-134a chemistry</b>		
$\text{CF}_3\text{CH}_2\text{F} + \text{OH} \rightarrow \text{CF}_3\text{CHF} + \text{H}_2\text{O}$	$1.7 \times 10^{-12} \exp(-1750/T)$	[13]
$\text{CF}_3\text{CHF} + \text{O}_2 \rightarrow \text{CF}_3\text{CHFO}_2$	very fast	
$\text{CF}_3\text{CHFO}_2 + \text{NO} \rightarrow \text{CF}_3\text{CHFO} + \text{NO}_2$	that of $\text{CClF}_2\text{O}_2$ is used	
$\text{CF}_3\text{CHFO}_2 + \text{NO}_2 \rightarrow \text{CF}_3\text{CHFOONO}_2$	as above	
$\text{CF}_3\text{CHFO}_2 + \text{HO}_2 \rightarrow \text{CF}_3\text{CHFOOH} + \text{O}_2$	as above	
$\text{CF}_3\text{CHFOONO}_2 \xrightarrow{M} \text{CF}_3\text{CHFO}_2 + \text{NO}_2$	that of $\text{CClF}_2\text{OONO}_2$ is used	

Table 2. continued

Reaction	Reaction rate k	Reference
$\text{CF}_3\text{CHFOOH} + \text{OH} \rightarrow \text{CF}_3\text{CHFO}_2 + \text{H}_2\text{O}$	$1.7 \times 10^{-12} \exp(220/T)$	that of $\text{C}_2\text{H}_5\text{O}_2$ [15, 18]
$\text{CF}_3\text{CHFOOH} \xrightarrow{h\nu} \text{CF}_3\text{CHFO} + \text{OH}$	that of $\text{CH}_3\text{OOH}$ is used	
$\text{CF}_3\text{CHFO} \xrightarrow{M1, Q2} \text{CF}_3\text{C(O)F} + \text{HO}_2$ ( $k_1$ )	$3.9 \times 10^{-15} \exp(-900/T)$	$0.1 \times K_{\text{CH}_3\text{O}+\text{O}_2}$ [13]
$\text{CF}_3\text{CHFO} \xrightarrow{M2} \text{CF}_3 + \text{HCOF}$ ( $k_2$ )		
The ratio of the two previous pathways ( $k_1$ )/( $k_2$ )	$1.58 \times 10^{-25} \exp(3600/T) \times (760/P)$ note 1 [22]	
$\text{CF}_3 + \text{O}_2 \rightarrow \text{CF}_3\text{O}_2$	very fast	
$\text{CF}_3\text{O}_2 + \text{HO}_2 \rightarrow \text{CF}_3\text{OOH} + \text{O}_2$	$3.8 \times 10^{-13} \exp(800/T)$	that of $\text{CH}_3\text{O}_2$ [13]
$\text{CF}_3\text{OOH} + \text{OH} \rightarrow \text{CF}_3\text{O}_2 + \text{H}_2\text{O}$	that of $\text{CH}_3\text{O}_2$	[15]
$\text{CF}_3\text{OOH} \xrightarrow{h\nu} \text{CF}_3\text{O} + \text{OH}$	that of $\text{CH}_3\text{OOH}$	
$\text{CF}_3\text{O}_2 + \text{NO} \rightarrow \text{FNO}_2 + \text{COF}_2$	$1.45 \times 10^{-11} (T/298)^{-1.2}$	[27]
$\text{CF}_3\text{O}_2 + \text{NO}_2 \rightarrow \text{CF}_3\text{OONO}_2$	$k_0 = 2.7 \times 10^{-29} (T/300)^{-5}$	[18]
	$k_\infty = 9 \times 10^{-12} (T/300)^{-0.7}$ , $F_c = \exp(-T/416)$	
$\text{CF}_3\text{OONO}_2 \xrightarrow{M} \text{CF}_3\text{O}_2 + \text{NO}_2$	that of $\text{CClF}_2\text{OONO}_2$	
$\text{CF}_3\text{OONO}_2 \xrightarrow{h\nu} \text{CF}_3\text{O}_2 + \text{NO}_2$	that of $\text{CClF}_2\text{OONO}_2$	
$\text{CF}_3\text{O} \rightarrow \text{COF}_2 + \text{F}$	simplification assumed to be very fast	
$\text{FNO}_2 \rightarrow \text{F} + \text{NO}_2$	very fast	
<b>HCFC-141b chemistry</b>		
$\text{CCl}_2\text{FCH}_3 + \text{OH} \rightarrow \text{CCl}_2\text{FCH}_2 + \text{H}_2\text{O}$	$1.3 \times 10^{-12} \exp(-1600/T)$	[13]
$\text{CCl}_2\text{FCH}_2 + \text{O}_2 \rightarrow \text{CCl}_2\text{FCH}_2\text{O}_2$	very fast	
$\text{CCl}_2\text{FCH}_2\text{O}_2 + \text{NO} \rightarrow \text{CCl}_2\text{FCH}_2\text{O} + \text{NO}_2$	$8.9 \times 10^{-12} \exp(0/T)$	that of $\text{C}_2\text{H}_5\text{O}_2$ [15, 18]
$\text{CCl}_2\text{FCH}_2\text{O}_2 + \text{NO}_2 \rightarrow \text{CCl}_2\text{FCH}_2\text{OONO}_2$	$k_0 = 1.9 \times 10^{-30} (T/298)^{-4}$	that of $\text{CH}_3\text{O}_2$ is used
	$k_\infty = 1. \times 10^{-11} (T/298)^{-1}$ , $F_c = 0.4$	[15, 18]
$\text{CCl}_2\text{FCH}_2\text{O}_2 + \text{HO}_2 \rightarrow \text{CCl}_2\text{FCH}_2\text{OOH} + \text{O}_2$	that of $\text{CClF}_2\text{O}_2$	
$\text{CCl}_2\text{FCH}_2\text{OOH} + \text{OH} \rightarrow \text{CCl}_2\text{FCH}_2\text{O}_2 + \text{H}_2\text{O}$	that of $\text{CClF}_2\text{OOH}$	
$\text{CCl}_2\text{FCH}_2\text{OONO}_2 \xrightarrow{M} \text{CCl}_2\text{FCH}_2\text{O}_2 + \text{NO}_2$	$k_0 = 0.09 \times 10^{-3} \exp(-9694/T)$	that of $\text{CH}_3\text{OONO}_2$
	$k_\infty = 1.1 \times 10^{16} \exp(-10560/T)$ , $F_c = 0.4$	[15, 18]
$\text{CCl}_2\text{FCH}_2\text{OONO}_2 \xrightarrow{h\nu} \text{CCl}_2\text{FCH}_2\text{O}_2 + \text{NO}_2$	that of $\text{CClF}_2\text{OONO}_2$	
$\text{CCl}_2\text{FCH}_2\text{OOH} \xrightarrow{h\nu} \text{CCl}_2\text{FCH}_2\text{O} + \text{OH}$	that of $\text{CH}_3\text{OOH}$	
$\text{CCl}_2\text{FCH}_2\text{O} \xrightarrow{Q2} \text{CCl}_2\text{FCHO} + \text{HO}_2$	very fast	
$\text{CCl}_2\text{FCHO} \xrightarrow{h\nu, 2Q2} \text{CCl}_2\text{FO}_2 + \text{CO} + \text{HO}_2$	cross sections form	[27]
$\text{CCl}_2\text{FCHO} + \text{OH} \xrightarrow{Q2} \text{CCl}_2\text{FC(O)O}_2 + \text{H}_2\text{O}$	$1.3 \times 10^{-13} \exp(250/T)$	note 2 [24]
$\text{CCl}_2\text{FC(O)O}_2 + \text{NO}_2 \rightarrow \text{CCl}_2\text{FC(O)OONO}_2$	$k_0 = 27 \times 10^{-29}$	that of PAN is used [18]
	$k_\infty = 12.1 \times 10^{12}$ , $F_c = 0.3$	
$\text{CCl}_2\text{FC(O)O}_2 + \text{HO}_2 \rightarrow \text{CCl}_2\text{FC(O)OOH} + \text{O}_2$ (ka)	$k_a + k_b = 4.3 \times 10^{-13} \exp(1040/T)$	that of $\text{CH}_3\text{C(O)O}_2$ [18]
$\text{CCl}_2\text{FC(O)O}_2 + \text{HO}_2 \rightarrow \text{CCl}_2\text{FCOOH} + \text{O}_3$ (kb)	$k_a/k_b = 330 \exp(-1430/T)$	that of $\text{CH}_3\text{C(O)O}_2$ [25]

Table 2. continued

Reaction	Reaction rate k	Reference
$\text{CCl}_2\text{FC(O)OONO}_2 \xrightarrow{M} \text{CCl}_2\text{FC(O)O}_2 + \text{NO}_2$	$k_0=4.9 \times 10^{-3} \exp(-12100/T)$ $k_\infty=3.7 \times 10^{16} \exp(-13603/T)$ , $F_c=0.3$	that of PAN [18]
$\text{CCl}_2\text{FC(O)OONO}_2 \xrightarrow{h\nu} \text{CCl}_2\text{FC(O)O}_2 + \text{NO}_2$	that of PAN	[26]
$\text{CCl}_2\text{FCOOH} + \text{OH} \rightarrow \text{CCl}_2\text{FCO}_2 + \text{H}_2\text{O}$	$1.3 \times 10^{-12} \exp(170/T)$	that of $\text{CH}_3\text{COOH}$
$\text{CCl}_2\text{FCO}_2 \rightarrow \text{CCl}_2\text{F} + \text{CO}_2$	very fast	
$\text{CCl}_2\text{FC(O)O}_2 + \text{NO} \rightarrow \text{CCl}_2\text{F} + \text{CO}_2 + \text{NO}_2$	$5.1 \times 10^{-12} \exp(220/T)$	[15]
$\text{CCl}_2\text{F} + \text{O}_2 \rightarrow \text{CCl}_2\text{FO}_2$	very fast	
$\text{CCl}_2\text{FO}_2 + \text{NO}_2 \rightarrow \text{CCl}_2\text{FOONO}_2$	$k_0=5.5 \times 10^{-29} (T/300)^{-5}$ $k_\infty=8.3 \times 10^{-12} (T/300)^{-0.7}$ , $F_c=0.42$	[15]
$\text{CCl}_2\text{FOONO}_2 \xrightarrow{M} \text{CCl}_2\text{FO}_2 + \text{NO}_2$	$k_0=3 \times 10^{-30} \exp(-10570/T)$ $k_\infty=2.1 \times 10^{16} \exp(-11980/T)$ , $F_c=0.4$	[15]
$\text{CCl}_2\text{FO}_2 + \text{HO}_2 \rightarrow \text{CCl}_2\text{FOOH} + \text{O}_2$	that of $\text{C}_2\text{H}_5\text{O}_2$	[18]
$\text{CCl}_2\text{FOOH} + \text{OH} \rightarrow \text{CCl}_2\text{FO}_2 + \text{H}_2\text{O}$	$1.7 \times 10^{-12} \exp(220/T)$	that of ROOH [15]
$\text{CCl}_2\text{FOOH} \xrightarrow{h\nu} \text{CCl}_2\text{FO} + \text{OH}$	that of $\text{CH}_3\text{OOH}$	
$\text{CCl}_2\text{FO}_2 + \text{NO} \rightarrow \text{CCl}_2\text{FO} + \text{NO}_2$	$3.1 \times 10^{-12} \exp(500/T)$	[13]
$\text{CCl}_2\text{FO} \rightarrow \text{COFCl} + \text{Cl}$	very fast	
$\text{COFCl} \xrightarrow{h\nu}$	very slow	
<b>HCFC-142b chemistry</b>		
$\text{CClF}_2\text{CH}_3 + \text{OH} \rightarrow \text{CClF}_2\text{CH}_2 + \text{H}_2\text{O}$	$1.4 \times 10^{-12} \exp(-1800/T)$	[13]
$\text{CClF}_2\text{CH}_2 + \text{O}_2 \rightarrow \text{CClF}_2\text{CH}_2\text{O}_2$	very fast	
$\text{CClF}_2\text{CH}_2\text{O}_2 + \text{NO}_2 \rightarrow \text{CClF}_2\text{CH}_2\text{OONO}_2$	that of $\text{CH}_3\text{OONO}_2$	[18]
$\text{CClF}_2\text{CH}_2\text{OONO}_2 \xrightarrow{M} \text{CClF}_2\text{CH}_2\text{O}_2 + \text{NO}_2$	that of $\text{CH}_3\text{OONO}_2$	[18]
$\text{CClF}_2\text{CH}_2\text{OONO}_2 \xrightarrow{h\nu} \text{CClF}_2\text{CH}_2\text{O}_2 + \text{NO}_2$	that of $\text{CClF}_2\text{OONO}_2$	
$\text{CClF}_2\text{CH}_2\text{O}_2 + \text{HO}_2 \rightarrow \text{CClF}_2\text{CH}_2\text{OOH} + \text{O}_2$	that of $\text{CClF}_2\text{O}_2$	
$\text{CClF}_2\text{CH}_2\text{O}_2 + \text{NO} \rightarrow \text{CClF}_2\text{CH}_2\text{O} + \text{NO}_2$	that of $\text{C}_2\text{H}_5\text{O}_2$	[18]
$\text{CClF}_2\text{CH}_2\text{OOH} + \text{OH} \rightarrow \text{CClF}_2\text{CH}_2\text{O}_2 + \text{H}_2\text{O}$	$1.7 \times 10^{-12} \exp(220/T)$	[15]
$\text{CClF}_2\text{CH}_2\text{OOH} \xrightarrow{h\nu} \text{CClF}_2\text{CH}_2\text{O} + \text{OH}$	that of $\text{CH}_3\text{OOH}$	
$\text{CClF}_2\text{CH}_2\text{O} \xrightarrow{O_2} \text{CClF}_2\text{CHO} + \text{HO}_2$	very fast	
$\text{CClF}_2\text{CHO} + \text{OH} \xrightarrow{O_2} \text{CClF}_2\text{C(O)O}_2 + \text{H}_2\text{O}$	that of $\text{CCl}_2\text{FCHO}$	
$\text{CClF}_2\text{CHO} \xrightarrow{h\nu, 2O_2} \text{CClF}_2\text{O}_2 + \text{CO} + \text{HO}_2$	cross sections from	[27]
$\text{CClF}_2\text{C(O)O}_2 + \text{NO}_2 \rightarrow \text{CClF}_2\text{C(O)O}_2\text{NO}_2$	that of PAN	[18]
$\text{CClF}_2\text{C(O)O}_2\text{NO}_2 \xrightarrow{M} \text{CClF}_2\text{C(O)O}_2 + \text{NO}_2$	that of PAN decomposition	[18]
$\text{CClF}_2\text{C(O)O}_2\text{NO}_2 \xrightarrow{h\nu} \text{CClF}_2\text{C(O)O}_2 + \text{NO}_2$	that of PAN	[26]
$\text{CClF}_2\text{C(O)O}_2 + \text{HO}_2 \rightarrow \text{CClF}_2\text{C(O)COH} + \text{O}_2$ (ka)	$k_a+k_b=4.3 \times 10^{-13} \exp(1040/T)$	that of $\text{CH}_3\text{C(O)O}_2$ [18]
$\text{CClF}_2\text{C(O)O}_2 + \text{HO}_2 \rightarrow \text{CClF}_2\text{COOH} + \text{O}_3$ (kb)	$k_a/k_b=330 \exp(-1430/T)$	that of $\text{CH}_3\text{C(O)O}_2$ [25]
$\text{CClF}_2\text{COOH} + \text{OH} \rightarrow \text{CClF}_2\text{CO}_2 + \text{H}_2\text{O}$	$1.3 \times 10^{-12} \exp(170/T)$	that of $\text{CH}_3\text{COOH}$

Table 2. continued

Reaction	Reaction rate k	Reference
CClF <sub>2</sub> C(O)O <sub>2</sub> + NO → CClF <sub>2</sub> + CO <sub>2</sub> + NO <sub>2</sub>	that of CCl <sub>2</sub> FC(O)O <sub>2</sub>	[15]
CClF <sub>2</sub> + O <sub>2</sub> → CClF <sub>2</sub> O <sub>2</sub>	very fast	

1. P: pressure in Torr, rate reported by Tuazon and Atkinson [23] is also used for comparison; 2. temperature dependence taken equal to that of CH<sub>3</sub>CHO;

\* Computing the photolysis rates of CClF<sub>2</sub>OONO<sub>2</sub>, the available literature data on the cross-section of CCl<sub>2</sub>FOONO<sub>2</sub> are used [17]. However, only cross-sections for wavelengths between 200 and 280 nm are available. An extrapolation of these data to longer wavelength, which is crucial for the tropospheric lifetime is carried out following the suggestions in the AFEAS report 1989.

† the following notation for three-body reactions is used:

$$K = \frac{k_0(T)M}{1 + K_0(T)M/K_\infty(T)} F (1 + [\log(K_0(T)M/K_\infty(T))]^2)^{-1}$$

The non-reactive rainout of HCFC-22, CClF<sub>2</sub>OONO<sub>2</sub>, CClF<sub>2</sub>OOH, COF<sub>2</sub>, COFCl, HCOF, CF<sub>3</sub>COF, CF<sub>3</sub>COCl, CCl<sub>2</sub>FCOOH and CClF<sub>2</sub>COOH is taken into consideration using the parameterization presented by Langner and Rodhe [28]. Input data for this scheme originate from measured climatological precipitation fields [29] and the distribution of the release of latent heat with height [30]. Furthermore, the scavenging efficiency depends on the solubility according to the Henry's law constants (Table 1).

The uptake and hydrolysis by the ocean of HCFC-22, HCFC-123, HCFC-124, HCFC-141b, HCFC-142b is parametrized as recommended by Butler et al. [10]. The uptake of the more reactive species COF<sub>2</sub>, COFCl, HCOF, CF<sub>3</sub>COF, CF<sub>3</sub>COCl, ROOH (where R: alkyl or halogenated alkyl), CCl<sub>2</sub>FC(O)OOH, CClF<sub>2</sub>C(O)OOH and CClF<sub>2</sub>OONO<sub>2</sub> is parameterized using an atmosphere-ocean resistance model [31].

Removal in clouds due to hydrolysis is introduced for COF<sub>2</sub>, COFCl, HCOF, CF<sub>3</sub>COF, CF<sub>3</sub>COCl, CCl<sub>2</sub>FC(O)OOH and CClF<sub>2</sub>C(O)OOH, whereas for the remaining species removal in clouds is expected to be slow [8].

Uptake and hydrolysis in clouds is considered using the statistical model of Rodhe and Grandell [32]. At a certain height, longitude and latitude, the lifetime due to loss in clouds is given by:

$$\tau = \tau_{nc} (1-f) + (f \cdot k_d)^{-1} \quad (1)$$

with:  $\tau$ : the overall lifetime due to loss in clouds (s);  
 $\tau_{nc}$ : the time that the air spends out of clouds (s);  
 f: cloud volume fraction;  
 $k_d$ : the pseudo-first order scavenging rate into clouds (s<sup>-1</sup>).

The first term of this sum ( $\tau_{nc} (1-f)$ ) accounts for the statistical probability for an air parcel of

0 1 3 9

being incorporated to clouds and the term  $(f \cdot k_d)^{-1}$  for the real removal rate in clouds. At high scavenging rates (i.e. when hydrolysis rates and Henry's Law coefficients are high), the total loss ( $\tau^{-1}$ ) is dependent on the frequency of cloud occurrence alone. On the other hand, when hydrolysis rates ( $k_H$ ) and Henry's Law coefficients ( $H$ ) are low, the loss rate ( $\tau^{-1}$ ) is determined by the cloud volume fraction, the liquid water content of the cloud and the  $H$  and  $k_H$  values. In range of the  $H$  and  $k_H$  values given in Table 1, the latter condition prevails. Thus, equation (1) can be simplified to:

$$\tau = (f \cdot k_d)^{-1} \quad (2)$$

where  $k_d$  is given by

$$k_d = k_H \cdot H \cdot R \cdot T \cdot LWC \cdot F_{AD} \quad (3)$$

with  $R = 0.083$  ( $\text{atm} \cdot \text{M}^{-1} \cdot \text{K}^{-1}$ );  $T$  is the temperature (K);  $LWC$  is the dimensionless liquid water content of the clouds; and  $F_{AD}$  a factor correcting for the effects of aqueous phase diffusion. Following Schwartz and Freiberg [33], the steady state solution for diffusion in cloud droplets can be expressed by relating the average concentration in the droplet  $C_m$  to the concentration at the surface of the droplet  $C_d$  through the equation:

$$F_{AD} = \frac{C_m}{C_d} = 3 \left( \frac{\coth q}{q} - \frac{1}{q^2} \right) \quad (4)$$

with  $q = r (k_H/D_a)^{1/2}$ ;  $r$  is the droplet radius (cm) and  $D_a$  the aqueous phase diffusion coefficient ( $\text{cm}^2/\text{s}$ ). For all compounds, we used a relatively slow aqueous phase diffusion coefficient of  $10^{-5} \text{ cm}^2\text{s}^{-1}$ . This correction is of no significance (correction factor almost 1) for slow hydrolysis rates and small droplets but becomes significant for large droplets and fast hydrolysis rates. For instance, using the set of parameters in Table 1, for a  $50 \mu\text{m}$  cloud droplet nucleated on seasalt aerosols in the marine environment, the correction factors for  $\text{COFCl}$ ,  $\text{CF}_3\text{COCl}$  and  $\text{CF}_3\text{COF}$ , are calculated to be 0.25, 0.10 and 0.20, respectively. Adopting a typical droplet radius of 10 mm, correction factors of 0.75, 0.50 and 0.65 were calculated for  $\text{COFCl}$ ,  $\text{CF}_3\text{COCl}$  and  $\text{CF}_3\text{COF}$ , respectively; the remaining species were not affected by aqueous phase diffusion limitation.

Note that in this parameterization the effects of uptake limitation by gas phase diffusion and transfer through the gas-aqueous interface were neglected. Gas phase diffusion limitation is negligible for the range of Henry's Law coefficients of species studied. This would not be the case if the Henry's Law coefficients were larger than those used here. Transport through the gas-droplet interface is dependent on the value of the sticking coefficient  $\alpha$  (the probability that, after collision, a gas phase molecule will remain on the droplet surface). The measurements by George et al. [34] and DeBruyn et al. [35] give no indication that  $\alpha$  would be small and, thus, we

neglect gas-droplet interfacial transport limitations.

**Stratospheric lifetimes:** Losses of HCFCs and HFC-134a to the stratosphere were parameterized using results of the 2-D stratospheric model of the Max-Planck Institute for Chemistry (Ch. Brühl, private communication). Monthly varying stratospheric loss rates of HCFC-22, HCFC-123, HCFC-124, HCFC-141b, HCFC-142b and HFC-134a, corresponding to lifetimes of 214, 62, 87, 90, 389 and 357 years respectively, are applied at the 100hPa model level. No stratospheric loss of the oxidation products from these halogenated hydrocarbons are taken into consideration. In fact, measurements by Wilson [36] in the NH suggested a flux of some halogenated carbonyl species (RCOX) from the stratosphere to the troposphere, but this has been neglected in the present study.

**Emissions:** Based on production and sales data, release of HCFC-22 was introduced for the period 1970-1990 [37]. This release is supplemented by an arbitrary amount of 5% to account for the production by non-reporting countries (mainly Russia, China and India). The HCFC-22 emissions were spatially distributed using the latitudinally and longitudinally varying F11 emissions given by Hartley and Prinn [38]. For the period after 1990, the "German Government Inquiry Report" emission scenario is used (see Figure 1). However, this scenario does not consider the phase out of HCFCs which is planned for the year 2030. Therefore, here we only present results for the period up to 2025. The same emission scenario which describes HCFC-123 is used for HCFC-124. Initial concentrations of HCFC-22 for 1970 (13 pptv in the Northern Hemisphere (NH) and of 10 pptv in the Southern Hemisphere (SH)) are used in this study, based on an extrapolation of measured concentrations. Initial 1990 concentrations of the remaining HCFCs and HFC-134a are assumed to be zero.

## Model results and Discussion

### a. Tropospheric Distributions

1. **HCFC-22 concentrations for the period 1970-1992:** The calculated HCFC-22 concentrations in June 1990 are somewhat lower than those reported in an earlier study [39] mainly because we use somewhat lower 1970 initial concentrations of HCFC-22 here. An annual increase of 6-7% in the tropospheric content of HCFC-22 is calculated for the period 1980-1990, corresponding to calculated increase of 5-9 pptv/year for Cape Meares (NH) and 4-7 pptv/year for Cape Grim (SH). Figure 2 shows the measured and calculated concentrations of HCFC-22 for the period 1970-1992. There is a large discrepancy between the observed HCFC-22 reported by the experimental groups which can mainly be attributed to differences in calibration standards. The mixing ratios of HCFC-22 determined by Khalil and Rasnussen [40] from ground-based chromatographic measurements in the Northern Hemisphere are 10-40% higher than those determined from long-path absorption measurements within the troposphere and lower stratosphere [42]. They are also higher than the grab sample measurements in the lower troposphere by Pollock et al. [43] and recently reported measurements of NH and SH air for the

period November 1991 to December 1992 [44]. These discrepancies in the experimental data prohibit better evaluation of the model results.

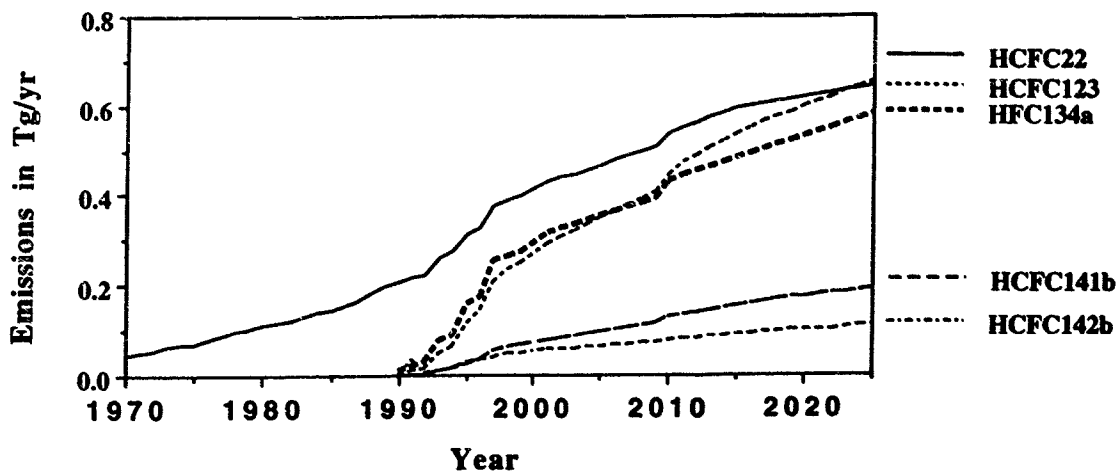


Figure 1. Emission scenario adopted for HCFCs and HFC-134a.

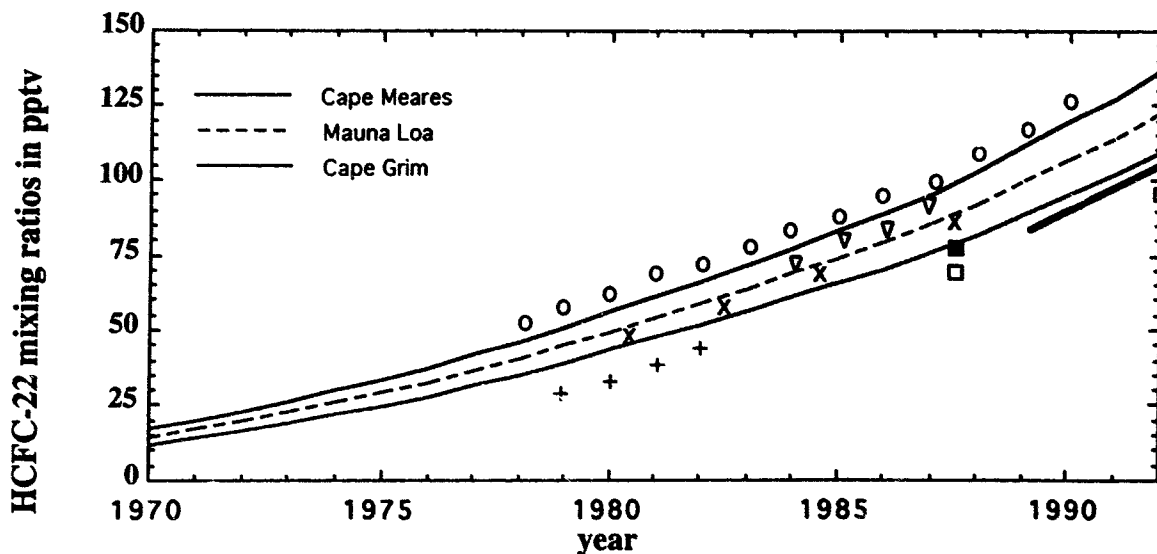


Figure 2. HCFC-22 mixing ratios for the period 1970-1992. Upper line: calculated concentrations for Cape Meares; Middle line: calculated concentrations for Mauna Loa; Lower line: calculated concentrations for Cape Grim; circles: measurements at Cape Meares, Oregon [40,41]; inverse triangles: measurements at Cape Grim, Tasmania [40]; short continuous line and closed square: N.H. measurements and open squares: S.H. measurements by Motzka et al. [44]; "x": spectroscopic measurements by [42] at 31-32°N.; "+": South pole measurements [40].

0 1 4 2

2. Future HCFCs and HFC-134a atmospheric concentrations: By using the "German Government Inquiry Report" scenario for the future emissions of substitutes (Figure 1) and assuming that these emissions will be geographically distributed like those of F11, we calculate the buildup of concentrations of the studied halogenated hydrocarbons. The phase out of HCFCs is not taken into consideration in the 'German Government Inquiry Report' scenario used in this study. Thus, future concentrations of HCFC-22 and of the other studied halogenated hydrocarbons presented below, may be lower than predicted if the phase out of HCFCs starts before 2025. HCFC-22, HFC-134a and HCFC-142b are the substitutes with the longest residence times in the atmosphere with lifetimes due to oxidation by OH radical of 13.7 years, 13.9 years and 20.3 years, respectively (Table 3). HCFC-22 and HFC-134a are expected to become the predominant compounds in the year 2025, reaching maximum volume mixing ratios of 540 pptv and 390 pptv in the NH, respectively. Near the surface the highest concentrations are found near the emission areas in the U.S., Europe and Japan. In the SH the concentration gradients are small, reflecting their long lifetime and relatively small SH emissions. The calculated mixing ratios of the HCFCs and HFC-134a from 1992 to 2025 are presented in Figure 3. HCFC-123, HCFC-141b and HCFC-142b mixing ratios are expected to remain lower than 100 pptv. The HCFC-124 mixing ratio exceeds 100 pptv but for this species the emission scenario of HCFC-123 has been used and this may prove not to be realistic.

**Table 3.** Atmospheric lifetimes for HCFCs, HFC-134a and some of their oxidation products.

Compound	oxidation	oceanic loss	in cloud loss	stratospheric loss*
CH <sub>3</sub> CCl <sub>3</sub>	6.5 yr	63 yr		54 yr
HCFC-22	13.7 yr	986 yr	-	214 yr
HFC-134a	13.9 yr	-	-	357 yr
HCFC-123	1.3 yr	306 yr	-	62 yr
HCFC-124	6.0 yr	1802 yr	-	87 yr
HCFC-141b	9.5 yr	1856 yr	-	90 yr
HCFC-142b	20.3yr	1455yr	-	389yr
<u>RCOX species</u>				
COF <sub>2</sub>	-	4.4 m	3.9 d	-
COFCl	-	2.3 yr	7.7 d	-
CF <sub>3</sub> COFCl	-	3.8 yr	5.9 d	-
CF <sub>3</sub> COF	-	2.9 yr	5.3 d	-
HCOF	-	76 yr	1.3 yr (1)	-

\* input to the model based on results of a 2-D stratospheric model [Ch. Brühl, private communication]

(1): no experimental data on Henry's Law coefficient (H) and hydrolysis rates ( $k_H$ ) are available.

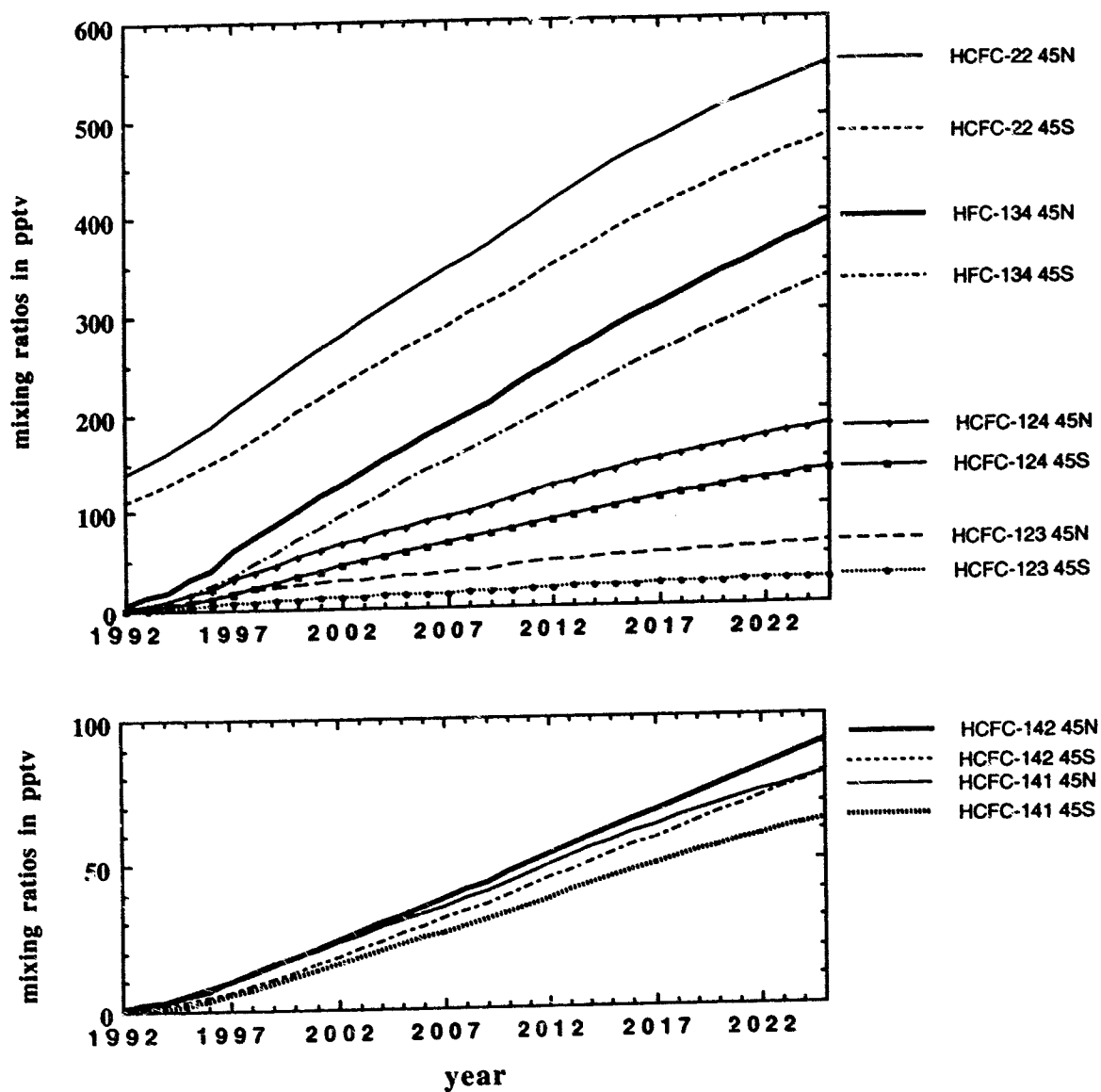


**Figure 3.** Volume mixing ratios of HCFC-22, HFC-134a, HCFC-123, HCFC-124, HCFC-141b and HCFC-142b (in pptv) at Cape Meares and at Cape Grim calculated for the period 1992-2025, based on the 'German Government Inquiry Report' scenario shown in figure 1.

**3. Carbonyl compounds** ( $\text{COF}_2$ ,  $\text{COFCl}$ ,  $\text{HCOF}$ ,  $\text{CF}_3\text{COF}$ ,  $\text{CF}_3\text{COCl}$ ): Heterogeneous processes are thought to be mainly responsible for the removal of carbonyl compounds ( $\text{RCOX}$ ). Based on the few measurements of the Henry's law coefficients,  $H$ , and unimolecular hydrolysis rates,  $k_H$ , the lifetimes of these species are calculated to range from a few days to years (see

Tables 1 and 3). The concentration distribution of the RCOX species reflects the net effect of oxidation of HCFCs and HFC-134a by OH and of removal from the atmosphere at the oceanic surface and by hydrolysis in clouds. Thus, the calculated concentrations strongly depend on the  $H$  and  $k_H$  values, adopted in the heterogeneous loss parameterization.

Because the formation of the gas phase degradation products of HCFCs and HFC-134a is closely connected to the presence of the OH radical, the tropics and sub-tropics with high water vapor concentrations and receiving the maximum of solar ultraviolet radiation are also the areas with the highest abundances of these species. The tropics, however, are also the regions of deep convective clouds associated with typical time scales of an hour. Within this period even for the fastest reacting RCOX species (Table 3), only a small fraction can hydrolyze in the Cb clouds. Thus, a fraction of some of the oxidation products could even be transported into the stratosphere, and subsidence of air masses from the higher troposphere to the surface in the downward branch of the Hadley circulation could carry most of the RCOX compounds into regions with higher hydrolysis rates, partly influencing the lifetimes of these species. A detailed quantitative analysis of this topic can not be achieved by the model we used. For the tropics, our model yields maximum surface mixing ratios of the pptv level for  $\text{COF}_2$ ,  $\text{COFCl}$ ,  $\text{HCOF}$ ,  $\text{CF}_3\text{COF}$ , and  $\text{CF}_3\text{COCl}$  for the year 2025. The highest concentrations are calculated for above 7 km in cloudless regions. As discussed above, because the RCOX species are hardly photolysed (lifetime due to photolysis is expected to be of the order of a thousand of years), the stratosphere might be an additional source for these species in the troposphere. This is not taken into consideration in the present study.

For the branching ratio between  $\text{CF}_3\text{COF}$  and  $\text{HCOF}$  formation from HFC-134a oxidation, we use the temperature and pressure dependence presented by Wallington [22]. A 30-35% higher branching ratio for the production of  $\text{CF}_3\text{COF}$  from HCFC-134a oxidation as recently determined by Tuazon and Atkinson [23] has been also used to evaluate uncertainties in the  $\text{CF}_3\text{COF}$  and  $\text{HCOF}$  yields. We calculate that 64-71% of the annually oxidized amount of HFC-134a in the model domain (between the surface and 100hPa), is converted to  $\text{HCOF}$ ; whereas 29-36% gives  $\text{CF}_3\text{COF}$ . In the present study  $\text{CF}_3\text{COF}$  is also produced from HCFC-124 oxidation and its mixing ratios which reach maximum values above 7 km do not exceed 5 pptv. Based on the adopted emission scenarios, we evaluate that 70-75% of the calculated  $\text{CF}_3\text{COF}$  concentrations are produced from the oxidation of HCFC-124 in the troposphere. After hydrolysis in clouds  $\text{CF}_3\text{COF}$  produces  $\text{CF}_3\text{COOH}$  which is of some environmental concern due to its extreme stability in the environment.

The calculated concentrations of  $\text{HCOF}$  strongly depend on the value assumptions made for  $H$  and  $K_H$ . Unfortunately, no experimental data are available for this carbonyl compound. In this study, we used the hydrolysis rate for  $\text{CH}_3\text{COF}$  [45] and Henry's law coefficient of 3 like for  $\text{CF}_3\text{COF}$ , which is 1000 times smaller than the Henry's law coefficient for  $\text{CH}_2\text{O}$  [46]. Our results, which rely totally on assumptions given in Tables 1 and 2, indicate that  $\text{HCOF}$  could build up in the troposphere and low stratosphere. Clearly measurements of the  $\text{HCOF}$  hydrolysis rate and Henry's law coefficient are needed, to properly assess its importance in the atmosphere.

Furthermore as shown in Table 1, we do not take into consideration variations of the

hydrolysis rates depending on the droplet pH, which has been reported [34, 35]. At high pH (basic solutions) the uptake rates of the studied RCOX species was observed to be enhanced, possibly due to OH<sup>-</sup> catalysis of RCOX hydrolysis [35]. In the present study reported values valid for a pH of 6 are used.

4. Other products resulting from HCFC-141b and HCFC-142b oxidation: The oxidation of CH<sub>3</sub>CCl<sub>2</sub>F and CH<sub>3</sub>CClF<sub>2</sub> in the troposphere produces CCl<sub>2</sub>FCHO and CClF<sub>2</sub>CHO which in turn are either photolysed or react with OH radicals.

Oxidation by the OH radical leads to the formation of the RCO radical (RCHO + OH → RCO + H<sub>2</sub>O; R: halogenated alkyl) which could subsequently produce PAN-like compounds (CCl<sub>2</sub>FC(O)O<sub>2</sub>NO<sub>2</sub> and CClF<sub>2</sub>C(O)O<sub>2</sub>NO<sub>2</sub>). These organic nitrates are of some concern because they could build up in the middle and high troposphere and contribute to the transport of reactive halogens to the stratosphere.

The photolysis of aldehydes produces halogenated methylperoxy radicals (CFCl<sub>2</sub>O<sub>2</sub> and CF<sub>2</sub>ClO<sub>2</sub>), without the intermediate production of a PAN-like species (RCHO  $\xrightarrow{h\nu+2O_2}$  RO<sub>2</sub>+CO+HO<sub>2</sub>). Absence of experimental data on the quantum yield of these photolytical reactions prohibits determination of the importance of the photolysis of these halogenated aldehydes relative to the reaction with OH. In the present study we assume a quantum yield equal to unity, which probably leads to an underestimate in the production of the PAN-like compounds. Furthermore, here we simulate the chemistry of these PAN-like species using the reaction and photodissociation rates of PAN. Based on these assumptions, the concentrations of CCl<sub>2</sub>FC(O)O<sub>2</sub>NO<sub>2</sub> and CClF<sub>2</sub>C(O)O<sub>2</sub>NO<sub>2</sub> calculated here are well below the pptv level. These results could change significantly when reaction and photolysis rates for the specific reactions will become available.

#### **b. Tropospheric lifetimes and environmental consequences.**

Oxidation by OH radical is responsible for the main loss of HCFCs and HFC-134a from the troposphere. The calculated tropospheric lifetimes (Table 3) resulting from oxidation by OH radicals are defined as the ratio of the annual mean tropospheric burden to the annual tropospheric loss by gas phase reaction with OH. For the RCOX species, hydrolysis in cloud droplets and in the ocean represent the major loss processes. Lifetimes resulting from the loss in clouds vary from several days to a year depending on the adopted Henry's Law coefficients and the hydrolysis rates. As mentioned above, large uncertainties persist on the experimental determination of these coefficients. In particular for HCOF, no experimental data are available. Therefore, to test the sensitivity of the hydrolysis rates, we also report in Table 4 the lifetimes of RCOX species calculated for 10 times higher and 10 times lower values than those reported in Table 1. These results are based on a single year simulation.

Table 4 shows that for all the species considered, hydrolysis in clouds is the dominant removal pathway. Interestingly, except for HCOF, the lifetimes due to hydrolysis in clouds are not very sensitive to the adopted hydrolysis rates. Instead, the lifetimes of these species seem rather to depend on meteorological processes like rapid transport into the upper troposphere by deep

convection, subsequent downward transport in the ITCZ and finally, incorporation in clouds. When removal by clouds becomes slower, oceanic removal gains importance because RCOX species are then long enough lived to be transported to the oceanic boundary layer. Thus, lifetimes in a 3-D model should be interpreted rather differently than when using the 0-D box model approach. The latter considers the potential lifetime of a species due to loss procedure and not the effective lifetime, as is the case in our 3-D model which includes the transport in the atmosphere.

Table 4 reveals the importance of obtaining experimental data on HCOF. Apparently, the calculated lifetimes and atmospheric concentrations of this species are very dependent on the adopted values of the Henry's law coefficient and hydrolysis rates.

**Table 4.** RCOX lifetimes resulting from the removal at the oceanic surface, rainout and loss in clouds A: using the Henry Law coefficients and Hydrolysis rates as reported in Table 1; B: using 10 times slower hydrolysis rates; C: using 10 times faster hydrolysis rates than in Table 1.

RCOX	in clouds loss			oceanic removal			rainout		
	A	B	C	A	B	C	A	B	C
COF <sub>2</sub>	3.9d	5.8d	3.7d	4.4m	2m	5.4m	74yr	31yr	99yr
CF <sub>3</sub> COCl	5.9d	6.5d	5.7d	3.8yr	2.1yr	4.4yr	870yr	511yr	1021yr
CF <sub>3</sub> COF	5.3d	6.0d	5.2d	2.9yr	1.6yr	3.3yr	625yr	365yr	730yr
HCOF	1.3yr	11.3yr	5m	76yr	88yr	83yr	>> 1000yr		

**Table 5.** Chlorine Loading Potentials of selected HCFCs and HFC-134a based on the tropospheric lifetimes calculated in this study.

Compound	oxidation by OHstratospheric loss*	total lifetime	CLP
HCFC-22	13.7yr	214yr	0.132
HFC-134a	13.9yr	357yr	-
HCFC-123	1.2yr	62yr	0.014
HCFC-124	6.0yr	87yr	0.036
HCFC-141b	9.5yr	90yr	0.126
HCFC-142b	20.3yr	389yr	0.015

On the basis of the model-derived lifetimes of HCFCs and HFC-134a (Table 3) and CFC-11 (53 yr), we can calculate the chlorine loading potential (CLP) of the species under consideration, which represents the upper limit of the steady-state effect of HCFCs and HFC-134a on ozone depletion relative to that of CFC-11. CLP is defined by the ratio of chlorine transported across

the tropopause to the stratosphere per unit of mass of HCFC or HFC emitted relative to the chlorine transported per unit of mass of CFC-11. The calculated CLP are reported in Table 5. According to our calculations HCFC-22 and HCFC-141b could be the most aggressive HCFCs towards stratospheric ozone. The other studied species are expected to be 30 to 100 times less effective in transporting chlorine from the troposphere to the stratosphere.

**Acknowledgements.** We thank the Alternative Fluorocarbons Environmental Acceptability Study Science Committee for financial support and for providing us information prior publication. Special thanks to Ch. Brühl for communicating us his 2-D stratospheric model results. We also thank J. Franklin, R. Atkinson, R. Prinn, D. Hartley, F. Zabel, R. Borchers and E.W. Elkins for providing us with information prior to publication. M.K. expresses gratitude to the CNRS and the CEA for facilities. We also thank C. Harris for proofreading this manuscript.

## REFERENCES

1. Crutzen P. J. and P. H. Zimmermann, Tellus, **43AB**, 136-151(1991).
2. Zimmermann P. H., J. Feichter, H. K. Rath, P. J. Crutzen, and W. Weiss, Atmos. Environ., **23**, 25-35 (1989).
3. Kanakidou M., and P. J. Crutzen, Chemosphere, **26**, 1-4, 787-802 (1993).
4. Dentener and Crutzen, J. Geophys. Res., april 20 (1993).
5. Lelieveld J., P. J. Crutzen, and H. Rodhe, UDC 551.510.4, CM-4. International Meteorological Institute in Stockholm (1989).
6. Dentener, PhD thesis, State University of Utrecht, The Netherlands (1993).
7. McLinden M. O., Scientific Assessment of Stratospheric Ozone: 1989, WMO, report N° 20, 11- 41 (1989).
8. Wine P. H., and W. I. Chameides, Scientific Assessment of Stratospheric Ozone: 1989, WMO, report N° 20, 273-298 (1989).
9. George C., J.L. Ponche, and P. Mirabel, paper presented at the STEP-HALOCSIDE/AFEAS workshop 23-25th March (1993).
10. Butler J., J. Elkins, and T. Thompson, B. Hall, T. Swanson, and V. Koropalov, J. Geophys. Res., **96**, 22347-22355 (1991).
11. Saathoff H. and R. Zellner, Chem. Phys. Lett., in press, (1993).  
Chen J., Zhu T., and Niki H., Geophys. Res. Lett., **19**, 2215-2218 (1992).
12. Franklin J., submitted to Chemosphere, march (1993).
13. DeMore W. B., S. P. Sander, D. M. Golden, R. F.Hampson, M.J. Kurylo, C. J. Horward, R. A. Ravishankara, M.G. Molina, JPL Publication 92-20, Evaluation N° 10, Jet Propulsion Laboratory, Pasadena, CA, (1992).
14. IUPAC, Evaluated kinetic and Photochemical data for Atmospheric Chemistry: Supplement III (1989), J. Phys. Chem. Ref. Data, **18**, 881- 1097 (1989).
15. Atkinson R. , in Scientific Assessment of Stratospheric Ozone: 1989, WMO, report N° 20, 165-208 (1989).
16. DeMore W. B., M. G. Molina, S. P. Sander, D. M. Golden, R. F.Hampson, M.J. Kurylo, C. J. Horward, and R. A. Ravishankara, JPL Publication 87-41, Evaluation N° 8, Jet Propulsion Laboratory, Pasadena, CA, 196 (1987).
17. Morel O., R. Simonaitis and J. Heicklen, Chemical Physics Letters, **73**, 38-42 (1980).
18. Lightfoot P.D., R.A. Cox, J.N.Crowley, M. Destriau, G.D. Hayman, M.E. Jenkin, G.K. Moortgat and F. Zabel, Atmos. Environ., **26A**, 10, 1805-1964 (1992).
19. Moortgat G.K., W. Klippel, K.H. Mobins, W. Seiler and S. Warneck, Rep. No FAA-EE-80-47, US dep. of Transport, Washington, D.C., 1980.20. Meller R., D. Boglu, and G.K.
20. Moortgat, proceedings of the STEP-HALOCSIDE/AFEAS workshop, Dublin 14-26 May, 110-116 (1991), and private communication.

21. Kirchner F., F. Zabel and K. H. Becker, proceedings of the STEP-HALOCSIDE/AFEAS workshop, Dublin 14-26 May, 73-78 (1991).
22. Wallington T.J., M. D. Hurley, J. C. Ball, and E. W. Kaiser, Environ. Sci. Technol., **26**, 1318-1324 (1992).
23. Tuazon E.C. and R. Atkinson, J. Atmos. Chem., in press (1993).
24. Hayman G.D., M.E. Jenkins and C.E. Johnson, AFEAS final report, 1991.
25. Horie O. and G.K. Moortgat, J. Chem. Soc. Faraday Trans., **88**, 3305-3312 (1992).
26. Senum G.I., Y.N. Lee, and J.S. Gaffney, J. Phys. Chem., **88**, 1269-1270 (1984).
27. Libuda H.G., F. Zabel and K.H. Becker, proceedings of the STEP-HALOCSIDE/AFEAS workshop, Dublin 14-26 May, 126-131 (1991).
28. Langner J. and H. Rodhe, J. Atmos. Chem., **23**, 225-263 (1991).
29. Jaeger L., Berichte des Dt. Wetterdienstes, 139 (1976).
30. Newell R. E., J. W. Kidson, D. G. Vincent, and G. L. Boer, The General Circulation of the Tropical Atmosphere and Interactions with Extratropical Latitudes, Vol. 2, MIT Press, Cambridge, Mass. (1974).
31. Kindler T. P., W. L. Chameides, P. H. Wine, D. Cunnold, and F. Alyea, proceedings of the AFEAS workshop on Atmospheric Wet and Dry Deposition of Carbonyl and Haloacetyl Halides, Sept. 22, Brussels, 33 - 43 (1992).
32. Rodhe H., and J. Grandell, Tellus, **24**, 442-454 (1972).
33. Schwartz S. E. and J. E. Freiberg, Atmos. Environ., **15**, 1129-1144 (1981).
34. George C., J. L. Ponche, and P. Mirabel, proceedings of the AFEAS workshop on Atmospheric Wet and Dry Deposition of Carbonyl and Haloacetyl Halides, Sept. 22, Brussels, 18 - 24, (1992).
35. DeBruyn W., J.A. Shorter, P. Davidovits, D.R. Worsnop, M.S. Zahniser, and C.E. Kolb, proceedings of the AFEAS workshop on Atmospheric Wet and Dry Deposition of Carbonyl and Haloacetyl Halides, Sept. 22, Brussels, 12- 17 (1992).
36. Wilson S.R., P.J. Crutzen, G. Schuster, D.W.T. Grifft, G. Hellas, Nature, **334**, 689-691 (1988).
37. Midgley P. M. and D. A. Fisher, submitted to Atmos. Environ. (1991).
38. Hartley D. and R. Prinn, J. Geophys. Res., **98**, 5183 -5198 (1993).
39. Kanakidou M., F. J. Dentener, P.H. Zimmernann, and P. J. Crutzen, proceedings of the AFEAS workshop on Atmospheric Wet and Dry Deposition of Carbonyl and Haloacetyl Halides, Sept. 22, Brussels, 103-117 (1992).
40. Khalil M. A. K. and R. A. Rasmussen, Baseline Atmospheric programme (Australia) 1985, edited by B.W. Morgan and P. J. Fraser, pp 26-29, Bureau of Meteorology/CSIRO (1987).  
Khalil M. A. K. and R.A. Rasmussen, Nature, **292**, 823-824 (1981).
41. Borchers R., Gunawardena R. and R. A. Rasmussen, paper presented at the Quadrennial Ozone Symposium, Charlottesville, Virginia, June 4-13 (1992).
42. Rinsland C., D. Johnson, A. Goldman, and J. Levine, Nature, **337**, 535-537 (1989).  
Rinsland C., A. Goldman, F. Murcray, R. Blatherwick, J. Kosters, D. Murcray, N. Sze and S. Massie, J. Geophys. Res., **95**, 16477-16490 (1990).
43. Pollock W.H., L.E. Heidt, R.A. Lueb, J.F. Vedder, M.J. Mills, and S. Solomon, J. Geophys. Res., **97**, 12993-12999 (1992).
44. Montzka S. A., R.C. Myers, J.H. Butler, S.C. Cummings, and J.W. Elkins, submitted to Geophys. Res. Lett., Dec. (1992).
45. Bunton C.A. and J.H. Fendler, J. Org. Chem., **31**, 2307-2312 (1966)
46. Ledbury W. and E. W. Blair, J. Chem. Soc., **127**, 2832-2839 (1925).

0 1 4 9

Absorption Cross-Sections and Photolysis Studies of Halogenated Carbonyl Compounds.  
Photooxidation Studies on CF<sub>3</sub>-containing CFC-Substitutes.

Richard Meller, Dimitrios Boglu and Geert K. Moortgat

Max-Planck-Institut für Chemie, Air Chemistry Department

Saarstrasse 23, D-6500 Mainz, Germany

### Introduction

The atmospheric degradation of the proposed hydrogen containing substitutes hydrochlorofluorocarbons (HCFCs) and hydrofluorocarbons (HFCs) produce a number of carbonyl compounds, whose atmospheric fate must be known. With this respect laboratory studies have been undertaken to obtain UV absorption spectra of CF<sub>3</sub>COCl, COFCl and CF<sub>3</sub>CHO. The photolysis of CF<sub>3</sub>COCl was investigated in order to determine the primary photolysis channels, and to establish the oxidation mechanism of the CF<sub>3</sub> radicals in air. In addition, the mechanism of the Cl-atom initiated degradation of small initial concentration HFC-134a (CF<sub>3</sub>CFH<sub>2</sub>) in air was investigated in view of the observed slow removal rate of CF<sub>3</sub>CFH<sub>2</sub>. Primary investigations on the observed degradation of CF<sub>3</sub>COOH are presented.

#### 1) UV Absorption Spectra of CF<sub>3</sub>COCl, COFCl and CF<sub>3</sub>CHO

The measurement of the UV absorption spectra were conducted in a 63 cm quartz cell at room temperature for CF<sub>3</sub>CHO, and in the temperature range 223-298K for COFCl and CF<sub>3</sub>COCl. A 200 W deuterium lamp was used as light source, and a 0.6 m monochromator was equipped with several holographic gratings (2400 grooves/mm for COFCl, or 600 grooves/mm for CF<sub>3</sub>COCl and CF<sub>3</sub>CHO) to yield a spectral resolution of 0.04 nm or 0.2 nm, respectively. The transmitted light was detected with a diode array detector, and calibration was performed with the emission lines of Zn-, Ir- and Fe-hollow cathode lamps. COFCl was synthesized by oxidizing CClF<sub>3</sub> by SO<sub>3</sub> as proposed by Siegemund [1]. Tri-fluoroacetaldehyde methyl hemiacetal was added dropwise to sulfuric acid and the formed CF<sub>3</sub>CHO distilled. The spectra of the cited carbonyl compounds are shown in Figures 1 to 3.

The absorption spectrum of CF<sub>3</sub>COCl is compared with the results obtained by Rattigan *et al.* [2]. Generally there exist excellent agreement (less than 5 % difference) between the two investigations, except at the minimum at 216 nm, where deviations up to 50 % are observed. These authors used a dual beam diode array detector interfaced to the cell with optical light fibers, which possess reduced transmittance below 220 nm. The relative deviation between both measurements is displayed in Figure 4.

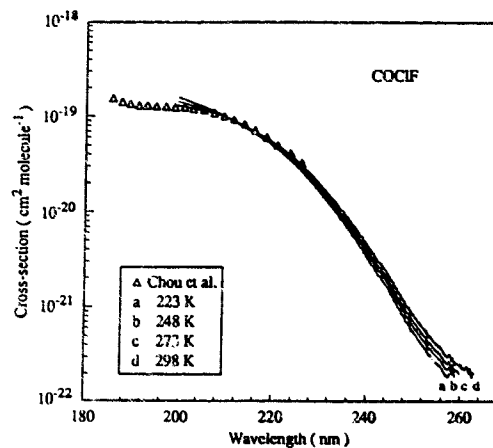


Fig.1 Temperature dependence of the UV Spectrum of COClF obtained in this laboratory [3] compared with data obtained by Chou *et al.* [4].

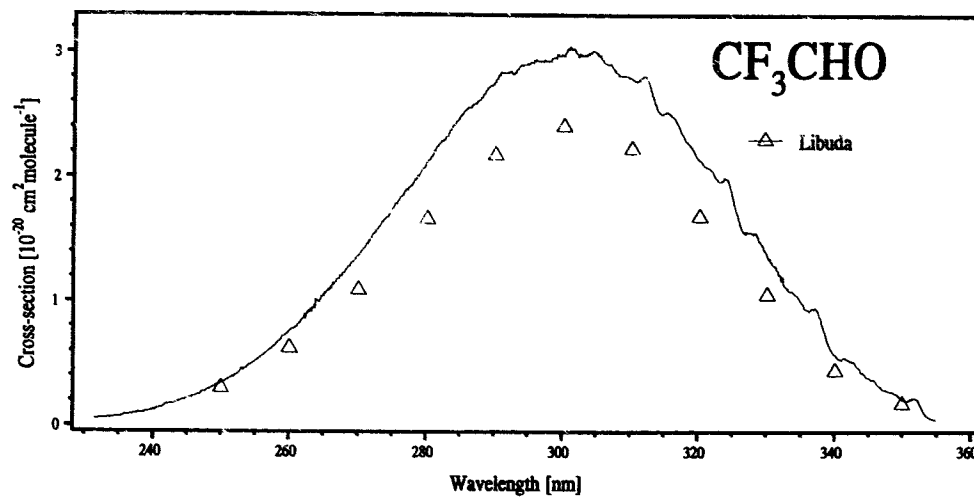


Fig. 2. UV absorption spectrum of  $\text{CF}_3\text{CHO}$ . The triangles refer to the data of Libuda *et al.* [5]

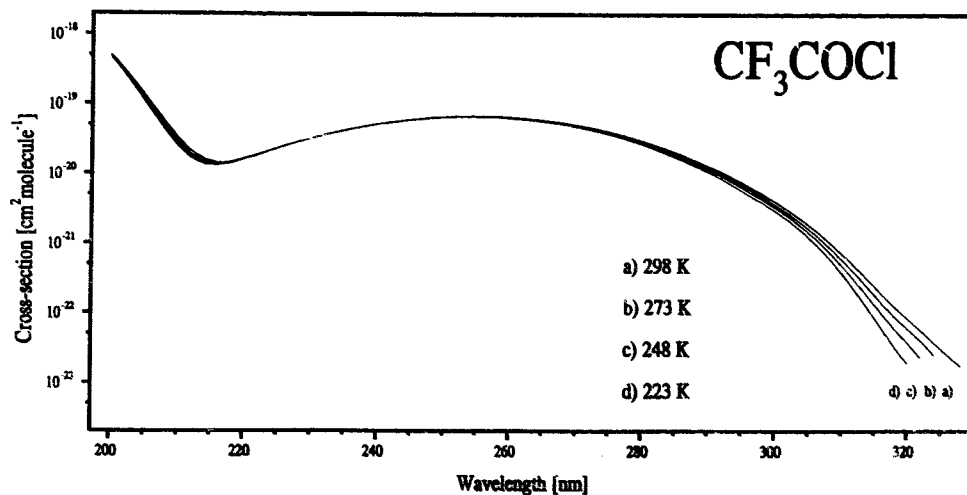


Fig.3. Temperature dependent absorption spectra of  $\text{CF}_3\text{COCl}$ .

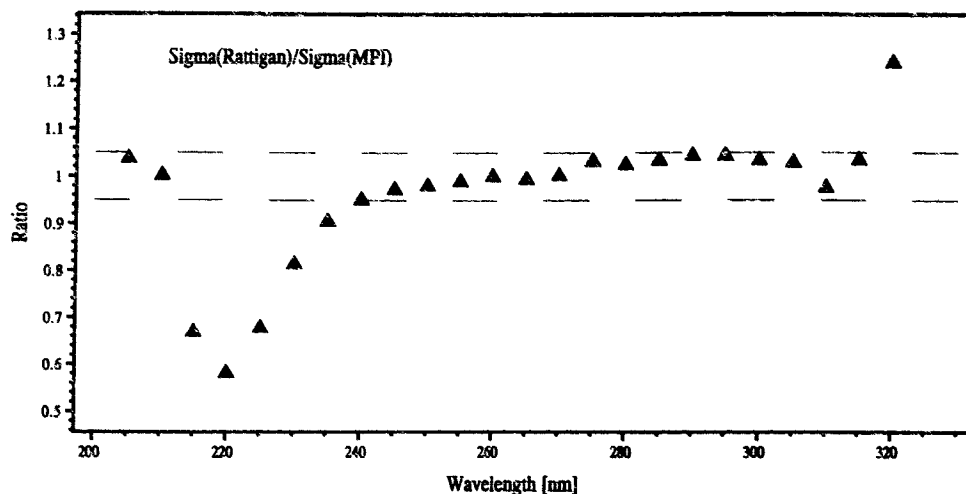


Fig.4 Relative deviation between the measurements obtained in this work and the data of Rattigan *et al.* [2].

## 2) Photolysis Studies on $\text{CF}_3\text{COCl}$

Photolysis experiments were carried out at ambient temperatures in a long-path multiple reflection quartz cell coupled to a Bomem DA8 series FTIR Spectrometer. Mixtures of  $\text{CF}_3\text{COCl}$  in synthetic air or  $\text{N}_2$  ( $0.9 - 6.0 \times 10^{14}$  molecule  $\text{cm}^{-3}$  in 760 Torr carrier gas) were photolysed at 254 nm with UV lamps.

First, the quantum yield of  $\text{CF}_3\text{COCl}$  removal in air and  $\text{N}_2$  at 254 nm was measured against the disappearance rate of  $\text{COCl}_2$ , with established quantum yield  $\phi = 1$ . The average of 10 measurements resulted in  $\phi = 0.95 \pm 0.05$  in air and of 7 experiments in  $\text{N}_2$   $\phi = 0.96 \pm 0.06$ . Measurements performed at pressures ranging from 50 Torr up to 400 Torr resulted in values between  $\phi = 0.93$  and 0.97, indicating that there is no pressure dependence. For the photolysis of  $\text{CF}_3\text{COF}$  in air, the average of 10 measurements resulted in  $\phi = 1.05 \pm 0.05$ , also measured against  $\text{COCl}_2$ .

$\text{CO}$ ,  $\text{CO}_2$ ,  $\text{COF}_2$  and  $\text{CF}_3\text{O}_3\text{CF}_3$  were the detected and identified main products of the photolysis of  $\text{CF}_3\text{COCl}$  in air. Trace amounts of  $\text{CF}_3\text{Cl}$  and  $\text{CF}_3\text{O}_2\text{CF}_3$  were also identified after trapping the products at 77 K and distilling the first fraction. Product-time profiles of the photolysis in air are shown in Fig. 5a and 5b for two different concentrations  $\text{CF}_3\text{COCl}$ . The ratio of the products produced versus  $\text{CF}_3\text{COCl}$  removed are displayed in Fig. 6a and 6b. Photolysis in  $\text{N}_2$  produced mainly  $\text{CO}$  and  $\text{CF}_3\text{Cl}$  as products.

0 1 5 2

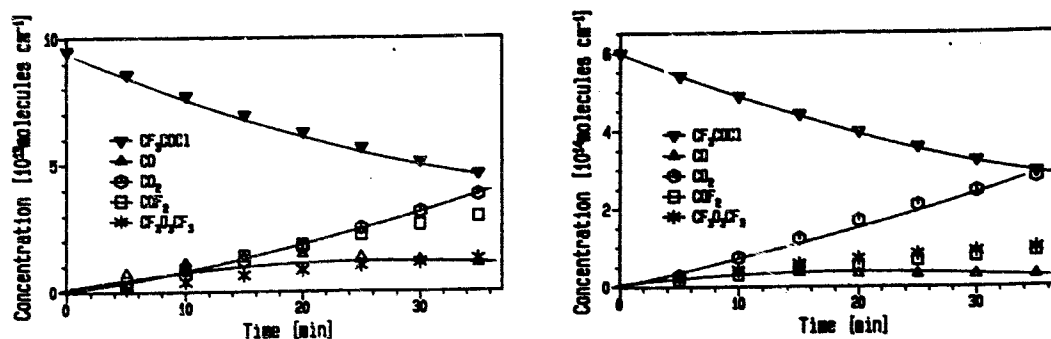


Fig. 5a and 5b. Product-time profiles of photolysis of  $0.9 \times 10^{14}$  and  $6.0 \times 10^{14}$  molecule  $\text{cm}^{-3}$   $\text{CF}_3\text{COCl}$ .

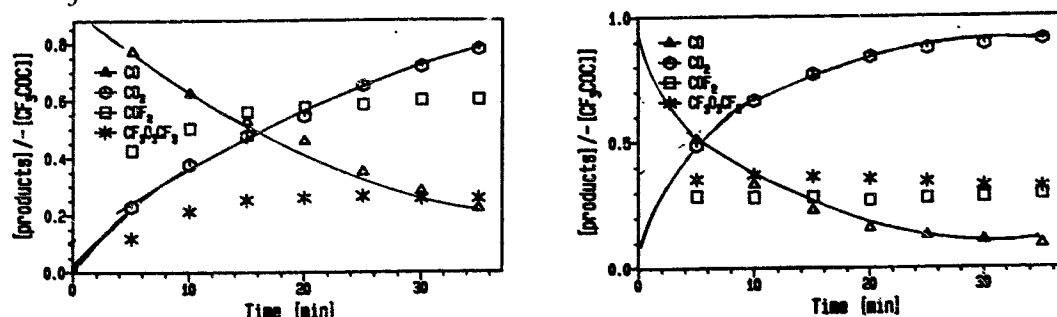
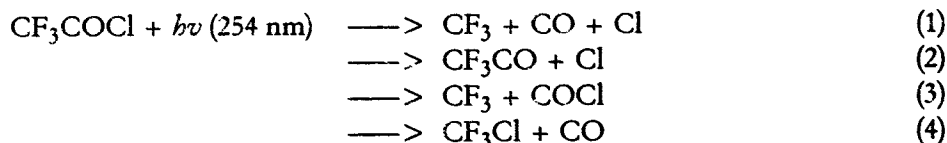
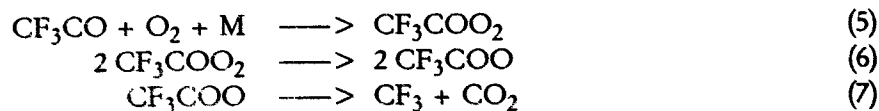


Fig. 6a and 6b. Ratio of the products formed versus  $\text{CF}_3\text{COCl}$  removed in the photolysis of  $0.9 \times 10^{14}$  and  $6.0 \times 10^{14}$  molecule  $\text{cm}^{-3}$   $\text{CF}_3\text{COCl}$ .

The possible primary photolysis steps are:



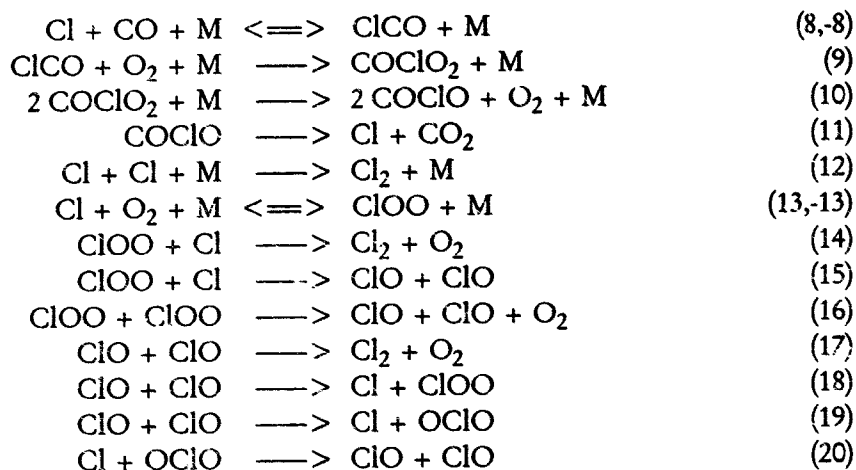
From the data shown in Figures 5a,b and 6a,b it can be concluded that CO is the main product at the beginning of the photolysis. The time profile of the formation of  $\text{CO}_2$  gives an important indication that  $\text{CO}_2$  is a secondary product not arising from reaction path (2), and the consecutive reactions (5) to (7). In a previous report [6], we had indicated that the high yield of  $\text{CO}_2$  at 25 min photolysis time could be explained by the reaction sequence initiated by the  $\text{CF}_3\text{CO}$  radical (analogous to the  $\text{CH}_3\text{COO}_2$  radical):



However, from the analysis of the experiments carried out in  $\text{N}_2$ , the products CO,  $\text{CF}_3\text{Cl}$  and  $\text{CF}_3\text{CF}_3$  were generated, with no evidence for the formation of  $\text{CF}_3\text{COCF}_3$

and  $\text{CF}_3\text{COCOCF}_3$ , which should have been formed if  $\text{CF}_3\text{CO}$  radicals were to be generated in step (2).

The formation of  $\text{CO}_2$  can be explained by the reaction chain initiated by the reaction Cl atoms with CO and  $\text{O}_2$ , producing molecular  $\text{Cl}_2$ , a product observed in this system:



This reaction scheme was checked in two other separate experiments, photolysing at  $\lambda = 254 \text{ nm}$

- i) mixtures  $\text{Cl}_2$  and CO in air, and
- ii) mixtures of  $\text{COCl}_2$  in air.

Fig. 7 displays CO-removal rates in the photolysis of 7 mTorr CO at various concentrations of  $\text{Cl}_2$  ranging from 7 to 70 mTorr in 760 Torr air. The presence of ClO radicals was observed by diode array spectroscopy, and is known to occur in earlier experiments performed by Clyne and Coxon [7]. A computer FACSIMILE simulation using the above reaction scheme and currently available rate constants [8] reproduces the product profiles observed in Figures 5a and 5b.

Additional evidence is found in the photolysis of  $\text{CF}_3\text{COCl}$  performed in air with added  $\text{C}_2\text{H}_6$ . The product ratio  $\Delta \text{CO} / \Delta \text{CF}_3\text{COCl}$  was found to be near unity and remaining constant over the photolysis period. Under these conditions, the Cl atoms are scavenged by  $\text{C}_2\text{H}_6$ , unable to start the further oxidation of CO to  $\text{CO}_2$ , via the reaction scheme (8) to (20).

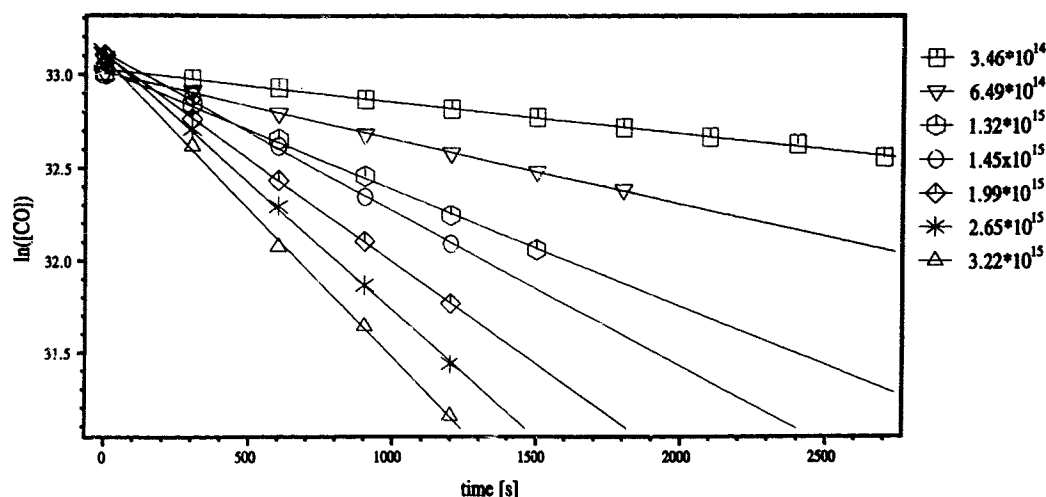
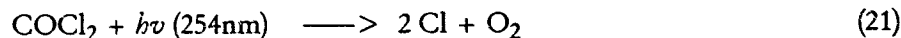


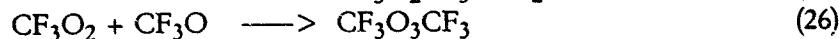
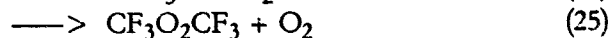
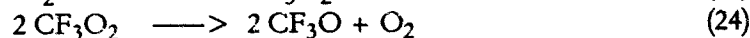
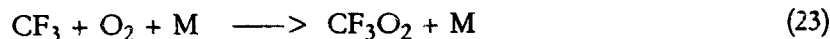
Fig. 7. First order decay rates in the photolysis of CO and Cl<sub>2</sub> mixtures in air.

It can therefore be concluded, that the earlier proposed primary reaction (2) is not a product channel in the photolysis of CF<sub>3</sub>COCl. Evidence against reaction channel (3) was found in the simulation of the COCl<sub>2</sub> + O<sub>2</sub> photolysis system, where only the photolysis via process (21) resulted in the observed slow formation of CO<sub>2</sub> with only few percent conversion. The formation of COCl (reaction 22) would cause a fast formation of CO<sub>2</sub> (100 % conversion), which is not observed, implying that no COCl species is formed primarily via channel (3):

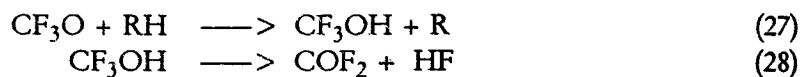


The formation of trace amounts of CF<sub>3</sub>Cl (upper limit 0.5 %) let us believe that direct molecular elimination occurs via reaction process (4). It must therefore be concluded that the main photolysis process at 254 nm of CF<sub>3</sub>COCl occurs via path (2). However it is possible that the yield of CF<sub>3</sub>Cl may be larger at lower wavelengths. The introduction of CF<sub>3</sub>Cl as Cl-containing compound in the stratosphere remains therefore a possibility.

The other main products observed COF<sub>2</sub>, CF<sub>3</sub>O<sub>3</sub>CF<sub>3</sub> and trace amounts of CF<sub>3</sub>O<sub>2</sub>CF<sub>3</sub> in the photolysis of CF<sub>3</sub>COCl originate from the oxidation of the CF<sub>3</sub> radicals:

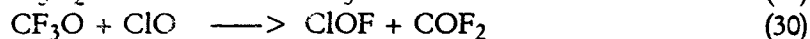
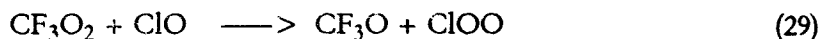


The fate of the CF<sub>3</sub>O and its further reaction to the main product COF<sub>2</sub> is not well understood. Sehested and Wallington [9] have proposed that CF<sub>3</sub>O radicals abstract and H-atom from hydrogen containing substances RH to form CF<sub>3</sub>OH which is unstable and decomposes to COF<sub>2</sub> and HF:



In our system, there is no RH present, except for impurities on the wall.

Computer simulations were carried out to investigate if there is a possible reaction between ClO and CF<sub>3</sub>O<sub>2</sub> to yield the observed COF<sub>2</sub>:

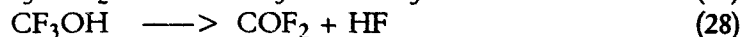


Using  $k_{29} = 2 \times 10^{-12}$ ,  $k_{30} = 1 \times 10^{-11}$  and  $k_{31} = 1 \times 10^{-11}$ , the calculated and observed COF<sub>2</sub> and CF<sub>3</sub>O<sub>3</sub>CF<sub>3</sub> concentrations after 35 minutes were respectively  $1.5 \times 10^{13}$  and  $1.3 \times 10^{14}$  (calculated) against  $9.9 \times 10^{13}$  and  $9.6 \times 10^{13}$  molecules cm<sup>-3</sup> (observed). These calculations indicated that reactions (29) and (30) are not responsible for the observed COF<sub>2</sub> formation.

### 3) Photooxidation Studies

In the study of the photooxidation of CF<sub>3</sub>CFH<sub>2</sub> (CFC-134a) described in our previous report [6], which was performed using small initial concentration of reactants (6 mTorr CF<sub>3</sub>CFH<sub>2</sub> and 60 mTorr Cl<sub>2</sub> at 700 Torr air), it was observed from the rate of disappearance of CF<sub>3</sub>CFH<sub>2</sub> that the calculated photolysis rate of Cl<sub>2</sub> was nearly 60 times slower than the measured photolysis rate using 7 TL12-lamps ( $2.5 \times 10^{-3} \text{ s}^{-1}$ ). FACSIMILE simulations have shown that the observed slow decay can be simulated if one takes into account the reactions (12) to (20). Due to the relatively small rate constant of the reaction Cl + CF<sub>3</sub>CFH<sub>2</sub> ( $k = 1.4 \times 10^{-15} \text{ cm}^3 \text{ molecule}^{-1} \text{ s}^{-1}$ ) and the low concentration of CF<sub>3</sub>CFH<sub>2</sub>, Cl atoms also react with O<sub>2</sub> (reaction 13) giving rise to the observed slower removal rate of CF<sub>3</sub>CFH<sub>2</sub>.

However the reaction scheme for the formation of COF<sub>2</sub>, proposed by Sehested and Wallington [9], and governed by reactions (27) and (28), where RH = CF<sub>3</sub>CFH<sub>2</sub>, does not explain the COF<sub>2</sub> yield observed in our study, using the proposed rate constants for reactions (32) and (28),  $k_{32} = 4.5 \times 10^{-16} \text{ cm}^3 \text{ molecule}^{-1} \text{ s}^{-1}$  and  $k_{28} = 4 \times 10^{-5} \text{ s}^{-1}$ .



Both reactions are too slow to explain the large yields of COF<sub>2</sub>. Obviously the mechanism for COF<sub>2</sub> is not understood for our experimental conditions.

#### 4) Chemistry of CF<sub>3</sub>COOH

Trifluoroacetic acid (TFA), CF<sub>3</sub>COOH, is known to be formed in the atmosphere by hydrolysis (in clouds) of CF<sub>3</sub>COF and CF<sub>3</sub>COCl, which are products arising from the degradation of HFC-134a, HCFC-124 and HCFC-123, respectively. The fate of the CF<sub>3</sub>COOH is however uncertain. CF<sub>3</sub>COOH exhibits a weak broad absorption band in the UV with a maximum near 215 nm ( $\sigma = 7.585 \times 10^{-20} \text{ cm}^2 \text{ molecule}^{-1}$ ) tailing off to zero at 275 nm [2].

a) Absorption experiments were performed in a 3 liter quartz reactor (base length 132 cm) without White optic mirrors. Absorption spectra were obtained using pressures up to 5.6 Torr CF<sub>3</sub>COOH (Fig. 8) and showed a dependence of the cross-section with pressure. The maximum of the absorptions was found at 212 nm.

We explain these measurements through the formation of dimers. Using the equation  $[\text{dimers}] = k_{\text{eq}} [\text{monomers}]^2$  the equilibrium constant  $k_{\text{eq}} = 0.45 \text{ Torr}^{-1}$  was obtained from the IR-spectra of CF<sub>3</sub>COOH at different pressures.

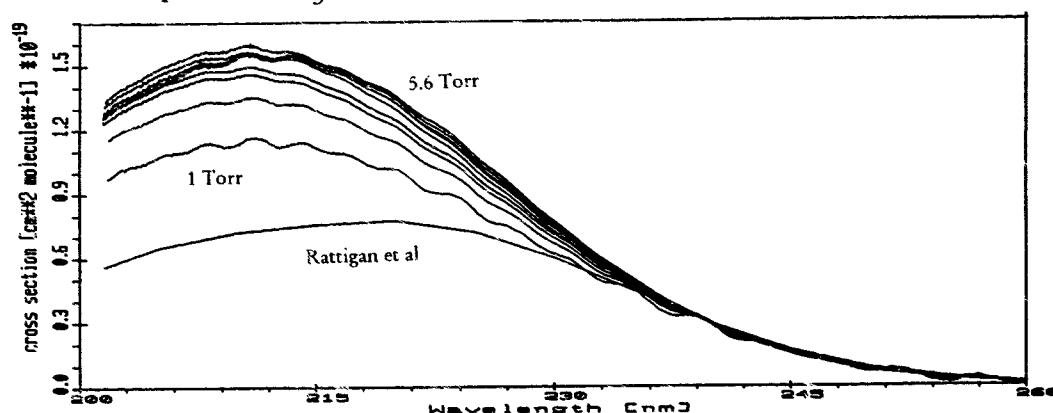


Fig. 8. UV spectra of CF<sub>3</sub>COOH at different pressures and comparison with UV spectrum obtained from Rattigan et al [2]. The ripple is an experimental artifact.

b) Experiments have been performed earlier in our laboratory, which seem to indicate that CF<sub>3</sub>COOH (Heraeus Feinchemikalien und Forschungsbedarf) decomposes by irradiation, *under specific conditions in our reactor*, into products COF<sub>2</sub> (60%), CO<sub>2</sub> (108 %) and CF<sub>3</sub>O<sub>3</sub>CF<sub>3</sub> (20%) with the yields based on initial rate measurements. Recently, additional investigations were undertaken using highly purified CF<sub>3</sub>COOH provided by the Solvay Fluor and Derivate GmbH, confirming our preliminary results.

The experiments were performed in a 46 l quartz reactor, equipped with White optic mirrors and coupled to a Bomem FTIR spectrometer. Photolysis of mixtures of 40, 8.5 and 1 mTorr CF<sub>3</sub>COOH in air with TL12 sun-lamps (emission in the wavelength range 280-360 nm) and/or UV lamps (254 nm) exhibited decomposition into the cited products, indicating C-C bond cleavage. In Figure 9 is shown the concentration time profiles of the photolysis of 8.5 mTorr CF<sub>3</sub>COOH in air with TL12 lamps. Figure 10 shows the IR-spectra of 8.5 mTorr CF<sub>3</sub>COOH at 760 Torr air before and after the photolysis, and the spectrum after stripping reference spectra of CF<sub>3</sub>COOH and COF<sub>2</sub> to show the formation of CF<sub>3</sub>O<sub>3</sub>CF<sub>3</sub>.

To scavenge possible impurities which might initiate a decomposition of CF<sub>3</sub>COOH, 6

Torr  $C_2H_6$  was added to some of the earlier experiments. The same initial decay of  $CF_3COOH$  was found with a 90 % yield of  $COF_2$ .

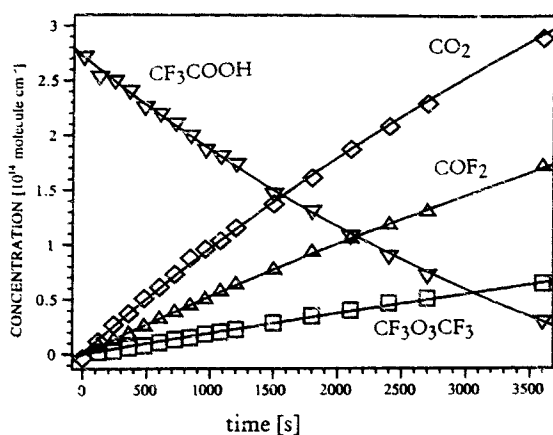


Fig. 9. Concentration-time profiles of the photolysis of  $CF_3COOH$  (8.5 mTorr) in air.

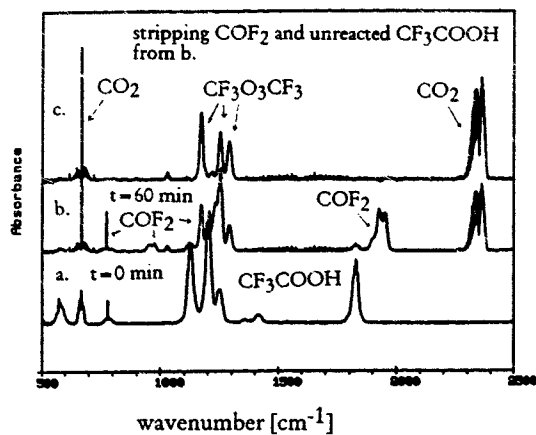


Fig. 10a-10c. IR-spectra of the photolysis of  $CF_3COOH$  (8.5 mTorr) in 760 Torr air with 7 TL12 lamps

These experiments indicate that *some (photolytic) catalytic decomposition* is taking place in the cell containing the White optic systems. This mirror system is mounted on stainless steel end-flanges, indicating that the decomposition may be accelerated by the presence of metal surfaces.

Certainly, further detailed experiments are needed to elucidate the observed behaviour of  $CF_3COOH$  and distinguish if the decomposition is accelerated by the presence of metal or quartz surfaces. If sunlight initiated decomposition on quartz is taking place, the atmosphere destruction of gas phase  $CF_3COOH$  on sand and mineral aerosols is possibly of importance.

#### References.

1. Siegemund G., *Angewandte Chemie. Intern. Ed.*, **12**, 918 (1973).
2. Rattigan O.V., Lutman E.R., Jones R.L. and Cox A.R., *J. Photochem. and Photobiol.*, in press (1993).
3. Nölle A., Heydtmann H., Meller R. and Moortgat G.K., *Geophys. Res. Lett.*, in press (1993).
4. Chou C.C., Crescentini G., Vera-Ruiz H., Smith W.S. and Rowland F.S., presented at 173rd ACS Meeting, New Orleans, 1977.
5. Libuda H.G., private communication.
6. Meller R., Boglu D. and Moortgat G.K., STEP-HALOCSIDE/AFEAS Workshop, p. 110, Dublin 1991.
7. Clyne M.A.A. and Coxon J.A., *Proc. Roy. Soc. London Ser. A.* **303**, 207 (1968).
8. DeMore W.B., Sander S.P., Golden D.M., Hampson R.F., Kurylo M.J., Howard C.J., Raviskankara A.R., Kolb C.E. and Molina M., JPL Publication 92-20 (1992).
9. Sehested J. and Wallington T.J., *Environ. Sci. Technol.*, **26**, 146 (1993).

0158

# RATE CONSTANTS FOR THE REACTION OF $CF_3O$ RADICALS WITH HYDROCARBONS AT 298 K.

Christina Kelly, Jack Treacy, and Howard W. Sidebottom  
*Department of Chemistry, University College Dublin, Dublin Ireland.*

and

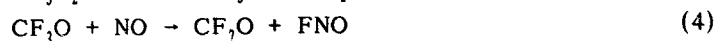
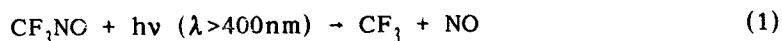
Ole John Nielsen  
*Chemical Reactivity Section, ES&T Department, Risø National Laboratory,  
DK-4000 Roskilde, Denmark.*

## Introduction

The catalytic destruction of ozone in the stratosphere by chlorine atoms is now well established [1]. In order to reduce the concentration of chlorine-containing compounds diffusing into the stratosphere it has been proposed that fully halogenated alkanes should be substituted by hydrofluorocarbons (HFCs) and hydrochlorofluoro-carbons (HCFCs). These compounds are, at least in part, oxidized in the troposphere via reaction with OH radicals, and hence their environmental impact depends on the oxidation products of the radical species produced following the reaction with OH radicals.

The available evidence suggests that  $CF_3$  radicals are produced as reaction intermediates in the atmospheric oxidation of compounds containing  $CF_3$ -groups [2,3]. In the atmosphere the  $CF_3$  radicals will react with oxygen and consecutively with NO [2,4] to give the corresponding alkoxy radical,  $CF_3O$ . The fate of the  $CF_3O$  radical under atmospheric conditions is unclear. Formation of  $CF_3O$  by either unimolecular decay with loss of a fluorine atom or by reaction with  $O_2$  is improbable, since both reactions are appreciably endothermic [5,6]. A number of experimental studies on the reactions of  $CF_3O$  radicals have recently been reported. Li and Francisco [7] observed laser induced fluorescence from the radical following infrared

multiphoton dissociation of  $\text{CF}_3\text{OOCF}_3$  and showed that the decay rate of  $\text{CF}_3\text{O}$  increased after addition of  $\text{NO}$  to the system. Product analysis by infrared spectroscopy indicated that  $\text{FNO}$  was a product of the reaction between  $\text{CF}_3\text{O}$  and  $\text{NO}$ . Chen et al. [8] investigated the photolysis of mixtures containing  $\text{CF}_3\text{NO}$  and  $\text{NO}$  in  $\text{O}_2/\text{N}_2$  mixtures at about 1 atmosphere total pressure. Analysis by long-path FTIR spectroscopy showed that  $\text{CF}_2\text{O}$ ,  $\text{FNO}$  and  $\text{NO}_2$  were formed in stoichiometric amounts based on the loss of  $\text{CF}_3\text{NO}$ . The authors rationalized their observations in terms of the reactions:



Chen et al. [9] have also found evidence that the  $\text{CF}_3\text{O}$  radical can abstract a hydrogen atom from alkanes:



Photolysis of  $\text{CF}_3\text{NO}/\text{NO}$  mixtures in air in the presence of ethane or propane gave  $\text{CF}_3\text{OH}$  and acetaldehyde or acetone, respectively. As previously reported [10]  $\text{CF}_3\text{OH}$  was found to be unstable and decomposes to give  $\text{CF}_2\text{O}$  and  $\text{HF}$ . Recent work by Zellner and Saathoff[11], Sehested and Wallington [12] and by Revilaqua et al. [13] has provided further evidence that H atom abstraction by  $\text{CF}_3\text{O}$  radicals is a relatively facile process.

The purpose of the present work was to further investigate the kinetics and mechanism for the reactions of  $\text{CF}_3\text{O}$  radicals with hydrocarbons. The results provide information on the importance of these reactions in the atmospheric chemistry of  $\text{CF}_3\text{O}$  radicals.

### Experimental

Kinetic and product analysis studies were carried out at  $298 \pm 2$  K and atmospheric pressure in an approximately 50 liter FEP Teflon cylindrical reaction chamber. The chamber was surrounded by 20 germicidal lamps (Phillips TUV 15W) providing UV-radiation with maximum intensity around 250 nm. Light intensity was varied by switching off various groups of

lamps. A uniform reaction temperature was achieved by the use of electric fans positioned below the reaction chamber. All pressure measurements were made using MKS Baratron capacitance manometers. Measured amounts of the reactants were flushed from calibrated Pyrex bulbs into the Teflon reaction chamber by a stream of Zero-Grade nitrogen (Air Products), which was then filled with either Zero-Grade nitrogen or Ultra-Pure air (Air Products). Reaction mixtures were allowed to mix for at least 30 minutes prior to photolysis. Quantitative analyses were carried out using gas chromatography (Gow Mac series 750 gas chromatograph equipped with a flame ionization detector) and FTIR spectroscopy (Mattson, Galaxy 5000,  $0.5 \text{ cm}^{-1}$  resolution). Gas tight syringes (Hamilton) or a Valco gas sampling valve were used to remove samples of the reaction mixtures from the Teflon bag for chromatographic analysis. FTIR spectra were obtained using an evacuable 2 litre Teflon-coated Wilks cell, containing a multi-pass White mirror arrangement (10m path-length), mounted in the cavity of the spectrometer. The reaction mixtures were expanded into the cell through 3 mm i.d. Teflon tubing, after various periods of photolysis.

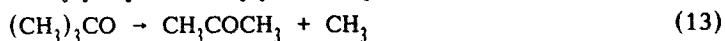
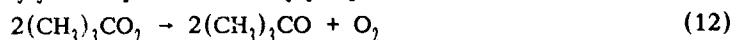
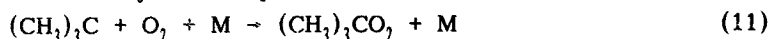
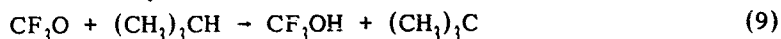
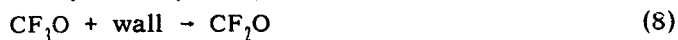
$\text{CF}_3\text{OOCF}_3$  (>99%, Fluorochem Ltd.) was further purified by vacuum distillation. Hydrocarbon gases were research grade products from Matheson and were used as received. Benzene (>99%, Aldrich) was trap to trap distilled prior to use.

## Results and Discussion

Photolysis of 10–60 ppm  $\text{CF}_3\text{OOCF}_3$  ( $1 \text{ ppm} = 2.46 \times 10^{13} \text{ molecules cm}^{-3}$  at 298 K) in air or nitrogen at atmospheric pressure for 5 hours resulted in about a 15% depletion of reactant and to the formation of stoichiometric amounts of  $\text{CF}_2\text{O}$ .  $\text{CF}_2\text{O}$  was stable in the dark for up to about 24 hours and photolysis at 250 nm was negligible over the time period of the present experiments. In the presence of a hydrocarbon, the loss of  $\text{CF}_3\text{OOCF}_3$  increased significantly, ~30% in 1 hour. For reactions carried out in air, the products detected by FTIR spectroscopy were  $\text{CF}_2\text{O}$  and other carbonyl compounds. In the initial stages of photolysis of  $\text{CF}_3\text{OOCF}_3$  in the presence of isobutane in air, the yields of  $\text{CF}_2\text{O}$  and  $\text{CH}_3\text{COCH}_3$  corresponded to the loss of  $\text{CF}_3\text{OOCF}_3$ ,

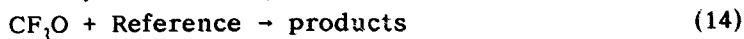
$\Delta\text{CF}_2\text{O}/-\Delta\text{CF}_3\text{OOCF}_3=2.1\pm0.3$  and  $\Delta\text{CH}_3\text{COCH}_3/-\Delta\text{CF}_3\text{OOCF}_3=2.0\pm0.2$ . At longer reaction times  $\text{CH}_3\text{COCH}_3$  was lost by photolysis. Similar results were

obtained from the photolysis of  $\text{CF}_3\text{OOCF}_3$  with ethane and propane, where the carbonyl compounds were acetaldehyde and acetone, respectively. The results are in agreement with Chen et al. [9], who also have provided evidence for the abstraction of hydrogen atoms from  $\text{C}_2\text{H}_6$  and  $\text{C}_3\text{H}_8$  by  $\text{CF}_3\text{O}$  radicals. These results are consistent with the following reactions:



Combination of  $\text{CF}_3\text{O}$  radicals in reaction (7) to reform the peroxide, appears to be the major reaction channel for these radicals after photolysis of  $\text{CF}_3\text{OOCF}_3$  in air or nitrogen. The small amounts of  $\text{CF}_2\text{O}$  detected are likely to arise from heterogeneous loss of  $\text{CF}_3\text{O}$  at the chamber walls. Reaction of  $\text{CF}_3\text{O}$  radicals with alkanes presumably involves a hydrogen abstraction process with the alkyl radical,  $(\text{CH}_3)_3\text{C}$  being oxidized in air to form acetone. In our system  $\text{CF}_3\text{OH}$  was not observed directly, but decomposed to give  $\text{CF}_2\text{O}$  and HF. Klöter and Seppelt [10] have previously shown that in the condensed phase  $\text{CF}_3\text{O}$  decomposes rapidly to form  $\text{CF}_2\text{O}$  and HF. However, in the gas phase at 12 torr, the lifetime appeared to be somewhat longer with a half-life of at least 5 minutes. From their gas phase experiments at 297 K Chen et al. [8] observed a lifetime for  $\text{CF}_3\text{OH}$  of about 12 minutes. Decomposition of  $\text{CF}_3\text{OH}$  to give  $\text{CF}_2\text{O}$  and HF is estimated to be approximately  $5 \text{ kcal mol}^{-1}$  exothermic [5,6]. In a recent theoretical treatment on the unimolecular decay of  $\text{CF}_3\text{OH}$ , Francisco [14] showed that the reaction had an appreciable barrier of around  $50 \text{ kcal mol}^{-1}$ , suggesting that the loss of  $\text{CF}_3\text{OH}$  observed by Klöter and Seppelt [10] and by Chen et al. [9] is probably surface catalyzed. In the present experiments the long photolysis times required to obtain measurable decays of  $\text{CF}_3\text{OOCF}_3$  precludes detection of  $\text{CF}_3\text{OH}$  with the result that  $\text{CF}_2\text{O}$  is the observed product of the reaction of  $\text{CF}_3\text{O}$  with alkanes.

Relative rate constants for the reaction of a number of hydrocarbons with  $\text{CF}_3\text{O}$  radicals were determined by comparison of the decay of the reactant hydrocarbon and that of a reference compound:



Assuming that reaction with  $\text{CF}_3\text{O}$  is the only significant loss process for both the reactant and the reference compound, it can be shown that:

$$\ln([\text{RH}]_0/[\text{RH}]_t) = k_5/k_{14} \ln([\text{Ref}]_0/[\text{Ref}]_t) \quad (I)$$

where the subscripts o and t indicate concentrations at the beginning of the experiment and at time t, respectively. Under the experimental conditions employed photolytic loss of the hydrocarbon was unimportant and the reaction mixtures were stable in the dark for at least 24 hours.

Photolysis of  $\text{CF}_3\text{OOCF}_3$ /hydrocarbon mixtures were carried out in either air or nitrogen at  $298 \pm 2$  K and 1 atmosphere total pressure;  $[\text{CF}_3\text{OOCF}_3]_0 = 10\text{--}60$  ppm,  $[\text{RH}]_0 = 1\text{--}10$  ppm. Concentration-time data for the hydrocarbon reactions investigated are plotted in the form of equation (I) in Figures 1 and 2.

The rate constant ratios  $k_5/k_{14}$ , where  $\text{C}_7\text{H}_6$  was the reference compound, are given in Table 1. These ratios were independent of reaction time, relative reactant concentration and light intensity in agreement with the proposed mechanism. At least five individual runs were carried out for each substrate and in order to test internal consistency of the rate constant ratios, each compound was run against another member of the series. In all cases the relative rate values were in excellent agreement with each other. Values of the rate constant ratios determined for each reactant pair were equal within experimental error for experiments run both in air and nitrogen. The eventual products arising from the alkyl radicals formed in these  $\text{CF}_3\text{O}$  initiated reactions would be expected to vary depending on whether air or  $\text{N}_2$  was the bath gas. Thus complications arising from either product interference in the analytical procedure or enhanced removal of one of the reactant components due to product radical reactions are unlikely to be significant. It is possible that some loss of hydrocarbon in our relative rate studies may arise from reactions of F atoms, which may be formed in heterogeneous reactions at the chamber wall. However, the degree of selectivity shown is inconsistent with a F atom loss process for the

0 1 6 3

Fig. 1. Concentration-time data for the reaction of  $\text{CF}_3\text{O}$  radicals with various hydrocarbons.

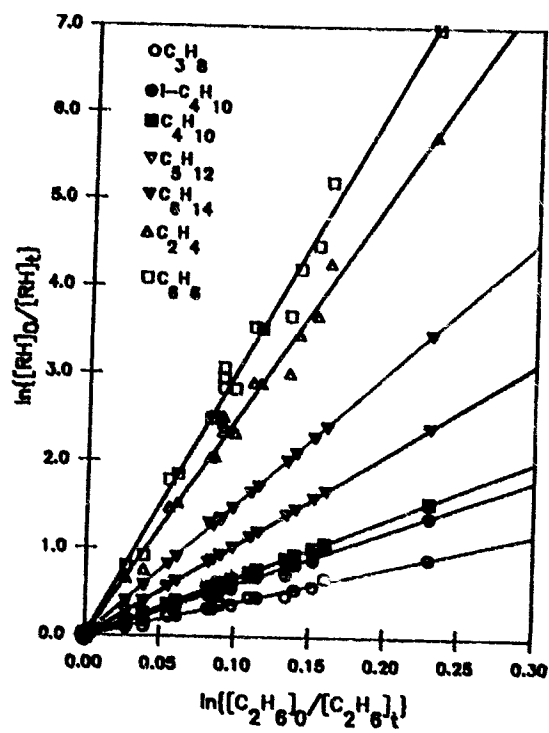
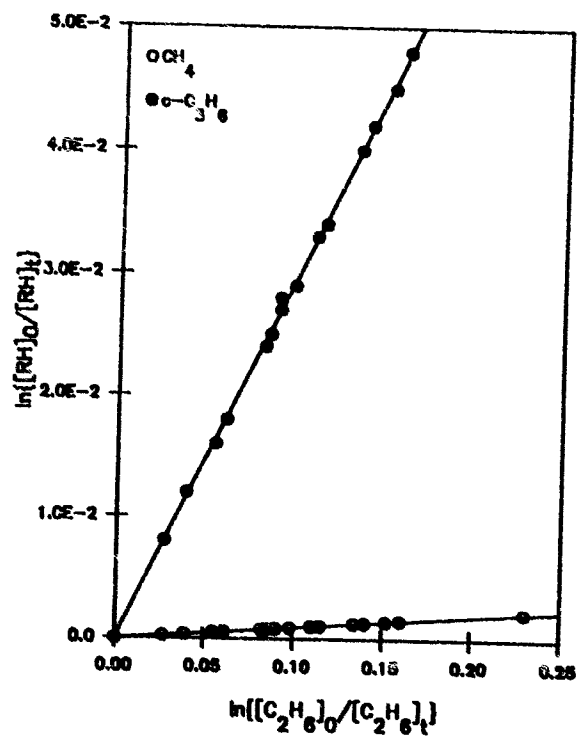


Fig. 2. Concentration-time data for the reaction of  $\text{CF}_3\text{O}$  radicals with  $\text{CH}_4$  and  $\text{c-C}_3\text{H}_8$ .



hydrocarbon. Furthermore, the addition of up to 100 ppm of  $\text{CH}_4$  did not change the rate constant ratios obtained for a pair of hydrocarbons. Addition of  $\text{CH}_4$  to the system would be expected to scavenge F atoms,  $k(\text{F}+\text{CH}_4)=8 \times 10^{-11} \text{ cm}^3 \text{ molecule}^{-1} \text{ s}^{-1}$  [15].

Table 1. Rate constant data for the gas-phase reactions of  $\text{CF}_3\text{O}$  radicals with hydrocarbons at  $298 \pm 2 \text{ K}$  and 1 atm. total pressure.

compound	$k(\text{CF}_3\text{O}+\text{RH})/k(\text{CF}_3\text{O}+\text{C}_2\text{H}_6)^{\text{a}}$	$10^{12}k(\text{CF}_3\text{O}+\text{RH})^{\text{b}}$	$k(\text{OH}+\text{RH})/k(\text{OH}+\text{C}_2\text{H}_6)^{\text{c}}$
$\text{CH}_4$	$0.010 \pm 0.001$	$0.012 \pm 0.001$	0.031
c- $\text{C}_3\text{H}_6$	$0.30 \pm 0.02$	$0.36 \pm 0.02$	0.26
$\text{C}_2\text{H}_6$	1.0	1.2	1.0
$\text{C}_3\text{H}_8$	$3.9 \pm 0.5$	$4.7 \pm 0.7$	4.3
$(\text{CH}_3)_3\text{CH}$	$6.0 \pm 0.4$	$7.2 \pm 0.5$	8.7
n- $\text{C}_4\text{H}_{10}$	$6.7 \pm 0.5$	$8.0 \pm 0.6$	9.5
n- $\text{C}_5\text{H}_{12}$	$10.4 \pm 0.4$	$12.5 \pm 0.5$	15
n- $\text{C}_6\text{H}_{14}$	$15 \pm 1$	$18 \pm 1$	21
$\text{C}_7\text{H}_8$	$25 \pm 1$	$30 \pm 1$	32
$\text{C}_6\text{H}_6$	$30 \pm 1$	$36 \pm 1$	4.6

<sup>a</sup> errors quoted represent  $\pm 2\sigma$  and represents precision only

<sup>b</sup> calculated using  $k(\text{CF}_3\text{O}+\text{C}_2\text{H}_6)=1.2 \times 10^{-11} \text{ cm}^3 \text{ molecule}^{-1} \text{ s}^{-1}$  [11], errors in this reference rate constant are not included.

<sup>c</sup> evaluated data taken from ref. [16]

The rate constants for reaction of  $\text{CF}_3\text{O}$  radicals with the hydrocarbons studied relative to the rate constant for reaction with ethane are given in Table 1. Chen et al [9] have previously reported the rate constant ratio  $k(\text{CF}_3\text{O}+\text{C}_3\text{H}_8)/k(\text{CF}_3\text{O}+\text{C}_2\text{H}_6)=2.5$  in reasonable agreement with our result. The rate constant ratios determined in this work for  $\text{CF}_3\text{O}$  reactions are compared to the values for the corresponding OH radical reactions in Table 1. The data show that  $\text{CF}_3\text{O}$  radicals have about the same degree of selectivity as the OH radical and thus may be expected to have the same level of reactivity. This rather surprising result is consistent with a recent laser flash photolysis - laser induced fluorescence study by Zellner [10] on the reaction

of  $\text{CF}_3\text{O}$  radicals with  $\text{C}_2\text{H}_6$ , for which a value of the rate constant,  $k(\text{CF}_3\text{O}+\text{C}_2\text{H}_6)=(1.2\pm 0.2)\times 10^{-12} \text{ cm}^3\text{molecule}^{-1}\text{s}^{-1}$  was obtained. Combining this rate constant with the rate constant ratios determined in this work provides estimates of the rate constants for the reaction of  $\text{CF}_3\text{O}$  radicals with the series of hydrocarbons investigated, Table 1. Bevilaqua et al. [12] employed a flow reactor coupled to a chemical ionization mass spectrometric detector to study the reaction of  $\text{CF}_3\text{O}$  radicals with isobutane. The preliminary estimate of  $k(\text{CF}_3\text{O}+\text{i-C}_4\text{H}_{10})=(5\pm 3)\times 10^{-12} \text{ cm}^3\text{molecule}^{-1}\text{s}^{-1}$  is in excellent agreement with the rate constant determined from the present work.

Figure 3 shows a plot of the rate constants for reaction of  $\text{CF}_3\text{O}$  radicals with a series of n-alkanes versus the number of  $\text{CH}_2$  groups. The linearity of the plot indicates that the reactions involve simple H-atom abstraction. Rate constants per abstracted H-atom from  $\text{CH}_4$ , primary, secondary and tertiary sites in hydrocarbons can be derived from the rate data in Table 1:  $k_{\text{prim}}=k_{\text{C}_2\text{H}_6}/6$ ;  $k_{\text{sec}}=(k_{\text{C}_3\text{H}_8}-k_{\text{C}_2\text{H}_6})/2$ ;  $k_{\text{tert}}=k_{(\text{CH}_3)_3\text{CH}}-(3/2)k_{\text{C}_2\text{H}_6}$ . As expected for H atom abstraction reactions the rate constants for reaction of  $\text{CF}_3\text{O}$  radicals with alkanes correlate very well with the C-H bond strengths [17], see Figure 4. The high reactivity of both  $\text{C}_2\text{H}_4$  and  $\text{C}_6\text{H}_6$  towards reaction with  $\text{CF}_3\text{O}$  indicates that addition to the unsaturated system is the major reaction channel in these systems. It is interesting to compare the rate constants for reactions of  $\text{CF}_3\text{O}$  radicals with alkanes to those for the corresponding  $\text{CH}_3\text{O}$  reactions. At 298 K the rate constant for reaction of  $\text{CF}_3\text{O}$  with ethane is over 5 orders of magnitude higher than that for  $\text{CH}_3\text{O}$ ,  $k(\text{CH}_3\text{O}+\text{C}_2\text{H}_6)=2.51\times 10^{-18} \text{ cm}^3\text{molecule}^{-1}\text{s}^{-1}$  [18]. This result can be rationalized in terms of strengthening of the O-H bond following fluorine substitution of the methyl group in  $\text{CH}_3\text{OH}$ ,  $D(\text{CF}_3\text{O}-\text{H})=109 \text{ kcal mol}^{-1}$  [5] and  $D(\text{CH}_3\text{O}-\text{H})=104 \text{ kcal mol}^{-1}$  [17]. It is surprising however that, the  $\text{CF}_3\text{O}$  radical is slightly more reactive towards hydrocarbons than the OH radical despite the fact that the reactions are about  $10 \text{ kcal mol}^{-1}$  less exothermic. Presumably, the high level of reactivity of the  $\text{CF}_3\text{O}$  radical is a consequence of both the strength of the O-H bond in  $\text{CF}_3\text{OH}$  and the high electronegativity of the radical.

As previously discussed, unimolecular decay with the loss of a F atom or reaction with  $\text{O}_2$  are unlikely to be important loss processes for  $\text{CF}_3\text{O}$  in the atmosphere. Reaction of  $\text{CF}_3\text{O}$  with oxides of nitrogen or hydrocarbons are possible sinks for  $\text{CF}_3\text{O}$  in the troposphere. The kinetic data obtained in this work, and in that of Chen et al. [9] and Bevilaqua et al. [12] indicate that reaction with hydrocarbons may be important. Bevilaqua et al. [12] have determined a value of the rate constant

Fig. 3 Rate constant for the reaction of  $\text{CF}_3\text{O}$  radicals with a series of n-alkanes versus the number of  $\text{CH}_2$  groups.

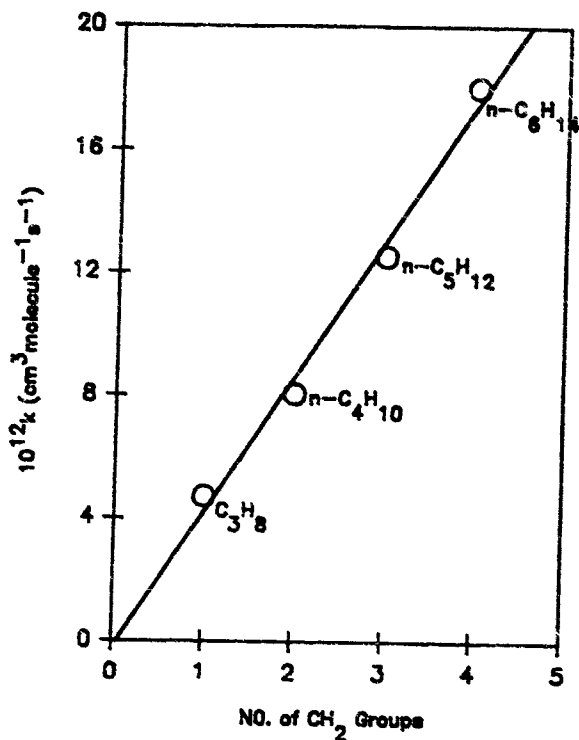
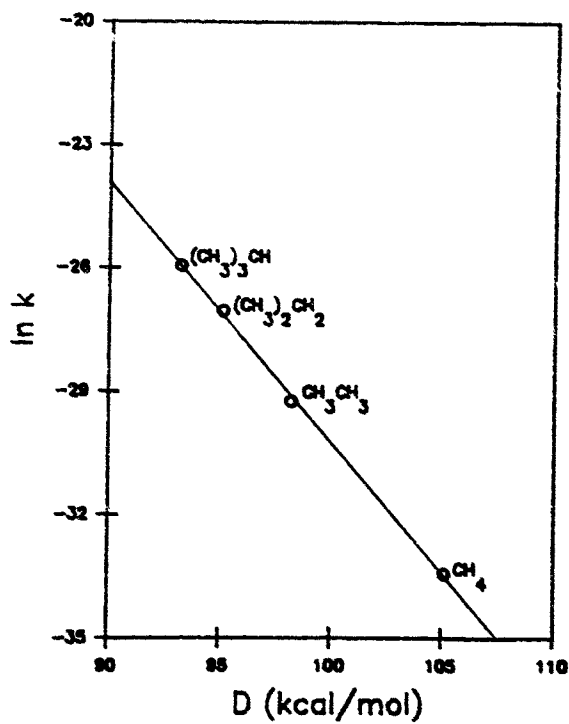


Fig. 4. Rate constants per abstractable H of the specified type as a function of the C-H bond strength.



for the reaction of  $\text{CF}_3\text{O}$  with  $\text{NO}$ ,  $k(\text{CF}_3\text{O}+\text{NO})=(2\pm 1)\times 10^{-11} \text{ cm}^3\text{molecule}^{-1}\text{s}^{-1}$ . Thus, as previously suggested by Chen et al. [9], at the hydrocarbon to  $\text{NO}$  mixing ratios typically found in the troposphere, the reaction with hydrocarbons will be a major sink for  $\text{CF}_3\text{O}$  radicals giving  $\text{CF}_3\text{OH}$ . Although  $\text{CF}_3\text{OH}$  is relatively unstable under laboratory conditions, the available data indicates that the decay may be mainly due to heterogeneous processes. It seems likely, therefore that  $\text{CF}_3\text{OH}$  loss in the troposphere will largely take place at aerosol surfaces or by hydrolysis in cloud water.

## REFERENCES

1. F.S. Rowland, *Ann. Rev. Phys. Chem.* 42 (1991) 731.
2. Scientific Assessment of Stratospheric Ozone, World Meteorological Organization Global Ozone Research and Monitoring Project, Report No. 20, Vol 2, Appendix: AFEAS Report, Chapter 6, (1989).
3. Scientific Assessment of Stratospheric Ozone, World Meteorological Organization Global Ozone Research and Monitoring Project, Report No. 25, Chapter 5, (1991).
4. A.M. Dognon, F. Caralp, and R. Lesclaux, *J. Chim. Phys.* 82 (1988) 349.
5. L. Batt and R. Walsh, *Int. J. Chem. Kinet.* 14 (1982) 933; L. Batt and R. Walsh, *Int. J. Chem. Kinet.* 15 (1983) 605.
6. S.W. Benson, "Thermochemical Kinetics", 2nd ed., Wiley, New York, (1976)
7. Z. Li and J.S. Francisco, *Chem. Phys. Lett.* 186 (1991) 336.
8. J. Chen, T. Zhu, and H. Niki, *J. Phys. Chem.* 96 (1992) 6115.
9. J. Chen, T. Zhu, H. Niki, and G.J. Mains, *Geophys. Res. Lett.* 19 (1992) 2215.
10. G. Klöter and K. Seppelt, *J. Am. Chem. Soc.* 101 (1979) 347.
11. R. Zellner and H. Saathoff, paper presented at the 12<sup>th</sup> International Symposium on Gas Kinetics, Reading (1992)
12. J. Sehested and T.J. Wallington, *Environ. Sci. Technol.* 27 (1993) 146.
13. T.J. Bevilaqua, D.R. Hanson, and C.J. Howard, accepted for publication in *J. Phys. Chem.* (1993).
14. J.S. Francisco, *Chem. Phys.* 19 (1991) 150.
15. W. B. DeMore, S. P. Sander, D. M. Golden, M. J. Molina, R. F. Hampson, M. J. Kurylo, C. J. Howard, and A. R. Ravishankara, JPL Publication 90-1 (1990).
16. R. Atkinson. *J. Phys. Chem. Ref. Data, Monograph 1* (1989)
17. D.F. McMillen and D.M. Golden, *Ann. Rev. Phys. Chem.* 87 (1983) 1812
18. W. Tang and R.F. Hampson, *J. Phys. Chem. Ref. Data.* 15 (1986) 1087

0 1 6 9

0 1 5 b

**LONG PATH-FTIR SPECTROSCOPIC STUDY OF THE REACTIONS  
OF CF<sub>3</sub>OO AND CF<sub>3</sub>O RADICALS WITH NO<sub>2</sub>**

**J. Chen, V. Young, T. Zhu and H. Niki**

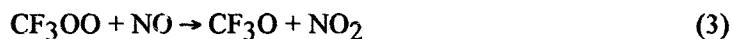
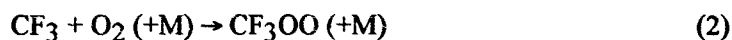
*Centre for Atmospheric Chemistry and Department of Chemistry, York University  
4700 Keele Street, North York, Ontario, Canada M3J 1P3*

**ABSTRACT**

Mechanisms of the reactions of CF<sub>3</sub>OO and CF<sub>3</sub>O radicals with NO<sub>2</sub> have been studied using the long path-FTIR method in the visible ( $\lambda \geq 400$  nm) photolysis of CF<sub>3</sub>NO in the presence of excess NO<sub>2</sub> (in mtorr range) in 700 torr of air at  $297 \pm 2$  K. In the early stage of the photolysis, the predominant F-containing product detected was CF<sub>3</sub>OONO<sub>2</sub> formed via the addition reaction  $\text{CF}_3\text{OO} + \text{NO}_2 (+\text{M}) \leftrightarrow \text{CF}_3\text{OONO}_2 (+\text{M})$ . An alternative decomposition channel of CF<sub>3</sub>OONO<sub>2</sub> to yield CF<sub>2</sub>O and FNO<sub>2</sub> as reported in the literature was not observed in the present study. Addition of excess NO to the above irradiated mixture in the dark led to the loss of CF<sub>3</sub>OONO<sub>2</sub> and concomitant production of CF<sub>3</sub>ONO<sub>2</sub>, FNO<sub>2</sub> and CF<sub>2</sub>O, consistent with the occurrence of  $\text{CF}_3\text{OO} + \text{NO} \rightarrow \text{CF}_3\text{O} + \text{NO}_2$  followed by the addition reaction  $\text{CF}_3\text{O} + \text{NO}_2 (+\text{M}) \rightarrow \text{CF}_3\text{ONO}_2 (+\text{M}) (\geq 90\%)$  and the F-transfer reaction  $\text{CF}_3\text{O} + \text{NO}_2 \rightarrow \text{CF}_2\text{O} + \text{FNO}_2 (\leq 10\%)$ .

## INTRODUCTION

The oxidation of the trifluoromethoxy radical ( $\text{CF}_3\text{O}$ ) is one of the major uncertainties in the mechanism of tropospheric degradation of hydrofluorocarbons (HFCs) and hydrochlorofluorocarbons (HCFCs) containing a  $\text{CF}_3$  group.<sup>1</sup> Recently, we have carried out a series of long path-FTIR-based studies of the reactions of  $\text{CF}_3\text{O}$  radicals with  $\text{NO}$ ,<sup>2</sup> alkanes<sup>3</sup> and alkenes,<sup>4</sup> using the visible photolysis of  $\text{CF}_3\text{NO}$  as the source of  $\text{CF}_3\text{O}$  radicals, i.e.,

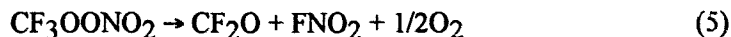


The present study is an extension of the above studies to the reactions of  $\text{CF}_3\text{OO}$  and  $\text{CF}_3\text{O}$  radicals with  $\text{NO}_2$ . To our knowledge, no kinetic or mechanistic studies made on these reactions under tropospheric conditions have been reported previously.

Similarly to the other  $\text{CX}_3\text{OO}$  ( $\text{X} = \text{H}$  or halogen atom) radicals,  $\text{CF}_3\text{OO}$  is expected to undergo an addition reaction with  $\text{NO}_2$  to form  $\text{CF}_3\text{OONO}_2$  which is thermally unstable and redissociates to  $\text{CF}_3\text{OO}$  and  $\text{NO}_2$ .<sup>5,6</sup>



Previously, Hohorst and DesMarteau<sup>7</sup> prepared pure  $\text{CF}_3\text{OONO}_2$  in a variety of low temperature ( $< -50$  °C) liquid-phase reactions, and characterized its spectroscopic and physico-chemical properties. These authors reported that  $\text{CF}_3\text{OONO}_2$  is the most stable alkyl peroxyxynitrate known, and that in pure gaseous form it slowly decomposed at 22 °C with an overall reaction given by:

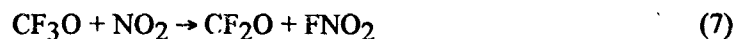


Thus,  $\text{CF}_3\text{OONO}_2$  may undergo dissociation via a mechanism other than reaction (-4) under the atmospheric conditions.

The  $\text{CF}_3\text{O} + \text{NO}_2$  reaction has two thermochemically possible channels, i.e. addition and F-atom transfer reactions:



and



Reactions analogous to reaction (6) are known to be the dominant channel for RO (R = H or alkyl group) radicals.<sup>8,9</sup> On the other hand, we have recently shown that the  $\text{CF}_3\text{O} + \text{NO}$  reaction exclusively undergoes F-atom transfer reaction to yield  $\text{CF}_2\text{O}$  and FNO rather than forming the addition product  $\text{CF}_3\text{ONO}$ .<sup>2</sup> Values of the rate constant for reaction (7) have been recently determined to be  $(2 \pm 1) \times 10^{-11}$ ,  $(2.5 \pm 0.4) \times 10^{-11}$  and  $(5.2 \pm 2.7) \times 10^{-11} \text{ cm}^3 \text{ molecule}^{-1} \text{ s}^{-1}$ .<sup>10-12</sup> The present study was undertaken to determine the relative importance of the possible channels for the  $\text{NO}_2$ -reactions of the  $\text{CF}_3\text{OO}$  and  $\text{CF}_3\text{O}$  radicals under atmospheric conditions.

#### EXPERIMENTAL

As in our previous studies of  $\text{CF}_3\text{O}$  radical reactions,<sup>2-4</sup> the visible ( $\lambda \geq 400 \text{ nm}$ ) photolysis of  $\text{CF}_3\text{NO}$  was used to produce the precursor  $\text{CF}_3$  radicals, i.e. reactions (1) and (2). For the study of the  $\text{CF}_3\text{OO} + \text{NO}_2$  reaction, mixtures containing  $\text{CF}_3\text{NO}$  (3 - 10 ppm, 1 ppm = 0.77 mtorr) and  $\text{NO}_2$  (4 - 10 ppm) in 700 torr of synthetic air were irradiated, at  $297 \pm 2 \text{ K}$ , in a 180-m path length IR absorption cell/photochemical reactor (30 cm diameter; 2 m long; 140 L Pyrex cylinder with internal gold-coated White cell mirrors) surrounded by visible fluorescent lamps (GE F40CW,  $\lambda \geq 400 \text{ nm}$ ).<sup>13</sup> For the study of the  $\text{CF}_3\text{O} + \text{NO}_2$  reaction, NO (1 - 2 ppm) was added to some of these mixtures in the dark following irradiation. IR absorbance spectra were typically recorded after each minute of irradiation with a resolution of  $1/16 \text{ cm}^{-1}$  in 90 s (16 scans) in the frequency range of  $500 - 3700 \text{ cm}^{-1}$  using a Ge-coated KBr beamsplitter and a liquid He-cooled Cu-Ge detector.  $\text{CF}_3\text{NO}$  (PCR, > 95%) was purified and handled as described previously.<sup>2-4</sup>  $\text{NO}_2$  (99%) and NO (99%) from Aldrich were used as received.

## RESULTS AND DISCUSSION

Displayed in Figure 1 are the typical spectra obtained in the photolysis of a mixture containing  $\text{CF}_3\text{NO}$  (3 ppm) and  $\text{NO}_2$  (4 ppm) in 700 torr of synthetic air. Prior to irradiation, the reactant mixture was kept in the cell in the dark for about 10 minutes. During this period, neither changes in the reactant concentrations nor the formation of any products were observed (Figure 1(A)). After 1 minute of photolysis (Figure 1(B)), approximately 0.05 ppm of the reactants  $\text{CF}_3\text{NO}$  and  $\text{NO}_2$  were consumed. At this low conversion of the reactants, the ratio  $[\text{NO}]/[\text{NO}_2] \approx 0.01$  was sufficiently low (Figure 1(B)) to ensure that the  $\text{CF}_3\text{OO}$  radicals reacted predominantly with  $\text{NO}_2$  rather than with  $\text{NO}$ . Displayed in Figure 1(C) is the difference spectrum obtained by subtracting Figure 1(A) from Figure 1(B). For clarity, the contribution of  $\text{CF}_3\text{NO}$  spectrum was also removed from Figure 1(C). In addition to  $\text{NO}$  formed from the photodissociation of  $\text{CF}_3\text{NO}$ , several bands attributable to  $\text{CF}_3\text{OONO}_2$  are seen in this spectrum. The gas phase IR spectrum of  $\text{CF}_3\text{OONO}_2$  was previously studied by Hohorst and DesMarteau.<sup>7</sup> The IR frequencies and peak intensities for  $\text{CF}_3\text{OONO}_2$  determined in the present work are in good agreement with those reported by Hohorst and DesMarteau,<sup>7</sup> as shown in Table 1. The indicated peak intensities were calculated from the observed absorbance and the  $\text{CF}_3\text{OONO}_2$  concentration derived from the material balance. Reactions similar to reaction (4) have been studied for  $\text{CCl}_3\text{OO}$ ,  $\text{CCl}_2\text{FOO}$  and  $\text{CClF}_2\text{OO}$  radicals by Niki *et al.*<sup>5</sup> and by Koeppenkastrop and Zabel.<sup>14</sup> The equilibrium constants for the  $\text{NO}_2$  addition were reported as  $3.04 \times 10^{-11}$ ,  $8.94 \times 10^{-11}$  and  $1.39 \times 10^{-10} \text{ cm}^3 \text{ molecule}^{-1}$  for  $\text{CCl}_3\text{OO}$ ,  $\text{CCl}_2\text{FOO}$  and  $\text{CClF}_2\text{OO}$ , respectively.<sup>14</sup> Similar experimental data are not available for the reaction of  $\text{CF}_3\text{OO}$  radicals with  $\text{NO}_2$ , but the substitution of F for Cl is expected to further stabilize the ensuing halomethyl peroxy nitrates.

At higher conversion of the reactants and correspondingly higher  $[\text{NO}]/[\text{NO}_2]$  ratios, additional products arising from the reactions of  $\text{CF}_3\text{O}$  formed in the  $\text{CF}_3\text{OO} + \text{NO}$  reaction were observed, as illustrated in Figure 2. Namely, when the identical reactant mixture as in Figure 1(A) was irradiated for 3 minutes (Figure 2(A)), the formation of  $\text{CF}_2\text{O}$  ( $1944$  and  $774 \text{ cm}^{-1}$ ),

CF<sub>3</sub>OONO<sub>2</sub> (1764, 1296, 1243, 1190, 956 and 787 cm<sup>-1</sup>) and FNO (1844 and 766 cm<sup>-1</sup>) plus several new bands were discernible in the difference spectrum (Figure 2(B)). Some of these new bands, (e.g. 956 and 1151 cm<sup>-1</sup>), were assigned to CF<sub>3</sub>ONO<sub>2</sub>, as discussed below. Two weak bands were also detected at 1790 and 1311 cm<sup>-1</sup> which correspond to the two strongest bands of FNO<sub>2</sub> spectrum reported by Bernitt et al.<sup>15</sup>

Consistent with the occurrence of reactions (4), (-4) and (3), the observed lifetimes of CF<sub>3</sub>OONO<sub>2</sub> were highly dependent on the [NO]/[NO<sub>2</sub>] ratio encountered in the reaction mixture following the photolysis. Namely, when the irradiated mixture shown in Figure 3 was aged in the dark, the NO and CF<sub>3</sub>OONO<sub>2</sub> were consumed nearly completely in about 10 minutes with the concomitant production of CF<sub>3</sub>ONO<sub>2</sub> and NO<sub>2</sub> (Figure 3). On the other hand, the addition of 1 ppm of NO after 1 minute of photolysis led to complete decay of the CF<sub>3</sub>OONO<sub>2</sub> and production of CF<sub>3</sub>ONO<sub>2</sub> and NO<sub>2</sub> during one min of dark aging, as shown in Figure 4.

IR spectrum of CF<sub>3</sub>ONO<sub>2</sub> has not been reported previously. However, by comparison with the known spectra of RONO<sub>2</sub>-type molecules, such as CH<sub>3</sub>ONO<sub>2</sub>,<sup>6</sup> C<sub>2</sub>H<sub>5</sub>ONO<sub>2</sub>,<sup>6</sup> ClONO<sub>2</sub> and FONO<sub>2</sub>,<sup>16</sup> the characteristic absorption bands associated with the NO<sub>2</sub> asymmetric and symmetric stretching modes are expected to be located in the frequency regions around 1650 - 1750 and 1300 cm<sup>-1</sup>, respectively; the C-O stretching mode around 950 - 1000 cm<sup>-1</sup>; and the NO<sub>2</sub> scissor mode around 800 - 850 cm<sup>-1</sup>. The IR peaks observed in Figure 3(C) at 1744, 1334, 924 and 791 cm<sup>-1</sup> are consistent with those of RONO<sub>2</sub>-type molecules. The three peaks at 1264, 1244 and 1151 cm<sup>-1</sup> are located in the frequency region of C-F stretches, similar to those observed for CF<sub>3</sub>NO,<sup>2</sup> CF<sub>3</sub>OH,<sup>4</sup> and CF<sub>3</sub>OONO<sub>2</sub>.<sup>5</sup> In addition, Niki and *et al.*<sup>6</sup> have reported that the NO<sub>2</sub> asymmetric stretching modes of RONO<sub>2</sub> type molecules are usually 20 to 60 cm<sup>-1</sup> lower than those of the corresponding ROONO<sub>2</sub> type molecules. The IR peak observed at 1744 cm<sup>-1</sup> is about 20 cm<sup>-1</sup> lower than the NO<sub>2</sub> asymmetric stretching mode of CF<sub>3</sub>OONO<sub>2</sub>, consistent with the present band assignment to CF<sub>3</sub>ONO<sub>2</sub>.

As described earlier, Hohorst and DesMarteau<sup>7</sup> observed CF<sub>2</sub>O and FNO<sub>2</sub> in the thermal decomposition of CF<sub>3</sub>OONO<sub>2</sub> at 22°C presumably via reaction (5). In their experiments, pure

CF<sub>3</sub>OONO<sub>2</sub> was used and NO was not present. The present results shown in Figures 3 and 4 suggest that the FNO<sub>2</sub> detected was formed as a minor product of the CF<sub>3</sub>O + NO<sub>2</sub> reaction rather than as the direct decomposition product of CF<sub>3</sub>OONO<sub>2</sub>. FNO<sub>2</sub> is reportedly stable at room temperature<sup>16,17</sup> and in the present study no decay of FNO<sub>2</sub> or CF<sub>3</sub>OONO<sub>2</sub> was observed during aging in the dark. Thus, the low yield of FNO<sub>2</sub> is not due to secondary reactions consuming FNO<sub>2</sub>. The rate constant ratio of  $k_7/(k_6 + k_7) = (0.1 \pm 0.02)$  can be estimated from the yield of CF<sub>2</sub>O per CF<sub>3</sub>NO consumed, assuming the identical yields of both CF<sub>2</sub>O and FNO<sub>2</sub> in these runs. Actually, the observed CF<sub>2</sub>O was produced via both reactions (7) and (8),<sup>2</sup> and the rate constant ratio of  $k_7/(k_6 + k_7)$  thus estimated should be considered as an upper limit.



Therefore, it is concluded that in the presence of 700 torr of air at least 90 per cent of the CF<sub>3</sub>O radicals are consumed via reaction (6) to yield CF<sub>3</sub>OONO<sub>2</sub>.

The above observations imply that CF<sub>3</sub>OONO<sub>2</sub> will, if formed, decay sufficiently rapidly back to CF<sub>3</sub>OO and NO<sub>2</sub> in the atmosphere. The CF<sub>3</sub>O + NO<sub>2</sub> reaction is a potentially important atmospheric reaction of the CF<sub>3</sub>O radicals. However, its kinetics as well as the atmospheric fate of the main product CF<sub>3</sub>OONO<sub>2</sub> remain to be determined.

#### ACKNOWLEDGMENT

We thank AFEAS, NSERC and British Gas/Consumers Gas for financial support. H. Niki is the holder of British Gas/Consumer Gas, NSERC and AES Industrial Research Chair in Atmospheric Chemistry. We thank C. J. Howard, O. J. Nielsen and R. Zellner for making preprints of their work available to us prior to publication.

## REFERENCES

- (1) Atkinson, R.; Cox, R.; Lesclaux, R.; Niki, H.; Zellner, R.; An assessment of Potential Degradation Products in the Gas-Phase Reactions of the Alternative Fluorocarbons in the Troposphere. World Meteorological Organization, Global Ozone Research and Monitoring Project; *AFEAS Report 20, 1991, Vol. II.*
- (2) Chen, J.; Zhu, T.; Niki, H.; *J. Phys. Chem.* **1992**, *96*, 6115.
- (3) Chen, J.; Zhu, T.; Mains, G.J.; Niki, H.; *Geophys. Res. Lett.* **1992**, *19*, 2215.
- (4) Chen, J.; Zhu, T.; Young, V.; Niki, H.; *J. Phys. Chem.* **1993**, (in press).
- (5) Niki, H.; Maker, P.D.; Savage, C.M.; Breitenbach, L.P.; *Chem. Phys. Lett.* **1979**, *61*, 100.
- (6) Niki, H.; Maker, P.D.; Savage, C.M.; Breitenbach, L.P.; *Chem. Phys. Lett.* **1978**, *55*, 289.
- (7) Hohorst, F.A.; DesMarteau, D.D.; *Inorg. Chem.* **1974**, *13*, 715.
- (8) Atkinson, R.; Baulch, D.L.; Cox, R.A.; Hampson, R.F.; Kerr, J.A.; Troe, J.; *J. Phys. Chem. Ref. Data* **1989**, *18*, 881.
- (9) Atkinson, R. *Atmos. Env.* **1990**, *24A*(1), 1.
- (10) Bevilacqua, T. J.; Hanson, D. R.; Howard, C. J.; *J. Phys. Chem.* **1993**, *97*, 350.
- (11) Zellner, R. private communication
- (12) J. Sehested and Nielsen, O.J; private communication
- (13) Niki, H.; Maker, P.D.; Savage, C.M.; Breitenbach, L.P.; *J. Mol. Struct.* **1980**, *59*, 1.
- (14) Koeppenkastrop, D.; Zabel, F.; *Int. J. Chem. Kinet.* **1991**, *23*, 1.
- (15) Bernitt, D.L.; Miller, R.H.; Hosatsune, I.C.; *Spectrochimica Acta*, **1967**, *23A*, 237.
- (16) Shimanouchi, T. *J. Phys. Chem. Ref. Data*, **1973**, *2*, 238.
- (17) Lee, T.J.; Rice, J.E.; *J. Chem. Phys.* **1992**, *97*, 4223.

**Table 1. Infrared Frequencies and Peak Intensities of CF<sub>3</sub>OONO<sub>2</sub>**

Assignment	Hohorst and DesMarteau <sup>(a)</sup>		This Work	
	Frequencies cm <sup>-1</sup>	Intensities	Frequencies/cm <sup>-1</sup>	Intensities <sup>(b)</sup>
NO <sub>2</sub> asym stretch	1760	vs	1764	1.7±0.6
NO <sub>2</sub> sym stretch	1292	vs	1296	1.5±0.5
CF <sub>3</sub> asym stretch	1244	vs	1243	2.8±0.9
CF <sub>3</sub> asym stretch	1186	vvs	1190	3.3±1.1
CO stretch	953	s	956	0.6±0.3
NO <sub>2</sub> scissor	783	vs	787	0.9±0.4

(a) Ref. 7

(b) Given in units of 10<sup>-3</sup> ppm<sup>-1</sup> m<sup>-1</sup> (base 10).

### FIGURE CAPTIONS

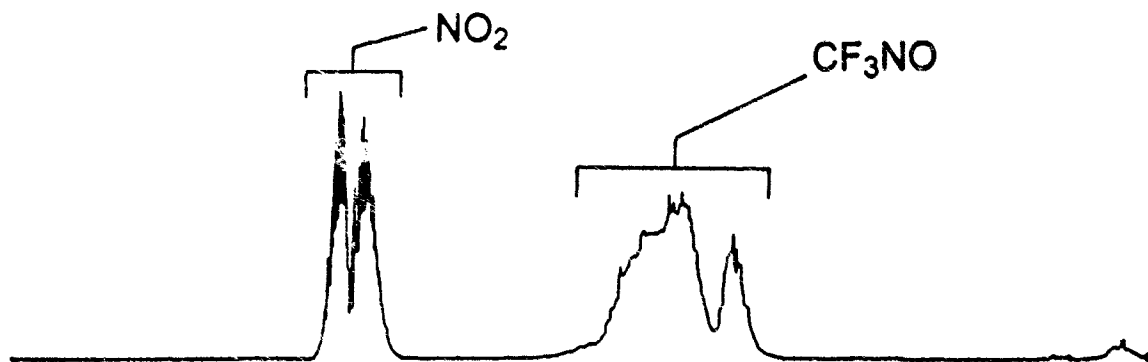
**Figure 1.** IR absorbance spectra in the frequency region  $650 - 2000 \text{ cm}^{-1}$  recorded in the photolysis of a mixture containing  $\text{CF}_3\text{NO}$  (3 ppm) and  $\text{NO}_2$  (4 ppm) in 700 torr of air. (A) before irradiation; (B) after 1 minute irradiation; (C) [(B) - (A)] scale expanded by  $\times 20$ .

**Figure 2.** Product spectra recorded at a longer irradiation of an identical mixture as in Figure 1. (A) after 3 minute irradiation; (B) difference spectrum [Fig. 2(A) - Fig. 1(A)] scale expanded by  $\times 10$ .

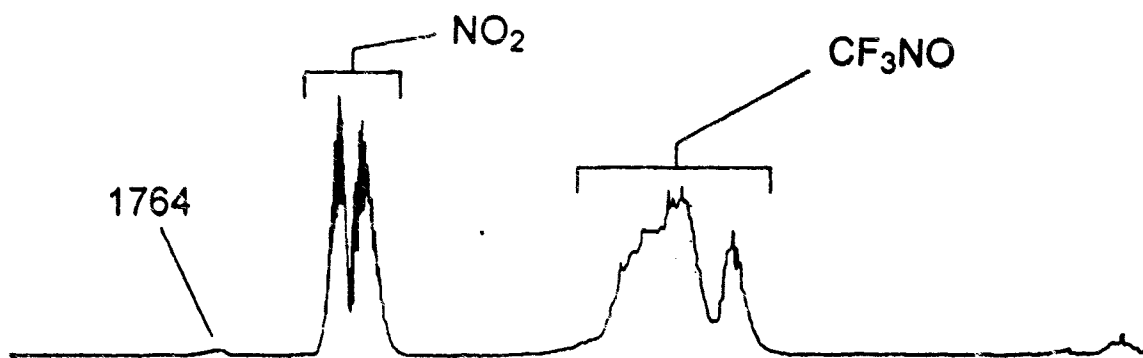
**Figure 3.** Spectral data obtained during dark aging of an irradiated mixture initially containing  $\text{CF}_3\text{NO}$  (3 ppm) and  $\text{NO}_2$  (4 ppm) in 700 torr of air. (A) after 3 minute irradiation and 10 min dark aging; (B) difference spectrum [Fig. 3(A) - Fig. 1(A)] scale expanded by  $\times 10$ .

**Figure 4.** IR absorbance spectra in the frequency region  $1700 - 2000 \text{ cm}^{-1}$  recorded in the photolysis of a mixture containing  $\text{CF}_3\text{NO}$  (9 ppm) and  $\text{NO}_2$  (9 ppm) in 700 torr of air. (A) after 1 minute irradiation; (B) after 10 minute dark aging; (C) after adding  $\text{NO}$  (1 ppm).

(A) Before irradiation



(B) After 1 min irradiation



(C) [(B) - (A)]  $\times 20$

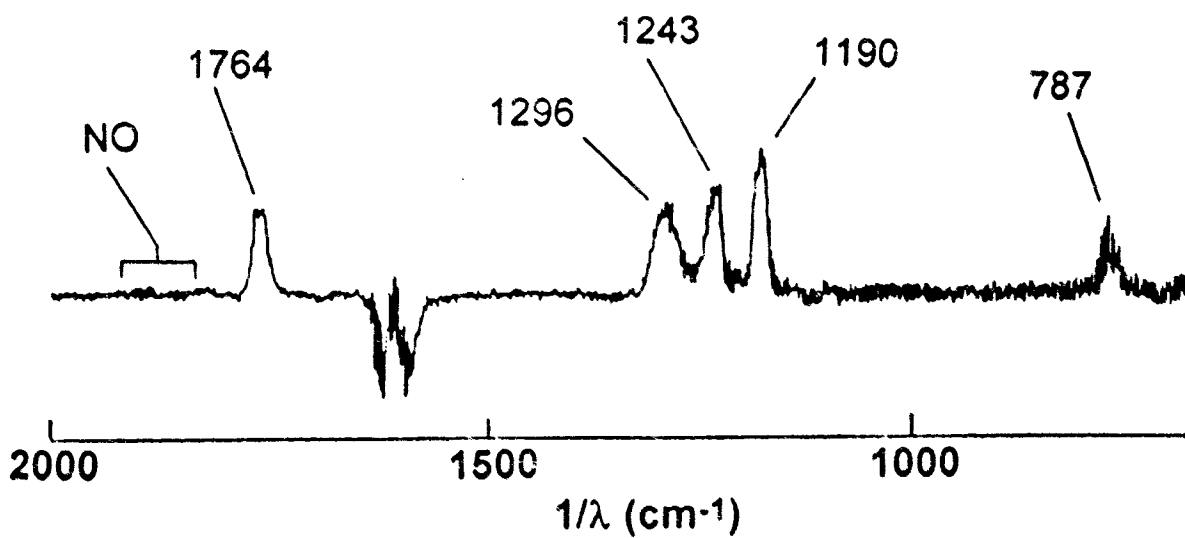
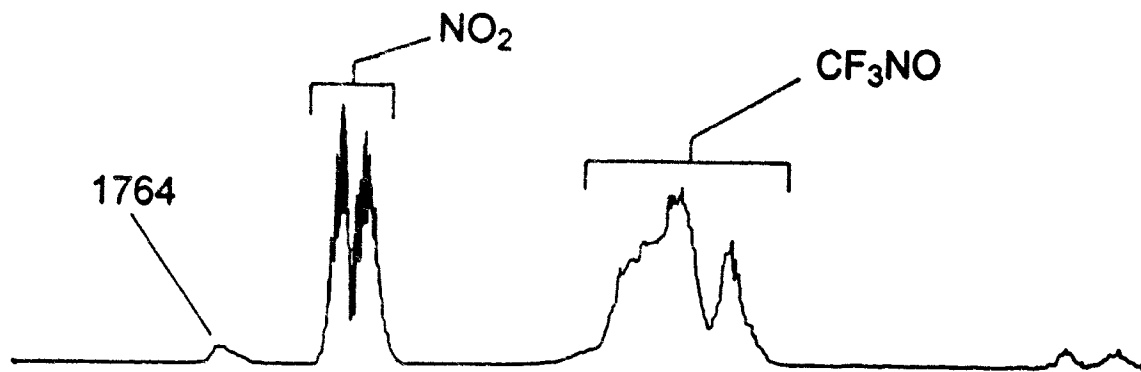


Figure 1

0179

(A) After 3 min irradiation



(B) [Fig.2(A) - Fig.1(A)]  $\times 10$

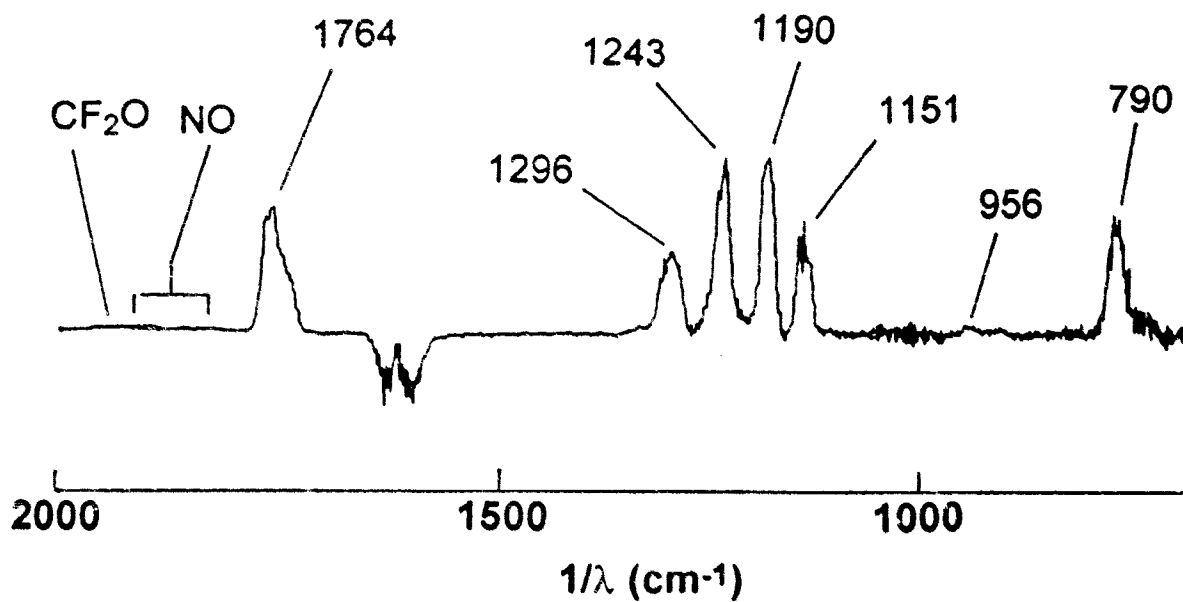
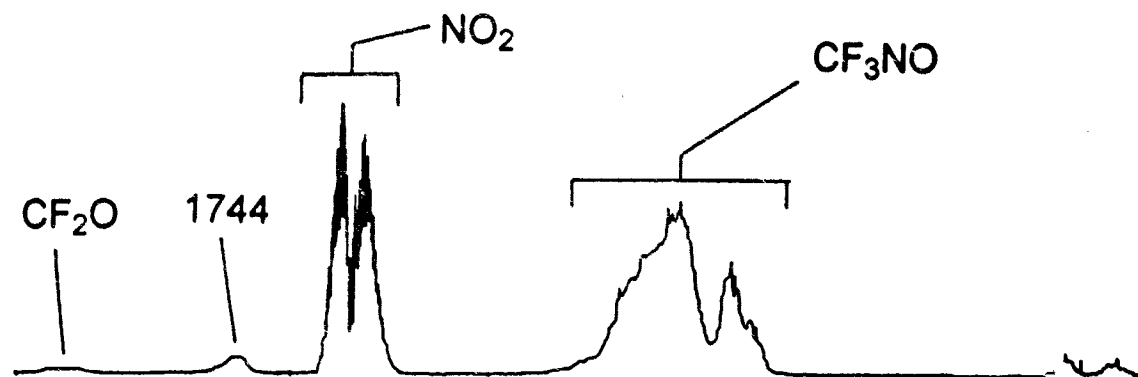


Figure 2

(A) After 3 min irradiation and 10 min dark aging



(B) [Fig.3(A) - Fig.1(A)]  $\times 10$

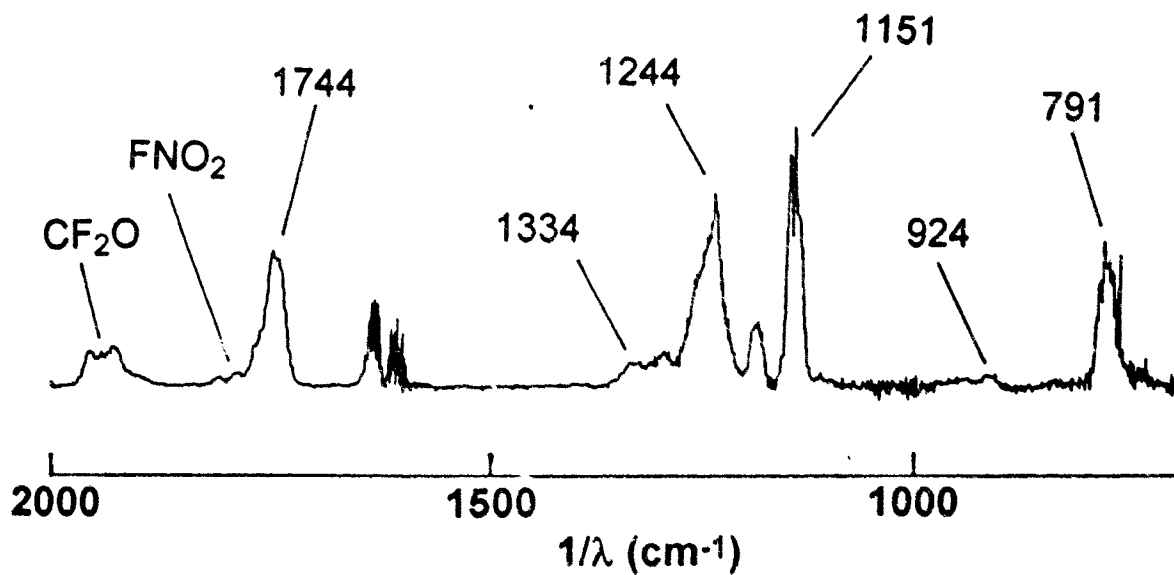
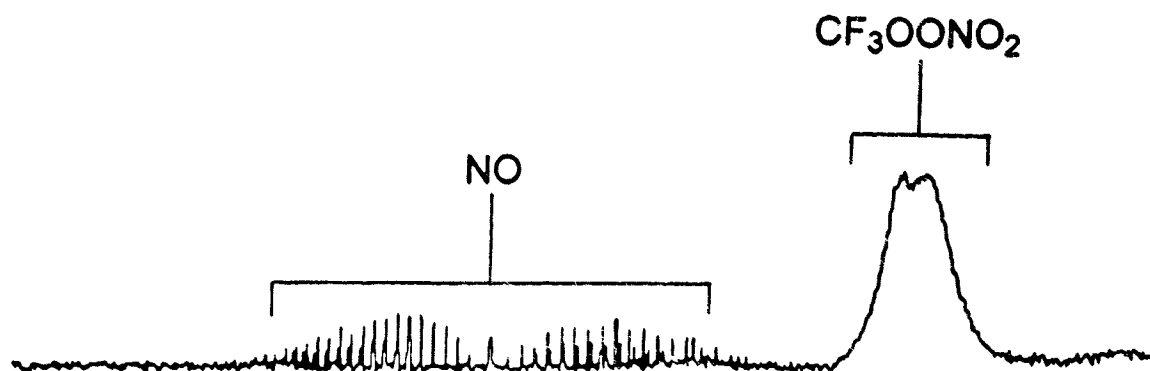
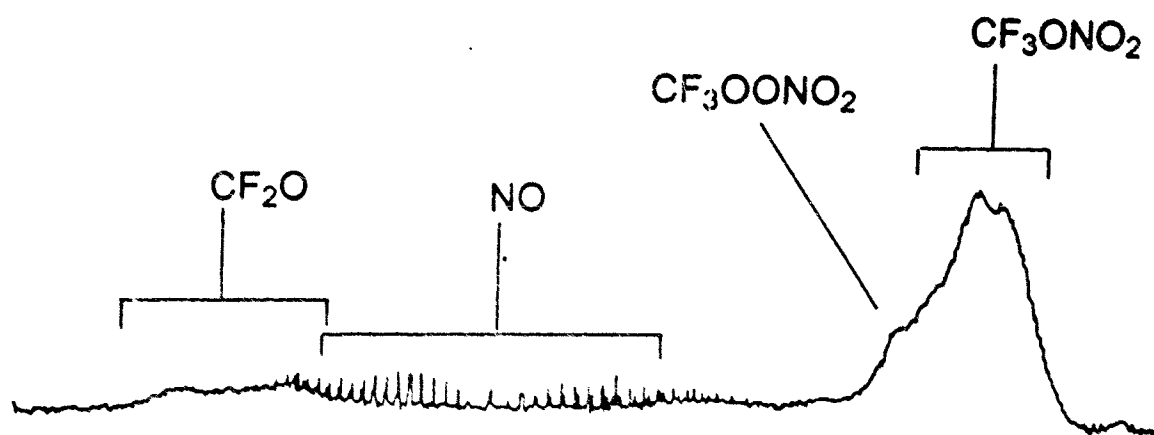


Figure 3

(A) After 1 min irradiation



(B) After 10 min dark aging



(C) After adding 1 ppm of NO

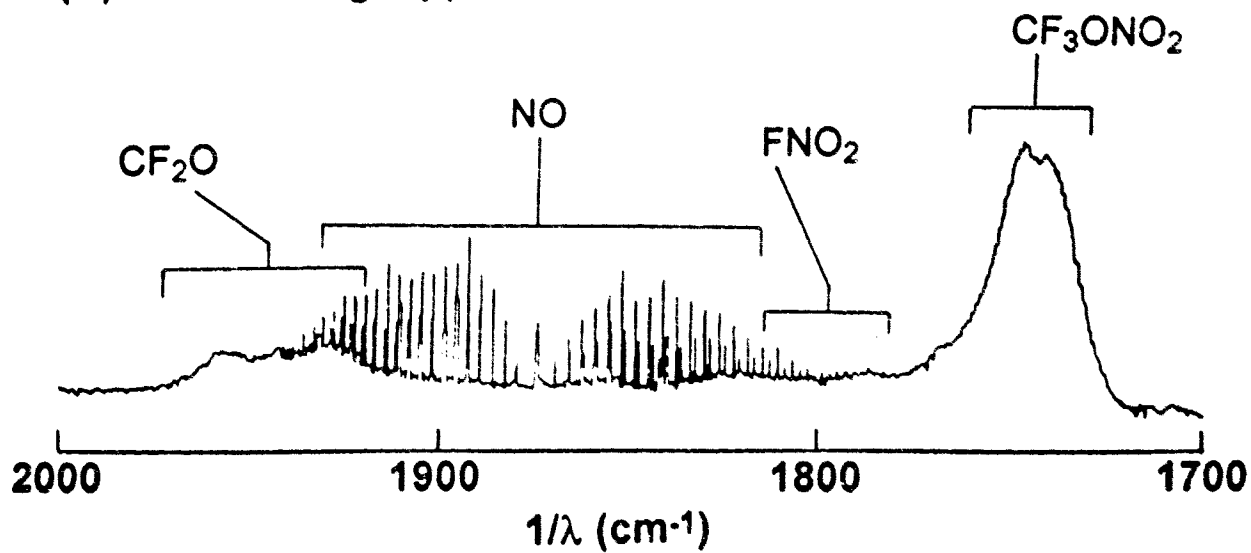


Figure 4

Studies of the atmospheric oxidation mechanisms of some CFC replacement compounds

T.J. Bevilacqua\*, D.R. Hanson\*\*, N.R. Jensen<sup>±</sup>, and C.J. Howard

NOAA, Aeronomy Laboratory, 325 Broadway, Boulder, CO 80303 USA

\* NOAA-NRC Postdoctoral Research Associate

\*\* NOAA-CIRES Postdoctoral Research Associate

± Danish Natural Science Research Council Postdoctoral Research Associate

### I. Introduction

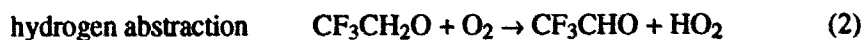
This paper is a brief report on the studies we have made of the atmospheric oxidation of the CFC replacement compounds. Due to the space limitations, we do not cite the contributions of other workers, many of whom are at this workshop, but describe only our own results and studies. The complete details are given in our journal publications. In an earlier paper, Dr. Schmoltner [1] reported on studies in our group of the primary processes that define the atmospheric lifetimes of some CFC replacements. In the present paper, we will focus on the subsequent processes that describe the degradation of these molecules. Here we are interested in the processes that account for breaking of the C-C, C-H, and C-X (where X is a halogen atom) bonds. We are seeking to identify intermediates formed in the oxidation process with special emphasis on the possible existence of stable species, which could have some environmental effects. Chapter VI of the AFEAS Report [2] gives several excellent reviews of the processes we are studying. Some of the studies reported here are being published elsewhere [3].

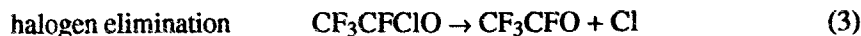
Our approach in these studies is to detect the reactants and products using chemical ionization mass spectrometry (CIMS) in a flow tube reactor. Thus we measure the rate coefficients of the elementary reactions. A key reaction involved in the breaking of many bonds involves the formation of an alkoxy radical. The driving force for the decomposition of this radical is the elimination of one functional group attached to the  $\alpha$  carbon and the formation of a carbonyl bond.

The oxidation process begins with the formation of an alkyl radical, typically by the abstraction of hydrogen from an HFC or HCFC molecule. The resulting alkyl radical rapidly adds molecular oxygen in the atmosphere. The alkylperoxy radical product of this reaction can undergo several different processes, one of which is reaction with nitric oxide:



The product alkoxy radical has three possible routes for decomposition depending upon what functional groups are bonded to the alkoxy  $\alpha$  carbon:





The latter two processes may occur spontaneously or involve activation through collisions with bath gas molecules.

## II. Experimental Methods

A sketch of the CIMS apparatus [4] is shown in Figure 1. It consists of two separate but connected flow tube reactors. The upper one is a typical radical flow tube reactor [5] and the lower one is a flowing afterglow (ion-neutral) reactor [6]. The basic idea is that we detect the trace neutral species from the radical flow tube as ions formed by means of an ion-neutral reaction in the flowing afterglow. The gas flow from the neutral reactor enters the ion reactor downstream of the electron impact ion source. The neutral reactor flow comprises about 10% of the total gas flow in the ion reactor. The ion products are sampled, mass analyzed, and detected in the chambers to the left of the flowing afterglow. The intensity of the ion signal is proportional to the concentration of the associated neutral species.

The important features of CIMS detection include the following: (i) Ion-neutral reactions are usually fast,  $k \approx 10^{-9}$  to  $10^{-10}$   $\text{cm}^3 \text{ molecule}^{-1} \text{ s}^{-1}$  and therefore efficient. (ii) Radicals are readily ionized because they tend to have low ionization potentials and high electron affinities. (iii) The ionization process can be designed to minimize fragmentation and to selectively ionize a species. (iv) Once a species is ionized, the ion is easy to detect at very low concentrations, e.g., as low as 1 to 10 ions  $\text{cm}^{-3}$ . This translates to a detection limit in the range  $10^8$  to  $10^{10}$   $\text{molecule cm}^{-3}$  for species in the neutral flow tube reactor. This technique also has some significant disadvantages. At the present time, our system operates only at low pressures, less than about 8 Torr. This limits how closely we can simulate the true conditions of the atmosphere. A second disadvantage is that our CIMS detector must be used with a flow tube reactor. Thus one must be cautious about possible surface reactions.

Either positive or negative ions can be used to ionize trace species. In our studies of the CFC replacement compounds, we have found  $\text{SF}_6^-$  to be a very versatile reagent ion. For example, in studies of the  $\text{CF}_3$  radical oxidation:



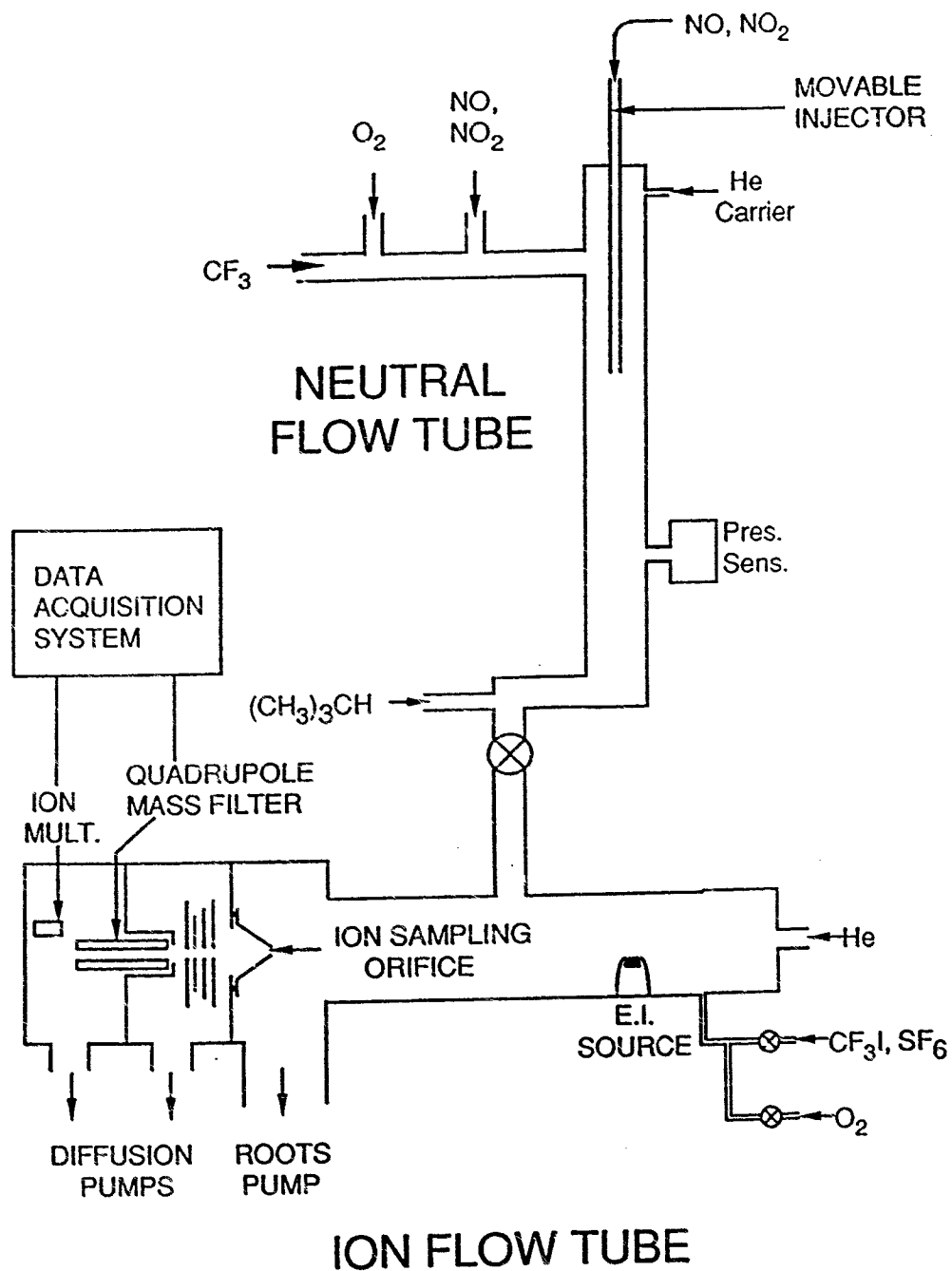
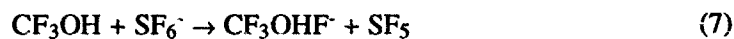


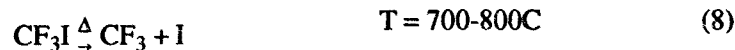
Figure 1. Sketch of chemical ionization mass spectrometer and flow tube reactor

0185



where (5) and (6) are simple charge transfer reactions and (7) is a fluoride ion transfer reactions. We have found the detection of haloalkylperoxy radicals via (5) to be a very effective general method.

Pyrolysis is the preferred method of generating radicals for the flow tube reactor. Trifluoromethyl iodide is a convenient source of  $\text{CF}_3$ :



Alternatively, we have used hydrogen atom abstraction using fluorine atoms to prepare fluoroalkyl radicals:

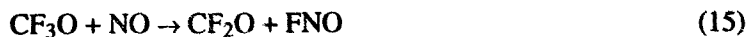


where the fluorine atoms are produced in a microwave discharge using a  $\text{CF}_4/\text{He}$  mixture.

The haloalkylperoxy radicals are generated in the sidearm reactor at the top of the neutral flow tube. For example, for  $\text{CF}_3\text{OO}$ :



where  $k_{10} \approx 10^{-12} \text{ cm}^3 \text{ molecule}^{-1} \text{ s}^{-1}$  at 298 K and 2 Torr. We have expended considerable effort trying to develop a clean source of  $\text{CF}_3\text{O}$  radicals, but have not as yet succeeded. Some of the schemes we have tested include the following:



Reaction (11a) is highly exothermic and the hot  $\text{CF}_3\text{O}$  product dissociates according to (11b). Reaction (12) is fast  $k \approx (1 \pm 0.7) \times 10^{-11}$  but it appears to proceed via an addition mechanism,

wherein the intermediate undergoes a four-center elimination to give  $\text{CF}_2\text{O}$  and  $\text{FNO}$  as the major products. Reaction (13) is too slow to be observed in our reactor  $k_{13} \leq 10^{-14} \text{ cm}^3 \text{ molecule}^{-1} \text{ s}^{-1}$ . Reaction (14) suffers from the complication that the  $\text{CF}_3\text{O}$  product is highly reactive toward the  $\text{NO}$  precursor as detailed in the next section.

All measurements were made at room temperature,  $297 \pm 2 \text{ K}$  unless noted otherwise.

### III. Results

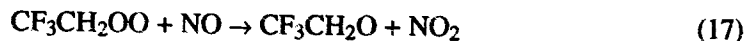
Our initial studies focused on the oxidation of the  $\text{CF}_3$  radical. The  $\text{CF}_3\text{OO}$  radical reacts with  $\text{NO}$  with a rate coefficient  $k_{14} = (1.53 \pm 0.2) \times 10^{-11} \text{ cm}^3 \text{ molecule}^{-1} \text{ s}^{-1}$  at  $297 \text{ K}$ . The product  $\text{CF}_3\text{O}$  radical is also very reactive toward  $\text{NO}$ ,  $k_{15} = (2 \pm 1) \times 10^{-11}$ . During the course of these studies using  $\text{SF}_6^-$  as a reagent ion, we observed an ion at  $105 \text{ amu}$ , which was identified as  $\text{CF}_3\text{OHF}^-$  formed via reaction (7). The source of  $\text{CF}_3\text{OH}$  was traced to the reaction of  $\text{CF}_3\text{O}$  with organic material in the neutral reactor. Cleaning the reactor surface by exposure to discharged oxygen ( $\text{O} + \text{O}_2$ ) reduced the production of  $\text{CF}_3\text{OH}$  from  $\text{CF}_3\text{O}$ .

The reactions of  $\text{CF}_3\text{O}$  with two hydrocarbons were studied. Since we did not have a clean source of  $\text{CF}_3\text{O}$ , the rate coefficients are only crudely determined.

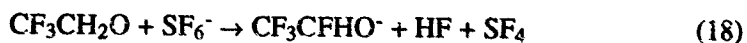


For  $\text{RH} = \text{CH}_4$ ,  $k = (3 \pm 2) \times 10^{-14}$ , and for  $\text{RH} = \text{isobutane}$ ,  $k = (5 \pm 3) \times 10^{-12} \text{ cm}^3 \text{ molecule}^{-1} \text{ s}^{-1}$ . The  $\text{CF}_3\text{OH}$  product was found to be quite stable, no decomposition was detected in  $2 \text{ Torr He}$ , when the reactor was heated to about  $130 \text{ C}$ . The residence time was only about  $50 \text{ ms}$  in the heated region.

A series of three different HFC radicals were investigated to examine the effects of fluorine substitution on the reactivity of the alkylperoxy radicals with  $\text{NO}$  and the decomposition routes of the alkoxy radical. For the reaction of  $\text{CF}_3\text{CH}_2\text{OO}$  with  $\text{NO}$ :



$k_{17} = (1.3 \pm 0.3) \times 10^{-11}$ . Although the  $\text{NO}_2$  product was detected, the  $\text{CF}_3\text{CH}_2\text{O}$  product was not observed with  $\text{SF}_6^-$  reagent ions. An ion corresponding to  $\text{CF}_3\text{CFHO}^-$  was observed, but this is likely to be due to a complex ion-neutral reaction such as:



The reaction of the  $\text{CF}_3\text{CH}_2\text{O}$  product with  $\text{O}_2$  could not be detected



in the presence of about  $3 \times 10^{15} \text{ O}_2 \text{ cm}^{-3}$ . This is not too surprising as alkoxy radical reactions with  $\text{O}_2$  are characteristically rather slow reactions.

The rate coefficients for the reaction of  $\text{CF}_3\text{CFHOO}$  with  $\text{NO}$  was also measured



$k_{20} = (1.3 \pm 0.3) \times 10^{-11}$ . The  $\text{NO}_2$  product was detected but the  $\text{C}_2$  product was not observed. The fragments  $\text{CF}_3\text{OO}$ ,  $\text{CF}_3\text{O}$ , and  $\text{CF}_2\text{O}$  were detected, indicating rapid decomposition of the  $\text{CF}_3\text{CFHO}$  radical.



Here the  $\text{CF}_3$  had undergone reactions (10), (14), and (15) with the excess  $\text{O}_2$  and  $\text{NO}$  in the flow tube to account for the product fragments observed.

Finally, the rate coefficient for the reaction of the  $\text{CF}_3\text{CF}_2\text{OO}$  radical with  $\text{NO}$  was measured.



$k_{22} = (1.6 \pm 0.3) \times 10^{-11}$ . The major products observed were  $\text{NO}_2$  and the fragments  $\text{CF}_3\text{OO}$ ,  $\text{CF}_3\text{O}$ , and  $\text{CF}_2\text{O}$ . Some  $\text{CF}_3\text{CF}_2\text{O}^\cdot$  and  $\text{CF}_3\text{CF}_2\text{OH}^\cdot$  were observed also, indicating that the alkoxy radical is somewhat stable and reactive toward organic material, much the same as the  $\text{CF}_3\text{O}$  radical. Breaking the C-C bond in  $\text{CF}_3\text{CF}_2\text{O}$  is expected to be a major decomposition route in the atmosphere as observed in our measurements.



#### IV. Discussion and Future Studies

The reactivity of all of the haloalkylperoxy radicals toward  $\text{NO}$  is high with rate coefficients in the range  $(1.2 \text{ to } 1.6) \times 10^{-11} \text{ cm}^3 \text{ molecule}^{-1} \text{ s}^{-1}$  at room temperature for the few species studied here. By analogy to other peroxy radicals, these reactions probably exhibit small negative temperature coefficients. The products observed in our studies at low pressure are alkoxy radicals and  $\text{NO}_2$  and in the case of the highly fluorinated radicals some C-C bond decomposition products were also found. At higher pressures such as is found in the troposphere, the possibility exists for an "Atkinson" [7] reaction, i.e.,



forming an alkyl nitrate. These nitrate molecules can have atmospheric lifetimes of the order of weeks to months. In regions of low NO, the RO<sub>2</sub> can react with HO<sub>2</sub> forming ROOH:



so these reactions should be investigated. Also the cross reactions of various different RO<sub>2</sub> species should be studied, as these reactions will also occur in low NO regions and can generate a variety of different products.

Our studies of the chemistry of the alkoxy radicals leaves many uncertainties. The failure to develop a clean source of CF<sub>3</sub>O has been a limitation to our studies of this interesting radical. The CF<sub>3</sub>O reactions with O<sub>3</sub>, CO, organic molecules, and NO<sub>2</sub> should be investigated. The fate of CF<sub>3</sub>OH, which we observed as a product of the CF<sub>3</sub>O reaction with organic molecules also must be investigated.

Finally, the fate of other C<sub>2</sub> alkoxy radicals must be studied further. The competition between α-hydrogen abstraction and C-C bond breaking is particularly important, notably for the CF<sub>3</sub>CFHO radical formed in the atmospheric oxidation of HFC 134a. We must develop a CIMS detection scheme for observing aldehyde products.

Acknowledgements. We are grateful for funding by The Alternative Fluorocarbons Environmental Acceptability Study (AFEAS) under contract no. CTR90-17/P90-006 to the NOAA-Environmental Research Laboratories/Aeronomy Laboratory and by NOAA under the Climate and Global Change Program.

- [1] Schmoltner, A.M., Talukdar, R.K., Warren, R.F., Mellouki, A., Goldfarb, L., Gierczak, T., McKeen, S.A., and Ravishankara, A.R., The third paper of these proceedings.
- [2] Scientific Assessment of Stratospheric Ozone: 1989, Volume II, Appendix: AFEAS Report, World Meteorological Organization, Global Ozone Research and Monitoring Project - Report No. 20.
- [3] Bevilacqua, T.J., Hanson, D.R., and Howard, C.J., *J. Phys. Chem.* **97** (1993) 3750.
- [4] Gleason, J.F., Sinha, A., and Howard, C.J., *J. Phys. Chem.* **91** (1987) 719.
- [5] Howard, C.J., *J. Phys. Chem.* **83** (1979) 3.
- [6] Ferguson, E.E., Fehsenfeld, F.C., and Schmeltekopf, A.L., *Adv. Atomic Molec. Phys.* **5** (1969) 1.
- [7] Atkinson, R., Aschmann, S.M., and Winer, A.M., *J. Atm. Chem.* **5** (1987) 91.

0 1 8 9

# ATMOSPHERIC CHEMISTRY OF CF<sub>3</sub>O RADICALS: REACTION WITH H<sub>2</sub>O.

Timothy J. Wallington, Michael D. Hurley, William F. Schneider  
Ford Research Laboratory, SRL-3083  
Ford Motor Company  
Dearborn, P. O. Box 2053  
Michigan 48121-2053, USA

Jens Sehested and Ole John Nielsen  
Section for Chemical Reactivity  
Environmental Science and Technology Department  
Risø National Laboratory  
DK-4000 Roskilde, Denmark

## Introduction

CF<sub>3</sub>O radicals are produced during the oxidation of HFC-134a, HFC-125 and HFC-23. The atmospheric fate of CF<sub>3</sub>O radicals is uncertain and the subject of a significant current research effort. Recently, it has been shown that CF<sub>3</sub>O radicals react with NO[1,2] and organic compounds[2,3,4]. To the best of our knowledge, the reaction of CF<sub>3</sub>O with H<sub>2</sub>O has not been considered as an atmospheric loss mechanism for CF<sub>3</sub>O radicals. We report herein a brief overview of results from a computational and experimental study of reaction (1). Further details are reported elsewhere[5].



## Experimental Details

The reaction chamber/FT-IR spectrometer system has been described previously[6]. White type multiple reflection optics were mounted in the reaction chamber to provide a total path length of 26.6 m for the IR analysis beam. The spectrometer was operated at a resolution of 0.25 cm<sup>-1</sup>. Infrared spectra were derived from 32 co-added interferograms.

CF<sub>3</sub>O radicals were generated by the chlorine-initiated oxidation of HFC-134a[4]. Chlorine atoms were generated by the photolysis of molecular chlorine using the output of 22 UV fluorescent lamps (GTE F40BLB). Initial concentrations used were: HFC-134a, 10-1040 mTorr; Cl<sub>2</sub>, 296-447 mTorr; and H<sub>2</sub>O, 0-916 mTorr. In all experiments, ultra pure air was used as diluent at a total pressure of 700 Torr. The temperature was 296±2K.

Products were quantified by fitting reference spectra of the pure compounds to the observed product spectra using integrated absorption features. Reference spectra were obtained by expanding known volumes of the reference material into the long pathlength cell.

The procedure was as follows. HFC-134a was first quantified and subtracted from the product spectra using characteristic absorption features over the wavelength region 800-1500 cm<sup>-1</sup>. HC(O)F, CF<sub>3</sub>COF, COF<sub>2</sub>, CF<sub>3</sub>O<sub>2</sub>CF<sub>3</sub>, and CF<sub>3</sub>OH were then identified and quantified using features over the following wavelength ranges: 1700-1900, 1000-1200 and 1800-2000, 700-800 and 1800-2000, 700-900 and 1100-1400, and 3600-3700 cm<sup>-1</sup> respectively.

## Computational Details

All calculations were performed with the Gaussian 88 program and employed standard basis sets[7]. The structures of all molecules were obtained by gradient optimization at the MP2/6-31G(d,p) level (unrestricted MP2 for the radicals). Using the MP2/6-31G(d,p) geometries, single point energies were evaluated at the UMP4/6-311+G(d,p) level, keeping the core orbitals frozen in the perturbation calculation.

0 1 9 8

The resultant total energies for these molecules has been reported elsewhere [11]. The force constant matrices and harmonic vibrational frequencies for all molecules were obtained by numerical differentiation of the analytical MP2/6-31G(d,p) gradients. The vibrational frequencies were used unscaled to obtain zero point vibrational energies. Internal translational, rotational, and vibrational energy corrections to 298.15 K were calculated using standard statistical mechanical methods[8,9]. The low frequency torsions in the two alcohol molecules, along with the umbrella mode of methyl radical, were treated as free rotations and thus contributed RT/2 to the internal energy. While inclusion of zero point energies has a substantial (up to 3 kcal/mol) effect on the calculated reaction heats, the thermal corrections have a fairly minor impact (< 0.5 kcal/mol) on our final results.

### Experimental Results

Experimental results are given in Table I. The first experiment involved the UV irradiation of a mixture of 1.04 Torr of HFC-134a and 300 mTorr of Cl<sub>2</sub> in 700 Torr of air diluent with, and without, the addition of 460 mTorr of H<sub>2</sub>O. The observed products were CF<sub>3</sub>COF, COF<sub>2</sub>, CF<sub>3</sub>O<sub>3</sub>CF<sub>3</sub>, HC(O)F and CF<sub>3</sub>OH. When reaction mixtures were allowed to stand in the dark the CF<sub>3</sub>OH was observed to decay rapidly to give COF<sub>2</sub>. The decay is attributed to heterogeneous decomposition on the reactor walls[4].



The addition of 460 mTorr of H<sub>2</sub>O to a reaction mixture containing approximately 1 Torr of HFC-134a caused no observable change in the products when the mixtures are irradiated. The CF<sub>3</sub>OH formation changed by <10%. CF<sub>3</sub>OH is produced from the reaction of CF<sub>3</sub>O radicals with HFC-134a[4]. Reaction (3) competes with reaction (4) for the available CF<sub>3</sub>O radicals.



In terms of a sink for CF<sub>3</sub>O radicals, 460 mTorr of H<sub>2</sub>O is less than 10% as effective as 1030 mTorr of HFC-134a. As  $k_3 < 1.8 \times 10^{-15} \text{ cm}^3 \text{ molecule}^{-1} \text{ s}^{-1}$ [4], then  $k_4 < 4 \times 10^{-16} \text{ cm}^3 \text{ molecule}^{-1} \text{ s}^{-1}$ .

Further investigation of the kinetics of reaction (1) requires use of larger values of the [H<sub>2</sub>O]/[HFC-134a] concentration ratio. The ratio [H<sub>2</sub>O]/[HFC-134a] was increased by decreasing [HFC-134a] to 9.9-24.1 mTorr. With such low initial concentrations the expected yields of CF<sub>3</sub>OH are close to, or below, the detection limit of approximately 1 mTorr, which precludes direct measurement of the CF<sub>3</sub>OH yield. Instead, the formation of CF<sub>3</sub>OH was measured indirectly by observing the yield of COF<sub>2</sub> formed after reaction mixtures were left to stand for 10 minutes in the dark. As discussed above, CF<sub>3</sub>OH rapidly decomposes into COF<sub>2</sub> in the reaction chamber. The detection limit of COF<sub>2</sub> was 0.02 mTorr. For experiments using low [HFC-134], the yields of HC(O)F and CF<sub>3</sub>COF were, within the experimental uncertainties, unaffected by the presence of H<sub>2</sub>O. In contrast, the yield of COF<sub>2</sub> increased significantly with increased [H<sub>2</sub>O]. Conversely, the measured CF<sub>3</sub>O<sub>3</sub>CF<sub>3</sub> yield decreased with increased [H<sub>2</sub>O]. This observation is consistent with a competition between reactions (1) and (4) for the available CF<sub>3</sub>O radicals.

To illustrate these observations, Figures 1A and 1B show spectra acquired before and after irradiation of a mixture of 9.9 mTorr of HFC-134a and 438 mTorr of Cl<sub>2</sub> in 700 Torr of air. Figures 1D and 1E show spectra taken before and after irradiation of a similar mixture but with 916 mTorr of H<sub>2</sub>O added. The yield of COF<sub>2</sub> is significantly larger in the presence of H<sub>2</sub>O.

The ratio of the COF<sub>2</sub> yield in the presence of H<sub>2</sub>O to that observed in the absence of H<sub>2</sub>O is plotted as a function of the concentration ratio [H<sub>2</sub>O]/[HFC-134a] in Figure 2. The solid line is a linear least squares fit forced through a y axis intercept of unity. Assuming that (i) COF<sub>2</sub> is formed solely from the decomposition of CF<sub>3</sub>OH, (ii) reactions (1) and (3) are the only sources of CF<sub>3</sub>OH, and (iii) formation of CF<sub>3</sub>OH is a relatively minor fate of CF<sub>3</sub>O radicals (i.e. there are CF<sub>3</sub>O radicals available which can be diverted by reaction with H<sub>2</sub>O to give CF<sub>3</sub>OH), then the following expression holds:

$$Y(\text{COF}_2)_{\text{H}_2\text{O}}/Y(\text{COF}_2) = 1 + (k_1/k_3) \times ([\text{H}_2\text{O}]/[\text{HFC-134a}])$$

$Y(\text{COF}_2)_{\text{H}_2\text{O}}$  is the molar yield of  $\text{COF}_2$  observed when  $\text{H}_2\text{O}$  is present,  $Y(\text{COF}_2)$  is the corresponding yield when  $\text{H}_2\text{O}$  is absent, and  $k_1/k_3$  is the ratio of the rate constants for reactions (1) and (3). Linear least squares analysis of the data in Figure 2 gives  $k_1/k_3 = (5.4 \pm 1.3) \times 10^{-3}$ . The quoted error represents 2 standard deviations.

### Discussion of Experimental Results

The observed product yields given in Table I can be compared to those expected based upon recent studies of the Cl atom initiated oxidation of HFC-134a in our laboratory[4]. Details concerning this comparison are given elsewhere[5] and are not discussed here. The literature chemical mechanism for the Cl atom initiated oxidation of HFC-134a[4] adequately simulates the product yields results given in Table I for experiments using initial [HFC-134a] of 1 Torr. However, the mechanism grossly underpredicts the  $\text{COF}_2$  yield for experiments where low initial [HFC-134a] was used. It was concluded that additional reactions that form either  $\text{CF}_3\text{OH}$ , or  $\text{COF}_2$ , or both, are missing from the chemical mechanism used in the simulations. Uncertainties remain in our understanding of the mechanism(s) by which  $\text{COF}_2$  is formed in experiments employing low HFC-134a concentrations.

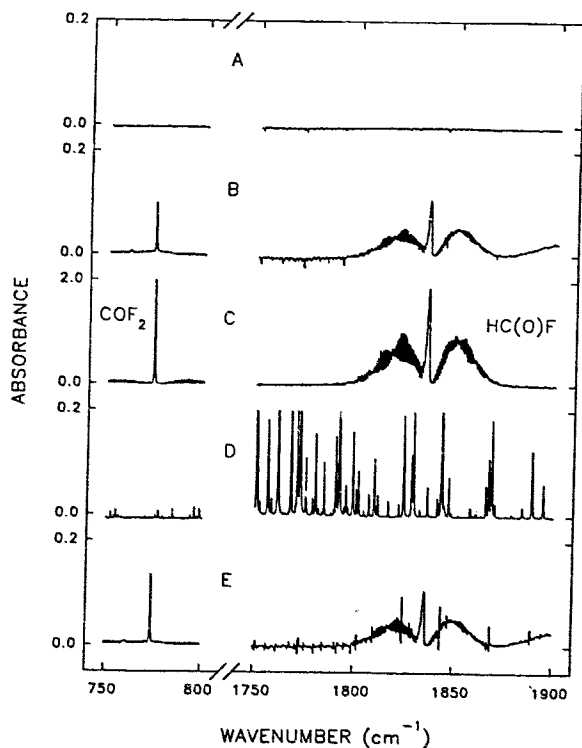


Figure 1: Spectra taken before (A) and after (B) 180 seconds irradiation of a mixture of 9.9 mTorr of HFC-134a, 438 mTorr of  $\text{Cl}_2$ , in 700 Torr of air diluent. Reference spectra of  $\text{HC(O)F}$  and  $\text{COF}_2$  are given in panel 1C. Spectra (D) and (E) were acquired before and after 180 seconds irradiation of a mixture of 10.1 mTorr of HFC-134a, 444 mTorr of  $\text{Cl}_2$ , and 916 mTorr of  $\text{H}_2\text{O}$ . The  $\text{H}_2\text{O}$  features in panel E have been subtracted for clarity.

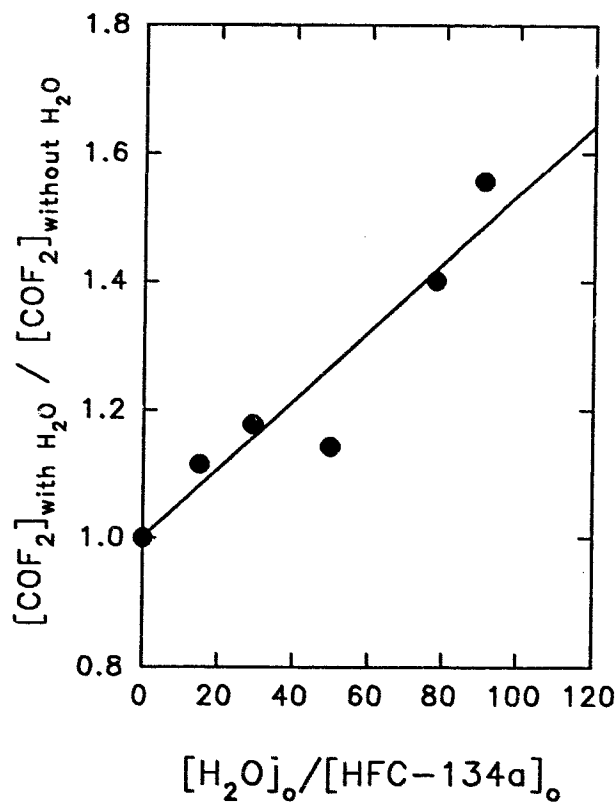


Figure 2: Ratio of  $\text{COF}_2$  yield observed in the presence of  $\text{H}_2\text{O}$  to that observed in the absence of  $\text{H}_2\text{O}$  versus  $[\text{H}_2\text{O}]_0/[\text{HFC-134a}]_0$ . See text for details.

Table I: Product yields<sup>a</sup> following the irradiation of HFC-134a/Cl<sub>2</sub>/H<sub>2</sub>O mixtures in 700 Torr of air.

Expt.	[HFC-134a] <sub>0</sub>	[Cl <sub>2</sub> ] <sub>0</sub>	[H <sub>2</sub> O] <sub>0</sub>	t <sub>irr</sub> (s)	Δ[HFC-134a]	Δ[HC(O)F]	Δ[CF <sub>3</sub> COF]	Δ[CF <sub>3</sub> O <sub>2</sub> CF <sub>3</sub> ]	Δ[COF <sub>2</sub> ]	Δ[CF <sub>3</sub> OH]
1	1040	296	0	75 <sup>b</sup>	na	11.1	3.3	3.9	1.0	2.4
2	1030	296	460	75 <sup>b</sup>	na	35.7	10.2	9.7	9.6	4.3
				240 <sup>b</sup>	na	10.6	3.0	2.4	0.9	2.1
3	9.9	438	0	180 <sup>c</sup>	na	35.7	10.2	10.2	9.7	4.0
4	10.1	444	502	180 <sup>c</sup>	2.28	1.38	0.51	0.58	0.47	
5	10.1	444	786	180 <sup>c</sup>	2.42	(61%) <sup>d</sup>	(22%)	(25%)	(21%)	
6	10.1	444	916	180 <sup>c</sup>	2.32	1.39	0.49	0.53	0.57	
7	23.8	444	0	180 <sup>c</sup>	2.12	(57%)	(20%)	(22%)	(24%)	
8	23.8	444	358	180 <sup>c</sup>	4.76	1.35	0.51	0.50	0.67	
9	24.1	447	0	300 <sup>c</sup>	7.23	(58%)	(22%)	(22%)	(29%)	
10	24.1	447	706	300 <sup>c</sup>	7.23	1.46	0.45	0.39	0.68	
						(69%)	(21%)	(18%)	(32%)	
						2.83	0.96	1.21	0.85	
						(59%)	(20%)	(25%)	(18%)	
						2.77	0.95	0.81	0.90	
						(61%)	(21%)	(18%)	(20%)	
						3.94	1.56	1.69	1.24	
						(55%)	(22%)	(23%)	(17%)	
						3.94	1.50	1.59	1.46	
						(55%)	(21%)	(22%)	(20%)	

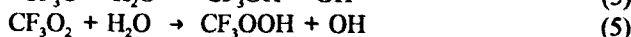
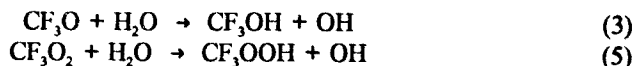
a: Observed concentrations in units of mTorr, with no corrections of any kind applied to data.

b: Irradiation time, analysis performed immediately after irradiation.

c: Irradiation time, analysis performed after reaction mixture sat in dark for 10 minutes to allow complete decomposition of CF<sub>3</sub>OH into COF<sub>2</sub>.

d: Values in parentheses are molar yields relative to HFC-134a loss.

The addition of H<sub>2</sub>O to reaction mixtures containing low initial HFC-134a concentrations leads to an increase in the yield of COF<sub>2</sub> and a decrease in that of CF<sub>3</sub>O<sub>2</sub>CF<sub>3</sub>. In contrast, the observed yields of HC(O)F and CF<sub>3</sub>COF were unchanged. The presence of H<sub>2</sub>O perturbs the chemistry associated with CF<sub>3</sub>O and/or CF<sub>3</sub>O<sub>2</sub> radicals. Two possibilities exist,



with the products, CF<sub>3</sub>OH or CF<sub>3</sub>OOH, decomposing to give COF<sub>2</sub>.

To check on the behavior of CF<sub>3</sub>OOH in the chamber a sample was introduced into the reaction chamber. There was no observable decay when CF<sub>3</sub>OOH was left to stand in the dark for 5 minutes with 275 mTorr of H<sub>2</sub>O added to the reaction mixture. We conclude that reaction (5) does not contribute to the increased COF<sub>2</sub> yield observed in experiments #3-10.

The possible reaction of CF<sub>3</sub>O and CF<sub>3</sub>O<sub>2</sub> radicals with species on the reaction chamber walls needs consideration. The lifetimes of CF<sub>3</sub>O and CF<sub>3</sub>O<sub>2</sub> radicals in the chamber with respect to gas phase reactions are calculated to be < 100 msec and < 600 msec, respectively[5]. These lifetimes preclude significant interaction with the chamber walls.

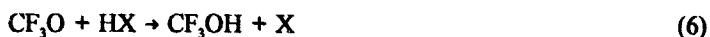
Finally, we need to consider the possibility that the trioxide, CF<sub>3</sub>O<sub>3</sub>CHF<sub>2</sub>CF<sub>3</sub>, which is a short lived product observed during the simulated atmospheric oxidation of HFC-134a[4], may react with H<sub>2</sub>O to form either CF<sub>3</sub>OH or COF<sub>2</sub>. CF<sub>3</sub>O<sub>3</sub>CHF<sub>2</sub>CF<sub>3</sub> decomposes into either CF<sub>3</sub>O<sub>2</sub> and CF<sub>3</sub>CHFO, or CF<sub>3</sub>O and CF<sub>3</sub>CFHO, radicals[4]. Reaction with H<sub>2</sub>O may compete with decomposition. However, such a competition would not be affected by the HFC-134a concentration used. Hence, if reaction of CF<sub>3</sub>O<sub>3</sub>CHF<sub>2</sub>CF<sub>3</sub> with H<sub>2</sub>O was important then increased CF<sub>3</sub>OH and/or COF<sub>2</sub> yields would be expected in experiments using both high and low initial HFC-134a concentrations. This is inconsistent with the experimental observations (for example compare experiments #2 and #4 in Table I) suggesting that reaction of CF<sub>3</sub>O<sub>3</sub>CHF<sub>2</sub>CF<sub>3</sub> with H<sub>2</sub>O is not a complication in the present work.

We believe that the most likely explanation for the observed increase of COF<sub>2</sub> product on addition of H<sub>2</sub>O is the gas phase reaction of CF<sub>3</sub>O radicals with H<sub>2</sub>O. To derive a value for k<sub>1</sub>, we need to construct a chemical mechanism which accurately predicts the product yields observed in the absence of H<sub>2</sub>O. Then we need to add reaction (1) to the model, and optimise k<sub>1</sub> to reproduce the experimentally observed product yields in the presence of H<sub>2</sub>O. Unfortunately, as discussed above, the mechanism by which COF<sub>2</sub> is formed in experiments using low HFC-134a concentrations is not completely understood. Thus, it is difficult to estimate the rate constant k<sub>1</sub>. However, we note that because of the presence of sources of COF<sub>2</sub> other than reaction (3), the rate constant ratio k<sub>1</sub>/k<sub>3</sub> derived from the data in Figure 2 is a lower limit. Hence, k<sub>1</sub>/k<sub>3</sub> > (5.4±1.3) × 10<sup>-3</sup>, using k<sub>3</sub> = (1.1±0.7) × 10<sup>-15</sup> then gives k<sub>1</sub> > 2 × 10<sup>-18</sup> cm<sup>3</sup> molecule<sup>-1</sup> s<sup>-1</sup>.

#### Computational Results and Discussion

The thermodynamics of reaction (1) are interesting both for its atmospheric significance and for its implications for the CF<sub>3</sub>O-H bond strength. If this reaction is spontaneous, then CF<sub>3</sub>O-H bond must be stronger than the O-H bond in water, which has an energy of 119.2 kcal/mol[10]. By comparison, the O-H bond strength in methanol, which is typical of most organic alcohols, is only 104.4 kcal/mol[11a]. Thus, if reaction (1) is exothermic, then the CF<sub>3</sub>O-H bond is at least 15 kcal/mol stronger than expected.

To explore the energetics of this reaction, ab initio computational methods have been applied to calculate the heat of reaction of CF<sub>3</sub>O with water, methane and hydrogen:



(X = H, OH, CH<sub>3</sub>). Additionally, the heats of the corresponding CH<sub>3</sub>O reactions were calculated for comparison with the available experimental results. The reaction energies were obtained by single point calculations at the MP4/6-311+G(d,p) level using fully optimized MP2/6-31G(d,p) geometries. This basis

Table II. Calculated and experimental heats of reaction.

	$\Delta H_{\text{calc}}^{298}$	$\Delta H_{\text{exp}}^{298}$
$\text{CF}_3\text{O} + \text{H}_2\text{O} \rightarrow \text{CF}_3\text{OH} + \text{OH}$	-1.7	
$\text{CF}_3\text{O} + \text{CH}_4 \rightarrow \text{CF}_3\text{OH} + \text{CH}_3$	-14.3	
$\text{CF}_3\text{O} + \text{H}_2 \rightarrow \text{CF}_3\text{OH} + \text{H}$	-15.2	
$\text{CH}_3\text{O} + \text{H}_2\text{O} \rightarrow \text{CH}_3\text{OH} + \text{OH}$	11.7	14.6
$\text{CH}_3\text{O} + \text{CH}_4 \rightarrow \text{CH}_3\text{OH} + \text{CH}_3$	-0.9	0.4
$\text{CH}_3\text{O} + \text{H}_2 \rightarrow \text{CH}_3\text{OH} + \text{H}$	-1.8	-0.2

set and degree of correlation were chosen as a compromise between the desired level of accuracy and computational expense, based on our own work and earlier calculations comparing various levels of correlation and extended triple-split-valence bases[12]. While these relatively extensive (and expensive) calculations are not sufficient to obtain accurate absolute molecular energies, they are expected to provide reasonably accurate ( $\pm 3$  kcal/mol) energy differences for the reactions under consideration. Vibrational frequencies obtained at the MP2/6-31G(d,p) level were used to correct the reaction energies for zero point and heat capacity effects to 298.15 K.

Table II contains the calculated heats of reaction of  $\text{CH}_3\text{O}$  with the three hydrogen donors. The table also contains experimental values for the three methoxy reactions, calculated from the X-H bond dissociation energies using the following equation[11]:

$$\Delta H^{298.15} = D_{298.15}^{\circ}(\text{CH}_3\text{O}-\text{H}) - D_{298.15}^{\circ}(\text{X}-\text{H})$$

A comparison of the experimental and theoretical results should help establish the accuracy of the computational method. The experimental bond energies are reportedly accurate to  $\pm 1$  kcal/mol. Thus, we can expect the experimental results in Table II to be accurate to within  $\pm 2$  kcal/mol. Given this level of uncertainty, the agreement between experimental and computed results is very good. As expected from the experimental data, the reaction of  $\text{CH}_3\text{O}$  with water is a strongly endothermic process. In contrast, the reactions of  $\text{CH}_3\text{O}$  with methane and hydrogen are nearly thermoneutral processes, reflecting the similarity of the  $\text{CH}_3\text{O}-\text{H}$ ,  $\text{H}-\text{H}$ , and  $\text{CH}_3-\text{H}$  bond strengths. The computational results systematically underestimate the experimental results by 1-3 kcal/mol, or slightly greater than the experimental uncertainty, which probably results from inadequacies in our basis set.

Table II also contains the calculated heats of reaction of the  $\text{CF}_3\text{O}$  radical with the three hydrogen donors. The energies are shifted downward 13.4 kcal/mol relative to the methoxy results. This shift reflects a corresponding increase in the computed O-H bond strength from methanol to trifluoromethanol. In contrast to the  $\text{CH}_3\text{O}$  results, the  $\text{CF}_3\text{O}$  reactions with the hydrogen molecule and methane are predicted to be strongly exothermic processes. Consistent with these results, the reaction of  $\text{CF}_3\text{O}$  radicals with methane has previously been observed[4].

The 13.4 kcal/mol shift from  $\text{CH}_3\text{O}$  to  $\text{CF}_3\text{O}$  is sufficient to make the reaction with water exothermic. The heat of reaction (1) is calculated to be -1.7 kcal/mol. Lower levels of theory, including the MP2/6-31G(d,p) calculations and the MP2 and MP3/6-311+G(d,p) results, give slightly (0-2 kcal/mol) more negative values. Given the likely level of error, including the systematic error observed in the methoxy results, we cannot definitely conclude that reaction (1) is exothermic. However, we can say that the reaction is close to thermoneutrality, and that unlike the reaction of typical alkoxy radicals with water, the abstraction of a hydrogen atom from water by trifluoromethoxy radical is energetically feasible.

While our calculations by themselves do not provide a good estimate of the O-H bond energy in trifluoromethanol, we can combine the heats of reaction in Table II with the experimental bond energies

of hydrogen, methane, or water, to obtain an "experimentally corrected" value. Using this approach yields an O-H bond energy of 119-121 kcal/mol, depending on the reaction used. A safe estimate, based on our results, is  $120 \pm 3$  kcal/mol. As already noted, this value is comparable to or greater than the bond energy of water, and is roughly 15 kcal/mol greater than that typically observed for an alcohol. Thus, the bond is among the strongest single bonds known.

#### Implications for Atmospheric Chemistry

At present, the atmospheric loss mechanism for  $\text{CF}_3\text{O}$  radicals is believed to be reaction with NO and hydrocarbons. Bevilacqua et al.[2] and Zellner[13] both report rate constants of  $2 \times 10^{-11} \text{ cm}^3 \text{ molecule}^{-1} \text{ s}^{-1}$  for reaction with NO, while Saathoff and Zellner[14] have measured  $k(\text{CF}_3\text{O}+\text{CH}_4) = 2.2 \times 10^{-14} \text{ cm}^3 \text{ molecule}^{-1} \text{ s}^{-1}$ . Reasonable estimates for the global tropospheric concentrations of NO,  $\text{CH}_4$ , and  $\text{H}_2\text{O}$  are  $2.5 \times 10^8$  (10ppt),  $5 \times 10^{13}$  (2ppm), and  $3 \times 10^{17} \text{ cm}^{-3}$  (50% relative humidity). Using  $k_1 = (0.2-40) \times 10^{-17} \text{ cm}^3 \text{ molecule}^{-1} \text{ s}^{-1}$  then leads to atmospheric lifetimes of  $\text{CF}_3\text{O}$  radicals (at room temperature) with respect to reaction with NO,  $\text{CH}_4$ , and  $\text{H}_2\text{O}$  of 200, 0.2, and 0.01-1.7 seconds, respectively. Reaction (1) may play a significant role in the atmospheric chemistry of  $\text{CF}_3\text{O}$  radicals, and hence, in the atmospheric degradation of CFC replacements such as HFC-134a.

#### Acknowledgements

We thank Ernie Tuazon (University of California, Riverside) for useful discussions concerning the IR spectrum of  $\text{CF}_3\text{OH}$ , and Geoff Tyndall (National Center for Atmospheric Research) for discussions regarding  $k_3$ .

#### References

1. Chen, J.; Zhu, T.; Niki, H., *J. Phys. Chem.*, **1992**, 96, 6115.
2. Bevilacqua, T. J.; Hanson, D. R.; Howard, C. J., *J. Phys. Chem.*, in press (1993).
3. Chen, J.; Zhu, T.; Niki, H.; Mains, G. J., *Geophys. Res. Lett.*, **1992**, 19, 2215.
4. Sehested, J.; Wallington, T. J.; *Environ. Sci. Tech.*, **1993**, 27, 146.
5. Wallington, T.J., Hurley, M. D., Schneider, W. F., Sehested, J., and Nielsen, O. J., *J. Phys. Chem.* in press (1993).
6. Wallington, T. J.; Gierczak, C. A.; Ball, J. C.; Japar, S. M. *Int. J. Chem. Kinet.*, **1989**, 21, 1077.
7. Gaussian 88. Frisch, M. J.; Head-Gordon, M.; Schlegel, H. B.; Raghavachari, K.; Binkley, J. S.; Gonzalez, C.; Defrees, D. J.; Fox, D. J.; Whiteside, R. A.; Seeger, R.; Melius, C. F.; Baker, J.; Martin, R.; Kahn, L. R.; Stewart, J. J. P.; Fluder, W. M.; Topiol, S.; Pople, J. A. Gaussian, Inc., Pittsburgh, PA 1988.
8. Del Bene, J. E.; Mettee, H. D.; Frisch, M. J.; Luke, B. T.; Pople, J. A., *J. Phys. Chem.*, **1983**, 87, 3279.
9. Lewis, G. N.; Randall, M., *Thermodynamics*, revised by K. S. Pitzer and L. Brewer, McGraw-Hill, New York, 1961.
10. Chase, M. W.; Davies, C. A.; Downey, J. R.; Frurip, D. J.; McDonald, R. A.; Syverud, A. N. *JANAF Thermochemical Tables*, Third Ed., *J. Phys. Chem. Ref. Data* **1985**, 14, Suppl. 1.
11. a. McMillen, D. F.; Golden, D. M., *Ann. Rev. Phys. Chem.*, **1982**, 33, 493. b. Baldwin, R. R.; Drewery, G. R.; Walker, R. W., *J. Chem. Soc., Faraday Trans. 1*, **1984**, 80, 2827.
12. Pople, J. A.; Luke, B. T.; Frisch, M. J.; Binkley, J. S., *J. Phys. Chem.*, **1985**, 89, 2198.
13. Zellner, R., private communication, 1.
14. Saathoff, H.; Zellner, R., **1993**, *Chem. Res. Lett.*, in press.

# The possible atmospheric importance of the reaction of CF<sub>3</sub>O radicals with ozone

P. Biggs, C.E. Canosa-Mas, D.E. Shallcross and R.P. Wayne  
*Physical Chemistry Laboratory, South Parks Rd., Oxford OX1 3QZ, UK*

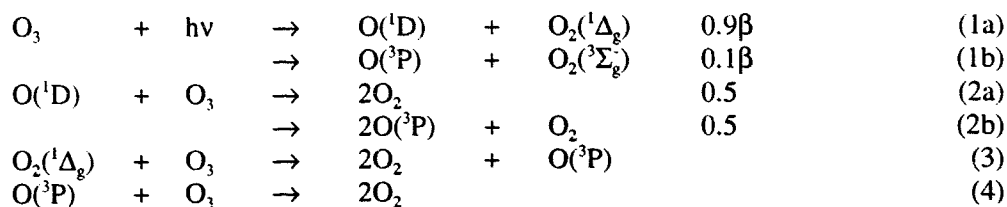
C. Kelly and H.W. Sidebottom  
*Chemistry Department, University College Dublin, Ireland*

## 1. Introduction

Over the past few years, a considerable effort has been put into investigating the tropospheric oxidation of hydrofluorocarbons (HFCs) and hydrochlorofluorocarbons (HCFCs) and the fate of the products of this oxidation. However, little research has been carried out on the stratospheric oxidation of these compounds and their degradation products, especially with regard to their reaction with the most important stratospheric species, ozone. The work described here is a re-examination of experimental results that give some indication of the reactivity of CF<sub>3</sub>O towards O<sub>3</sub>. The data were obtained during a study of the fate of the organic fragment resulting from chlorine-atom abstraction from a series of chlorofluorocarbons [1,2]. Although these experiments were not designed to study reactions of the CF<sub>3</sub>O radical directly, an analysis of the behaviour of ozone in the system suggests that CF<sub>3</sub> behaves very differently from CF<sub>2</sub>Cl or CFC<sub>1,2</sub>, probably because of the special nature of CF<sub>3</sub>.

## 2. Experimental

The experimental setup has been described in detail elsewhere [1,2]. A simplified block diagram of the system is shown in figure 1. The apparatus consists of a quartz flow tube, around which is a helical low-pressure mercury lamp. The flow tube is connected to a quadrupole mass spectrometer, the interface between the two being a differentially pumped sampling system. A mixture of helium and ozone passes down the flow tube, with the concentration of ozone in the system being monitored by the mass spectrometer. When the photolysis lamp is turned on, the concentration of ozone in the system decreases: the fractional loss of ozone depends on the concentration of ozone present, the residence time within the photolysis region ( $t_1$ ) and the contact time after photolysis ( $t_2$ ). The reactions occurring in this ozone-only system are



0 1 9 3

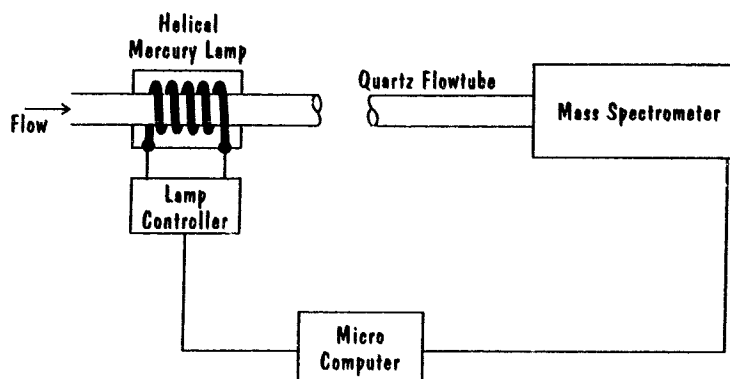
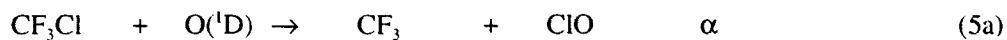


Figure 1 Block diagram of the experimental system.

The value of  $\beta$  (the rate of photolysis of ozone) was determined by using  $N_2$  instead of helium as the carrier gas: the  $N_2$  efficiently quenches the  $O(^1D)$ , thus inhibiting reaction (2). Numerical techniques were then used to model the reaction system, with the value of  $\beta$  being determined as 0.45.

### 3. Results

On addition of a CFC to the flow mixture, the  $O(^1D)$  produced in the photolysis of  $O_3$  will interact with the CFC: either chlorine atom abstraction or physical quenching of the excited oxygen atom will occur. The product of the chlorine abstraction will then react further with ozone giving rise to the following reaction steps in the case of CFC-13



The change in the fractional loss of ozone on adding the CFC will obviously depend on the relative rates of reaction (2) and reactions (5) and (6). A first, approximate, approach to interpreting the system can be attempted if we consider only reactions (1a), (2), (5a) and (6), and if it is assumed that  $O(^1D)$  is in steady state during photolysis. The stoichiometry factor,  $n$ , can be shown to be given by the equation

$$n = 1 + \frac{k_5[CF_3Cl] + k_2[O_3]_0}{\alpha k_5[CF_3Cl]} \left[ \frac{\Delta[O_3]}{0.9\beta[O_3]_0\tau_1} - 2 \right]$$

where  $\Delta[\text{O}_3]$  is the decrease in ozone concentration observed on irradiation. Figure 2 shows a plot of  $n$  against  $[\text{O}_3]_0$  (the initial ozone concentration) for the system with  $\text{CF}_3\text{Cl}$  present; the open circles are experimental points. Although it can clearly be seen that no single value of  $n$  can describe the experimental data, and that the value of  $n$  increases with increasing  $[\text{O}_3]_0$ , the values of  $n$  are surprisingly high ( $6 < n < 14$ ), suggesting that there is some form of chain reaction occurring in the system.

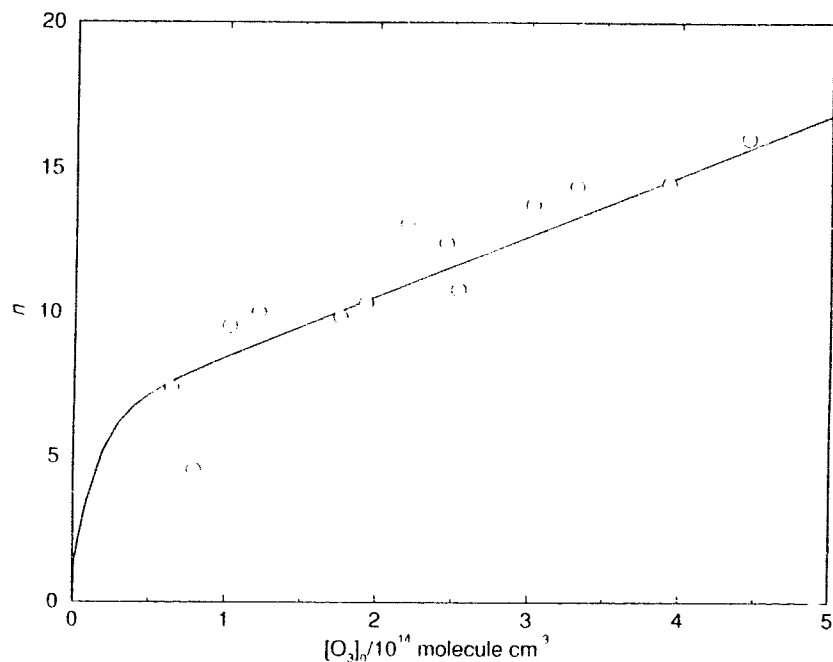
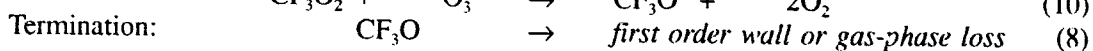
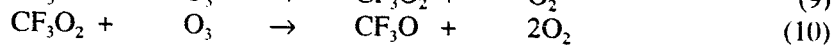
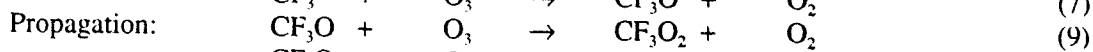
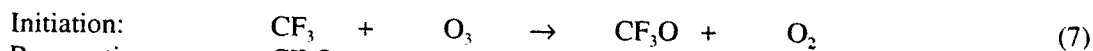


Figure 2 Plot of  $n$  against  $[\text{O}_3]_0$ . The points and line are explained in the text.

The reaction of the  $\text{CF}_3$  radical with ozone is most likely to produce  $\text{CF}_3\text{O}$ : any other product is either thermodynamically unlikely, or would not lead to any further ozone loss so that  $n$  would be unity. However, there are two possible fates for the  $\text{CF}_3\text{O}$  radical in our system: either reaction with ozone or first-order loss (including unimolecular decomposition and wall reactions). The reaction with ozone seems likely to produce the peroxy radical,  $\text{CF}_3\text{O}_2$ , which, in our  $\text{NO}_x$  free system, is also likely to react with ozone. If the products of the reaction of  $\text{CF}_3\text{O}_2$  with  $\text{O}_3$  are  $\text{CF}_3\text{O}$  and  $\text{O}_2$ , regeneration of  $\text{CF}_3\text{O}$  will lead to a chain reaction. The chain therefore consists of the following reactions



It can readily be shown from the scheme of reactions (1a), (2), (5) and (7)–(10) that in the steady state

$$n = \frac{2k_9[\text{O}_3]_0}{k_8} + 1$$

Figure 2 shows that for  $[O_3]_0 > 1-2 \times 10^{14}$  molecule  $cm^{-3}$ , the relation is approximately linear. At lower concentrations,  $n$  appears to be too low, probably because there is insufficient reaction time for the steady state to establish itself. The solid curve on the figure shows the result of a numerical model, to be described later, that incorporates the true reaction periods, and it is consistent with the experimental results. For the purposes of estimation of rate coefficients, it is appropriate to take a spot value of  $n$  within the steady state region. For an  $[O_3]_0$  of around  $2 \times 10^{14}$  molecule  $cm^{-3}$ ,  $n$  is approximately 10, this relation suggesting that  $k_9/k_8 \approx 2 \times 10^{-14}$   $cm^3$  molecule $^{-1}$ . For radicals such as  $CH_3O$  in similar reaction systems,  $k_8$  is of the order of 30–100  $s^{-1}$ . Taking these values for  $CF_3O$  as well, our ratio suggests that  $k_9$  is in the range  $6 \times 10^{-13}$ – $2 \times 10^{-12}$   $cm^3$  molecule $^{-1}$   $s^{-1}$ , which we use as the starting value for numerical modeling. We note, however, that the simplified scheme omits some secondary reactions (especially of  $ClO$ ) that will contribute, so that the true value of  $k_9$  is likely to be somewhat smaller than the value derived by the approximate method.

Figure 3 shows a plot of  $[O_3]_0$  against  $\Delta[O_3]$ , with the experimental data points once again being marked by open circles. The solid line in the figure represents the loss of ozone as calculated by a numerical model. The model uses a 13-reaction scheme which includes reactions not only of the primary participants, but also of the possible secondary products (such as  $O_2(^1\Delta_g)$ ,  $F$ ,  $Cl$ ,  $FO$  and  $ClO$ ). In order to produce a fit to the experimental data,  $k_9$  (the rate of the reaction of  $CF_3O$  with  $O_3$ ) was used as a fitting parameter and  $k_8$  was set to a value of 100  $s^{-1}$ ;  $k_{10}$  was constrained to be the same as  $k_9$ . The dashed lines in the figure are for values of  $k_9$  which show noticeably worse fits to the experimental data. For the central value, the fit to the experimental data is excellent, and it can be seen that the value of  $k_9/k_8$  obtained from the model ( $\approx 10^{-14}$   $cm^3$  molecule $^{-1}$ ) is quite close to that derived analytically. This ratio remains virtually unaltered if the assumed value of  $k_8$  is changed by a factor of ten, so that the value of  $k_9$  need to fit the experimental data scales with  $k_8$ .

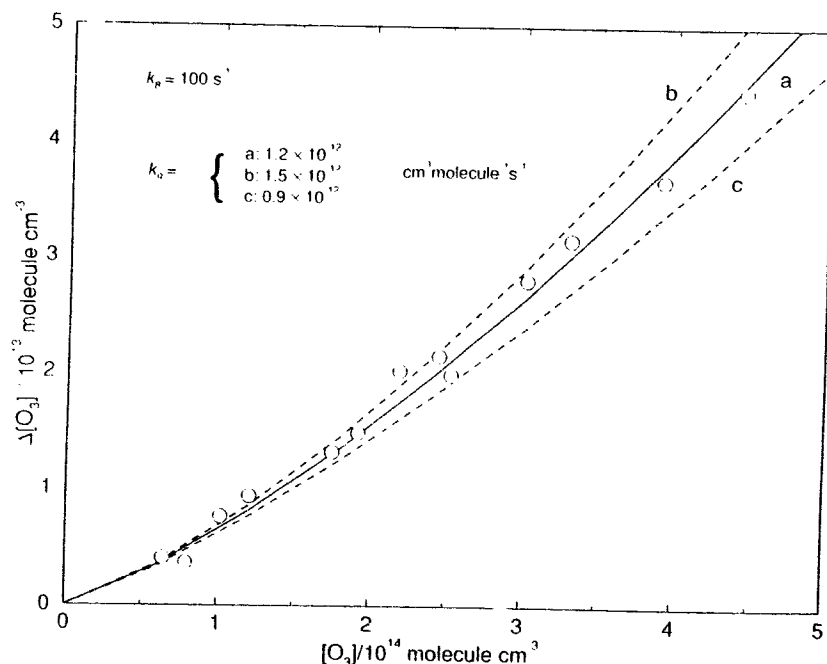


Figure 3 Plot of  $[O_3]_0$  against  $\Delta[O_3]$ .

#### 4. Atmospheric significance

Table 1 shows the rates of the reactions of  $\text{CF}_3\text{O}$  with various stratospherically important species. The table also shows the estimated lifetime of  $\text{CF}_3\text{O}$  with respect to each species (calculated as  $1/k[\text{X}]$ , the rate constants being those presented at the AFEAS meeting in Dublin, 1993).

Reaction	Rate / $\text{cm}^3\text{molecule}^{-1}\text{s}^{-1}$	concentration of co-reactant at 30 km / $\text{molecule cm}^{-3}$	Lifetime / s
$\text{CF}_3\text{O} + \text{O}_3 \rightarrow \text{CF}_3\text{O}_2 + \text{O}_2$	$1 \times 10^{-12}$	$10^{12}$	1
$\text{CF}_3\text{O} + \text{NO} \rightarrow \text{CF}_2\text{O} + \text{FNO}$	$2.5 \times 10^{-11}$	$10^9$	40
$\text{CF}_3\text{O} + \text{NO}_2 \rightarrow \text{CF}_3\text{ONO}_2$	$9 \times 10^{-12}$	$10^9$	100
$\text{CF}_3\text{O} + \text{CO} \rightarrow \text{CF}_2\text{O} + \text{COF}$	$4.4 \times 10^{-14}$	$10^{10}$	2200
$\text{CF}_3\text{O} + \text{CH}_4 \rightarrow \text{CF}_3\text{OH} + \text{CH}_3$	$2.2 \times 10^{-14}$	$10^{11}$	450

It can clearly be seen that reaction with ozone is very important in determining the lifetime of  $\text{CF}_3\text{O}$ ; even if the rate constant quoted here is too high, then reaction with ozone could still be an important fate of  $\text{CF}_3\text{O}$  in the stratosphere. Further, in the atmosphere the product of the reaction with ozone,  $\text{CF}_3\text{O}_2$ , will most likely react with either NO or O atoms, both of which will regenerate  $\text{CF}_3\text{O}$ . The only significant process that will lead to a permanent loss of ozone-destroying species from the stratosphere is reaction of  $\text{CF}_3\text{O}$  with NO.

#### 5. Conclusions

Although these results do not directly demonstrate the occurrence of a reaction between  $\text{CF}_3\text{O}$  and  $\text{O}_3$ , they are strongly suggestive of such a process. We have performed analogous experiments to those described here with the CFCs  $\text{CF}_2\text{Cl}_2$  and  $\text{CFCl}_3$ . This is not the place to discuss the data or their analyses. However, it is apparent that less ozone is decomposed in the presence of these species: the radicals  $\text{CF}_2\text{ClO}$  and  $\text{CFCl}_2\text{O}$  are known to rapidly lose a Cl atom, so that the interaction with ozone is suppressed and chains of the type described here are correspondingly much shorter. Instead, excess ClO appears in the system (as detected mass spectrometrically) and the values of  $n$  are lower.

The significance of the reactions in atmospheric chemistry needs to be assessed quantitatively. Although any chains may be relatively short, some effect on ozone might occur if  $\text{CF}_3$  precursors become abundant in the stratosphere. Direct laboratory measurements are clearly needed to obtain the kinetic and mechanistic data that will allow a firmer interpretation.

#### 6. References

- [1] P. Biggs, *D.Phil. Thesis*, Oxford University (1987)
- [2] D.G. Ralph and R.P. Wayne, *J. Chem. Soc., Faraday Trans. 2*, **78**, 1815 (1982)

# The Photolysis and Chlorine-Initiated Photo-oxidation of Trifluoroacetaldehyde

Hannah R. Richer, John R. Sodeau and Ian Barnes\*

School of Chemical Sciences, University of East Anglia, NORWICH,  
Norfolk, NR4 7TJ, U.K.

\*Bergische Universitat-Gesamthochschule Wuppertal, Physikalische  
Chemie FB-9, Gausstrasse 20, 5600 Wuppertal 1, Germany.

## Introduction

Trifluoroacetaldehyde is a possible degradation product of the halogenated alkanes  $\text{CF}_3\text{CH}_3$  (143a) and  $\text{CF}_3\text{CClH}_2$  (133a). Little is known concerning the photo-oxidation of this aldehyde. The u.v. spectrum has been obtained by various authors [1,2 and 3]; it is shown to absorb strongly in the region 240 to 360nm. Previous photolysis experiments ( $\lambda=313\text{nm}$ ) [4] have indicated that the major products are  $\text{CF}_3\text{H}$  and  $\text{CO}$ . The authors proposed that the pathway forming  $\text{CF}_3\text{H}$  in their system was due to the reaction of  $\text{CF}_3$  radicals with the aldehyde;



However, as the experiments reported in this communication are performed in 950mbar of air, process (1) will not occur because peroxy radicals ( $\text{CF}_3\text{O}_2$ ) are formed.

An alternative degradation mechanism of  $\text{CF}_3\text{CHO}$  in the atmosphere is *via* abstraction of a hydrogen atom by a hydroxyl radical;



In the laboratory it is often simpler to use chlorine atoms to mimic hydroxyl radicals, as reaction is more rapid, shorter wavelength light is not required (ie products which are photo-sensitive are more likely to remain) and by-products of OH formation are avoided.

## Experimental

Initial experiments with  $\text{CF}_3\text{CHO}$  were carried out in a 1080 dm<sup>3</sup> quartz reaction chamber with pathlength 468m. A more detailed description of the apparatus has been given in ref [5].

Further experiments were carried out in a 18dm<sup>3</sup> quartz chamber with pathlength 12m. In both cases visible ( $\lambda_{\text{max}}=360$ ) or uv ( $\lambda_{\text{max}}=253.7\text{nm}$ ) lamps were employed for photolysis of gas mixtures.

Both reaction chambers were used in conjunction with FTIR spectroscopy, Bruker (IFS-88) and Biorad (FTS-7) respectively. Absorption spectra were obtained by co-addition of 64-256 interferograms at a spectral resolution of 1cm<sup>-1</sup>. Reaction times were dependent on the exact study, usually of the order of 30 minutes to an hour, except for photo-oxidation initiated by lamps in the visible region alone, when longer photolysis times were required.

Chemicals were introduced into the system by means of a vacuum line or by direct injection. The concentrations of  $\text{CF}_3\text{CHO}$  were typically of the order of 0.5 ppmv in the large reaction chamber and 50ppmv in the small reaction chamber. Where chlorine was used it was generally added such that it did not exceed half the concentration of the aldehyde. Ethane was also used in some studies and was present in excess. Mixtures were made up to 950mbar with synthetic air.

The gases were obtained from BOC or Messer Griesheim and were used as received. The trifluoroacetaldehyde was prepared by dehydration of the hydrate with  $\text{P}_4\text{O}_{10}$  under vacuum. The deuterated sample was prepared by the  $\text{LiAlD}_4$  reduction of  $\text{CF}_3\text{C}(\text{O})\text{OH}$  [6] and dehydration of the resultant hydrate. The products were vacuum distilled and found to have no impurities detected by FTIR spectroscopy.

## Results and Discussion

### *Photo-oxidation $\lambda_{\text{max}}=253.7\text{nm}$ and $\lambda_{\text{max}}=366\text{nm}$*

The uv initiated photo-oxidation of  $\text{CF}_3\text{CHO}$  gives two major (C-F containing) products;  $\text{CF}_3\text{H}$  and  $\text{CF}_2\text{O}$ . Other products observed are  $\text{CO}$ ,  $\text{CO}_2$  and  $\text{HF}$ . With a concentration of 70ppm the products are formed in the following proportions;  $\text{CF}_3\text{H}$ (14%),  $\text{CF}_2\text{O}$ (80%),  $\text{CO}$ (65%),

CO<sub>2</sub>(45%). CO<sub>2</sub> is found with a higher concentration than might be expected possibly due to wall reactions. A minor product having weak absorbances is also noted and decays in the dark to give CF<sub>2</sub>O. (see table 1)

When ethane is added to the system the percentage of CF<sub>2</sub>O formed is seen to fall, the minor product noted above is no longer visible and no large increase in CF<sub>2</sub>O is observed after the product mixture is left in the dark. However, the rate of formation of CF<sub>3</sub>H remains constant. With a concentration of 250ppm ethane the products are now seen in different proportions CF<sub>3</sub>H (56%) and CF<sub>2</sub>O (42%). The yield of CO also increases to a little over 100% and some CO<sub>2</sub> is also noted, probably due to photolysis of products of ethane oxidation. Preliminary quantum yield studies suggest that CF<sub>3</sub>H and CF<sub>2</sub>O are formed with approximately equal efficiency, however, further work needs to be carried out in this area in order to reduce the uncertainty. If the concentration of ethane is increased no further change in the product concentrations is observed. Photolysis of CF<sub>3</sub>CDO in air leads to the expected products CF<sub>2</sub>O and CF<sub>3</sub>D.

Experiments with visible photolysis lamps showed that on long photolysis times (>6 hours) CF<sub>3</sub>CHO is seen to undergo a small degree of photolysis. The major products observed are CF<sub>2</sub>O and CO<sub>2</sub>.

#### *Cl<sub>2</sub> Initiated Photo-oxidation*

With low concentrations (<1ppm) of reactants the only major products observed were CF<sub>2</sub>O and CO<sub>2</sub>. However, when Cl<sub>2</sub> and/or CF<sub>3</sub>CHO concentrations were increased it could be seen that at least one intermediate was present in the formation of CF<sub>2</sub>O, (see table 1 for I.R. frequencies). In the smaller cell with higher concentrations of reactants the "intermediates" were likewise found in much higher concentrations. Not all the absorbance bands were found to have the same formation and decay characteristics. The bands at 1858 and 1053cm<sup>-1</sup> (intermediate Y) were seen to decay much more rapidly, on being left in the dark or on photolysis with 253.7nm light, than the remaining bands intermediate X). This decay in Y does in fact correspond to an increase in X which then decays to CF<sub>2</sub>O and HF.

Experiments starting with the deuterated compound  $\text{CF}_3\text{CDO}$  gave both the same "intermediates" as found previously and also a new unknown. The deuterated intermediate formed decays to  $\text{CF}_2\text{O}$  and  $\text{DF}$ . The spectra of the normal and deuterated intermediate have characteristic OH and OD stretches, the only other absorbance band to be significantly changed between the isotopically altered species is that assigned to the OH bend. With this information and that available from the literature, ref. [7] and more recently ref. [8], it can be concluded that the intermediate X is  $\text{CF}_3\text{OH}$ .

Less information is available as to the identity of intermediate Y which goes on to form  $\text{CF}_3\text{OH}$ . It has a characteristic carbonyl stretching frequency and appears to decompose readily to give the radical  $\text{CF}_3\text{O}$ . Possibilities for the intermediate Y, which has also been detected in other work, ref. [9], may be  $\text{CF}_3\text{C}(\text{O})\text{OOCF}_3$  or  $\text{CF}_3\text{C}(\text{O})\text{OOOCF}_3$ . A literature reference is available for the peroxy compound [10] and the absorption wavenumbers are similar ( $1859$  and  $1068\text{cm}^{-1}$ ) but not the same. From a mechanistic point of view the latter species would appear to be more likely. Thus Y can be identified with the molecule  $\text{CF}_3\text{C}(\text{O})\text{OOOCF}_3$ .

**Table 1 Absorbance Frequencies of Intermediates in the Reaction of  $\text{CF}_3\text{CHO}$  and  $\text{Cl}$ , in Air**

Frequencies $\text{cm}^{-1}$			Relative Intensity	assignment
<b>X</b>				
This work	Ref. [7]	Ref. [8]		
3664	3675	3665	m	OH stretch
1399	1401	1400	m	$\text{CF}_3$ asym str
1361	1363	1361	m	
1281	1283	1281	vs	CO stretch
1182	1187	1183	s	$\text{CF}_3$ asym str
1118	1117	1119	s	OH bend
<b>Y</b>				
1859			w	CO stretch
1053			w	

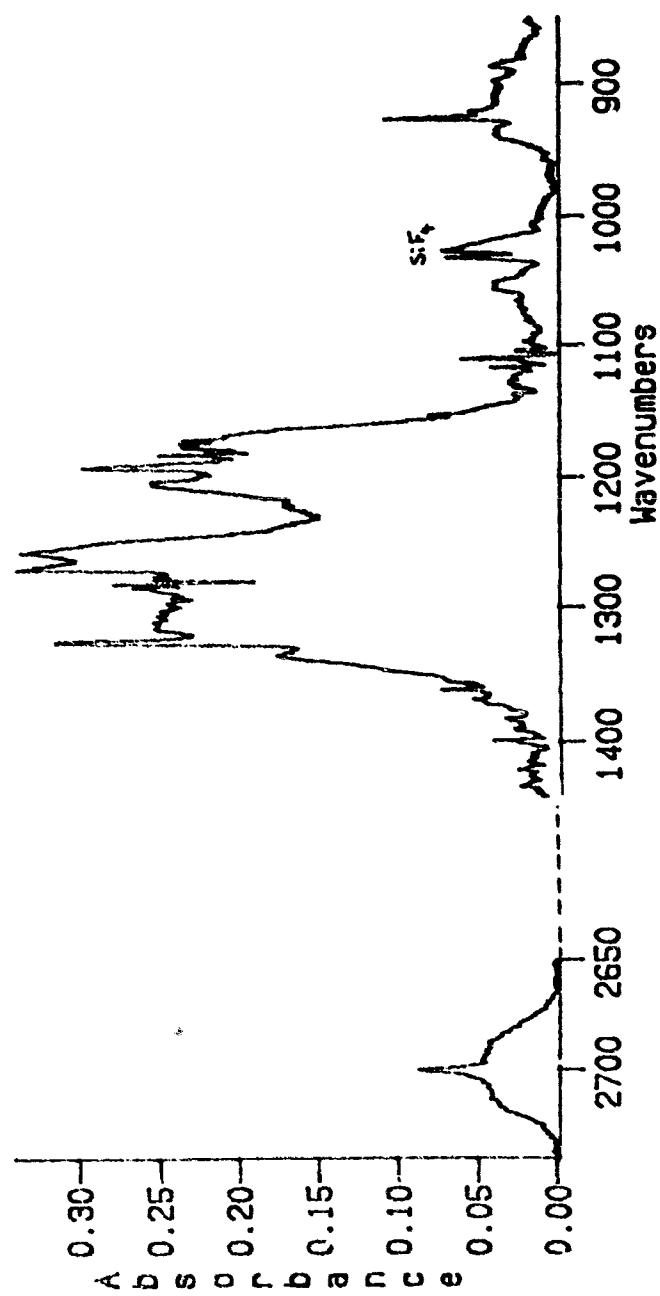


Figure 1 Spectrum of Deuterated Intermediate, assigned as  $\text{CF}_3\text{OD}$

## Summary

It can be concluded that at 254nm there are at least two major photolysis pathways; the molecular pathway to form  $\text{CF}_3\text{H}$  and  $\text{CO}$

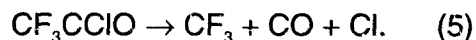


and a pathway leading to  $\text{CF}_2\text{O}$  is also of importance. This product is likely to originate from process (4);



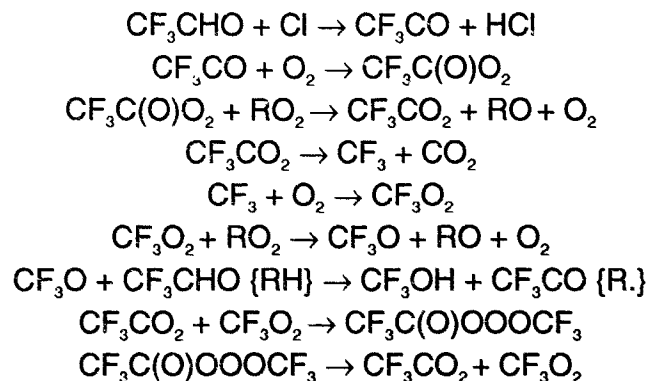
Fission of the CH bond would also be a possibility but this requires greater energy [11] and would lead to the formation of  $\text{CO}_2$  rather than  $\text{CO}$ .

It has been noted by Moortgat et al. [3] that for the carbonyl compound  $\text{CF}_3\text{C}(\text{O})\text{Cl}$  the major pathway is via;



This may also be a possibility here, however, with the current evidence it is not possible to distinguish between reactions (4) and (5). Theoretical work, [11], suggests formation of  $\text{CFHO}$  and  $\text{CF}_2$  as the lowest energy process but neither species has been detected in this study.

Chlorine initiated studies suggest the following mechanism;



## Environmental Implications

One interesting result of the study of photolysis, at 254nm, of  $\text{CF}_3\text{CHO}$  in air, is the formation of  $\text{CF}_3\text{H}$  in a comparatively large yield.  $\text{CF}_3\text{H}$  has a long atmospheric lifetime, estimated as 270 years [12] and has the possibility to build up in the stratosphere. A much greater understanding of  $\text{CF}_3\text{O}$  radical reactions has developed over the last two years. It is now known that  $\text{CF}_3\text{O}$  radicals react with hydrocarbons and also appear to react with water [9]. However, certain points have yet to be clarified, e.g. the possible role of  $\text{CF}_3\text{O}$  radicals in the stratosphere.

## References

- [1] Libruda G., personal communication
- [2] Rattigan O., personal communication
- [3] Moortgat G.K., STEP-HALOCSIDE/AFEAS Workshop (1993)
- [4] Dodd R.E. and Watson Smith J., J. Chem. Soc. (1957) 1465
- [5] Becker K.H., Barnes I., Bastian V., Fink E.H., Kriesche V., Nelsen W., Zabel F., Abschlussbericht des Forschungsvorhabens FKZ 07EU 708/3 (1991)
- [6] Braid M., Iserson H. and Lawlor F.E., J. Am. Chem. Soc., 76, (1954) 4027
- [7] Kloter G. and Seppelt K., J. Am. Chem. Soc., 101, (1979) 347
- [8] Chen J., Zhu T., and Niki H., Geophys. Res. Letts. 19 (1992) 2215
- [9] Wallington T., personal communication
- [10] Hohorst F. A. and DesMarteau D.D., J. Am. Chem. Soc. 93 (1971) 3882
- [11] Francisco J.S., Chem. Phys., 163 (1992) 27
- [12] Schmoltner A.M., STEP-HALOCSIDE/AFEAS Workshop (1993)

## Thermodynamic Properties for Atmospheric Degradation of HFC-134a and HFC-23

David A. Dixon and Richard Fernandez  
DuPont Central Research and Development  
Experimental Station E328  
Wilmington, DE 19880-0328

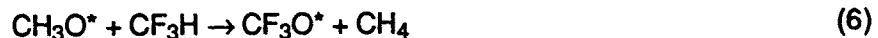
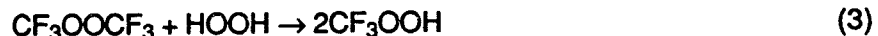
There is significant interest in the environmental fate of man-made materials, especially those that are released into the atmosphere. The atmospheric fate of HFC-134a is of great interest to the chemical industry because of its proposed use as a replacement for CFCs in refrigeration systems. The pathway for atmospheric destruction has been developed based on known species in the atmosphere and on hydrocarbon combustion chemistry.[1] Although there is a significant amount of kinetic work on the decomposition of HFC-134a, there is very little known about the actual thermodynamics governing the decomposition pathways other than what has been obtained from group additivity models. Because of this lack of kinetic information, we decided to calculate as much of the thermochemistry as possible based on ab initio molecular orbital methods and the few pieces of known experimental data. We have previously been successful in calculating the thermodynamics of a variety of simple alkanes containing H, F and Cl as substituents.[2]

The calculations were done as follows. The geometries were optimized with a polarized double zeta basis set [3] at the Hartree-Fock RHF (closed shell) or ROHF (open shell) levels with the program GRADSCF [4] by using analytic gradient methods.[5] Force fields were calculated at these levels analytically.[6] The final geometry parameters were used in MP2/PUMP2 calculations [7,8] with a polarized double zeta basis set. These calculations were done with the program GAUSSIAN 92.[9]

The results of the calculations are a set of total electronic energies and zero point energies. These can be used to predict the reaction energy of a variety of reactions( preferably isodesmic or related types) of the form



From the energy of the reaction and the known heats of formation of A, B, and C, it is possible to calculate the unknown heat of formation of D. Of course, this process relies on the fact that the known heats of formation do not have significant errors. If such errors are present, these will be incorporated into the calculated values. Examples of the types of reactions used in this study to calculate the heats of formation of the species in Table I are given below. (An asterisk denotes a radical species.)



The results in Table I can be used to calculate the reaction enthalpies for the decomposition processes in Table II for HFC-134a and the simpler model system HFC-23. The results for HFC-32 have some interesting features, notably the O-H bond energy in  $\text{CF}_3\text{OH}$  is predicted to be essentially the same as that of  $\text{H}_2\text{O}$ , much higher than the OH bond in methanol. The important channel for atmospheric degradation of HFC-134a is the decomposition of the intermediate  $\text{CF}_3\text{CHFO}^*$ . Our calculated values show that beta scission of the C-C bond is an exothermic process by about 6 kcal.mol. The fact that we can optimize the structure of  $\text{CF}_3\text{CHFO}^*$  shows that the alkoxy radical is an intermediate and has a barrier to C-C bond cleavage. The other possible cleavage pathways of the alkoxy radical are predicted to be endothermic. The reaction of  $\text{CF}_3\text{CHFO}^*$  to produce  $\text{HOO}^*$  and the acid fluoride is predicted to be very exothermic.

**Table I. Heats of Formation (kJ/mol) for Atmospheric Decomposition Reactions of HFC-134a and HFC-23.**

Formula	DuPont <sup>a</sup> (calc)	Zellner <sup>b</sup> (AFEAS)	Batt <sup>c</sup> & Walsh
HOO*	2.1±8.4	10.5	
CH <sub>3</sub> O <sub>2</sub> *	16.7±8.4 <sup>d</sup>	15.9	
CF <sub>3</sub> O <sub>2</sub> *	-646.3	-674.8	
CF <sub>3</sub> CHFOO*	-835.6		
OH*	39.0±1.2	39.3	
CH <sub>3</sub> O*	16.7±4.2 <sup>d</sup>	16.7	
CF <sub>3</sub> O*	-637.4	-606.7	-655.6
CF <sub>3</sub> CHFO*	-848.9	-807.5	
CH <sub>4</sub>	-74.9±0.3		
CF <sub>3</sub> H	-697.0±3.3		
CF <sub>3</sub> CFH <sub>2</sub>	-897.2 <sup>e</sup>		
O*	249.2±0.1		
H*	218.0±0.0		
F*	79.4±0.3	79.1	
Cl*	121.3±0.0	120.9	
CH <sub>3</sub> *	145.7±0.8	146.9	
CF <sub>3</sub> *	-470.3±4.2	-468.6	
CF <sub>3</sub> CFH*	-678.0		
C(O)F <sub>2</sub>	-638.9±1.7	-636.0	
C(O)H <sub>2</sub>	-115.9±6.3	-108.8	
C(O)Cl <sub>2</sub>	-219.1±0.5	-220.1	
CH <sub>3</sub> C(O)F	-442.1±3.3 <sup>f</sup>		
CH <sub>3</sub> C(O)Cl	-242.8±0.8 <sup>f</sup>		
CH <sub>3</sub> C(O)H	-166.1		

CH(O)F	-404.6	-372.0	
CH(O)Cl	-185.8		
CF(O)Cl	-427.2	-428.0	
CF <sub>3</sub> C(O)Cl	-821.1	-828.4(-861.9)	
CF <sub>3</sub> C(O)F	-1029.1	-983.2(-1050.6)	
CF <sub>3</sub> C(O)H	-764.2		
H <sub>2</sub> O	-241.8±0.0		
CH <sub>3</sub> OH	-201.5±0.3 <sup>f</sup>	-201.3	
CF <sub>3</sub> OH	-916.2	-893.3	
CF <sub>3</sub> CFHOH	-1088.7		
HOOH	-136.1 <sup>g</sup>		
CF <sub>3</sub> OOH	-806.7	-821.7	[-821.5]
CF <sub>3</sub> CHFOOH	-998.9		
CH <sub>3</sub> OOCH <sub>3</sub>	-125.7	-125.9	
CF <sub>3</sub> OOCF <sub>3</sub>	-1458.1	-1507.1	-1507.1

<sup>a</sup> Experimental values have error limits and unless noted are from JANAF Tables, Ref. 10.

<sup>b</sup> R. Zellner in Ref 1(a), p. 249. Value in [ ] from R. Atkinson in Ref 1(a) p. 163.

<sup>c</sup> Ref. 11. Values in ( ) from Ref. 12 based on values in Ref. 11.

<sup>d</sup> Ref. 13

<sup>e</sup> Value estimated by group additivity in Ref. 14 is -904.2.

<sup>f</sup> Ref. 15

<sup>g</sup> No error limits given in Ref. 10.

---

Our values in Table I can be compared to the most extensive set that is available, that of Zellner (Ref 1(a), p. 249). Where our values differ, we tend to have more negative heats of formation, except for the heats of formation of the peroxides and CF<sub>3</sub>C(O)Cl where our values are more positive. For the important beta scission C-C bond cleavage of CF<sub>3</sub>CHFO\*, Zellner's values yield -7.9 kcal/mol, in good agreement with our calculated value of -6.2 kcal/mol.

**Table II. Atmospheric Decomposition Pathways for HFC-134a and HFC-23**

Reaction	$\Delta H(\text{kcal/mol})$
HFC-134a	
$\text{CF}_3\text{CH}_2\text{F} + \text{OH}^* \rightarrow \text{CF}_3\text{CHF}^* + \text{H}_2\text{O}$	-14.7
$\text{CF}_3\text{CFH}^* + \text{O}_2 \rightarrow \text{CF}_3\text{CFHOO}^*$	-37.7
$\text{CF}_3\text{CFHOO}^* + \text{H}_2\text{O} \rightarrow \text{CF}_3\text{CFHOOH} + \text{OH}^*$	28.1
$\text{CF}_3\text{CFHOO}^* + \text{OOH}^* \rightarrow \text{CF}_3\text{CFHOOH} + \text{O}_2$	-39.5
$\text{CF}_3\text{CHFOOH} + h\nu \rightarrow \text{CF}_3\text{CHFO}^* + \text{OH}^*$	45.2 (15,810 $\text{cm}^{-1}$ )
$\text{CF}_3\text{CHFO}^* \rightarrow \text{CF}_3^* + \text{CHFO}$	-6.2
$\rightarrow \text{CF}_3\text{CHO} + \text{F}^*$	39.2
$\rightarrow \text{CF}_3\text{CFO} + \text{H}^*$	9.0
$\text{CF}_3\text{CHFO}^* + \text{O}_2 \rightarrow \text{CF}_3\text{CFO} + \text{HOO}^*$	-42.6
$\text{CF}_3\text{CHFO}^* + \text{H}_2\text{O} \rightarrow \text{CF}_3\text{CHFOH} + \text{OH}^*$	9.8
HFC-23	
$\text{CF}_3\text{H} + \text{OH} \rightarrow \text{CF}_3^* + \text{H}_2\text{O}$	-13.3
$\text{CF}_3^* + \text{O}_2 \rightarrow \text{CF}_3\text{OO}^*$	-42.1
$\text{CF}_3\text{OO}^* + \text{H}_2\text{O} \rightarrow \text{CF}_3\text{OOH} + \text{OH}^*$	28.8
$\text{CF}_3\text{OO}^* + \text{OOH}^* \rightarrow \text{CF}_3\text{OOH} + \text{O}_2$	-38.8
$\text{CF}_3\text{OOH} + h\nu \rightarrow \text{CF}_3\text{O} + \text{OH}$	49.8 (17,420 $\text{cm}^{-1}$ )
$\text{CF}_3\text{O}^* \rightarrow \text{CF}_2\text{O} + \text{F}^*$	18.6
$\text{CF}_3\text{O}^* + \text{H}_2\text{O} \rightarrow \text{CF}_3\text{OH} + \text{OH}^*$	0.5

In conclusion, we have calculated the heats of formation of a variety of species important in the atmospheric decomposition of HFC-134a by means of ab initio molecular orbital theory and appropriately chosen chemical reactions.

## References

1. a) "Scientific Assessment of Stratospheric Ozone: 1989, Volume II, Appendix: AFEAS Report, World Meteorological Organization, Global Ozone Research and Monitoring Project - Report No. 20, p. 249, 1989; b) "Kinetics and Mechanisms for the Reactions of Halogenated Organic Compounds in the Troposphere" Step-Halocside/AFEAS Workshop, University College, Dublin, Ireland, 1991.
2. a) Dixon, D. A.; Smart, B. E. *Chem. Eng. Comm.*, **98**, (1990) 173. b) Dixon, D. A. *J. Phys. Chem.*, **92**, (1988) 86.
3. Dunning, T. H., Jr.; Hay, P. J. in "Methods of Electronic Structure Theory," Schaefer, H. F., III, Ed., Plenum Press: New York, 1977, Ch. 1.
4. GRADSCF is an ab initio program system designed and written by A. Komornicki at Polyatomics Research.
5. a) Komornicki, A.; Ishida, K.; Morokuma, K.; Ditchfield, R.; Conrad, M. *Chem. Phys. Lett.*, **45**, (1977) 595. b) McIver, J. W., Jr.; Komornicki, A. *Chem. Phys. Lett.*, **10**, (1971) 202. c) Pulay, P. in "Applications of Electronic Structure Theory," Schaefer, H. F. III, Ed.; Plenum Press: New York, 1977, p.153.
6. a) King, H. F.; Komornicki, A. *J. Chem. Phys.*, **84**, (1986) 5465. b) King, H. F.; Komornicki, A. in "Geometrical Derivatives of Energy Surfaces and Molecular Properties" Jorgenson, P.; Simons, J. Eds. NATO ASI Series C. Vol. 166, D. Reidel: Dordrecht 1986, p. 207.
7. a) Møller, C.; Plesset, M. S. *Phys. Rev.*, **46**, (1934) 618; b) Pople, J. A.; Binkley, J. S.; Seeger, R. *Int. J. Quantum Chem. Symp.*, **10**, (1976) 1; c) Pople, J. A.; Krishnan, R.; Schlegel, H. B.; Binkley, J. S.; *Int. J. Quantum Chem. Symp.*, **13**, (1979) 325; d) Handy, N. C.; Schaefer, III *J. Chem. Phys.*, **81**, (1984) 5031.
8. Schlegel, H. B. *J. Chem. Phys.*, **84**, (1986) 4530.

9. GAUSSIAN 92. Frisch, M. J.; Trucks, G. W.; Head-Gordon, M.; Gill, P. M. W.; Wong, M. W.; Foresman, J. B.; Johnson, B. G.; Schlegel, H. B.; Robb, M. A.; Replogle, E. S.; Gomperts, R.; Andres, J. L.; Raghavachari, K.; Binkley, J. S.; Gonzalez, C.; Martin, R. L.; Fox, D. J.; DeFrees, D. J.; Baker, J.; Stewart, J. J. P.; Pople, J. A., Gaussian Inc., Pittsburgh, PA 1992.
10. Chase, Jr., M. W.; Davies, C. A.; Downey, Jr., J. R.; Frurip, D. J.; MacDonald, R. A.; Syverud, A. N. *J. Phys. Chem. Ref. Data*, **14**, *Supple. 1*, (1985). (JANAF Tables)
11. Batt, L.; Walsh, R. *Int. J. Chem. Kinet.*, **14**, (1982) 933; **15**, (1983) 605.
12. Francisco, J. S.; Williams, I. H. *Int. J. Chem. Kinet.*, **20**, (1988) 455.
13. DeMore, W. B.; Sander, S. P.; Golden, D. M.; Hampson, R. F.; Kurylo, M. J.; Howard, C. J.; Ravishankara, A. R.; Kolb, C. E.; Molina, M. J. "Chemical Kinetics and Photochemical Data for Use in Stratospheric Modeling. Evaluation No. 10" JPL 92-20, Jet Propulsion Laboratory, Pasadena, CA 1992
14. Chen, Y.; Rauk, A.; Tschuikow-Roux, E. *J. Chem. Phys.*, **94**, (1991) 7299.
15. Pedley, J. B.; Naylor, R. D.; Kirby, S. P. "Thermochemical Data of Organic Compounds, 2nd Ed. Chapman and Hall: London 1986.

0 2 1 5

## Experimental determination of uptake coefficient for acid halides.

George Ch., Ponche J.L., Mirabel Ph.  
Laboratoire de Physico-Chimie de l'Atmosphère.  
Centre de Géochimie de la Surface and  
Chemistry department, Université Louis Pasteur  
28,, rue Goethe  
F-67083 STRASBOURG Cedex

### 1. Introduction.

The substitution of CFC's by HCFC's is based on their much larger tropospheric reactivity. The accepted homogeneous gas phase degradation mechanism of HCFC's leads to the formation of carbonyl ( $\text{COX}_2$ ) and haloacetyl halides (RCOX). The HCFC's lifetime through this degradation pathway will therefore be in the range of 1 to 5 years. But the fate of the secondary oxidation products (RCOX) is yet not clear and their lifetime is expected to be long is only gas phase processes are considered [1]. Thus the fate of these carbonyl and haloacetyl halides will depend on the heterogeneous processes i.e. dissolution in water. Some studies [2-6] have shown that the uptake rate of these species by the aqueous phase is slow, governed by their hydrolysis rate (described by the hydrolysis rate constant  $k$ ) in water, but is also limited by their low solubility (described by the Henry's law constant  $H$ ). However, these parameters are still under studies and their values open to questions.

We report in this study experimental measurements of uptake rates in water of some carbonyl and haloacetyl halides ( $\text{CCl}_3\text{COCl}$ ,  $\text{CF}_3\text{COCl}$ ,  $\text{CF}_3\text{COF}$  and  $\text{COF}_2$ ) with the droplet train apparatus. This technique allows the deconvolution of the hydrolysis and solubility steps of the uptake i.e. make it possible to estimate  $H$  and  $k$  for each compound.

### 2. Experimental.

A detailed description of the experimental set-up has already been given previously [7] and will not be repeated here. We shall, however, briefly recall the principles of operation. A stream of monodispersed droplets (100 to 110  $\mu\text{m}$  of diameter), generated by the vibrating orifice method, is exposed in the interaction chamber to known amounts of the halogenated compound under study diluted in nitrogen. The experimental set-up is a low pressure (20-25 torr, in order to increase gas phase diffusion) flow tube reactor which length can be varied allowing contact times between the droplets and the gas phase in the range of 4 to 16 ms. An important aspect of this droplets train technique is the control of the water vapour pressure in the reactor since it controls the surface temperature of the droplets [8]. In our experiments the gas phase was saturated, before

0 2 1 6

entering the interaction chamber, with water vapour in such a way that the temperature was varied between 274 and 294 K. The droplets are then collected in order to be analysed by means of ion chromatography using a Waters IC-Pack A HR column with an IC-Pack guard column. For the acid halides of interests ( $\text{COF}_2$ ,  $\text{CY}_3\text{COX}$  with X and Y= F or Cl) we have analysed the presence of the halides  $\text{X}^-$  in the solution by conductimetry using a borate/gluconate eluant, and the presence of the acid  $\text{CF}_3\text{COOH}$  by U.V. detection using an octanesulfonic acid sodium salt eluant (2.5mM). These two techniques give the same results for the amount of trace gas incorporated in our experiments within 7%, which corresponds roughly to the accuracy of the chromatographic system. Furthermore, the conductimetric method is closed to its detection limit while the U.V. method is still very sensitive.

The gas phase concentrations obtained by dilution of a known flux of the halogenated compounds in nitrogen are also measured by means of liquid chromatography after dissolution of a known volume of gas in water. Care was taken to have complete hydrolysis of the halogenated compounds and for this the dissolution time was varied between 1 and 24 hours without any changes. The products ( $\text{CF}_3\text{COCl}$ ,  $\text{CF}_3\text{COF}$  and  $\text{COF}_2$ ) were obtained from Fluorochem, while  $\text{CCl}_3\text{COCl}$  was obtained from Aldrich, and were used without further purification.

The chemical analysis of the collected liquid phase leads to a measure of the aqueous concentration of trace gas absorbed by the liquid phase  $n_{\text{abs}}$ , which can be related to the volume rate of flow  $F_g$  ( $\text{cm}^3 \cdot \text{s}^{-1}$ ) of the carrier gas and to the change of the trace gas concentration  $\Delta n$  by:

$$n_{\text{abs.}} = F_g \cdot \Delta n. \quad (1)$$

We can then calculate the observed uptake coefficient  $\gamma_{\text{obs.}}$ , which reflects the different factors affecting the uptake of a gaseous specie [7,8] by:

$$\gamma_{\text{obs.}} = \frac{F_g}{\frac{1}{4} \bar{c} N S_d} \cdot \frac{\Delta n}{n} \quad (2)$$

where  $n$  is the trace gas concentration,  $\bar{c}$  is the trace gas thermal velocity ( $\text{cm} \cdot \text{s}^{-1}$ ) and  $N S_d$  the total area ( $\text{cm}^2$ ) exposed by the  $N$  droplets present in the interaction zone. In this apparatus, the train of droplets and the gas flow pass coaxially through the flow tube leading to the possible existence of a concentration gradient along the length of the interaction chamber. Integrating the uptake over the length of the flow tube gives [7, 8]:

$$\gamma_{\text{obs.}} = \frac{F_g}{\frac{1}{4} c N S_d} \ln \left( \frac{n^{\text{in}}}{n^{\text{in}} - \Delta n} \right) \quad (3)$$

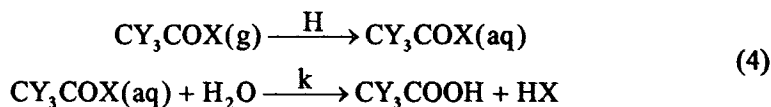
where  $n^{\text{in}}$  is the inlet gas phase concentration.

This uptake coefficient reflects a convolution of all the processes which may influence the rate of mass transfer between the aqueous and gaseous phases. In the next section, we discuss the different steps present in the incorporation of these halogenated compounds.

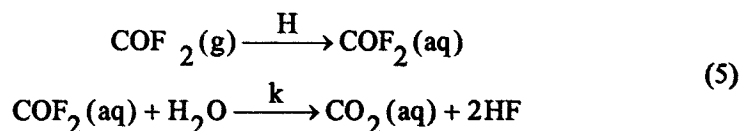
### 3. Results

Experiments were performed for the four compounds of interests ( $\text{COF}_2$ ,  $\text{CCl}_3\text{COCl}$ ,  $\text{CF}_3\text{COCl}$  and  $\text{CF}_3\text{COF}$ ) in which the dependency of the uptake coefficient with the interaction time and the initial pH of the droplets were studied for temperatures in the range of 273 to 294 K. The interaction time was varied between 4 and 16 ms and the pH between 3 and 12, leading to uptake coefficients in the range  $5 \cdot 10^{-4}$  to  $5 \cdot 10^{-3}$ . Figure 1 shows the results obtain for these compounds. It is visible that no significant variation was observed when the initial pH of the droplets was changed. However, a slight temperature dependency was observed for  $\text{CF}_3\text{COF}$  and  $\text{COF}_2$  whereas a small time variation was noted for all four compounds. This last variation is more important in the case of the carbonyl fluoride compared to the three other halogenated acetyl.

To explain these observations, we have to take into account all sub-processes involved in the incorporation of the gaseous compounds. In regards to previously published data [3, 4], the controlling steps may be the solubility and the rate of hydrolysis. The small time decrease of the uptake coefficient reflects a convolution of saturation of the droplets surface due to low solubility and low hydrolysis rate. Thus, the haloacetyl halides react with water to form the trihalogenated acid according to the following equations:



whereas the carbonyl fluoride reacts with water leading to:



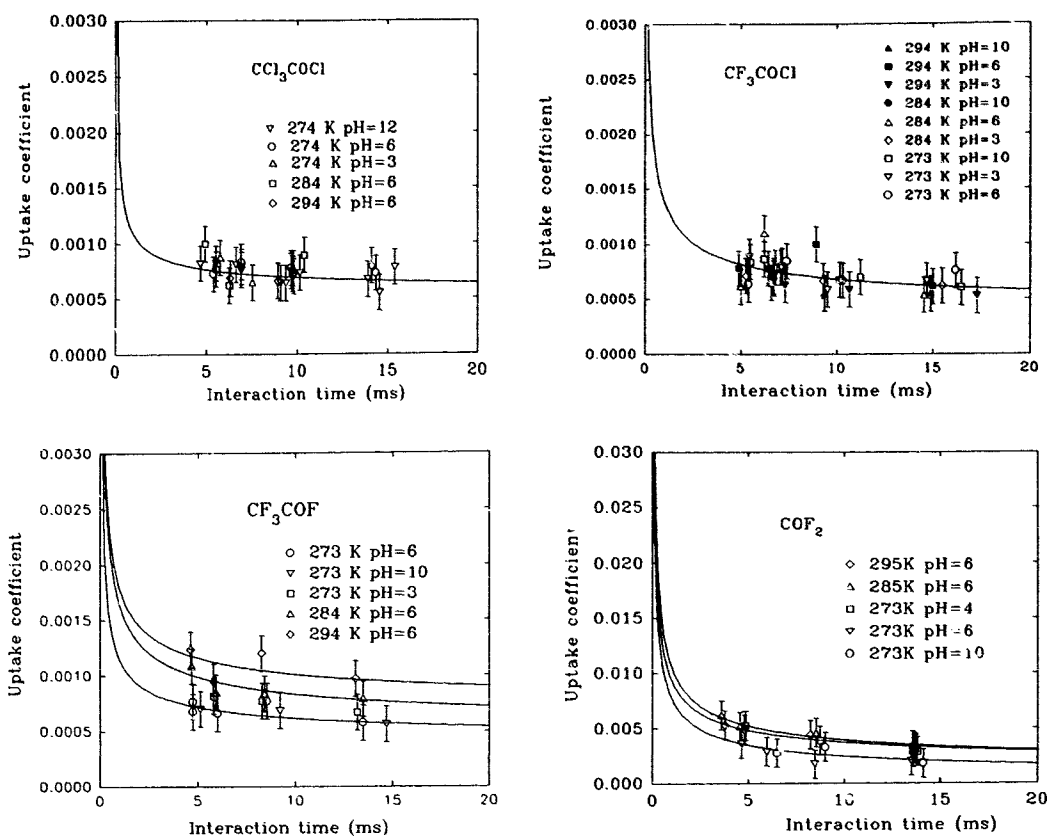


**Figure 1:** measured uptake coefficients  $\gamma_{obs}$  for  $CCl_3COCl$ ,  $CF_3COCl$ ,  $CF_3COF$  and  $COF_2$  as a function of interaction time, initial pH and temperature. The solid lines represent the fit of equation (6) to our data.

The combination of the establishment of the gas/liquid equilibrium (described by the Henry's law constant) followed by the hydrolysis (first order rate constant  $k$ ) corresponds to the overall kinetic of the uptake of the halogenated compounds [3,4]. The steady state between surface saturation and chemical reaction can be described by equation (6) [9]:

$$\gamma_{obs} = \frac{4HRT\sqrt{D_{aq}}}{\bar{c}} \times \left( \frac{1}{\sqrt{t}} + \sqrt{k} \right) \quad (6)$$

where  $R$  is the gas constant,  $D_{aq}$  the aqueous phase diffusion coefficient (calculated by the Wilke and Chang formula [10]) and  $t$  the interaction time. This relationship will allow us to deconvolute  $H$  and  $k$  and makes it possible to estimate these two constants.

The results of the fit of equation (6) to our data for the different investigated pH and temperatures are plotted in figure 1 (solid line). These results show no significant variation of  $H$  nor

k when the initial pH of the droplets was changed. For the two chlorides no significant variation was observed when the temperature was changed whereas for the two fluorides a slight increase of the uptake coefficient with temperature was observed. In tables I and II we present average values for H and k which uncertainties are about a factor 2 and 3 respectively.

**Table I:** estimated hydrolysis rate constants k and Henry's law constants H for the two chlorides under study (average values for the studied pH range).

	H (M.atm <sup>-1</sup> )	k (s <sup>-1</sup> )
CCl <sub>3</sub> COCl	1.9	520
CF <sub>3</sub> COCl	2.5	200

The independence of the hydrolysis rate constant with pH seems to be in apparent disagreement with the observed acid and alkaline catalysed hydrolysis of acids halides [11,12]. However, this can be explained by considering that the dissolution of the acids halides followed by their hydrolysis, which products undergo acid-base dissociation, will change the droplets surface pH. Assuming that the gaseous species is always in equilibrium with the liquid droplets surface and that the hydrolysis is a first order kinetic, it becomes possible to estimate the pH at the surface of the droplets [7,8]. This estimation shows that the dissolution of the halides acidify the surface of the droplets even for an initial pH=12. In fact, whatever is the initial pH value of the droplets, the pH at the surface after a few milliseconds exposure to the gas phase is always very small (pH ≤ 4). This point explains the apparent independence of the estimated hydrolysis rate constant with the initial pH of the droplets.

**Table II:** estimated Henry's law and hydrolysis rate constant for CF<sub>3</sub>COF and COF<sub>2</sub> for an initial pH=6 as a function of temperature.

	273 K	284 K	294 K
<b>COF<sub>2</sub></b>			
H (M.atm <sup>-1</sup> )	21	20	15
k (s <sup>-1</sup> )	< 1	8	18
<b>CF<sub>3</sub>COF</b>			
H (M.atm <sup>-1</sup> )	3.2	3.2	2.6
k (s <sup>-1</sup> )	71	147	326

### **Comparison with other results.**

The order of magnitude of the uptake coefficients reported here is consistent with those reported by previous studies. In all cases low uptake coefficients were observed [2,6]. However, all these results show that the uptake by an aqueous phase will lead to short estimated lifetime of the studied species.

De Bryun *et al.* [3, 4]. have developed a new experimental technique which allows, in a similar way as the one presented here, to deconvolute the hydrolysis and solubility effects. The principle of their method is based on the reaction of a column of bubbles with water, during given contact times which can be varied between 0.1 and 2 s. Their estimates show similar orders of magnitude for H but large differences for k (figure 2). The large discrepancy between the two methods is not yet clear, even if the two methods appear to be similar in principle and use the same treatment of the data, except that the time scales are different.

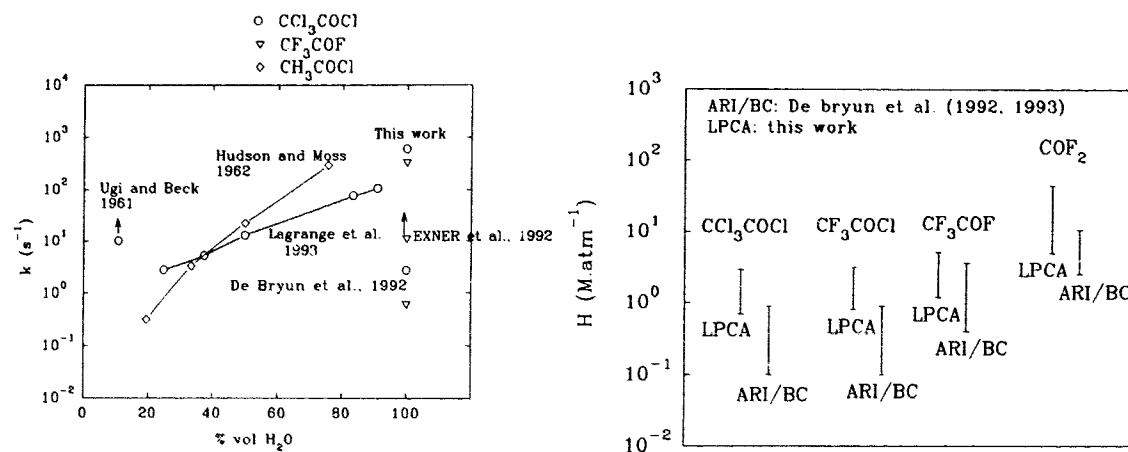


Figure 2: comparison with the estimated values of H and k with literature data.

Unfortunately, there exists only a few measurements of rate law of hydrolysis for some acetyl fluorides or chlorides, and mostly in poor water containing solutions in order to limit the rate which is, otherwise, too fast to be observed directly. Exner *et al.* [13] have measured the hydrolysis rate constant of CF<sub>3</sub>COF in solutions containing less than 1% water in volume in organic solvents. They have extrapolated linearly their data to pure water and obtained a value of 11 s<sup>-1</sup> which has to be considered as a lower limit to the actual hydrolysis rate constant. In fact, Bunton and Fendler [11], George *et al.* [12] conducted studies in which the effect of the amount of water in organic solutions was studied. These results clearly show that the hydrolysis rate constant increases exponentially with the concentration of water (figure 2). In collaboration with Pr. J. Lagrange in Strasbourg, we have also performed direct measurements of the hydrolysis rate law of CCl<sub>3</sub>COCl using a stop flow technique [12], which leads to  $k=152$  s<sup>-1</sup> for a pH between 4 and 7. Outside this pH range, the rate constant increased, leading to values too high to be measured by the experimental technique. If we consider that our pH at the surface is always acidic (pH ≤ 4), our estimated  $k$  is in good agreement with the direct observations as plotted in figure 2. In addition, Ugi and Beck [14] have followed the hydrolysis of CCl<sub>3</sub>COCl in 10.9% vol water and 89.1% vol acetone at 253K and found a lower limit of  $k > 10$  s<sup>-1</sup> also consistent with our estimated value of  $k$ .

Hudson and Moss [16] have studied the hydrolysis of acetyl chloride (figure 2), and measured  $k=292 \text{ s}^{-1}$  in a 75.6% vol. water and 24.4 % vol. dioxan at 300 K. Swain and Scott [15] also studied the hydrolysis of acetyl chloride and fluoride in a 25%vol. water and 75% vol acetone mixture at 298 K, they found  $k=0.86$  and  $0.0001 \text{ s}^{-1}$  for the chloride and fluoride respectively. However, all these rates of hydrolysis are expected to be even faster in pure water [11, 12].

With all these observations in mind, we believe that the estimated rate of hydrolysis and solubilities will give interesting input data for modeling studies of the atmospheric lifetime and deposition of these halogenated compounds. The reported values are large enough so that the expected lifetime due to heterogeneous processes should be short and therefore will limit the impact of these chlorine containing species.

### 3. References

- [1] BUTLER R. and SNELSON A., *J. Air pollut. Control assoc.*, **29** (1979), 833.
- [2] WORSNOP D.R., ROBINSON G.N., ZAHNISER M.S., KOLB C.E., DUAN S.X., DeBRUYN W., SHI X. and DAVIDOVITS P., STEP-HALOCSIDE/AFEAS WORKSHOP Dublin 14-16 May 1991,132.
- [3] De BRUYN W.J., DUAN S.X., SHI X.Q., DAVODOVITS P., WORSNOP D.R., ZAHNISER M.S. and KOLB C.E., *Geophys. Res. Lett.*, **19** (1992), 1939.
- [4] De BRUYN W.J., SHORTER J.A., DAVODOVITS P., WORSNOP D.R., ZAHNISER M.S., and KOLB C.E., *AFEAS Workshop Proceedings, Brussels 1992*.
- [5] IBUSUKI T., TAKEUCHI K., KUTSUNA S., *AFEAS Workshop Proceedings, Brussels 1992*.
- [6] De BRUYN W.J., SHORTER J.A., DAVODOVITS P., WORSNOP D.R., ZAHNISER M.S., and KOLB C.E., STEP-HALOCSIDE/AFEAS WORKSHOP Dublin 22-24 March 1993, this book.
- [7] PONCHE J.L., GEORGE Ch. and MIRABEL Ph., *J. Atmos. Chem.*, **16** (1993), 1.
- [8] WORSNOP, D.R., ZAHNISER, M.S., KOLB, C.E., GARDNER, J.A., JAYNE, J.T., WATSON, L.R., VAN DOREN, J.M., DAVIDOVITS, P., *J. Phys. Chem.*, **93** (1989), 1159.
- [9] JAYNE J.T., DUAN S.X., DAVIDOVITS P., WORSNOP D.R., ZAHNISER M.S. and KOLB C.E., *J. Phys. Chem.*, **96** (1992), 5452-5460.
- [10] REID, C.R., SHERWOOD, T.K., "The properties of gases and liquids", ed. Mc Graw Hill Company, 520, 1986.
- [11] BUNTON C.A. and FENDLER J.H., *J. Org. Chem.*, **31** (1966) 2307.
- [12] GEORGE Ch, PONCHE J.L. , Ph. MIRABEL, LAGRANGE J., PALLARES C. and LAGRANGE Ph., Final report to ECSA, 1993.
- [13] EXNER M., HERRMANN H., MICHEL J. and ZELLNER R., *AFEAS Workshop Proceedings, Brussels 1992*.
- [14] UGI I., BECK F., *Chem. Ber.*, **94** (1961), 1839.
- [15] SWAIN C.G. and SCOTT C.B., *J. Am. Chem. Soc.*, **75** (1953)246.
- [16] HUDSON R.F., MOSS G.E., *J. Chem. Soc.*, 5157-5163, 1962.

# An Aerosol Chamber Technique for the Determination of the Uptake of Carbonyl Halides by Submicron Aqueous Solution Droplets : Phosgene

Wolfgang Behnke, Manfred Elend, Heinz-Ulrich Krüger and Cornelius Zetzsch

Fraunhofer-Institut für Toxikologie und Aerosolforschung  
Nikolai-Fuchs-Str. 1  
W-3000 Hannover 61  
F. R. Germany

## Introduction

The tropospheric degradation of halogenated hydrocarbons, HCFC's and HFC's is known to lead to carbonyl and acid halides, which are expected to be hydrolyzed to the corresponding acids rapidly. Either heterogeneous reactions with aerosols (leading to washout) or surface contact with the oceans may then remove the carbonyl halides. Only a few data on the hydrolysis rates of carbonyl chlorides are available, mostly from time resolved conductivity measurements at  $-20^{\circ}\text{C}$  in acetone, containing a mole fraction of 0.333 of water [1] where the following rate constants were observed:  $\text{CH}_3\text{CClO}$ :  $0.001\text{s}^{-1}$ ,  $\text{ClCH}_2\text{CClO}$ :  $0.02\text{s}^{-1}$ ,  $\text{Cl}_2\text{CHCClO}$ :  $3.1\text{s}^{-1}$ ,  $\text{COCl}_2$ :  $1\text{s}^{-1}$ ,  $\text{CCl}_3\text{CClO}$ :  $> 10\text{s}^{-1}$ . It should be noted that an extrapolation of these data to pure water according to the exponential dependence on mole fraction is fairly uncertain. Such an extrapolation may yield values for phosgene around  $80\text{s}^{-1}$  at  $-50^{\circ}\text{C}$  and  $400\text{s}^{-1}$  at  $-20^{\circ}\text{C}$ , i.e. considerably higher than  $10^3\text{s}^{-1}$  at room temperature. This contrasts with results [2] from a liquid jet method in pure water: In measurements of Henry's law constant,  $H$ , of phosgene, an interference of hydrolysis was observed at 35 and  $45.5^{\circ}\text{C}$  and extrapolated to a value of  $6\text{s}^{-1}$  at  $25^{\circ}\text{C}$  (the rate constant for the hydrolysis by  $\text{OH}^-$  was obtained in separate measurements with added  $\text{NaOH}$  to be  $1.6 \cdot 10^4\text{mol}^{-1}\text{s}^{-1}$  at  $25^{\circ}\text{C}$ ). It should be noted that the hydrolysis of phosgene occurs in two consecutive steps, which could not be distinguished in the studies (i.e. the second step was assumed to be faster than the first step, taken to be irreversible). According to a recent assessment [3] the tropospheric lifetime of phosgene is limited to a few days mainly by hydrolysis and rainout.

Because of the systematic behaviour of an increase with electron-withdrawing substituents, faster hydrolysis rates are expected for the analogous fluorinated compounds, where a safe lower limit of  $k > 10^3\text{s}^{-1}$  has been proposed [4]. Since it was assumed to be highly probable (although not certain at that time) that trifluoroacetyl fluoride is scavenged by clouds, a detailed global model calculation on the expected rainout of trifluoroacetic acid has recently been carried out [5].

The mass accommodation coefficient,  $\alpha$ , determines if thermodynamic equilibration between the gas and aqueous species of the clouds can be fast enough for rainout, and only at  $\alpha < 10^{-6}$  uptake by the sea surface may be more important. At larger  $\alpha$  the accommodation will have a negligible impact on equilibration in clouds, and the overall uptake will be determined by  $H$  and  $k$ . For  $H$  values in the range  $10^{-6} - 1\text{mol l}^{-1}\text{atm}^{-1}$  and  $k > 10^2\text{s}^{-1}$  uptake by clouds will dominate while for  $k < 10^2\text{s}^{-1}$ , ocean deposition will be the major pathway.

On the other hand, cloud formation and rainout are dependent on seasons and sometimes and in some regions of the globe rare events. Then the uptake and hydrolysis of the carbonyl halides may occur by much smaller aerosols: the ubiquitous condensation nuclei (which are required to form clouds and remain after reevaporation of clouds). The impact of cloud condensation nuclei on tropospheric chemistry is demonstrated e.g. by the observation of a sudden decrease of  $\text{NO}_3$  (observed by DOAS, see [6]) during nighttime. The disappearance coincides with rising humidity by cooling, and  $\text{NO}_3$  (that is in equilibrium with  $\text{N}_2\text{O}_5$ ) disappears often soon after midnight in the summer months, even before the dewpoint is reached at ground level. Cloud condensation nuclei are assumed to be responsible for the rapid removal of  $\text{NO}_3$  and  $\text{N}_2\text{O}_5$  and for a coinciding increase of  $\text{HNO}_3$  and  $\text{HONO}$ . These cloud condensation nuclei are simulated by the saline, humidified aerosols of the present study.

Lifetime measurements of carbonyl halides in glass vessels appear to have a poor reproducibility and are thus difficult to transfer to environmental behaviour. For phosgene, half-lives ranging from a few minutes to several days are observed in glass vessels at different surface/volume ratios and with inserted surfaces [7]. An inhibiting effect of  $\text{HCl}$  on the hydrolysis at long reaction times and promoting effects of phosgene at high concentration levels and of the surface/volume ratio,  $S/V$ , were observed and summarized in the rate law: 
$$-d[\text{COCl}_2]/dt = k_1 [\text{COCl}_2]^2 [\text{H}_2\text{O}]^{0.5} + k_2 [\text{COCl}_2] S/V$$
 to obtain a homogeneous rate constant of  $k_1 = 0.5\text{bar}^{-2.5}\text{s}^{-1}$  and a heterogeneous removal rate constant of  $k_2 = 3 \cdot 10^{-6}\text{cm s}^{-1}$  (at  $\approx 296\text{K}$  and low partial pressures of phosgene). The heterogeneous removal rate,  $k_2 S/V$ , can be converted by simple kinetic theory (neglecting turbulent diffusive mixing) to an uptake coefficient of the order of  $10^{-10}$ . Therefore (and because of a probable saturation of the chamber walls with  $\text{HCl}$  in those experiments and the influence of turbulent diffusion),

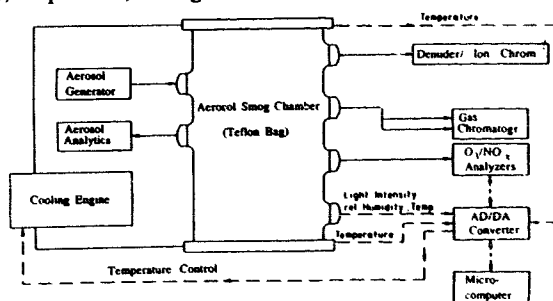
these results might be difficult to transfer to atmospheric aerosols. A lifetime of 20 h is observed in our experiment in the plain 2400 l glass chamber. This can be converted to an uptake coefficient of  $6 \cdot 10^{-8}$ , considering the S/V ratio of our vessel. A minimum uptake coefficient of  $\gamma > 10^{-6}$  has been estimated [8] from hydrolysis and Henry's law constant obtained in early liquid jet experiments [2], and  $\gamma > 3 \cdot 10^{-6}$  has similarly been estimated for the fluorinated carbonyl chlorides [4].

For aerosol chamber experiments with aqueous aerosol, some salt content is required to stabilize the droplet size (at well defined rel. humidity). The results are expected to be independent of the type of electrolyte (besides a minor influence of ionic strength on gas solubility; for the potential influence of pH: see above). Since the chloride from the hydrolysis of phosgene cannot be detected in NaCl,  $\text{NaNO}_3$  (already employed in [2]) is used for the experiments of the present study.

#### Aerosol Chamber Experiments and Raw Data

The smog chamber facility at Hanover, shown in fig. 1 [9 - 11], is used to investigate the behaviour of the carbonyl halides in the present study. It is connected on-line with high resolution GC and equipped with aerosol production and characterization instrumentation. Some experience in the analytics of phosgene, dichloroacetyl chloride and trichloroacetyl chloride by direct gas chromatography and by ion chromatography with denuder techniques exists from a previous project [12, 13] - denuders are internally coated tubes, which can discriminate between gaseous compounds and the aerosol; in practice, HCl gas can be determined in NaCl aerosol with less than 3 % interference from the particles).

Fig. 1: Schematic diagram of the aerosol chamber facility at Hanover. A new Teflon bag ( $\approx 500$  l volume) is inserted for each run.



Since at typical tropospheric aerosol surface densities of  $10^5 \text{ cm}^2/\text{cm}^3$  the heterogeneous removal rate constant [7] yields a lifetime of the order of 1000 years for phosgene, about one month is expected in our smog chamber facility at its S/V ratio of  $0.1 \text{ cm}^{-1}$ . The experiments were carried out in teflon bags (FEP 200A, a fairly hydrophobic material, was chosen to avoid hydrolysis on the chamber walls) of  $\approx 500$  l volume at constant concentration of gaseous phosgene, that is monitored by gas chromatography [12, 13]. In contrast to the expectation of about one month, a typical lifetime of 250 h was observed for phosgene at  $66\%$  r.h. in the bags, that is most probably given by permeation, and an even shorter lifetime of 40 h is observed for HCl gas. Fairly monodisperse aerosol at high density is obtained by atomizing aqueous salt solutions [14], where charged particles are removed by pre-aging the aerosol in a storage bag before filling it into the final bag of the experiment. The size distribution is characterized by a differential mobility particle sizer (TSI 3071 + 3020) and rapid scanning over 50 size classes [11, 14]. Since data on the uptake and hydrolysis of phosgene in aqueous  $\text{NaNO}_3$  solutions exist [2], this salt was chosen as an aerosol, and fig. 2 shows aerosol size distributions obtained at  $66\%$  r.h., where the droplets are concentrated electrolytes, corresponding to  $\approx 8$  molar solution. The aerosol in fig. 2 can be described by a log-normal distribution with an initial standard deviation of 1.75 in the final bag, becoming slightly sharper with time (a standard deviation of 1.55 is attained after 6 h). Because of the hygroscopic properties, the mean diameter is dependent on only minor variations of the room temperature in the (air conditioned) laboratory.

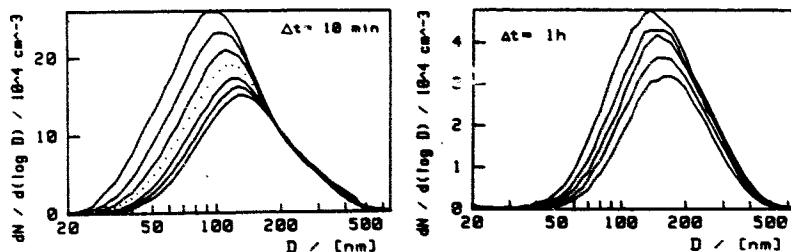


Fig. 2: Size distribution of aqueous  $\text{NaNO}_3$  aerosol, produced by atomizing an aqueous solution, immediately after production and 10 min later each in the pre-switched aerosol-supply bag (a), and behaviour of the aerosol after release into the final bag one hour later each (b). The dotted line marks a determination of the total mass density by microgravimetry on a filter sample.

The total aerosol mass density is determined by ion chromatography of  $\text{NO}_3^-$  and  $\text{Cl}^-$  combined with formation on size distribution, number density and hygroscopic properties (considering the relative humidity under the experimental conditions) and is calibrated by microgravimetry of teflon filter samples on a microbalance with a precision of  $1 \mu\text{g}$ . It is of the order of  $100 \mu\text{g m}^{-3}$  of aqueous  $\text{NaNO}_3$  solution droplets (exposed to phosgene in our experiments), representing a surface area of  $5 \cdot 10^5 \text{cm}^2/\text{cm}^3$ . Assuming an uptake coefficient of  $10^{-7}$  and phosgene levels of  $\approx 1 \text{ppm}$ , the uptake by the aerosol is estimated to be  $8 \cdot 10^{-13} \text{mol cm}^{-3} \text{h}^{-1}$ , and the corresponding  $2 \text{Cl}^-$  ions resulting from hydrolysis can be detected from hourly 50 l samples (of  $\approx 10\%$  of the aerosol mass) by ion chromatography.

Fig. 3 shows an example of a time profile observed for the ratio  $\text{Cl}^-/\text{NO}_3^-$  in the presence of 0.9 ppm of phosgene. A strong uptake of  $\text{Cl}^-$  is observed immediately after the injection of phosgene (that would correspond to an uptake coefficient of the order of  $10^{-5}$ , dashed line; this initial, sharp increase is much smaller in the presence of  $\text{NaHCO}_3$  buffer in the aerosol and is therefore believed to be an artifact). A much slower increase of  $\text{Cl}^-$  occurs subsequently, that is approximated by a straight line here. At uptake coefficients  $> 10^{-3}$ , the equation of Fuchs and Sutugin [15]:

$$\phi_{\text{COCl}_2}(r)/\text{cm}^3\text{s}^{-1} = (4\pi\lambda/3)(8kT/\pi m)^{1/2} \{r/[1+(\Gamma(r) + 4/3(1-\gamma)/\gamma)\lambda/r]\}, \quad (\text{I})$$

has to be applied, where  $\phi_{\text{COCl}_2}(r)$  denotes the loss rate of  $\text{COCl}_2$  in the presence of an aerosol particle as a function of its radius  $r$ ,  $\lambda$  the mean free path,  $k$  and  $T$  Boltzmann constant and temperature,  $m$  the mass of the  $\text{COCl}_2$  molecule, and  $\Gamma(r)$  a function correcting for the anisotropic velocity distribution close to the surface at large diameter.

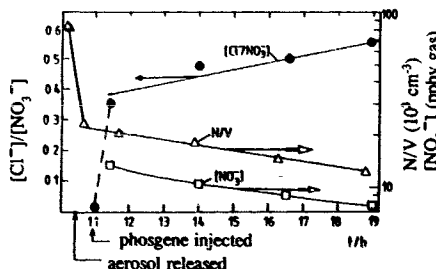


Fig. 3: Time profile of the ratio  $\text{Cl}^-/\text{NO}_3^-$  (left hand ordinate) observed in humidified  $\text{NaNO}_3$  aerosol (73.4% r.h.) after the injection of 0.9 ppm of phosgene. Time profiles of the number density,  $N/V$  (determined by a condensation nuclei counter) and the  $\text{NO}_3^-$  concentration (from ion chromatography of aerosol filter samples, given in ppb units, i.e. a hypothetical mixing ratio in the gas volume for comparison with phosgene) on a semilogarithmic scale (right hand ordinate). The time profiles of  $\text{NO}_3^-$  and  $\text{Cl}^-$ , combined with information on size distribution, number density and hygroscopic properties, are used to obtain (compute) the total absolute mass density of the moist aerosol under the experimental conditions.

For small values of  $\gamma$  ( $< 10^{-3}$ , as observed here for phosgene), the formula from the kinetic theory of gases is sufficient:

$$\phi_{\text{COCl}_2}(r)/\text{cm}^3\text{s}^{-1} = \pi r^2 \gamma (8kT/\pi m)^{1/2} \quad (\text{II})$$

The coefficient,  $\gamma$  (i.e. the ratio of reactive to total collisions), is fitted by using Newtons approximation for nonlinear functions to obtain agreement with  $k_{\text{observed}}$ , according to the equation

$$k_{\text{observed}} = \sum_i n_i \cdot \phi_{\text{COCl}_2}(r_i), \quad (\text{III})$$

where  $n_i$  denotes the number density of an individual aerosol size class,  $i$ . A rough estimate of the uptake coefficient by equation II, using the initial mean aerosol diameter, leads to a preliminary value of  $\gamma \approx 2.5 \cdot 10^{-7}$ .

Fig. 3 includes time profiles of  $\text{NO}_3^-$  and the number density. Subsequent to the release of the aerosol from the first into the second bag (causing a decrease to 1/3 of the density of the supply bag), a slow decrease of the number density with a lifetime of 10 to 15 h is observed.

The profile of  $\text{NO}_3^-$  shows a similar behaviour, indicating that no loss of nitric acid (by acidification and volatilization) occurs under these conditions. A significant loss of  $\text{NO}_3^-$  was observed at higher levels of phosgene (at 3 and 10 ppm and lower aerosol densities). In a supplementing run, the pH of the aerosol was controlled by adding  $\text{NaHCO}_3$  (79.6% r.h., since  $\text{NaHCO}_3$  is much less hygroscopic than  $\text{NaNO}_3$ ). This experiment, leading to an uptake coefficient of about  $2 \cdot 10^{-7}$ , did not differ significantly from our results with  $\text{NaNO}_3$  at 0.9 ppm. A summary of the aerosol chamber runs is given in table 1.

Table 1: Coefficients,  $\gamma$ , for the uptake of phosgene by submicron  $\text{NaNO}_3$  aerosol in Teflon bags, specifying the relative humidity (r.h., at 298 K), the mixing ratio of  $\text{COCl}_2$  injected and the initial aerosol volume density in the differential mobility particle sizer (v/V, including the liquid water content),  $V_{\text{liq}}/V_{\text{air}}$  (filter samples 1-4) and  $\phi_i$  (filter samples 2-4)

Run #	r.h. (%)	$[\text{COCl}_2]$ (ppb)	v/V ( $\mu\text{m}^3/\text{cm}^3$ )	$\gamma'$ ( $10^{-7}$ )	$(\gamma_2, \gamma_3, \gamma_4)^*$	$V_{\text{liq}}/V_{\text{air}}$ ( $10^{-10}$ )	$\phi_i$ ( $10^8 \text{s}^{-1}$ )
N640T	66.0	-	92	-			
N788T	71.5	8820	100	- <sup>a</sup>			
G789T	73.3	3010	-	- <sup>b</sup>			
N790T	75.0	3140	37	- <sup>a</sup>			
N791T	73.4	890	100	2.5 <sup>c</sup>			
N792T	71.5	977	192	1.4	(1.48, 1.91, 1.72)	4.2 3.8 3.6 3.2	3.7 4.4 3.5
N793T	75.7	970	-	- <sup>d</sup>			
N794T	85.5	951	15	0.1 <sup>a</sup>			
N795T	93.0	893	360	1.6	(1.25, 1.84, 2.17)	22 11.7 6.2 3.7	5.6 5.1 4.2 <sup>e</sup>
N796T	84.5	1040	420	1.5	(1.82, 1.84, 1.35)	11.4 6.9 5.5 4.5	6.5 5.3 3.4
H797T	79.6	948	102	2.5	(0.49, 1.52, 1.79) <sup>e</sup>	3.2 2.8 2.6 2.5	0.96 2.7 3.0
N798T	79.5	2025	210	1.2	(1.19, 1.25, 1.20)	6.1 5.2 4.6 4.2	3.6 3.3 2.8
N799T	80.5	1003	360	2.3	(2.90, 2.05, 1.72) <sup>f</sup>	14.2 7.7 5.6 3.2	7.5 4.1 2.1

\* Uptake coefficients  $\gamma'$  are rough estimates from the mean aerosol diameter, neglecting the shape of the size distribution and the decay of aerosol density, and  $\gamma_i$  are values obtained from individual filter samples with respect to the sample prior to injection of phosgene.

<sup>a</sup> Volatilization by acidification at high levels of  $\text{COCl}_2$  and low levels of  $\text{NaNO}_3$

<sup>b</sup> Residence times:  $\text{COCl}_2 \approx 250$  h,  $\text{H}_2\text{O} \approx 100$  h ( $\text{HCl} \approx 40$ h)

<sup>c</sup>  $\text{Cl}^-$  - interference in  $\text{NaF}$ -coated denuders corresponding to 0.28% loss of  $\text{COCl}_2$

<sup>d</sup> Not evaluated because of an unexpected decrease of  $\text{Cl}^-$  or rapid loss of aerosol density, respectively

<sup>e</sup> Blank experiment on the uptake of  $\text{COCl}_2$  by  $\text{NaNO}_3$ -loaded filters ( $x_{\text{Cl}^-} < 0.025$ )

<sup>f</sup> Aerosol buffered with  $\text{NaHCO}_3$  ( $x = 0.2$ )

<sup>g</sup> Run optimized for large aerosol diameter of  $\approx 0.3 \mu\text{m}$

### Final Evaluation and Discussion

A detailed evaluation of the data by comparing the uptake rates,  $k$ , with integrals of the size distribution [11] can be performed and the results are included in table 1. It should be noted, that  $\text{NaNO}_3$  is much less hygroscopic than  $\text{NaCl}$ . A corresponding shrinking can be observed when  $\text{NaCl}$  aerosol is converted to  $\text{NaNO}_3$  by the fast reaction with  $\text{NO}_2$  [16, 17]. A growth of  $\text{NaNO}_3$  is accordingly induced by the uptake of  $\text{Cl}^-$ . The final evaluation of the uptake coefficient has to include the size dependent loss of aerosol, the changing hygroscopic properties and the influence of humidity on aerosol size and surface area.

The limitation by the half-life of the aerosol in our teflon bags ( $\approx 15$ h), leads to a limit of  $\gamma \cdot [\text{COCl}_2] > 10^{-7}$  ppm for the minimum uptake coefficient required to determine a significant uptake. The maximum uptake coefficient to be determined will be about  $\gamma = 10^{-4}$ , limited by the time resolution given by the mixing time of the carbonyl halide with the aerosol. This limitation may preclude a measurement of the uptake coefficients of  $\text{CCl}_3\text{COCl}$  and  $\text{CF}_3\text{COCl}$ , where values of  $3 \cdot 10^{-3}$  (at pH = 12) and  $2 \cdot 10^{-4}$  (at pH = 7, dependent on pH between 3 and 10) have been obtained at 273 K [18]. Furthermore, (employing small gas bubbles [19] since the droplet train method was unable to detect a significant loss of gaseous phosgene [8]), uptake coefficients of  $4 \cdot 10^{-5}$  for  $\text{CF}_3\text{COF}$ ,  $1 \cdot 10^{-5}$  for  $\text{CF}_3\text{COCl}$  and  $5 \cdot 10^{-6}$  were obtained for phosgene at 290 K and pH = 6 [19], in a range accessible by our method. On the other hand, the latter value for phosgene contrasts with our determination of  $2 \cdot 10^{-7}$  for the same quantity on aerosols with high ionic strength. It should be noted that a similar value,  $2 \cdot 10^{-6}$ , has been obtained in our laboratory [20] by a wetted-wall flow tube technique [16] for phosgene on aqueous solutions (independent of pH between 0 and 10, increasing strongly at higher pH to almost  $10^{-4}$  at pH = 14). A slightly smaller value of  $1 \cdot 10^{-6}$  is observed at high ionic strength (2 molar  $\text{NaNO}_3$  solution). These observations clearly indicate that the existing measurements of the uptake coefficient are dependent on the hydrolysis rate constant (and therefore solubility-limited and do not constitute mass accommodation coefficients).

The extremely small diameter of the droplets in our measurements needs special consideration. The differential equation describing diffusive transport of phosgene (concentration in the droplet:  $c$ ) from the surface to the center of the droplet (radius:  $R$ ) and simultaneous hydrolysis is given (in polar coordinates,  $r$ ) by:

$$dc/dt = \frac{D}{r^2} \frac{d(r^2 dc/dr)}{dr} - k c, \quad (IV)$$

where  $D$  denotes the diffusion coefficient of phosgene in the liquid phase. The equation can be solved in steady state ( $dc/dt = 0$ ) and with the boundary conditions  $c = c_R$  for  $r = R$  (given by Henry's law constant) and  $dc/dr = 0$  for  $R = 0$  to lead to the equation:

$$c(r) = c_R \frac{R}{r} \frac{e^{r\sqrt{k/D}} - e^{-r\sqrt{k/D}}}{e^{R\sqrt{k/D}} - e^{-R\sqrt{k/D}}} \quad (V)$$

for the dependence of  $c$  on the radius  $r$ , where  $c_R$  is the steady state concentration at the droplet surface. Assuming an aerosol diameter of  $0.7 \mu\text{m}$  (the upper limit in our experiments) at a diffusion coefficient of  $D = 10^{-5} \text{ cm}^2 \text{ s}^{-1}$ , a hydrolysis rate constant  $k > 10^5 \text{ s}^{-1}$  would be required to obtain a surface concentration 10% larger than the average concentration of phosgene in the droplet. At smaller hydrolysis rate constants, the consumption of phosgene becomes proportional to the volume of the droplet (i.e.  $\gamma \sim r$ ):

$$-d[\text{COCl}_2]/dt = [\text{COCl}_2] H k V_{\text{liq}}/V_{\text{air}}, \quad (VI)$$

after integration:

$$\tau_{\text{phosgene}}^{-1} = H k V_{\text{liq}}/V_{\text{air}}. \quad (VII)$$

Only at much larger hydrolysis rate constants (or larger diameters) the consumption of phosgene becomes proportional to the surface of the droplets (i.e.  $\gamma$  independent of  $r$ ). An evaluation of our data of table 1 according to this equation is shown in fig. 4, where the decay rate of phosgene (obtained from the increase of  $\text{Cl}^-$  in the droplets, divided by 2) is plotted versus the aerosol volume. The figure confirms that the decay rate of phosgene is proportional to the aerosol volume (that is varied not only by aerosol diameter but also by number density). The product  $H \cdot k$  is obtained to be  $92 \pm 32 \text{ s}^{-1}$  in the droplets (using the dimensionless Henry's law constant of eq. VI and VII), corresponding to  $H \cdot k = 3.8 \pm 1.3 \text{ mol l}^{-1} \text{ atm}^{-1} \text{ s}^{-1}$ . An extrapolation of Henry's law constant obtained [2] to saturated  $\text{NaNO}_3$  solution ( $H = 0.04 \text{ mol l}^{-1} \text{ atm}^{-1}$ ) leads to a hydrolysis rate constant of  $95 \pm 33 \text{ s}^{-1}$ .

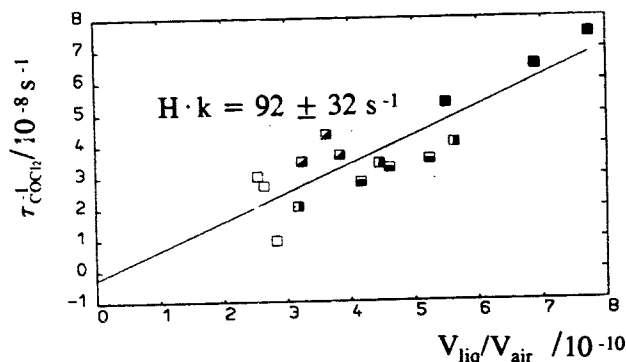
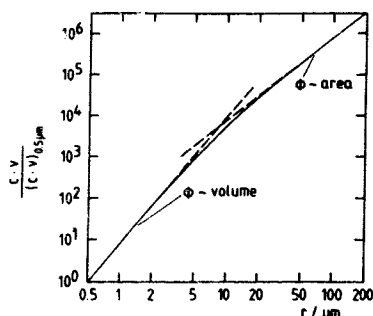


Fig. 4: Decay rate of phosgene (determined from the uptake of  $\text{Cl}^-$ ) in submicron saturated  $\text{NaNO}_3$  aerosol droplets vs the ratio of aerosol and gas volume. The data points stem from individual analyses of the runs (relative humidity in brackets) N792T (■, 71.5%), N798T (□, 79.5%), N799T (■, 80.5%), N796T (■, 84.5%), and N797T (□, 79.6%, buffered with  $\text{NaHCO}_3$ ).

The data of fig. 4 demonstrate that the decay rate of phosgene is proportional to the droplet volume below  $r = 2 \mu\text{m}$ . At much larger droplet sizes, complete saturation with phosgene is attained only in the surface layer, and the decay rate of phosgene would become proportional to the droplet surface area. This is illustrated in fig. 5, where the total amount of phosgene dissolved in the droplets in steady state is computed according to equation V (using  $D = 10^{-5} \text{ cm}^2 \text{ s}^{-1}$  and  $k = 100 \text{ s}^{-1}$ ) as a function of droplet size; above a droplet radius of  $50 \mu\text{m}$  the uptake becomes proportional to the surface area.

It should be noted that the change in uptake behaviour to  $\phi \sim \text{area}$  is dependent on the diffusion coefficient in the droplets. Turbulent diffusion may contribute above  $r = 50 \mu\text{m}$  and thereby shift this region significantly to larger values of  $r$ . Diffusive mixing leads to larger penetration depths of phosgene and consequently to larger  $\phi$  than shown in the upper half of fig. 5.

Fig. 5: Dependence of the uptake of phosgene on droplet size. The double logarithmic diagram is scaled to a droplet radius of 0.5  $\mu\text{m}$ . The limiting cases  $\phi \sim r^3$  for  $r < 2\mu\text{m}$  and  $\phi \sim r^2$  for  $r > 50\mu\text{m}$  are indicated by the straight lines.

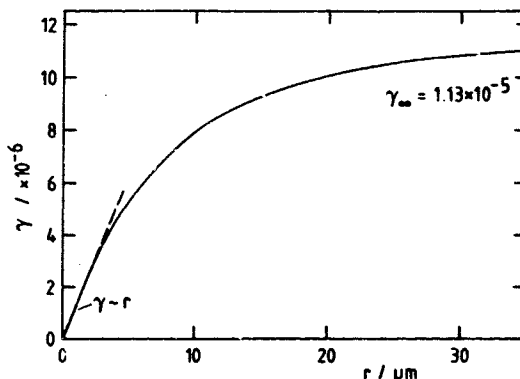


According to the kinetic theory, the corresponding loss rate of phosgene from the gas phase can be calculated from equation II to obtain  $\gamma$  by comparison with  $\phi = dc/dt$  from equation IV:

$$\phi_{\text{COCl}_2}(r) / \pi r^2 (8kT/\pi m)^{1/2}. \quad (\text{VIII})$$

Fig. 6 shows the computed dependence of  $\gamma$  on droplet size that leads to a limiting value of  $\gamma = 1.1 \cdot 10^{-5}$  at large droplet size (again considering molecular diffusion in the droplet alone). Since the uptake coefficient is solubility-limited, it may be larger by about a factor of 2 for pure water.

Fig. 6: Dependence of the uptake coefficient of phosgene on droplet size, computed from the curve of fig. 5 for saturated  $\text{NaNO}_3$  solution. Note the linear dependence of  $\gamma$  on  $r$  at submicron aerosol sizes.



It should be noted again, that this extrapolation to large droplet diameters (dependent on  $H \cdot k/D$ ) is obtained for an assumed value of  $(D/k)^{1/2}$  of  $3.2 \cdot 10^{-4}$  cm, based on our measurement of  $H \cdot k$  and the solubility extrapolated from [2]. An extrapolation of  $\gamma = 2 \cdot 10^{-6}$  (from our wetted-wall flow tube measurements and using  $H = 0.1 \text{ mol l}^{-1} \text{ atm}^{-1}$ ) would yield a value of  $510 \text{ cm}^{-1}$  for  $(k/D)^{1/2}$ , leading to  $D = 3.8 \cdot 10^{-4} \text{ cm}^2 \text{ s}^{-1}$  for  $k = 100 \text{ s}^{-1}$ . The uncertainty may well result from the measurement of  $H$  [2], that is based on calculated values of  $D$  ( $H \cdot D^{1/2}$  is the quantity derived from their experiment).

On the other hand, the quantity derived directly from our aerosol experiment,  $H \cdot k$ , is the quantity desired for the estimate of the removal of phosgene by cloud droplets. Our value of  $3.8 \text{ mol l}^{-1} \text{ atm}^{-1} \text{ s}^{-1}$  in saturated  $\text{NaNO}_3$  is almost an order of magnitude higher than the value of  $\approx 0.5 \text{ mol l}^{-1} \text{ atm}^{-1} \text{ s}^{-1}$  at 290 K, inferred from the recent experiments by the bubbler method [19] (based on  $D = 2 \cdot 10^{-5} \text{ cm}^2 \text{ s}^{-1}$  for pure water and leading to a tropospheric residence time of phosgene of about 20 days) and is expected to be even higher for pure water. Since  $\gamma > 10^{-6}$  appears to be accepted for phosgene, the mass accommodation coefficient does not limit the uptake by clouds by the resistance of the droplet surface. A recent 2-D/two-layer model calculation [21], employing  $H \cdot k = 0.1 \text{ mol l}^{-1} \text{ atm}^{-1} \text{ s}^{-1}$  at 293 K (Arrhenius-like extrapolations of the measurements of [2] from higher temperatures to 293 K yield  $H \cdot k^{1/2} = 0.19 \text{ mol l}^{-1} \text{ atm}^{-1} \text{ s}^{-1/2}$  or  $H \cdot k = 0.4 \text{ mol l}^{-1} \text{ atm}^{-1} \text{ s}^{-1}$ ) and leading to a total lifetime of about 50 days of phosgene due to wet deposition, may therefore require revision.

### Conclusions

The uptake of phosgene by submicron aerosol of saturated  $\text{NaNO}_3$  is limited by solubility and hydrolysis. The product of hydrolysis rate and Henry's law constant,  $k \cdot H$ , can be determined with reasonable precision by this technique, leading to  $H \cdot k = (3.8 \pm 1.3) \text{ mol l}^{-1} \text{ atm}^{-1} \text{ s}^{-1}$  in the droplets. This important quantity, governing tropospheric washout of the carbonyl halides, is expected to be about a factor of two higher for pure water

because of higher solubility (assuming that hydrolysis is not affected). A hydrolysis rate constant of the order of  $\approx 100 \text{ s}^{-1}$  can be inferred from the measurements at room temperature (much larger than a previous estimate from a liquid water jet method that delivers  $\text{H} \cdot \text{k}^{1/2}$ , confirmed by wetted-wall flow tube measurements of our laboratory). Although further experimental work is required for a reliable separation of H and k, the measurement of  $\text{H} \cdot \text{k}$  implies that the tropospheric lifetime of phosgene due to wet deposition is of the order of only 1 day. Additional sources of phosgene are required to balance this larger loss rate.

**Acknowledgements** This work was supported by AFEAS. The authors wish to thank J. Franklin (Solvay), J.-M. Libre (ATOCHEM), H. Pruppacher (University of Mainz) and U. Schurath (University of Bonn) and I. Ugi (Techn. University of Munich) for discussions, P. Mirabel and C. George (University of Strasbourg) and P. Wine and Th. Kindler (GeorgiaTech, Atlanta) for communication of unpublished results and V. Scheer (FhG) for supplementing measurements with a wetted-wall flow tube.

#### References

1. Ugi, I. and Beck, F. *Chem. Ber.* **94** (1961) 1839.
2. Manogue, W.H., and Pigford, L.A. *I.Ch.E. Journal* **6** (1960) 494.
3. Helas, G., and Wilson, S.R. *Atmos. Environment* **26A** (1992) 2975.
4. Wine, P., and Chameides, W.L. *Kinetics and Mechanisms for the Reactions of Halogenated Organic Compounds in the Troposphere. Scientific Assessment of Stratospheric Ozone: 1989, World Meteorology Organization, Report* **20** (1989) 273.
5. Rodriguez, J.M., Ko, M.K.W., Sze, N.D. and Heisey, C.W. In: *Kinetics and Mechanisms for the Reactions of Halogenated Organic Compounds in the Troposphere. STEP/HALOCSIDE/AFEAS workshop* (eds. M. McFarland and H. Sidebottom), pp. 138-143, Dublin 1991; Rodriguez, J.M., Ko, M.K.W., Sze, N.D. and Heisey, C.W. In: *Atmospheric Wet and Dry Deposition of Carbonyl and Haloacetyl Halides, Proc. AFEAS workshop*, pp. 25-32, Solvay Research and Technology Center, Brussels 1992.
6. Pitts, J.N. Jr., Biermann, H.W., Atkinson, R. and Winer, A.M. *Geophys. Res. Lett.* **11** (1984) 558.
7. Keiser, H. and Reichold, E. *Staub-Reinh. Luft* **48** (1988) 239.
8. Worsnop, D.R., Robinson, G.N., Zahniser, M.S. and Kolb, C.E., Duan, S.X., DeBruyn, W., Shi, X. and Davidovits, P. In: *Kinetics and Mechanisms for the Reactions of Halogenated Organic Compounds in the Troposphere. STEP/HALOCSIDE/AFEAS workshop* (eds. M. McFarland and H. Sidebottom), pp. 132-137, Dublin 1991; DeBruyn, W., Duan, S.X., Shi, X.Q., Davidovits, P., Worsnop, D.R., Zahniser, M.S. and Kolb, C.E. *Geophys. Res. Letters* **19** (1992) 1939.
9. Behnke, W., Holländer, W., Koch, W., Nolting, F. and Zetzsch, C. *Atmos. Environ.* **22** (1988) 1113.
10. Nolting, F., Behnke, W. and Zetzsch, C. *J. Atmos. Chem.* **6** (1988) 47.
11. Zetzsch, C., and Behnke, W. *Ber. Bunsenges. Phys. Chem.* **96** (1992) 488.
12. Behnke, W. and Zetzsch, C. In: *Kinetics and Mechanisms for the Reactions of Halogenated Organic Compounds in the Troposphere. STEP/HALOCSIDE/AFEAS workshop* (eds. M. McFarland and H. Sidebottom), pp. 144-149, Dublin 1991.
13. Behnke, W. and Zetzsch, C. *The yield of carbon tetrachloride from the tropospheric photochemical degradation of perchloroethene. Final report to ECSA and HSIA, Fraunhofer-Institute ITA, Hannover 1991.*
14. Behnke, W., Krüger, H.-U., Scheer, V. and Zetzsch, C. *J. Aerosol Sci.* **22** (S1) (1991) 609.
15. Fuchs, N. A., and Sutugin, A.G. In: *Int. Rev. of Aerosol Physics and Chemistry, Vol. 2* (eds. M. Hidy and J.R. Brock), pp. 1-60, Pergamon, New York 1971.
16. Behnke, W., Krüger, H.-U., Scheer, V. and Zetzsch, C. *J. Aerosol Sci.* **23** (1992) (S1) 933.
17. Behnke, W., Krüger, H.-U., Scheer, V. and Zetzsch, C. In: *Photo-oxidants and Precursors. Proc. EUROTRAC Sympos. '92* (eds. P.M. Borrell, P. Borrell, T. Cvitas and W. Seiler), pp. 565-570, SPB Academic Publ., Den Haag 1993.
18. George, C., Ponche, J.L. and Mirabel, P. In: *Atmospheric Wet and Dry Deposition of Carbonyl and Haloacetyl Halides, Proc. AFEAS workshop*, pp. 18-24, Solvay Research and Technology Center, Brussels 1992 (see also contribution to this workshop).
19. DeBruyn, W., Shorter, J.A., Davidovits, P., Worsnop, D.R., Zahniser, M.S. and Kolb, C.E. In: *Atmospheric Wet and Dry Deposition of Carbonyl and Haloacetyl Halides, Proc. AFEAS workshop*, pp. 12-17, Solvay Research and Technology Center, Brussels 1992 (see also contribution to this workshop).
20. Scheer, V., Behnke, W. and Zetzsch, C. (unpublished results)
21. Kindler, T.P., Chameides, W.L., Wine, P.H., Cunnold, D. and Alyea F. In: *Atmospheric Wet and Dry Deposition of Carbonyl and Haloacetyl Halides, Proc. AFEAS workshop*, pp. 33-43, Solvay Research and Technology Center, Brussels 1992.

# Formation of OClO and Cl<sub>2</sub>O<sub>3</sub> on ice in the Cl/O<sub>3</sub>-system at temperatures below -60°C and some results from the Br/O<sub>3</sub>-System.

U. Kirchner, M. Liesner, Th. Benter and R.N. Schindler

*Institut für Physikalische Chemie der Universität Kiel,  
Ludewig-Meyn-Str. 8, D-2300 Kiel 1*

## 1 Introduction

Both groundbased and air-born remote-sensing using UV/VIS absorption spectroscopy have shown that in periods of highly disturbed chlorine chemistry in the Antarctic as well as in the Arctic stratosphere, the OClO levels are considerably enhanced. Solomon [1] reports enhancement factors up to 100. It is generally accepted that the OClO observed is formed in a homogeneous reaction between ClO and BrO for which the rate constant and branching ratios have been determined recently [2 - 4]. No other atmospheric OClO-sources have been suggested. However, analysing stratospheric O<sub>3</sub> losses in periods of disturbed chemistry on the basis of air-born ClO and BrO measurements using the accepted kinetic parameters discrepancies as large as 35% between observations and model calculations were noted [5].

Laboratory experiments carried out in flowing Cl/O<sub>3</sub> mixtures at low temperatures persistently pointed towards an additional route of OClO formation in the presence of humidity [6] not considered up to now in atmospheric chemistry. This route does not involve bromine species. In the present investigation it is demonstrated that at temperatures low enough for polar stratospheric cloud formation, OClO is generated in a heterogenous process on ice. The results suggested that the OClO formed remains in/on the ice and reacts with further ClO to form Cl<sub>2</sub>O<sub>3</sub>. This also suggests that Cl<sub>2</sub>O<sub>3</sub> should be considered as an additional Cl-reservoir species.

The study also yielded UV/VIS absorption spectroscopic evidence that in the presence of bromine in the system a new, up to now in atmospheric studies unreported bromine oxide species is formed the high mass signals of which correspond to the oxide Br<sub>2</sub>O.

## 2 Experimental

The reactions were started by passing measured amounts of precooled O<sub>3</sub>/He and Cl/He gas flows at a total pressure of ~ 2 mbar through a cooled flow tube equipped with quartz windows for optical analysis. The ozone was swept out from a cold silica gel reservoir. Cl-atoms were generated by passing highly diluted Cl<sub>2</sub> through a microwave-powered discharge. The starting concentrations were [O<sub>3</sub>]<sub>0</sub> ≈ 2 · 10<sup>14</sup> cm<sup>-3</sup> and [Cl]<sub>0</sub> ≈ 10<sup>14</sup> cm<sup>-3</sup>. At the low temperatures used part of the reactants and products were collected at the walls of the flow tube acting as a cold trap. The reactions were stopped at predefined times by interrupting the reactant gas flows.

After pumping down the flow system to ~ 10<sup>-3</sup> mbar and isolating it from pumps, product analysis were performed, while slowly warming up the flow tube. The analysis occurred

simultaneously by in situ UV/VIS absorption spectroscopy using a diode array arrangement in connection with a White-cell of 2 m total path length and by mass spectroscopy. A time-of-flight MS was employed in this study being directly connected to the absorption cell by a molecular beam sampling inlet.

### 3 Results and Discussion

In fig. 1 a series of consecutive absorption spectra is shown as received at different times during the warm-up period. The flow tube had been precovered with frost for these experiments. The tube was held at  $T \sim 200\text{K}$  during the reaction and warmed up to  $T \sim 250\text{K}$  within about 30 minutes. It should be kept in mind that during the whole period the tube was connected to the MS through a 0.1 mm orifice in the skimmer.

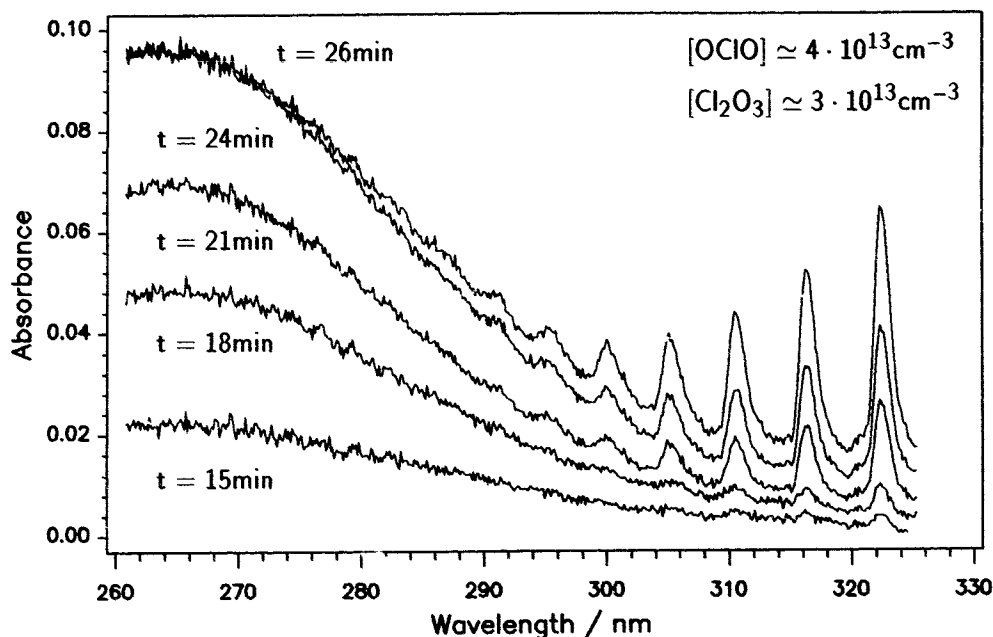


Fig. 1: Series of optical absorption spectra obtained during warming of ice-covered tube

The absorption with maximum around 265 nm that develops with time is due to  $\text{Cl}_2\text{O}_3$  [7]. Surprisingly OCIO appears to evaporate from the cooled wall after  $\text{Cl}_2\text{O}_3$ . As seen its concentration still increases with time when  $[\text{Cl}_2\text{O}_3]$  had reached a plateau. This observation is taken as evidence that the OCIO observed under these conditions results from dissociation of  $\text{Cl}_2\text{O}_3$ . The dissociation energy is reported to be  $\Delta H_d = 62 \text{kJ} \cdot \text{mol}^{-1}$  [8]. Thus at equilibrium the  $[\text{Cl}_2\text{O}_3]/[\text{OCIO}]$  ratio observed would correspond to a temperature of roughly 240 K in acceptable agreement with experimental conditions. Unfortunately no information on  $\text{Cl}_2\text{O}_3$  generation/dissociation could be obtained from MS analysis. The mass spectrometer is extremely insensitive to  $\text{Cl}_2\text{O}_3$  on its parent mass.

Results from absorption measurements at wavelength  $\lambda < 260 \text{nm}$ , not presented here, indicated that  $\text{Cl}_2\text{O}_2$  was not formed in the experiments on ice. Because of the low total

pressure during the reaction, only negligible contributions from a homogenous three body recombination would be expected. The heterogenous ClO-dimerisation appears to be prevented by the massive presence of ice. Cl<sub>2</sub>O<sub>2</sub> formation was shown to occur, however, heterogeneously in the absence of frost (see below).

No information is obtained from UV/VIS absorption measurements on the generation of Cl<sub>2</sub>O in the present experiments (about MS data for Cl<sub>2</sub>O see below). This species is a rather weak absorber with an absorption cross section about an order of magnitude lower than that of Cl<sub>2</sub>O<sub>3</sub> at its absorption maximum around 265 nm [8].

HOCl was not expected to come off the tube wall to a noticeable extent around 250 K, even if present in the ice [9].

The simultaneously recorded MS spectra nicely complemented the results obtained in absorption measurements. In fig. 2 is presented a typical spectrum in the range 40 < amu < 130 at t ~ 25 min.

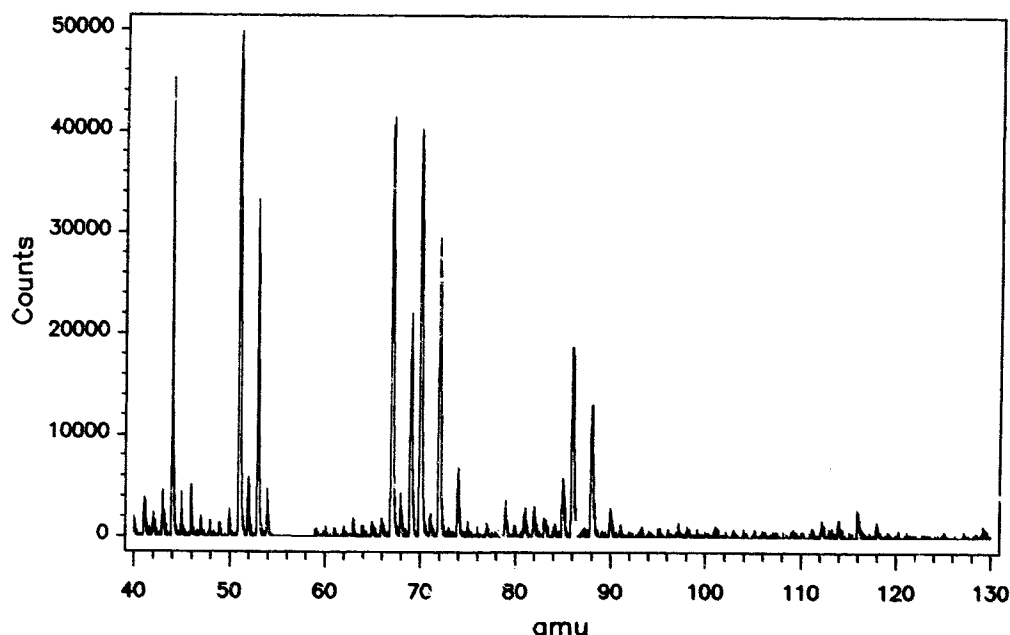
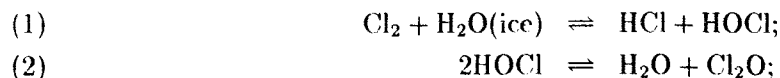


Fig. 2: Mass spectrum registered during the warming of the ice-covered tube.

The signal at 44 amu demonstrates the presence of CO<sub>2</sub> from covering the flow tube with frost before the experiments, which was done with the tube being open to air. The ClO<sup>+</sup>-signals at 51, 53 amu are fragments from OClO<sup>+</sup> and Cl<sub>2</sub>O<sup>+</sup> with parent signals at 67, 69 and at 86, 88 and 90 amu, respectively. Presumably also Cl<sub>2</sub>O<sub>3</sub> contributes to these signals. No detailed fragment analysis was carried out at this stage of the investigation. The signal at 85 amu constitutes an unaccounted background signal present in the MS. The main contribution to the signals at 70, 72 and 74 amu are due to unreacted Cl<sub>2</sub>. Clearly no ion signals for Cl<sub>2</sub>O<sub>2</sub> were obtained in the experiments on ice in contrast to experiments in its absence (see below).

It was shown that Cl<sub>2</sub>O formation occurs already when Cl<sub>2</sub>/He is passed over ice in the absence of O<sub>3</sub>. It is suggested that Cl<sub>2</sub>O results from Cl<sub>2</sub> disproportionation on ice (1) followed

by step (2):



It had been shown in experiments with gaseous HOCl that its  $\text{Cl}_2\text{O}$  content could be adjusted in a wide range by varying the temperature of a trap over which HOCl was transported with He as carrier gas [9].

At present only speculations can be offered on the formation of OClO in the Cl/O<sub>3</sub>-system over ice. Certainly oxidation of ClO by O<sub>3</sub> could be considered as option, although refuted by others [10]. The concept of disproportionation on ice of neutral ClO radicals with their chlorine in the formal valence state +2 into Cl atoms and OClO with chlorine in the valence states ±0 and 4, respectively, is not violated by formulating an overall step like (3):



In the gas phase this process is endothermic by  $3.1 \pm 2 \text{ kcal} \cdot \text{mol}^{-1}$  and would have a very low probability only to occur at low temperature. But no data are available for changes in solvation energies for the species involved in the processes on ice. Certainly, the Cl atoms will immediately react on ice in exothermic steps to yield solvated Cl<sup>-</sup> and H<sup>+</sup>-ions. Solvation of H<sup>+</sup> is known to be one of the most exothermic processes [11, 12].

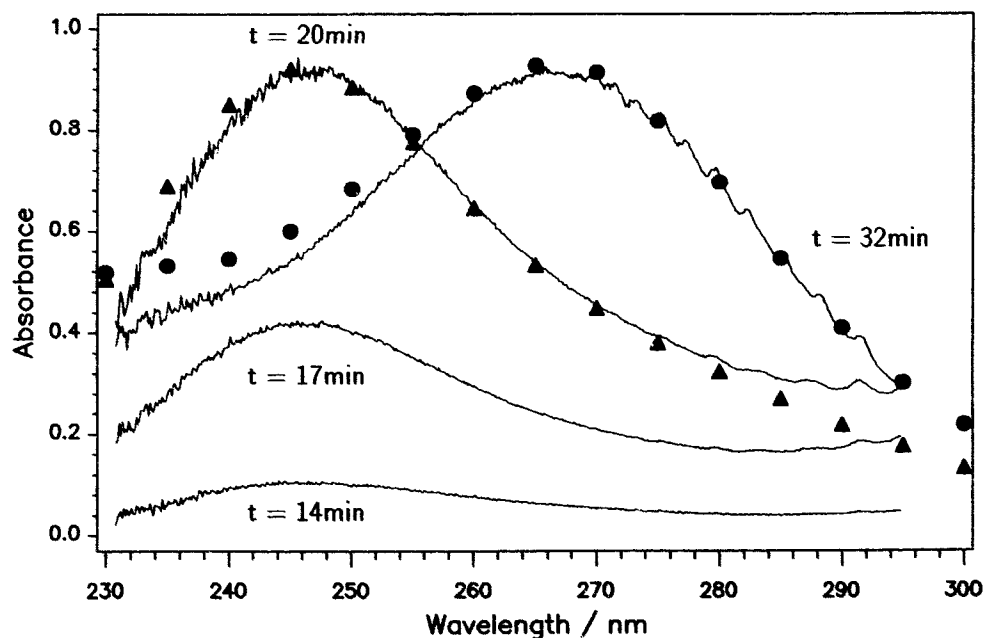


Fig. 3: UV/VIS absorption spectra registered at different times  $t$  during the warm-up period of the tube not precovered with frost (see text); triangles represent reference data taken from [15]; circles represent data points taken from ref [16], note discrepancy at  $\lambda < 250 \text{ nm}$

It must be pointed out, that in experiments in which the flow tube had not been precovered with frost products were collected at the flow tube wall with very much lower yields only. A

reduction in collection efficiency by a factor of 10-50 at a temperature  $\sim 200$  K was observed. As pointed out above, formation of  $\text{Cl}_2\text{O}_2$  in the uncovered tube, in contrast to observations on ice, is considered to be a significant difference.

To collect enough reactants and products for convenient analysis the temperature of the flow tube in these experiments was lowered in steps from run to run down to  $\sim (110 \pm 20)$  K. The large error given reflects experimental problems to control the temperature in this range. Also we were unable to exclude humidity rigorously from the system. Since no traces of frost could be detected on the walls after warming the tube to  $\sim 230$  K, it can only be stated that humidity was too low to be visually observable.

In fig. 3 is shown a series of consecutive UV/VIS absorption spectra received at different times during the warming-up period of the tube not precovered with frost. Clearly under these conditions  $\text{Cl}_2\text{O}_2$  was found in the reaction. It was identified by the shape of its absorption with  $\lambda(\text{max}) = 245$  nm.  $\text{Cl}_2\text{O}_2$  evaporates from the tube wall in a narrow temperature range prior to  $\text{Cl}_2\text{O}_3$ . Good agreement exists between the observed  $\text{Cl}_2\text{O}_2$  absorption spectrum and previously reported data — except in the range of  $\text{OClO}$  absorption [13-16]. A discrepancy is apparent at short wave length for  $\text{Cl}_2\text{O}_3$  between the present finding and data reported in [16]. At higher temperatures  $\text{OClO}$  became dominant similar to the situation presented in fig. 1.

Fig. 4 shows a simultaneously registered mass spectrum. As in the UV/VIS spectra also mass spectrometrically  $\text{Cl}_2\text{O}_2$  is unequivocally identified as product. No higher chlorine oxides could be detected, although looked for. If formed they might have decomposed in the MS inlet, which was not cooled cryomatically.

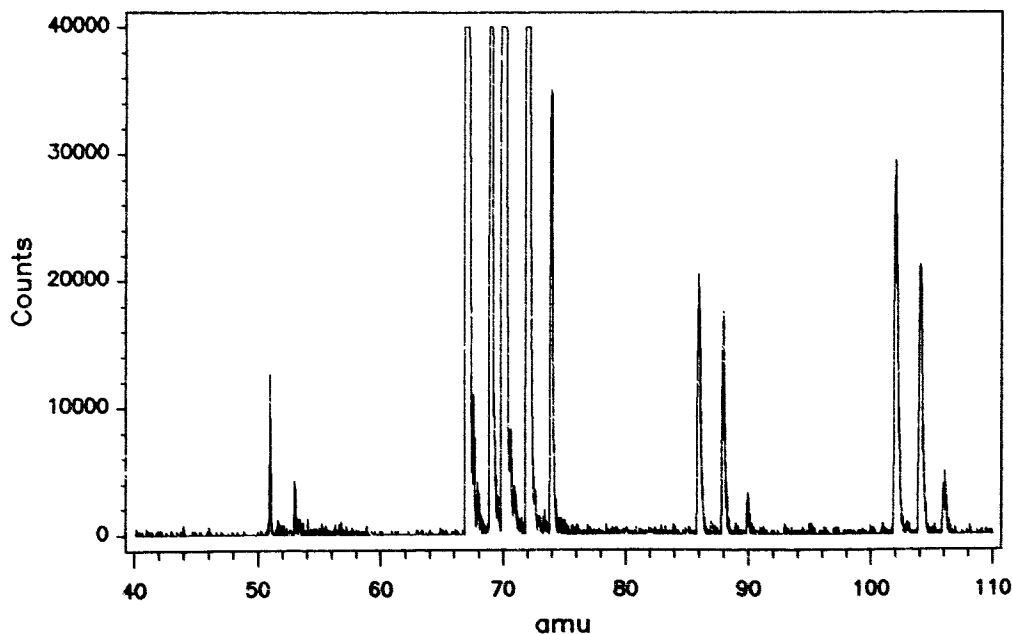


Fig. 4: Mass spectrum registered at  $t \sim 20$  min during the warm-up period of the tube. The background was subtracted in this spectrum.

The latter experiments in a tube not covered with frost are not relevant to atmosphere chemistry. The results seem to hint, however, on a subtle difference in  $\text{ClO}$  low temperature

chemistry: OClO formation from ClO radicals followed by Cl<sub>2</sub>O<sub>3</sub> generation seems to require only traces of humidity on the tube surface and is not effected by excess of ice, whereas dimerisation of ClO radicals is significantly inhibited by ice on the flow tube wall. Also, if OClO were formed in a heterogenous oxidation by O<sub>3</sub> radicals the results would suggest that this reaction is immune to presence of ice whereas the ClO dimerisation is not.

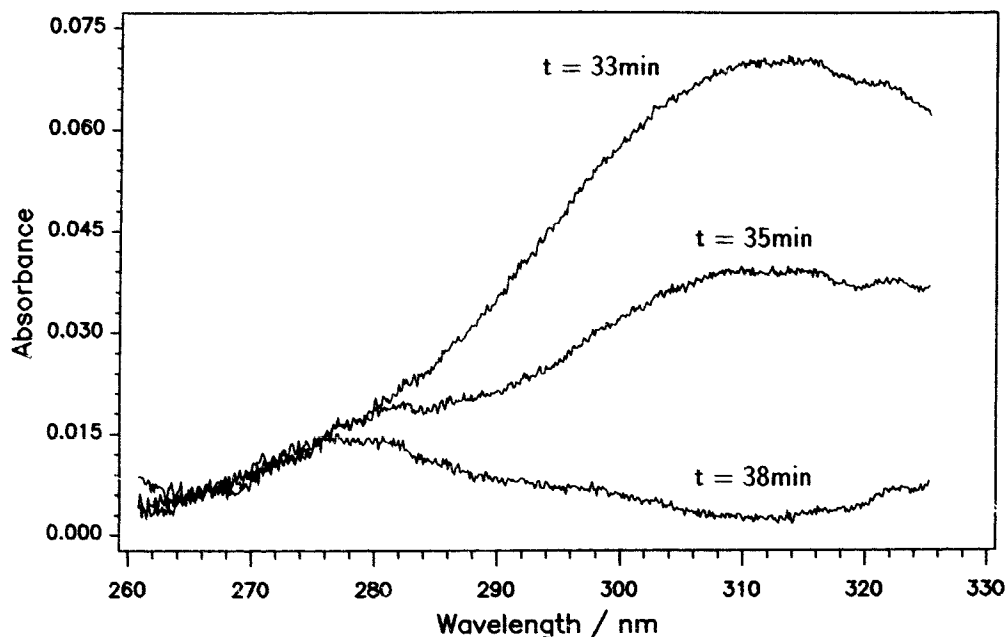


Fig. 5: UV/VIS absorption spectra obtained in the Br/O<sub>3</sub> system

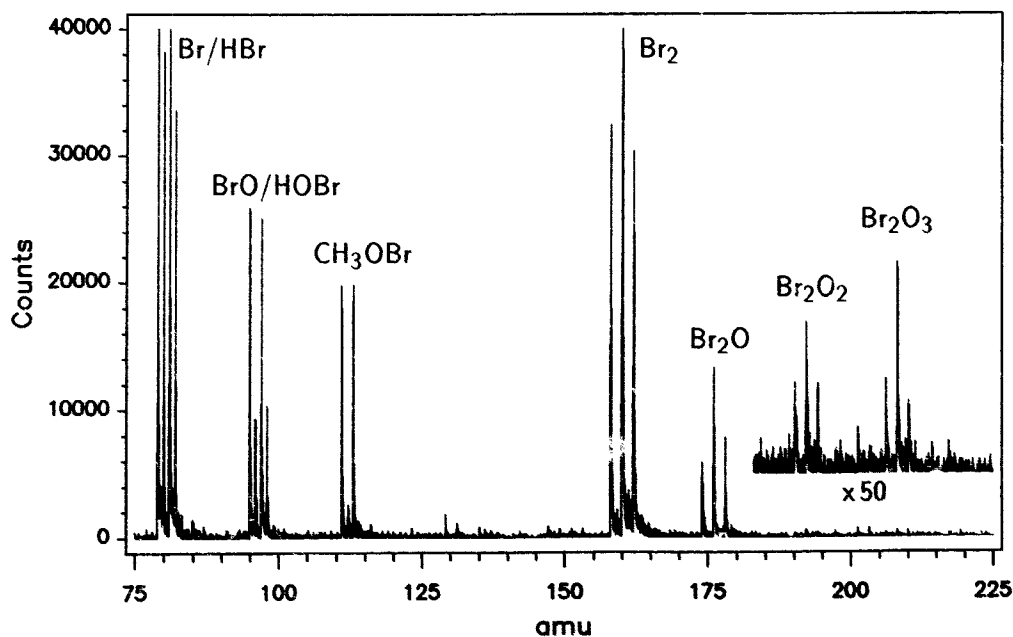


Fig. 6: mass spectrum registered in the Br/O<sub>3</sub> system during warming.

0.235

The results obtained in a comprehensive study of the Br/O<sub>3</sub> system carried out under comparable conditions shall be mentioned only briefly. These data are prepared for publication in a separate contribution [16]. An up to now unreported continuous absorption with maximum at  $\lambda \sim 312$  nm was detected upon warming the tube. A series of UV/VIS spectra from these experiments is shown in fig. 5. It appears that more than one species contributes to the spectra since two residual absorptions at  $\lambda \sim 280$  nm and  $\lambda \sim 323$  nm remain after the main absorber disappeared. On the basis of the MS data presented below the absorption at  $\lambda \sim 312$  nm is proposed to be Br<sub>2</sub>O. The contribution at 280 nm seems to be due to HOBr [17]. The absorption at  $\lambda \sim 323$  nm can not be accounted for at present.

A corresponding mass spectrum is given in fig. 6. The signals shown are labeled (for CH<sub>3</sub>OBr signals see below). The oxides Br<sub>2</sub>O<sub>2</sub> and Br<sub>2</sub>O<sub>3</sub> were present in the system only in negligible amounts (see insert in fig. 6).

An interesting additional information was obtained through an experimental mishap: In the course of these experiments a tiny crack developed in the flow tube and allowed traces of the coolant CH<sub>3</sub>OH to leak into the flow tube. The signals at 111 and 113 amu indicate generation of CH<sub>3</sub>OBr of the low temperature experiment. An ionic reaction mechanism for its formation can be conceived with Br<sub>2</sub>O as reactant.

#### 4 References

- [1] Solomon, S., *Nature* **347** (1990) 347.
- [2] Friedl, R.R. and Sander, S.P., *J. Phys. Chem.* **93** (1989) 4756.
- [3] Sander, S.P. and Friedl R.R., *J. Phys. Chem.* **93** (1989) 4764.
- [4] Poulet, G., Lencar, I.T., Laverdet, G. and Le Bras, G., *J. Phys. Chem.* **94** (1990) 278.
- [5] Anderson, J.G., Toohey, D.W. and Brune, W.H., *Science* **251** (1991) 39.
- [6] Molina, M.J., Colussi, A.J., Molina, L.T., Schindler, R.N. and Tso, T.L., *Chem. Phys. Lett.* **173** (1990) 310.
- [7] Hayman, G.D. and Cox, R.A., *Chem. Phys. Lett.* **155** (1989) 1.
- [8] NASA-Panel for Data Evaluation, "Chemical kinetics and photochemical data for use in stratospheric modelling", *Evaluation number 10*, Jet Propulsion Laboratory, Pasadena, California (1992).
- [9] Vogt, R., Schindler, R.N., *Ber. Bunsenges. Phys. Chem.* **93** (1993) in press.
- [10] DeMore, W.B., private communication.
- [11] Henglein, A., *Ber. Bunsenges. Phys. Chem.* **78** (1974) 1078.
- [12] Principally, J., Bockris, O.M. and Reddy, A.K.M., *Modern electrochemistry*, Vol. 1, Plenum press (1970).
- [13] Cox, R.A. and Hayman, G.D., *Nature* **332** (1988) 796.
- [14] Permien, T., Vogt, R. and Schindler, R.N., paper presented at the COST 611 Meeting, Norwich, Sept. 1988.
- [15] DeMore, W.B. and Tschuikow-Roux, E., *J. Phys. Chem.* **94** (1990) 5856.
- [16] Burkholder, J.B., Orlando, J.J. and Howard, C.J. *J. Phys. Chem.* **94** (1990) 687.
- [17] Kirchner, U. and Schindler, R.N., prepared for publication.
- [18] Permien, T. and Schindler, R.N., unpublished.